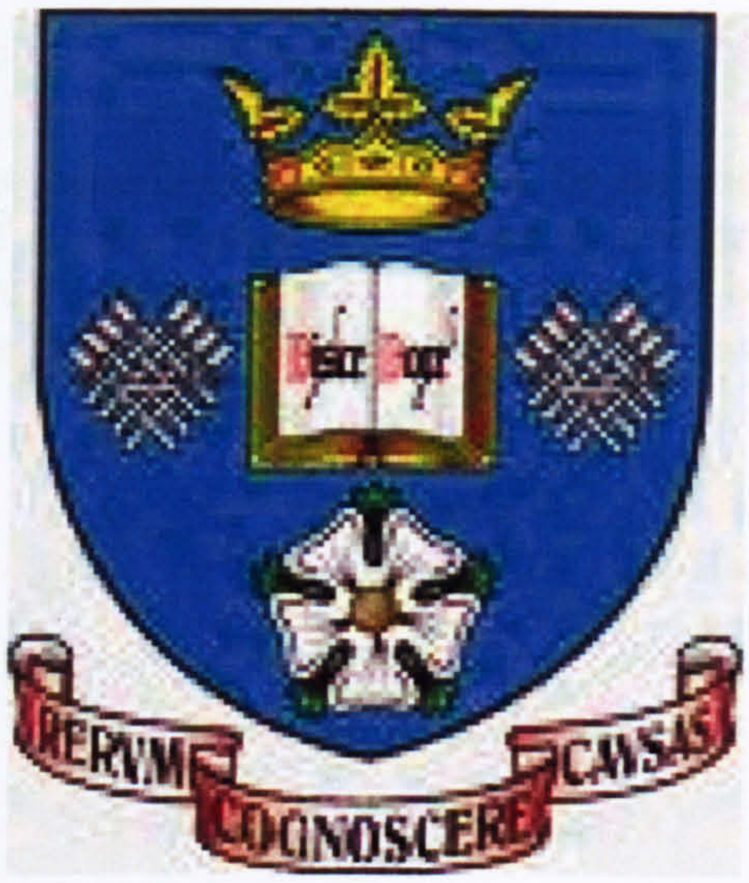


# Hydrological Performance of Green Roofs

**Hartini Kasmin**

**This thesis is submitted in partial fulfilment of the requirements for the Degree of Doctor of Philosophy**

**University of Sheffield**

**Department of Civil & Structural Engineering**

**June 2010**

# DECLARATION

I declare that the work in this thesis has been composed by me and no portion of the work has been submitted in support of an application for another degree or qualification of this or any other university or other institute of learning. The work has been my own except where indicated and all quotation marks and the sources of information have been acknowledged.

Hartini Kasmin, 30th June 2010

Hydrological Performance of Green Roofs

Hartini Kasmin

## ABSTRACT

Due to an increase in impermeable hard surfaces, urbanization has led to the deterioration of urban watercourses and increased the quantity of stormwater runoff. It may be argued that the current norm of impermeable roofs represents a wasted opportunity. Green roofs have the potential to replace some of the hydrological characteristics of natural catchments that are normally lost as a consequence of urbanization and the removal of vegetation.

The overall aim of this study was to develop a generic green roof rainfall runoff response model capable of predicting the temporal variations within any configuration of green roof in response to an arbitrary rainfall input. It was recognized that the preliminary investigations has led to the identification of a subset of processes/parameters for a green roof which warranted more detailed investigation. In this case the substrate moisture holding capacity and the losses due to evapotranspiration were identified as key controlling variables to be identified. To simulate the function of stormwater drainage, a direct observation of the system's behaviour is required. Hence, an established 'typical' small scale green roof (1.0 m × 3.0 m) on the roof of Sheffield University has been monitored with the intention to relate both retention and detention with fundamental, measurable, physical properties of the system.

A continuous long time-series of data, in the period of 29 months, from the test rig was analysed and interpreted. Laboratory analyses on physical properties and evaporation of the substrates were undertaken and relationships between measureable physical properties and model parameter values were identified. The empirical (requiring site-specific calibration using monitored data) conceptual model now has been developed into a physically-based model. Although the model still needs to be refined, independent physically-based methods have been identified for defining two key parameters (evapotranspiration (ET) and the maximum moisture-holding capacity ($WC_{max}$)). ET can be estimated using a modified form of Thornthwaite's equation, and $WC_{max}$ may be determined by physical laboratory assessment of the substrate. The proposed hydrological model has been shown to reproduce monitored data, both during a storm event, and over a longer continuous simulation period.

"It was the best of times, it was the worst of times, it was the age of wisdom, it was the age of foolishness, it was the epoch of belief, it was the epoch of incredulity,..."
— Charles Dickens (A Tale of Two Cities)

. .suffering has been stronger than all other teaching, and has taught me to understand what your heart used to be. I have been bent and broken, but - I hope - into a better shape"
— Charles Dickens (Great Expectations)

# ACKNOWLEDGEMENTS

First of all, I would like to say Alhamdulillah, for giving me the strength and health to do this research work until it done.

I am heartily thankful to my supervisor, **Dr. Virginia Stovin**, for her excellent guidance, consistent encouragement and patience throughout the course of this research, help me to develop an understanding of the subject.

I would also like to thank the Green Roof Centre of Sheffield's staffs especially Dr. Nigel Dunnet and Jeff Sorrill for providing green roof's facilities for my experiment, sharing their knowledge and giving me the opportunity to explore the real of green roof world.

I wish to thank all of my colleagues of the Pennine Water Group, University of Sheffield especially Dr. Abigail Hathway, Dr Alma Schellart, Fred Sonnenwald, and Joerg Werdin, for their help and stimulating discussions.

This project would not be possible without the helpful assistance of the following departmental technical staffs; Paul Osborne, Mark Foster, Lee Jervis, David Callaghan, Glenn Brawn, Mick Moore, Alex Cargill and Dick Smith.

Special thanks to Minister of Higher Education Malaysia and Universiti Tun Hussien Onn, Malaysia for their financial support during the full term of this research.

It is a pleasure to thank those who made this thesis possible such as my parents, Hj Kasmin Abu Yamin and Hjh Pauzeah Ahmad, and the whole lovely family who gave me the moral support, endless advice and encouragement.

Special thanks also go to my best friends, Mahar Diana Hamid, Nor Hayati Abdul Ghafar, Ahmad Badruddin Che Kasim, Mariyam Jamilah Homam, Tuan Norhayati Tuan Chik, Norazizi Yusoff and Sabariah Julaihi for their spiritual support during the study.

Lastly, I offer my regards and blessings to all of those who supported me in any respect during the completion of the study.

## A. TABLE OF CONTENTS

**PAGES**

## CHAPTER 7 MODEL DEVELOPMENT



## CHAPTER 8 CONCLUSIONS AND SUGGESTIONS FOR FURTHER WORK

## B. LIST OF TABLES

**PAGES**

## C. LIST OF FIGURES

**PAGES**

# NOTATIONS

| Symbol | Definition | Unit |
|---|---|---|
| A | Cross sectional area | $m^2$ |
| ADWP | Antecedent dry weather period | hours |
| AFp | Air-filled porosity | % |
| D | Drainage water to the groundwater | mm |
| Ddry | Bulk density (dry) | $g/cm^3$ |
| Dmoist | Bulk density (moist) | $g/cm^3$ |
| Dmax | Bulk density (maximum water condition) | $g/cm^3$ |
| Dp | Particle density | $g/cm^3$ |
| E | Evaporation | mm |
| $E_e$ | Experiment Evaporation | mm |
| ET | Evapotranspiration | mm |
| $ET_{th}$ | Evapotranspiration from the Thornthwaite equation | mm |
| $ET_f$ | Evapotranspiration from fitted values | mm |
| H | Height of the water level | mm |
| I | Inflow | $mm^3/5min$ |
| i | Intensity | mm/5min |
| IL | Initial losses | mm |
| k | Runoff routing coefficient | |
| mod $K_f$ | Water permeability | cm/s |
| $MC_0$ | Initial moisture content/Moisture content at time 0 | % |
| $MC_{min}$ | Minimum moisture content | % |
| $MC_t$ | Moisture content at time t | % |
| n | Runoff routing coefficient | |
| O | Outflow | $mm^3/5min$ |
| P | Precipitation | mm |
| Q | Direct runoff | mm |
| Qp | Peak runoff intensity | mm/5min |
| PA | Peak attenuation | % |
| PE | Potential Evaporation | mm |
| R | Rainfall | mm |
| RD | Rainfall duration | hours |
| Rp | Peak rainfall intensity | mm/5min |
| $R^2$ | Best goodness of fit | % |
| $R_t^2$ | Best goodness of fit (time-series) | % |
| Ta | Time to start runoff | hours |
| Tlag | Time to peak rainfall to peak runoff | min |
| TP | Total rainfall | mm |
| TR | Total runoff | mm |
| Tp | Total porosity | % |
| TRD | Total retention depth | mm |
| VR | Volume retention | % |
| $WC_{max}$ | Maximum moisture-holding capacity, Water-Filled Porosity | % |
| $\Delta S$ | Change in water storage in the soil | $mm^3$ |
| $\Delta t$ | Time interval | min |
| $\rho_w$ | Water density | $kg/m^3$ |

# ABBREVIATIONS

| | |
|---|---|
| Al-HL | Alumasc Heather with Lavender |
| Al-Sedum | Alumasc Sedum |
| CSOs | Combined Sewer Overflows |
| FLL | Guidelines for the Planning, Execution and Upkeep of Green-Roof Sites |
| FSR | Flood Studies Report |
| GE | Green Estate |
| LECA | Light Expanded Clay Aggregate |
| SUDS | Sustainable (Urban) Drainage Systems |
| UH | Unit Hydrograph |

# CHAPTER 1

# INTRODUCTION

## 1.1 Background to the Study

Urbanization has altered the natural hydrological process by providing more impervious areas within developed countries. Due to the adverse effects of increase in flow rate and the volume of stormwater runoff, water engineers have introduced Sustainable (Urban) Drainage Systems (SUDS) provides a natural approach to manage stormwater (Swan *et al.*, 1999; Reeves & Lewy, 2002; Hutchinson, *et al.*, 2003; Villarreal, *et al.*, 2004; Taylor, *et al.*, 2005; Taylor, 2006; Rowe, *et al.*, 2003, 2006, CIRIA, 2007). SUDS are believed to be more sustainable than conventional drainage methods because they can manage runoff flowrates, reducing the impact of urbanization on flooding by dealing with runoff close to where the rain falls (CIRIA, 2007). SUDS reproduce the natural process of the hydrological cycle by infiltrating, storing and controlling the amount of water that flows to natural streams. Swales, retention ponds, detention basins, permeable paving, filter drains and green roofs are examples of SUDS structures. Each of these structures has their own role to play by mimicking the natural water cycle processes.

Urbanization has deteriorated urban watercourses, associated with increasing quantities of stormwater runoff due to an increase of impermeable hard surfaces. This reduces the level of spare capacity in the conventional drainage systems, which may lead to flooding and/or overflow events. Existing urban areas continue to have impacts on the quantity and the quality of urban watercourses (Macdonald & Jefferies, 2003). There is a need to have a better solution and it has been suggested that retrofitting SUDS might be an option for resolving the catchment hydraulics problem (Stovin & Swan, 2003).

In order to achieve greater influence on flow mitigation, the stormwater management train approach is an effective surface water/drainage approach that provides balanced treatment for the quality and the quantity of the runoff (Figure 1.1). The aim of this management train is to reduce the total volume and rate of runoff from the SUDS structures, and retain the pollutants

that may be picked up from surrounding materials and atmospheric deposition. The SUDS train system implies three levels of stormwater train management from source control (individual premises), to a larger downstream site and regional control (CIRIA, 2007).

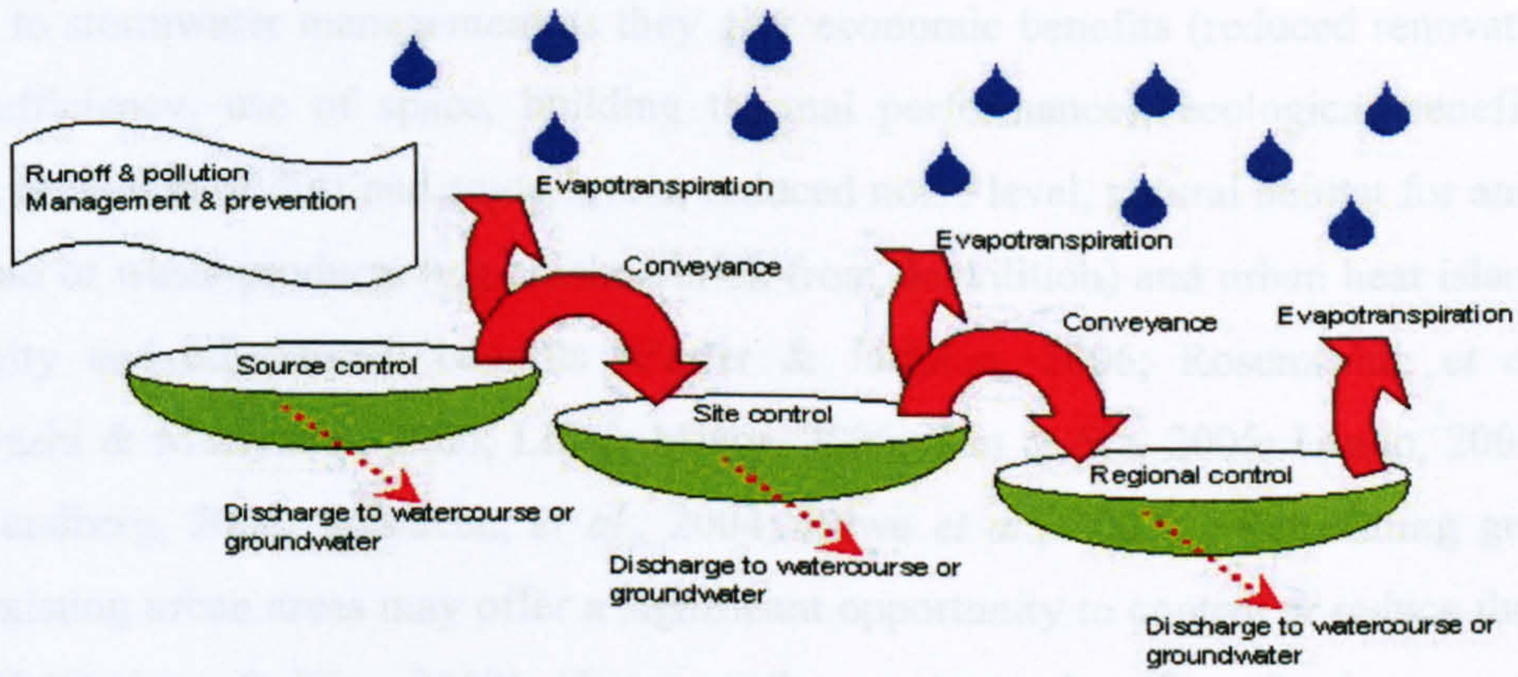


Figure 1.1: SUDS management train (Source: CIRIA, 2007)

The stormwater train technologies attempt to solve/control the problem by mimicking nature through infiltration, storage and evapotranspiration processes within those three levels of controls. SUDS are defined as a sequence of management practices and control structures designed to drain surface water in a 'more sustainable' fashion than some conventional techniques (CIRIA, 2007). SUDS structures at source control includes: soakaways, garden ponds, green roofs and water butts. Site controls include porous pavements, swales and infiltration trenches and in regional controls, basin and ponds are the structures that are typically involved.

While most of the SUDS structures are applied into new developments, SUDS retrofitting within existing development might provide additional scope for controlling the stormwater runoff (Stovin & Swan, 2003; Macdonald & Jones, 2006). The source control system has a greater influence on flows than the site and regional control systems (Macdonald & Jefferies, 2003). This comparison was made due to water quality performance, where majority of suburban area and car parking areas (source control systems) results on low contamination flows while two sites control had a risk of high level. These findings might suggest that green roofs, which could replace significant areas of urban impermeable surface, should be studied in more detail. In addition, it may be argued that it is a suitable time to gain some benefits from using the largely wasted rooftop spaces in urban environments (Liptan & Strecker, 2003).

Green roof is a roof structure for drainage and irrigation system that is covered with vegetation and growing media. It has been recognized as providing a source control SUDS drainage structure which replicates natural catchment processes. Green roofs offers other benefits in addition to stormwater management as they give economic benefits (reduced renovation costs, energy efficiency, use of space, building thermal performance), ecological benefits (urban ecology, reduction of dust and smog levels, reduced noise level, natural habitat for animals and plants, use of waste products (e.g crushed brick from demolition) and urban heat island effect), community and educational benefits (Carter & Jackson, 2006; Rosenzweig *et al.*, 2006; Takebayashi & Moriyama, 2006; Liu & Minor, 2005; Tan & Sia, 2005; Lando, 2004; Miller, 2004; Lundberg, 2004; Schraven, *et al.*, 2004; Rowe *et al.*, 2003). Retrofitting green roofs within existing urban areas may offer a significant opportunity to control or reduce the quantity of runoff (Graham & Kim, 2003). However, the maximum benefits of using green roofs to influence the flow mitigation will arise when they are used in combination with other SUDS structures (Villarreal *et al.*, 2004).

## 1.2 Objective of the Study

Drainage engineers require models in order to simulate the function of stormwater drainage. The overall aim of this study is to develop a generic green roof rainfall runoff response model capable of predicting the temporal variations within any configuration of green roof in response to an arbitrary rainfall input.

Although several studies of green roof hydrological performance have been reported in the literature, there are several reasons why it was felt necessary to collect new, local, experimental data as part of this research project. Key motivations for this decision were as follows:

- Direct observation of the system's behaviour is invaluable for understanding key processes;
- Ownership of the test facility provides greater opportunity to manage and understand the quality and limitations of the collected data set;
- None of the reported studies correspond to roof configurations typically utilised in the UK, or to UK climatic inputs – as such the long-term performance characteristics may not be indicative of what might be expected locally;
- As the study's ultimate aim is to develop a generic modelling tool which would be able to predict runoff for a roof with a previously unmonitored configuration in response to an arbitrary rainfall event, it is important to have additional supplies of components

available for complementary physical tests and analyses. In particular, samples of the substrates were retained for analysis of physical characteristics such as porosity and moisture-holding capacity.

The research programme is therefore developed to make use of data generated from a single, typical, green roof test bed which had been established shortly before the present research commenced (Stovin *et al.*, 2007). It is anticipated that the data obtained from this test bed would be used to inform the development of a simple hydrological rainfall-runoff model, and to identify key controlling processes and configuration variables/model parameters. In order to fulfil the requirement for a generic model, the research also needed to include a programme of laboratory tests aimed at relating the model parameter values to measureable substrate physical characteristics.

It was recognized that the preliminary investigations would lead to the identification of a subset of processes/parameters which warranted more detailed investigation. In this case the substrate moisture holding capacity and the losses due to evapotranspiration were identified as key controlling variables. Laboratory analyses of alternative substrates were undertaken and model predictions of their impacts upon runoff responses made. As it is always desirable to validate model predictions, the final stage of the research programme was aimed at establishing new test rigs which would enable field data focusing on these specific variables to be collected.

The objective of the research may be summarized as follows:

- Analyse and interpret a continuous long time-series data from a 'typical' green roof configuration test rig under UK climatic conditions;
- Propose an appropriate, generic, conceptual rainfall/runoff model;
- Utilize experimental data from the 'typical' test rig to calibrate and verify the proposed model;
- Undertake complementary laboratory experiments and analyses to identify relationships between measureable physical properties and model parameter values;
- Use the model to predict how runoff responses will vary in response to specific configuration modifications, and establish additional experimental test beds to enable predictions to be tested.

Note that 'typical' green roof configuration is referred to the standard configuration supplied by ZinCo (Alumasc Exterior Building Products) for planted roof system.

## 1.3 Structure of the Thesis

This thesis is divided into eight main chapters. The first contains summary information on general introduction to the main problem of the study, as well as the aim and the objectives of the research. Chapter 1 also contains summary information on the structure of the report.

Chapter 2 provides a literature review. The introduction contains the general background of the study on the urbanization problems on stormwater runoff which leads to the adoption of Sustainable Urban Drainage System (SUDS) as well as the green roof as one type of SUDS structure. Several studies were reviewed in this chapter including the instrumentation used in their studies as well as their green roof stormwater performance. General background for data-based and process-based modelling highlights the need of the monitoring of local hydrological data for green roof. Hence the literature review provides a brief introduction to urban hydrology, basic approaches of data-based and process-based modelling followed by an assessment of previous work relating to the hydrological monitoring and modelling of green roofs.

The conceptual model is outlined in Chapter 3 based on information from Chapter 2 and our objectives. The conceptual model includes the theoretical parameters related to loss estimation in retention compartment and storage routing in detention part that going to be used in our model. Chapter 4 covers the methodologies that have been used in this study, including the description of the current green roof test rig configurations, the rainfall-runoff monitoring approaches, instrumentation and outlined programme of laboratory tests.

Chapter 5 consists of results and performance analyses from 29 months monitored storm-event from the established test rig. Storm by storm event, monthly, seasonal and regression analyses are presented in this chapter. Chapter 6 presents the results from the experimental work; the substrate physical characteristics test and evaporation test of three different substrates. Further model development is explained in Chapter 7 with further calibration using storm data from the monitored test rig from Chapter 5 and model validation using substrates properties result from Chapter 6. This followed then by the final Chapter 8; conclusion and suggestion for further work. In this chapter, conclusions based on main chapters; 5, 6 and 7 are presented.

# CHAPTER 2

# LITERATURE REVIEW

## 2.1 Hydrological Performance of Natural and Urban Catchments

The hydrological performance of natural catchments is mainly influenced by three basic categories of processes (Figure 2.1):

1. Those controlled by climate – water movement to the catchment area is determined by the rates of precipitation (rain and snow);
2. Those controlled by vegetation – water movement to the catchment surface is determined by interception, transpiration and affects of infiltration rates;
3. The process influenced by various surface and subsurface pathways – water movement to the nearest stream is determined by the process of precipitation, evapotranspiration, infiltration and runoff.

Urbanization, which has been associated with more paved areas, road drains and city sewer systems, has altered rates of transpiration, evaporation and infiltration resulting in higher magnitude and earlier flood peaks during urban flood events (Figure 2.1).

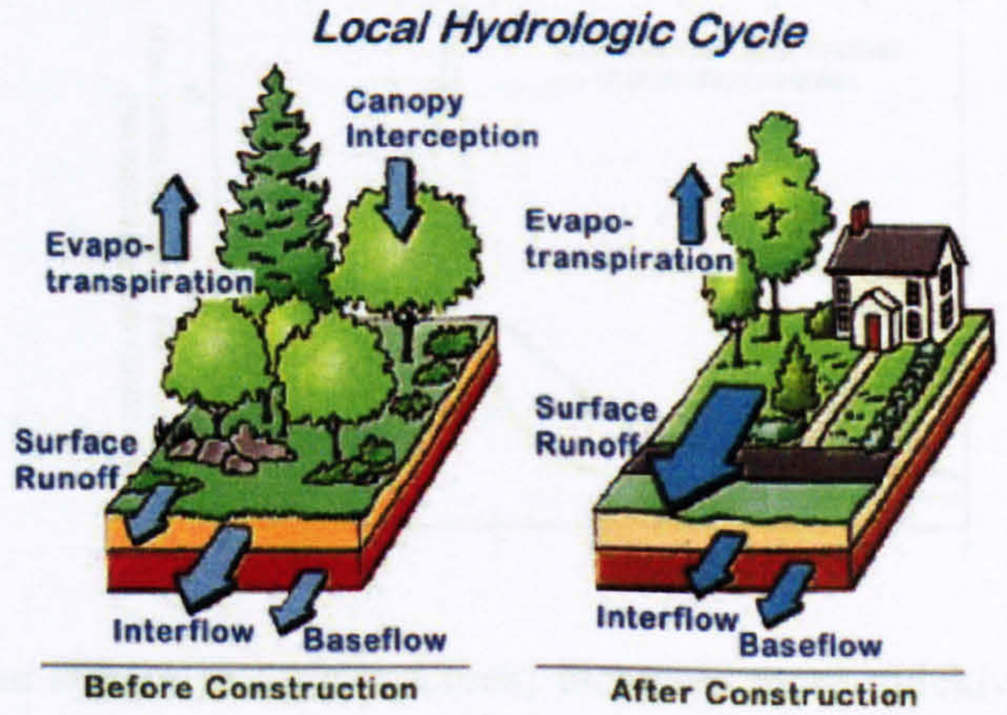


Figure 2.1: Local hydrological cycle and the flow path of runoff before and after construction (Source: MDE, 2002)

Evidence of hydrologic effects in urban development was shown; for example in Western Washington, by comparing Novelty Hill, a forested catchment and Klahanie, a catchment with residential land use (Burges *et al.*, 1998). During storms, Klahanie produced different runoff patterns to Novelty as Klahanie has a higher runoff volume and higher peak discharge (Figure 2.2). A report from Konrad (2005) also indicates that Newaukum Creek (rural) and Mercer Creek (urban) in Washington State show the same results as Burges (Figure 2.3). These two examples indicate that the water cycle in urban catchment changed when there were changes in vegetation and surface permeability. These changes affect the rate of interception, evapotranspiration and surface runoff.

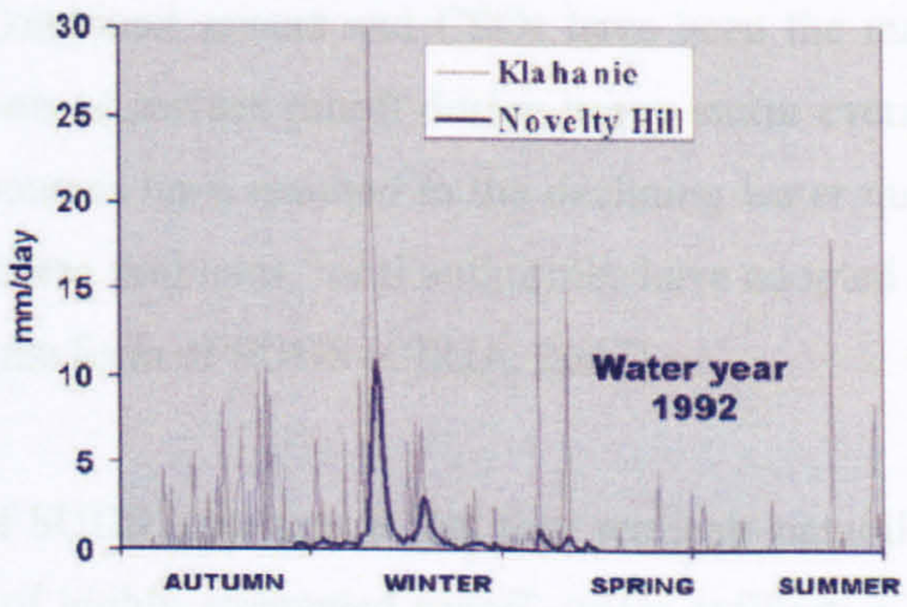


Figure 2.2: Hydrograph for an urban (Klahanie) and a rural watershed (Novelty Hill). Stormflows increase in magnitude and frequency in the urban watershed. (Source: Burges *et al.*, 1998)

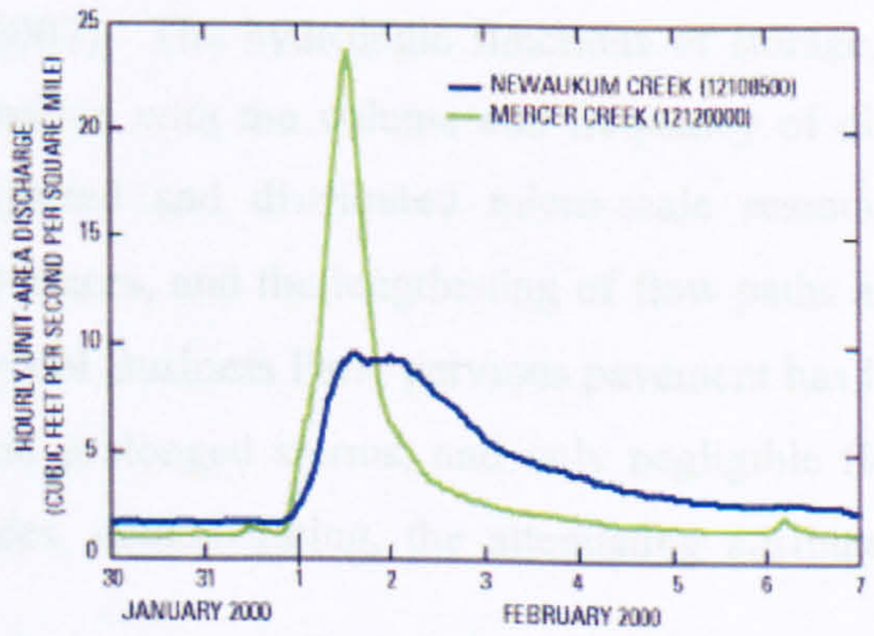


Figure 2.3: An urban stream in Mercer Creek, increases more quickly, reaches a higher peak discharge and a larger volume than streamflow in Newaukum Creek, a nearby rural stream (Source: Konrad, 2005)

These examples show that urbanisation leads to an increased flood risk in urban areas. Corresponding to this increase in impermeable area, high levels of surface runoff are experienced in urban areas during heavy rainfall events (Environment Agency (EA), 2007). The movement of the runoff from upstream gathers all the dirt and waste during flash floods. Combined Sewer Overflows (CSOs) will cause raw sewage to be dumped in local watercourses which leads to poor water quality, unsightly environments and produces the negative effects of harmful chemicals on biodiversity.

According to the Environment Agency (EA) (2003), removing water using conventional drainage systems leads to a range of impacts; including increased runoff, as well as higher water levels and flow rates. Combined sewers and CSOs have been the main systems of drainage within the UK. High levels of surface runoff during heavy storm events and the effluent from domestic and industrial sources have resulted in the declining water quality standards of urban rivers. In order to tackle these problems, local authorities have adopted strategies of sustainable drainage development in the form of SUDS (CIRIA, 2007).

The unique advantages of SUDS structures is that they replicate natural hydrological processes, including characteristics of highly attenuated runoff, water exfiltration, storage and infiltration (Reeves & Lewy, 2002; Defra, 2005), rainfall absorption and filtration (EA, 2003). Furthermore, they have the following benefits: they control the quantity of runoff; they improve the quality of runoff and enhance the nature conservation, landscape and amenity value of the site (EA, 2003; CIRIA, 2007). The hydrologic functions of storage, infiltration, and ground water recharge, in combination with the volume and frequency of discharges, are maintained through the use of integrated and distributed micro-scale retention and detention areas, reduction of impervious surfaces, and the lengthening of flow paths and runoff time (Coffman 2000). For example in Bristol Business Park, pervious pavement has been observed during and after a range of heavy and prolonged storms, and only negligible flows have been observed discharging into the swales, demonstrating, the attenuating attributes of the paving system (CIRIA, 2007).

SUDS have been applied in new developments in almost all developed countries for more than a decade, for example in the UK (Bettes, 1996; CIRIA, 2007), USA (USEPA; Stahre & Urbanos, 1990), Germany (Grotehusmann, *et al.*, 1993), Australia (Argue, & Pezzati, 1998) and Japan (Akagawa, *et al.*, 1997). To date SUDS have been widely used within new developments

and have provided a practical solution. However existing urban areas continue to create significant drainage and surface water problems. The term retrofit is employed when SUDS-type approaches are intended to replace and/or augment an existing drainage system in a developed catchment (Stovin & Swan, 2003).

The principle promoted by SUDS and retrofit has led to the increase usage of green roofs. Green roofs may be applicable in both new build and retrofit contexts. Villareal *et al.*, (2004) has demonstrated that the implementation of retrofit stormwater system at Augustenborg, Malmö, Sweden not only improved stormwater management in the area, but also improved the performance of the combined sewer system serving the surrounding area. The combined sewer system was disconnected from this impervious area and the SUDS structures were retrofitted with a range of green roofs, open channels and detention ponds; due to the availability of land, safety and public expectations. The system now drains wastewater almost exclusively; indeed, the volume of stormwater draining to the combined system is now negligible. This scheme included green roofs as part of a SUDS treatment train and it was found that green roofs are effective at lowering total runoff (Villareal *et al.*, 2004).

## 2.2 Green Roofs

A SUDS system implies three levels of stormwater management; from source control (individual premises), to a larger downstream site and regional control (CIRIA, 2007). Green roofs represent multi-beneficial structural components at a controlled source; where there is a building roof structure for drainage and an irrigation system that is covered with vegetation and growing media. Green roofs, or vegetated roofs, offer not only a significant opportunity to provide environmental sustainability, improve rainwater management, water and air quality. Above all, green roofs do not require any new space or land, but use waste urban areas, i.e. suitable rooftops, to restore green spaces within urban areas. The benefits of green roofs are site specific (Villarreal & Bengtsson, 2005).

In addition to their roles as SUDS structures, green roofs have also been suggested to provide various benefits including reduction of the urban heat island effect (Loder & Peck, 2004; Taube, 2005; Cabugos *et al.*, 2007), water and air purification (Moran *et al.*, 2004; MacMillan, 2004) and reduction in thermal and energy consumption (Whitelaw, 2005; Liu & Minor, 2005).

### 2.2.1 Green roof configurations

As a SUDS device, the function of green roofs is to reduce storm runoff at source. To have permeable green plants within impermeable urban areas might offer some benefits towards restoring a natural water cycle. The configurations of a green roof, which simply replicate the actual function of a hydrological mechanism include the following (Figure 2.4):

1. The slope
2. A vegetation/plant layer
3. A substrate layer and the depth
4. A drainage layer

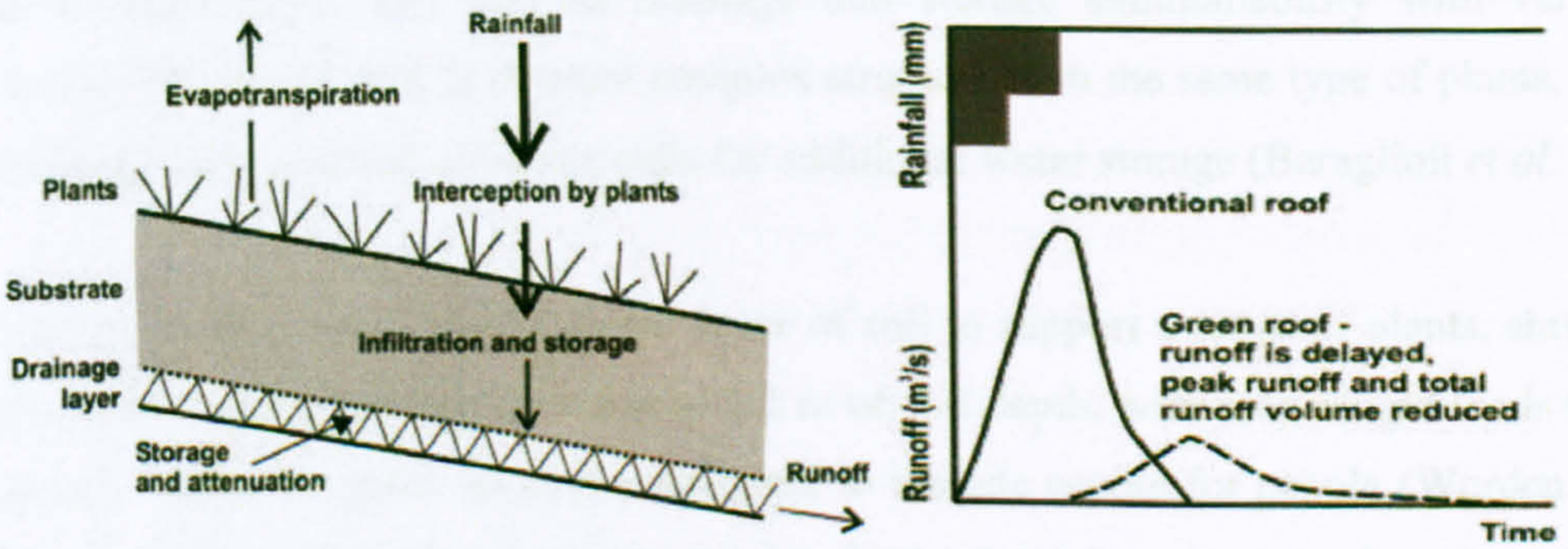


(a) (b)

Figure 2.4: (a) The hydrological mechanism of green roofs; (b) Theoretical impacts on runoff (Source: Stovin, *et al*., 2007)

Based on the normal hydrological mechanism (Figure 2.4 (a)), in vegetation layers, rainfall could be intercepted and with some loss due to evapotranspiration. The rainfall will then be infiltrated and stored in the substrate and the drainage layer of the green roofs to then become runoff (Liu, 2002; Bass & Baskaran, 2001). Green roofs could be expected to retain a percentage of the storm runoff, but there are many factors controlling the response of a specific roof to an individual storm event. It will depend on the various types of plant/vegetation and substrate, the depth of the substrate, the slope, the size of the green roofs (VanWoert, *et al*., 2005; Rowe, *et al*., 2003, 2006; Hutchinson *et al*., 2003), the storage availability, evapotranspiration, antecedent conditions (Seters, *et al*., 2007; Liu & Minor, 2005; Moran *et al*., 2005, 2004; MacMillan, 2004) and the characteristics of the rainfall event (Seters *et al*., 2007; Mentens, *et al*., 2006; LaBerge, *et al*., 2005). The saturated hydraulic conductivity, porosity and storage capacity/moisture retention of the growth media and transmissibility of the drainage

layer strongly influence hydrologic performance and the reliability of the design (Miller & Pyke, 1999; Mansell, 2003). The excess of stormwater runoff that has been filtered will be drained off with a temporal delay known as attenuation. Attenuation is the reduction of peak flow and increased duration of a flow event (CIRIA, 2007).

There are two main types of green roof; extensive and intensive. Extensive green roofs have a shallow soil layer (usually crushed recycled brick) with a depth of approximately 25 to 180 mm and a weight up to 73 kg/m$^2$. They will be planted directly with small plants (usually sedum). They are frequently designed to satisfy specific engineering (in term of weight and load) and performance goals (in term of landscape ecstatic or engineering) required for each specific area. The extensive green roof structure can be: 1) A simple extensive structure comprising substrate as a single layer that acts as drainage and storage simultaneously with very low water consuming plants; and 2) A more complex structure with the same type of plants, a substrate, a drainage layer and non-draining cells for additional water storage (Baraglioli *et al.* 2008).

Intensive green roofs have a deeper layer of soil to support a range of plants, shrubs and trees. They have approximately 200 mm to 1.2 m of soil depth, with roof weight loads from 390-800 kg/m$^2$. Intensive green roofs are designed to include access for people (Worden *et al.*, 2004). The intensive green roof structure can be: 1) An intensive structure that supports plants with more considerable water requirements; and 2) An intensive structure with a complementary rainwater storage arrangement made up of non-draining cells (Baraglioli *et al.* 2008).

The hydrological processes described above and illustrated in Figure 2.4 (b) show the expected runoff in green roofs for one single event as compared with a conventional roof. The figure emphasizes the contrasts of a conventional roof with a green roof. Runoff is expected to be delayed in time, and result in a reduction/retention in peak flow and total runoff volume. These rainfall runoff responses of green roofs are the main hydrological parameters that need to be explored before any modelling can be built.

## 2.3 Hydrological Performance from existing Green Roofs

Understanding the characteristics of hydrological performance from established green roofs around the world could provide information about how typical hydrological responses could occur in a certain design of vegetated roofs. There are several parameters/variables that affect the hydrological performances (as described in 2.2.1), which can be categorized in two main

parts; 1) within the roof itself; and 2) surrounding climate characteristics. In each green roof, three main entities need to be observed: the roof (type, size, slope and age), the substrate (type, depth and properties) and the vegetation (type, maturity), while climate characteristics include rainfall characteristics (volume, duration) and temperature (seasonal, wet, dry). This section will review the existing established roof designs and their performance in terms of their climate regime characteristics.

From the existing studies, many reports describe similar approaches to investigating the rainfall runoff responses. Monitoring of various small scale or full-scale green roof by Uhl & Schiedt, 2008; Fassmann, 2008; Getter *et al.*, 2007; Carter & Rasmussen, 2006; Rowe *et al.*, 2003, show that runoff retention is affected by roof slope, substrates depth, and vegetation type. Type of growing media, types of roof (Straet *et al.*, 2008; Carter & Jackson, 2006, Moran *et al.*, 2005), temperatures (Seters *et al.*, 2007; LaBerge *et al.*, 2005), rainfall characteristics (Straet *et al.*, 2008) and climate conditions (Uhl & Schiedt, 2008; Kohler, *et al.*, 2001) will also influence runoff responses. Some of these studies highlighted the importance of substrate moisture storage which influences the percentage of water retention in green roofs and is related to substrate properties and vegetation transpiration rates (Fassman *et al.*, 2008; Fassman, 2008; Rezaei & Jarret, 2006; Miller, 2004, 2003).

Before considering these performances reviews in detail, some observation on instrumentation methods will be presented below.

### 2.3.1 Instrumentation

In order to investigate the hydrological performance of green roofs, certain instruments are required during the monitoring period. The rainfall-runoff data relationship needs to be obtained by installing the rainfall and runoff monitoring instruments. Tipping bucket rain gauges have been used to gather and measure the precipitation (Seters *et al.*, 2007; Taylor, 2006; Carter & Rassmuss, 2005, 2006; Taylor, *et al.*, 2005; Macmillan, 2004; Hutchinson *et al.*, 2003; Mentens *et al.*, 2003; Rowe *et al.*, 2003). For runoff monitoring, several different approaches have been used. There are two basic types of approach: rate-based and volume-based measurement systems. Rate-based devices employ primary devices such as a shaped flume, weir or orifice; and secondary devices, such as a pressure transducer or gas bubbler are used to measure water depth (head) (Taylor, 2006). These approaches are chosen depending on

the size of the green roofs, full-scale or small-scale test beds, and the type of roof. All the data collected using these devices will be stored by a data logger.

### 2.3.1.1 Runoff measurement for full-scale roofs

In most studies, rate-based devices which employ both primary and secondary devices have been used to monitor runoff in full-scale green roofs. Rate-based systems need a specific and calibrated hydraulic device to establish the rate of flow from water depth at any given instant (Taylor, 2006). The full-scale Ecoroof studies at the Hamilton Apartments in Portland, USA, considered roof sizes ranging from 146 $m^2$ to 168.5 $m^2$. They used a small, $60^0$, V-trapezoidal Plasti-Fab flume and an American Sigma Model 950 bubbler-type flow meter to measure the water level in each flume (Hutchinson, 2003). Studies of another full-scale green roof at North Carolina University (NCU), USA, used roofs ranging from 27 $m^2$ to 180 $m^2$. A V-notch weir was used to measure flow from the green roof and the control roof; the control weir box was $30^0$ and the green roof was $23^0$. The smaller angle was selected for the green roof due to the smaller surface area of the green roof and, the resulting low flows expected (Moran *et al.*, 2004). To steady the water flow over the weir, each weir box was equipped with one baffle at the center point. Instead of a level sensor to measure the height of the water above the weir notch, a bubbler flow meter was used (Moran *et al.*, 2005).

However, Macmillan (2004) and their extended studies (Seters *et al.*, 2007) at York University, Toronto used a somewhat different approach and instruments. Runoff flows from both the greened (241 $m^2$) and control roof (131 $m^2$) were monitored continuously with two electromagnetic Hauser Promag 50 flow meters. The flow meters determine flow rates and volume via water conductivity. All of the monitoring devices at York University's studies have been networked to a single logger and network and communicates measured data via the internet. The internet connection also provides real-time measurements of monitoring activities (e.g. rainfall) and could be accessed from anywhere in the world. A similar method was applied in the City of Toronto, where a 460 $m^2$ roof drainage system was retrofitted. Runoffs from the three roof sections were directed into individual magnetic induction instruments (MAGmeters) flowmeters for measurement purposes. All sensors were connected to a data acquisition system, which can be remotely accessed via a modem, for continuous monitoring (Liu & Minor, 2005). The Vancouver Public Library (VPL) monitoring project has approximately 1850 $m^2$ of intensive green area and also applied a similar approach (Johnston *et al.*, 2004). They used two types of water meters on the system, one for measuring large flow and the other for measuring

low flow. The large flow meter was a 2" T-10 Meter which was calibrated to register 10 litres/pulse and the low flow meter was a 5/8" T-10 NSF61 Meter which was calibrated to register 1 litre/pulse. Both works depended on the water pressure on the nutating disk.

Wachter *et al.*, (2007) in their policy paper explored several types of instruments for green roof sites in the City of Seattle. The purpose of their research was a continuous hydrologic model development, for which a complete hydrologic mass balance monitoring of rainfall, evapotranspiration, soil storage and runoff needed to be measured. Therefore they needed to develop consistent monitoring methodologies across all the monitored rooftops. A wide range of flow rates were expected, so that accurate measurements of water inputs onto the roof and runoff from the roof must be made. A two stage flow monitoring system for each green roof was developed to provide accurate measurements of very low flow rates ($6.3 \times 10^{-6}$ $m^3/s$ or less) and higher flow rates (up to 0.013 $m^3/s$ per downspout). For two study sites, Zoomazium and Fire Station 10, they proposed a monitoring system consisting of a tipping bucket to accurately measure very low flow, which was then bypassed during higher flow which was then measured using a magmeter. For another site, a tipping bucket was used at low flow and at higher flow, water from a tipping bucket was discharged into an HS flume (type of flume designed to measure small flow rates with a high accuracy) where the level was measured with a pressure transducer and flow calculated using the flume's rating curve.

In Italy, Palla *et al.*, (2008) from University of Genoa transformed existing flat green roofs with three independent levels with a surface area of approximately 1000 $m^2$ into an experiment site; with the next new extension of a green roof of 350 $m^2$ in an area on the central part of the same roof with new solutions for substrate configuration. The experimental site has been fully equipped with on-site meteorological, hygrometric and flow rate measurement sensors. For the subsurface-flow monitoring, a rectangular channel equipped with a triangular weir and a level sensor was used. The channel was equipped with a small lateral orifice that was designed to obtain suitable flow rates compatible with the tipping bucket capacity. The triangular weir and the tipping bucket device were calibrated in the laboratory. To obtain a high accuracy within all the measurement ranges; the triangular weir calibration curve was employed if the effluent rates were higher than 0.4 l/s; while for effluent rates lower than 0.4 l/s the tipping bucket calibration curve was used.

### 2.3.1.2 Runoff Measurement for Test Rigs

Small scale test beds use different approaches depending on the aim of the studies. Runoff measurement for test beds can use either volume-based or rate-based systems. The principle of volume-based measurement is that the volume of runoff is a function of the depth of water in the collection instruments such as barrels, tanks or cisterns. Villarreal & Bengtsson (2005) used the simplest rate-based method to measure runoff volume using beakers at 1 minute intervals. During this experiment, they devised artificial rain events and sprinkled water over the 0.8 m x 1.93 m green plots manually collecting runoff using beakers. Straet *et al.*, (2008) also used the method by collecting the runoff using a metallic box containing pavements and substrate after the substrate became saturated, after 5 hours and 2 days saturation. They collected the runoff after simulating natural rain using fixed nozzles, a rain simulator on 600 x 600 mm test boxes was used to evaluate the infiltration behaviour of two types of greened porous pavement in comparison with open-jointed paving blocks. Moreover, Fassman (2008) also practiced the same method to collect runoff by using a measuring cup in 30s increments (typically measured every 1 to 3 mins) from three of 1m x 2m test plots. In this study, synthetic rainfall was also applied at a constant intensity to the test beds.

Studies carried out at Michigan State University (MSU), aimed to quantify the differences in water retention as a function of roof vegetation types, slope and substrate depths. They used a rate-based system, where TE525WS tipping bucket rain gauges were mounted under the drain of each of the fifteen platform section with overall dimensions of 2.44 m x 2.44 m to quantify stormwater runoff every five minutes (Rowe *et al.*, 2003; Getter *et al.*, (2007). They also used other tipping buckets to collect rainfall every 5 minutes, for 24 hours a day using a Campbell Scientific CR10X datalogger. However, they also reported on the reliability of data recorded from tipping buckets as diminished during freezing temperatures.

Carter & Rasmussen (2005) in their study at the University of Georgia tested 5.2m x 8.2m sized vegetated roof test plots. They aimed to build a large green roof test plot that would be monitored for its stormwater retention performance relative to a typical gravel roof and also modelled performance data. They used a rate-based approach using weirs, a Druck PDCR 1800 pressure transducer and linked to a Campbell Scientific CR23x data logger. The weir was designed using a two-stage riser setup. They used a 120cm x 30cm x 30cm stainless steel box containing the primary weir outlet, a 2.54cm open orifice located 15.24cm from the bottom of

the weir box. A secondary rectangular weir outlet was placed at the top of each weir box to accommodate the runoff during extreme events (Carter & Rasmussen, 2006).

In Pennsylvania State University, a study by DeNardo *et al.* (2003) was conducted on six 4.65m$^2$ small buildings; three green roofs and three conventional roofs. Each building had its own water collection system including a roof gutter, downspout and a 205 litres runoff barrel. A pressure transducer was fitted in each barrel and a signal sent to a central datalogger at 30 second intervals. All rain events were recorded by a weather station, which provided precipitation depths at one-hour intervals, and their interest focused on large events rather than continuous performance.

The City of Chicago Department of Environment was conducting an experiment under local conditions comparing green roofs versus conventional roofs to investigate stormwater runoff and temperature characteristics. The 3.34m$^2$ green roof test plots were designed using a specific concept design to collect data on continuous storm events and compare the results across different green roofs and conventional applications. Nine green roof sheds had a slot draining into an internal PVC gutter system that conveyed water to a 205 litre plastic rain barrel with a functional rain barrel capacity of 182 litres. Within the rain barrel was a pressure transducer powered by a 12-volt car battery; a logger recorded data every 6 minutes. Each roof was imbedded with temperature sensors while only seven of them were all equipped with stormwater instruments (LaBerge *et al.*, 2005).

### 2.3.1.3 Conclusion

In summary, the reviews from the case studies show that for different performance goals of green roofs, different approaches or systems could be used. The instruments were chosen depending on the practicality, cost, accuracy and reliability of the systems. It can be seen from Villarreal & Bengtsson (2005), Straet *et al.*, (2008) and Fassman (2008) that there were studies, where the runoff collection was made using beaker, box and cup for small test plots. Practically, the experiments provided interesting information regarding the hydrological performances of the test plots for a short term in response to a synthetic rainfall event. However, the manual use of a beaker as an instrument to collect runoff for bigger plots or for long term monitoring could not provide a practical accurate performance for the system. Moreover; this manual approach, like artificial rain, is only suitable for non-continuous monitoring.

The usage of tipping bucket occurred for both test beds (Rowe *et al.*, 2003) and full scales (Palla *et al.*, 2008). Using the tipping bucket, Rowe *et al.*, (2003) in their paper provided information on the accuracy of the tipping bucket approach for different flow rates (higher flow) but later on as described by Palla *et al.* (2008). The tipping bucket was used to collect low flow measurements, with a combination of channel weirs to measure the high flow for accuracy measurement ranges.

Whereas for the test plot used in LaBerge *et al.*,'s (2005) studies, may provide a simple yet accurate approach to collecting runoff measurements; a logger recorded data every 6 minutes using a pressure transducer as well as a similar approach used by Carter & Rasmussen (2006). The accuracy of Carter & Rasmussen (2006) might be better as they provided two stages of runoff collection; the primary weir outlet for normal flow event and a secondary rectangular weir outlet for extreme event. As reported by Carter & Rasmussen (2006) on their instruments, no storm event produced enough runoff to overflow into the second outlet. It may suggest that, their instrument design was not suitable for smaller plots and it was sufficiently sensitive to small rainfall events. Therefore, it can be concluded that, for a test plot to be designed, the use of a rain barrel and a pressure transducer could be a practical approach to measuring the volume of the runoff. However to provide measurement accuracy, to differ both low flow and high flow measurement should be considered. While for a full-scale green roof, rate-based which employs weir or orifice and the secondary devices such as pressure transducer could be a reliable instrument for use.

## 2.4 Performance Monitoring Results

Based on previous general studies reviews, the stormwater performance of green roofs are shown to depend on several factors, including the variation of storm event characteristics, roof configuration variables and planting and various climatic differences from different locations. Further in this section, it is interesting to see how the hydrological performances of water volume, peak flow reduction and attenuation can differ from or be similar to various roof characteristics and climatic variables regarding several case studies in detail. It will then be reviewed, initially for full-scale studies, and then for test beds:

### 2.4.1 Full-Scale Studies

Most full-scale studies have had a significant impact on water retention, reduced peak flows and delays in runoff. In North Carolina State University (NCSU), three green roofs were built: a flat green roof on the original rooftop of the storage building at Wayne Community College (WCC) in Goldsboro (17 months monitoring), a 3% pitch green roof at Neuseway Nature Centre in Kinston, NC (4 months monitoring) and a 7% green roof slope atop the Brown & Jones Architects, Inc building, Raleigh, NC (3 months monitoring). The soil depth, ranging from 50 to 100mm, was planted with typical sedum plants. Moran, *et al.*, (2004, 2005) reported that the averages of water retention on these three green roofs were 62% (from April 2003 to September 2004 – Figure 2.5), 63% (of part of July 2003, August 2003, November 2003 and December 2003) and 55% (from July 2004 to September 2004) respectively. The length of the study period with each different roof slopes had no greater impact on the overall average of water retention. The variation of retention as shown in Figure 2.5 (a) also depends on the amount of rainfall for each month, and a higher retention rate would be expected to occur with several dry days rather than a month with numerous rainfalls within a few consecutive days. This indicates that the substrate storage capacity plays an important role in water retention, where higher intensity storms will result in reduced retention rates.

Moran, *et al.*, (2004, 2005) also reported on peak flow reduction observed at the WCC green roof for events larger than 38 mm averaged 51% and increased for smaller storm events. An example of storm responses from WCC green roof can be observed in Figure 2.5 (b) for a 23 mm rainfall event on 7 April 2003 with a retention of 75%; the peak rainfall was 37mm/hr and the peak runoff was 3.7mm/hr with 90% reduction in peak flow. With averages of 36 to 44 mm/hr of peak rainfall, almost 90% of the rain events experienced delays in the onset the average runoff of 19 – 4.6 mm/hr (of the green roof) with 60% having a minimum of 30 minutes delays. The peak runoff from the green roofs was also reduced at WCC, Kinston and Raleigh by 87%, 87% and 57% respectively. This finding describes the ability of the green roof to attenuate almost all small storm events and is reduced for larger events.

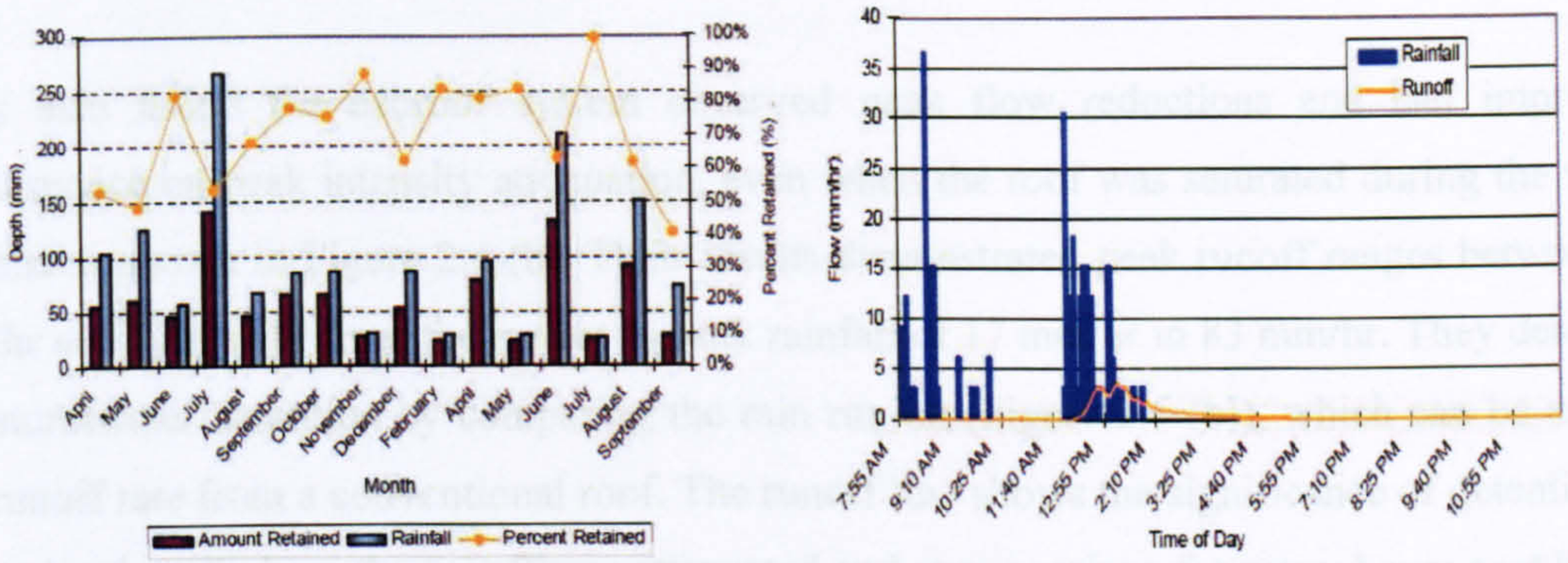


(a) (b)

Figure 2.5: (a) Monthly retention rates at WCC green roof from April 2003 to September 2004; (b) Peak flow reduction of green roof runoff at WCC green roof on April 7, 2003 (Source: Moran *et al.*, 2005)

Two ecoroofs for the stormwater management study were reported on by Hutchinson *et al.*, (2003) and were constructed in The City of Portland, Oregon, USA. Ecoroof is a combination of a green roof that supports vegetation and a cool roof that reflects thermal energy. Over 75 species of plants were installed on these 234m$^2$ and 243m$^2$ ecoroofs including varieties of sedum, numerous grasses and herbaceous plants. Hutchinson *et al.*, (2003) in their study of a 15 months monitoring period on the west ecoroof they reported that overall 69% of the total rainfall had been retained for the 100 to 130 mm growing medium depth. The retention over two periods within 15 months of monitoring has been compared; i) January to March 2002 with an average of 20 - 30% retention, and ii) January to March 2003 where retention was 59% and for most warm weather storms retention was almost 100% (Figure 2.6 (a)). Both ecoroofs had shown various amounts of stormwater retention relative to seasonal influences. Rainfall patterns within these two years (of the same 3 months periods) were different wherein 2002 there was a relatively even rainfall distribution while in 2003 there was a greater variability of rainfall (with long dry periods between storms). They concluded that the long dry periods in 2003 may account for greater evapotranspiration and increased water holding capacity in the ecoroofs. Hutchinson *et al.*, (2003) also reported that the potential evapotranspiration due to temperature differences may account for higher retention rates, where a further potential factor contributing to high retention was the maturity of the vegetation. As the retention performance appears to be increasing with time (from the same period of January to March in 2002 to the same period in 2003), it might also be associated with a few factors such as rainfall distribution, intensity pattern, air temperature, the maturity of vegetation/substrate ecosystem and influences.

They also found the ecoroof system observed peak flow reductions and had impressive performance on peak intensity attenuation, even when the roof was saturated during the winter months as shown in Figure 2.6 (b). Their results demonstrated peak runoff ranges between 3.3 mm/hr and 52 mm/hr from the ranges in peak rainfall of 17 mm/hr to 83 mm/hr. They described the stormwater detention by comparing the rain run-on (Figure 2.6 (b)), which can be used as the runoff rate from a conventional roof. The runoff line shows the significance of detention for a vegetated roof where the runoff was attenuated and may continue for many hours past the last recorded rain. They concluded that long dry periods may account for greater evapotranspiration and increased water holding capacity, and the system can still attenuate the flow even when the substrate was saturated.

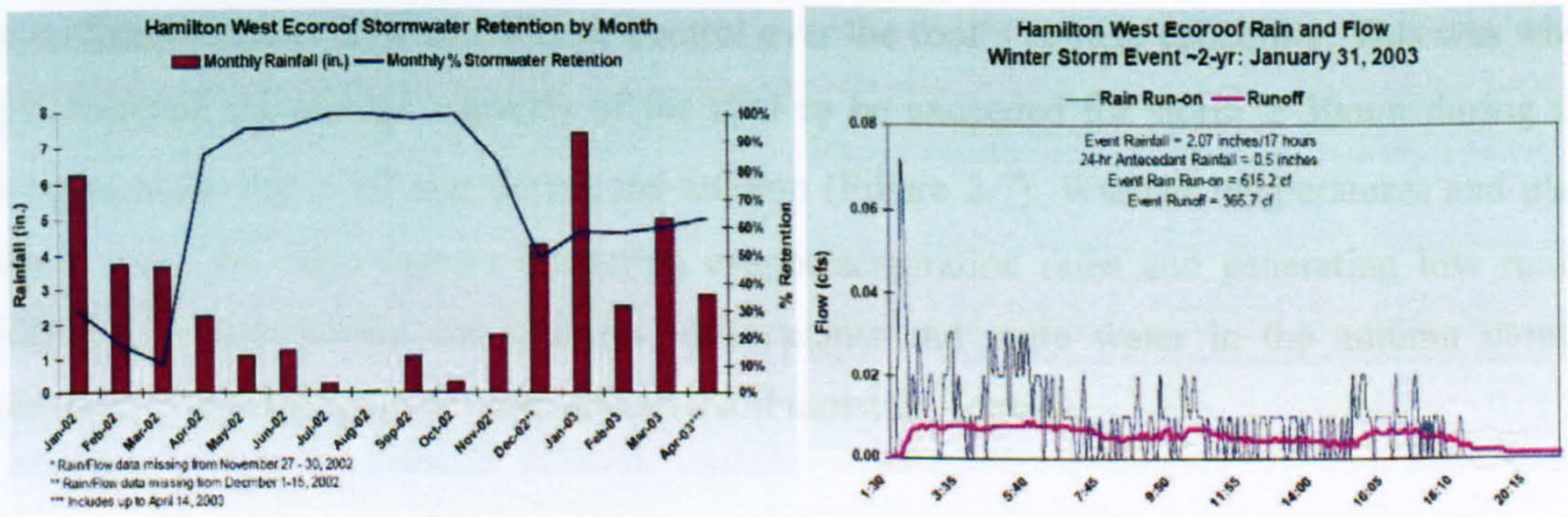


(a) (b)

Figure 2.6: (a) Hamilton West Ecoroof retention by month; (b) Example of low intensity, high volume winter storm (Source: Hutchinson, 2003)

The MacMillan (2004) study from May to November 2003 on the quality and quantity of York University rooftop garden in Toronto concluded that the 10% slope and 140 mm soil depth with wildflowers garden reduces the total runoff volume by approximately 55%. They experienced 800 mm of annual total rainfall. During the spring/summer months, the garden reduced runoff volume by 76% and by 37% in the autumn. They suggested that the roof performance was affected by seasonality and the continuous saturation of the garden soils during autumn months decreased storage capability. Their observations of peak flow shows that the reductions decreased with larger storm events (Table 2.1) with the ranges of runoff lag time from 4 to 88% during the spring/summer months and 3 to 18% during autumn months. Lag time is the time from the centre of a mass of rainfall to the peak of the hydrograph. They also reported that this

lag time variable is a direct result of antecedent conditions, event precipitation volumes and irrigation contributions.

Table 2.1: Peak flow reduction for storm events between 10 mm to > 40 mm (Source: Macmillan, 2004)

| Rainfall ranges (mm) | Average peak flow reduction (%) |
|---|---|
| 10 – 19 | 85 |
| 20 – 29 | 82 |
| 30 – 39 | 68 |
| > or equal to 40 | 46 |

They concluded that antecedent conditions within different seasons with these variable factors; soil moisture, variable rainfall intensity, temperatures and evaporation rates, significantly affect the roof performance in terms of their control over the roof's storage capability. This was when they observed the storage capacity of the roof to be exceeded for storm ≥ 30mm during the spring/summer and ≥ 20 mm during the autumn (Figure 2.7). Warmer temperatures and plant growth were the main factors impacting evapotranspiration rates and generating low runoff coefficients while cooler temperatures, dead plants and more water in the autumn months decreased evapotranspiration rates and also soil moisture content.

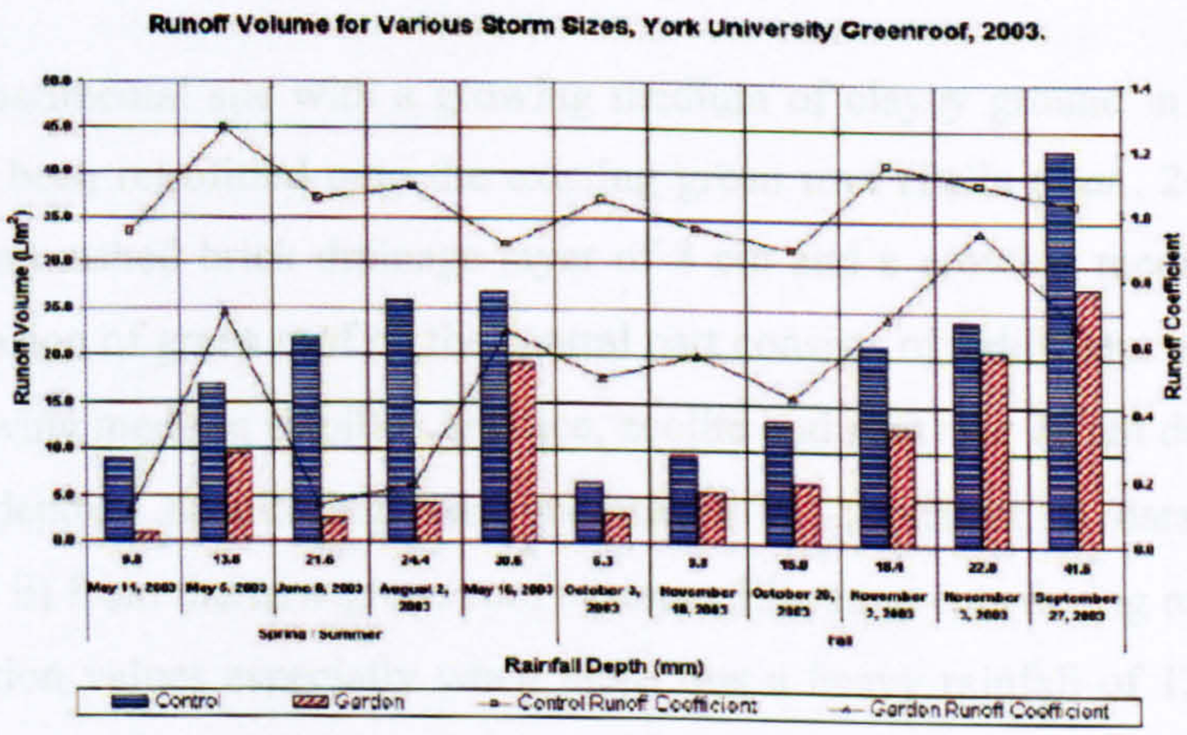


Figure 2.7: Event performance for various sized storms; chart is arranged by events from smallest to largest and by season (Source: Macmillan, 2004)

Their extended study (Seters *et al.*, 2007) monitored 154 runoff events from May to November 2003, June to November 2004 and April to August 2005, and showed 54% retention in 2003, while in 2004 and 2005 approximately 75% of precipitation was retained. Summer events were

between 78 and 85% and 39 and 64 % for spring and autumn. They also concluded that the key factors explaining monthly and event-by-event variations in green roof retention rates, lag times variables and storage capacity performance were inclusive of rainfall volumes, evapotranspiration rates, antecedent moisture content, irrigation distribution and temperature.

Liu & Minor (2005) also discovered a 57% annual reduction in runoff volume from two green roofs in the City of Toronto. Two extensive green roofs contained 75 to 100 mm depth of lightweight growing medium with a variety of vegetation. Both systems contained the same components, but differed in materials and designs. The Green Roof System G has 100 mm of lightweight growing medium with small light-coloured granules consisting of a composite semi-rigid polymeric drainage and filter mat and a root-anchoring mat. However, the other roof, called Green Roof System S is made of expanded polystyrene drainage panels and a geotextile filter fabric with a lightweight dark-coloured growing medium of a depth of 75 mm containing porous ceramic granules. A maximum reduction of 100% (on an event by event basis) occurred during summer months for certain rain events that totalled less than 15 mm. However during wet conditions, the Roof G reduced the volume consistently while the Roof S media became saturated, the response rates behaved similarly to the control roof. Calculated peak flow rate reductions ranged from 25% to 60% and showed a lag time (detention time) of 20 to 40 minutes.

A green roof experimental site with a growing medium of clayey ground in the University of Genoa, Italy has been retrofitted onto the existing green roof (Palla *et al.*, 2008). The green roof consists of a crushed brick drainage layer of 8 cm and a growing medium of 35 cm. A further new extension of green roof on the central part consists of a different configuration; with a mixture of growing medium (lapillus, pumice, zeolite and peat) for 20 cm depth and 15 cm of drainage layer depth. Monitoring was undertaken in 2 phases; i) data collection from impervious roof; ii) from the new green roof system. Eleven events during monitoring showed significant retention values especially when there was a heavy rainfall of 138.2 mm that still retained rainfall volumes at 10% with an average of 85% retention. The peak flow reduction with an average value of 97% and runoff delay for a heavy rainfall event of 148 min. They reported on the delay values observed during their monitoring as relevant to the view of usual concentration times in urban catchments. Furthermore, a green roof system has the ability to significantly reduce the runoff generation in Mediterranean regions in term of runoff volume reduction, peak attenuation and increase of delay time.

## 2.4.2 Small-Scale Test Plot Studies

Green roof test plots are the best way to investigate critical technologies that can be applied to large commercial buildings with minimal additional costs (Lando, 2004). Following are several studies that demonstrated the performance of stormwater in green roof test plots.

Pennsylvania State University (DeNardo *et al*., 2003) undertook a study of an 89 mm green roof and investigated it for its stormwater retention and detention capabilities. The green roof system with a 1:12 sloped roof consisted of porous medium substrate with a 12mm thick Enka-drainage layer, 25 mm of Porous Expanded Polypropylene (PEPP) and *Sedum spurium* vegetation. Measured porosities for the medium were 55% with a field capacity of 34% ranging from a 17% to 28.5% for PEPP formulation porosity. These combination layers of green roof had a saturated hydraulic conductivity of 11mm/s with a maximum retention of 30 mm (34%). This maximum retention is assumed to be reached due to evapotranspiration; all available water from the media has been transpired by the plants and the remaining moisture was removed by evaporation. The variation retention during October and November of 2002 were between 19 and 98%. Figure 2.8 (a) demonstrates the response of the green roof system with a retention of 4.6 mm and a 4hr delay at the start of runoff. Figure 2.8 (b) demonstrated the ability of the green roof to attenuate the peak flow, from 6.6 mm/hr to a runoff rate of 4.1mm/hr with a 38% reduction. The average of green roof's delaying the start of runoff, when compared to the rainfall, is 5.7 hours with an average delay of 45% from the seven storms evaluated. Average peak runoff rate was reduced to 2.4 mm/hr from the peak rainfall rate of 4.3 mm/hr with peak runoff delayed on average by 2 hours.

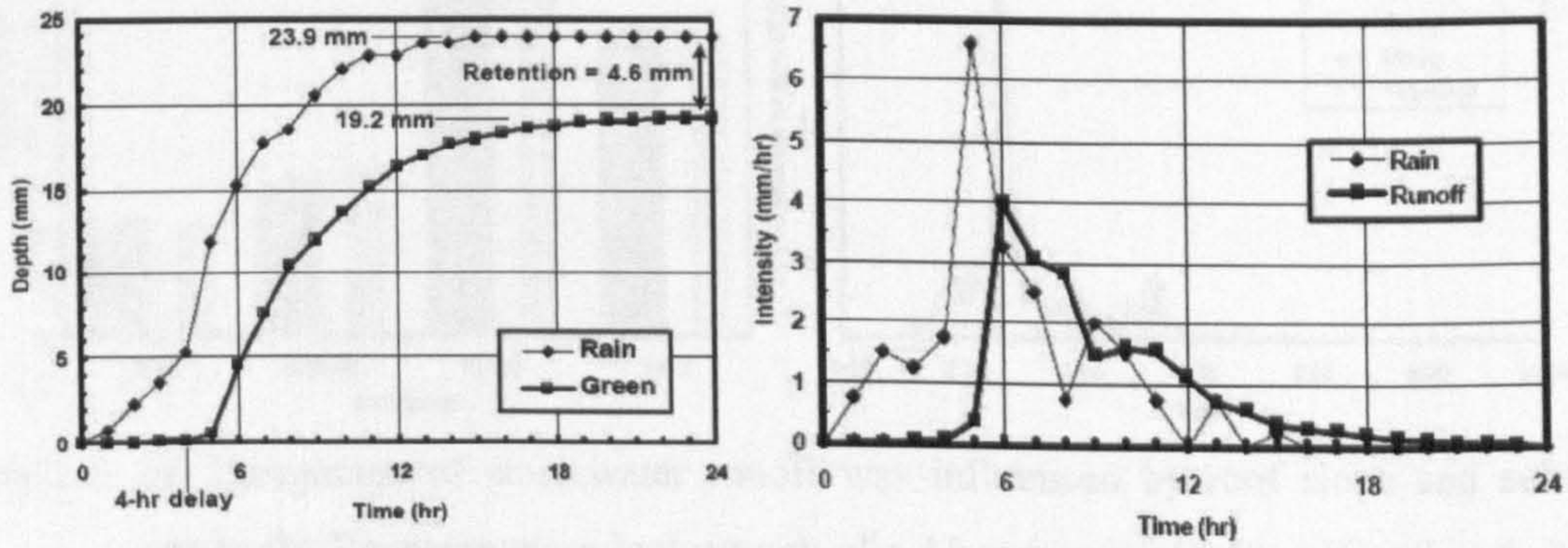


(a) (b)

Figure 2.8: (a) Rainfall and green roof response for the October 25, 2002 storm; and (b) Rainfall intensity and green roof runoff rate (Source: DeNardo *et al*.. 2003)

Rowe, *et al.*, (2003) from Michigan State University examined runoff performance with respect to green roof slope, substrate depth and vegetation. Using the same size of test plot roofs, 2.44 m x 2.44 m, 12 roofs for slope and depth studies and 3 roofs for vegetation studies were studied. As shown in Figure 2.9 (a), three different substrate depths (2.5 cm, 4 cm and 6 cm) were compared with two different slopes (2% and 6.5%) to show the influence of roof slope and substrate depth on the percentage of stormwater runoff. In this study a rainfall event was defined by two rainfalls being separated by six hours or more, and each individual rainfall event was defined as light (< 2 mm/hr), medium (2 to 4 mm/hr) or heavy (> 4 mm/hr). While for vegetation treatment the comparison was between sedum, substrate only and gravel roofs. Overall, the retained rainfall ranged from 74% (2% slope and 4cm substrate), to 69% (6.5% slope and 4cm substrate). The test plot that contained 100% of sedum cover retained 66% of the rainfall compared to 63% of the test plot with substrate only and 25% for gravel roofs (Figure 2.9 (b)). At a 2% slope, 40 mm and 25 mm depths retained 74% and 70% respectively, whilst at a 6.5% slope, the water retained was 72% and 69% at depths of 60 mm and 40 mm, respectively. Logically, a greater amount of water would be retained by a deeper substrate with more vegetation cover. The performance from a rainfall event using a constant 40 mm depth but at a different slope shows that the 6.5% slope platforms produced more runoff than the 2% slope. They concluded that a shallower substrate depth and a steeper roof slope resulted in greater runoff, furthermore the substrate moisture content prior to a rainfall was found to influence the retention capacity of the roof (Rowe, *et al.*, 2003).

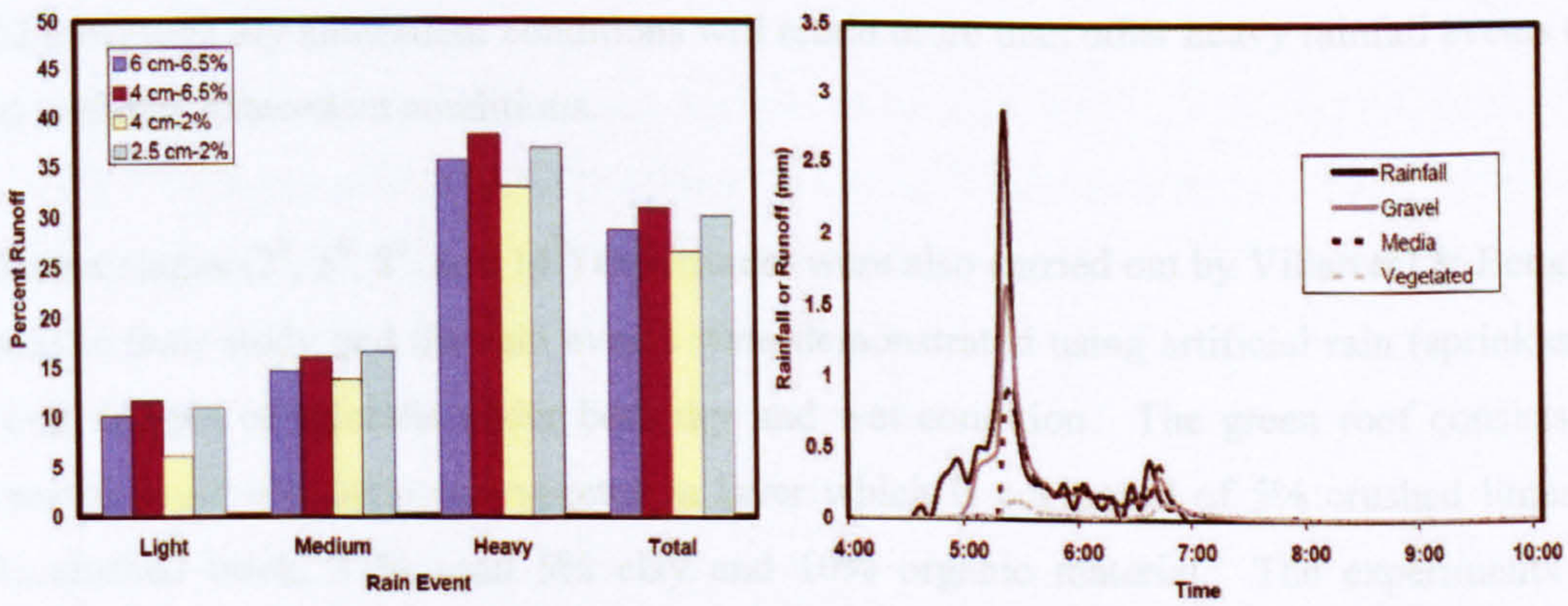


Figure 2.9: (a) Percentage of stormwater runoff was influenced by roof slope and substrate depth; (b) Representative hydrograph of a 10 mm rainfall event (October 4, 2002); (Source: Rowe, *et al.*, 2003)

Another extended study in Michigan State University by Getter *et al.*, (2007) using the same 12 roof plots as Rowe *et al.*, (2003) analysed runoff performances at four different slopes 2%, 7%, 15% and 25%. It found that the average retention value is 80.8% where the least retention is at the 25% slope (76.4%) and the greatest at the 2% slope (85.6%) where it was demonstrated that as the slope increased, the retention values decreased. Retention is also highest for light rain events (94.2%) and lowest for heavy rain events (63.3%) demonstrating the limited storage capacity of the substrate; once it is saturated by precipitation run off. Runoff was also found to be delayed and distributed over a long period of time with final runoff lasting 4 h 20 min (light event), 10 hr 45 min (medium event) and 13 hr 45 min (heavy event). The initial runoff delay for these rain events is minimal for all slopes, perhaps due to high rainfall intensity or the moisture conditions of the substrate. In addition, they concluded that the roof ecosystem was also important to quantify the runoff, where greater maturity and factors like roof age may affect the hydraulic conductivity of the substrate in terms of greater values for porosity, free airspace, organic matter, and water holding capacity relative to the initial substrate. They also compared the results of substrate physical properties – water holding capacity, organic matter, pore space and free airspace for the substrate between initial substrate (prior to planting) and mature substrate (after 5 years). They demonstrated that this comparison shows that the mature substrate exhibited greater values for porosity, free airspace, organic matter and water holding capacity relative to the initial substrate's physical properties; it is of increased likelihood that this will also affect retention volume. Their findings on antecedent moisture conditions show considerable deviation for varying storm volumes; where the results for heavy rainfall event (42.2 mm) with dry antecedent conditions will retain more than other heavy rainfall events (28.7 mm) with wet antecedent conditions.

Different slopes ($2^0$, $5^0$, $8^0$, and $14^0$) experiment were also carried out by Villarreal & Bengtsson (2005) in their study and the rain events were demonstrated using artificial rain (sprinkler) for several designs of rainfalls under both dry and wet condition. The green roof consists of a geotextile layer with 4cm soil-vegetation layer which is composed of 5% crushed limestone, 43% crushed brick, 37% sand 5% clay and 10% organic material. The experiments were undertaken both on dry days (7 days without precipitation) and with wet initial conditions (i.e. at field capacity). They also conducted several experiments regarding dry initial conditions with constant rainfall intensity in order to determine the amount of initial loss when they found between only 6 and 12 mm of rain were necessary to initiate runoff. According to their experiments, the slope does influence retention volumes for dry initial volumes. With a uniform

intensity rainfall of 0.4 mm/min, 62%, 43%, and 39% of the total rainfall was retained on the green roofs with slopes of $2^0$, $8^0$, and $14^0$, respectively (Table 2.2).

Table 2.2: Retained precipitation – dry initial conditions (values in parentheses are % with respect to P) (Source: Villarreal & Bengtsson, 2005)

| Rain (mm/min) | Duration (min) | Total precipitation, *P* (mm) | Rain to start runoff (mm) | Total runoff | Retention (mm) |
|---|---|---|---|---|---|
| Slope $2^0$ | | | | | |
| 0.4 | 60 | 24 | 12 | 9.2 (38%) | 14.8 (62%) |
| 0.8 | 30 | 24 | 10 | 11.0 (46%) | 13.0 (54%) |
| 1.3 | 30 | 39 | 9 | 31.0 (79%) | 8.0 (21%) |
| Slope $8^0$ | | | | | |
| 0.4 | 50 | 20 | 8 | 11.4 (57%) | 8.6 (43%) |
| 0.8 | 30 | 24 | 7 | 16.7 (70%) | 7.3 (30%) |
| Slope $14^0$ | | | | | |
| 0.4 | 60 | 24 | 8 | 14.6 (61%) | 9.4 (39%) |
| 0.8 | 60 | 48 | 7 | 38 (79%) | 10.0 (21%) |
| 1.3 | 60 | 78 | 6 | 70.0 (90%) | 8.0 (10%) |

The corresponding retentions for a 0.8 mm/min rainfall were 54%, 30%, and 21%; and for a 1.3 mm/min rain, 21% and 10% were retained for $2^0$ and $14^0$ slopes. They concluded that for a specific rainfall event, retention diminishes as the slope increases, and for a specific slope, retention is greatest for low intensity events; however, roof slope had no effect on the shape of direct runoff hydrograph (peak flows, stormwater volumes) although it does influence retention volume for dry initial conditions of retention and detention.

Two test plots for Carter & Rasmussen (2005) were retrofitted onto an existing flat (<2% slope) roof in the University of Georgia. They showed that for 32 storm events recorded, the retention of rainfall volume ranged from 39 to 100% based on separated events. For storm events less than 12.7 mm, more than 90% of the rainfall volume was retained with a 4.1 mm event 100% retained. For a larger storm event of 54 mm, the stormwater was retained at 39%. They concluded that with only a thin layer a green roof system can still accommodate retention of almost 100% for most frequent smaller storm events, but as it reaches saturation the retention performance looks relatively similar to a black roof. This indicates that the roof operates as a retention instrument for a particular water volume rather than detaining and slowly releasing significant amounts of stormwater after percolation through the soil, even for small storm events. They continued their studies (Carter & Rasmussen, 2006) and their green roof storm hydrographs consistently showed similar retention/abstraction/characteristics compared to the

black roof, which produced greater runoff volume during the same initial period (Figure 2.10 (a)). Most stormwater retention occurs at the beginning of storms as the growing media absorbs the initial rainfall until it reaches saturation (Table 2.3). They concluded that these results had provided an indication that the roof can essentially operates as a retention instrument rather than detaining and slowly releasing the water.

Table 2.3: Water retention summary (Source: Carter & Rasmussen, 2006)

| Storms (mm) | Water retention (%) |
|---|---|
| Small storms (< 25.4mm) | Nearly 88 |
| Medium storms (25.4 – 76.2 mm) | More than 54 |
| Large storms (> 76.2 mm) | Nearly 48 |

Another performance parameters observed was peak discharge rate, which tends to increase with the increasing depth of precipitation, although it is not always the case (Figure 2.10 (b)) when some larger storms have lower peak discharge rates than intermediate storms. They also reported on the increase in runoff ratio as precipitation depth increases; with the conclusion that the increase of runoff ratio could be attributed to increased water content within the soil medium, resulting in the increased runoff rates. The ability of the green roof to detain, or delay the runoff was reported; as only 5% (two storms) did not delay the peak flow, while most were delayed (57%) between 0 and 10 minutes. The longest delay was approximately two hours. The delays varied from storm to storm due to variation in precipitation intensity as well as antecedent soil moisture conditions, leading to complex runoff behaviour (Carter & Rasmussen, 2006). They also concluded that seasonal and temperature factors play a large role in retention; where it can affect the amount of soil moisture because of evapotranspiration. Furthermore, the timing and storm duration also affects the retention performance, in urbanized areas, even if the total storm volume is intense it can still produce substantial runoff using a green roof.

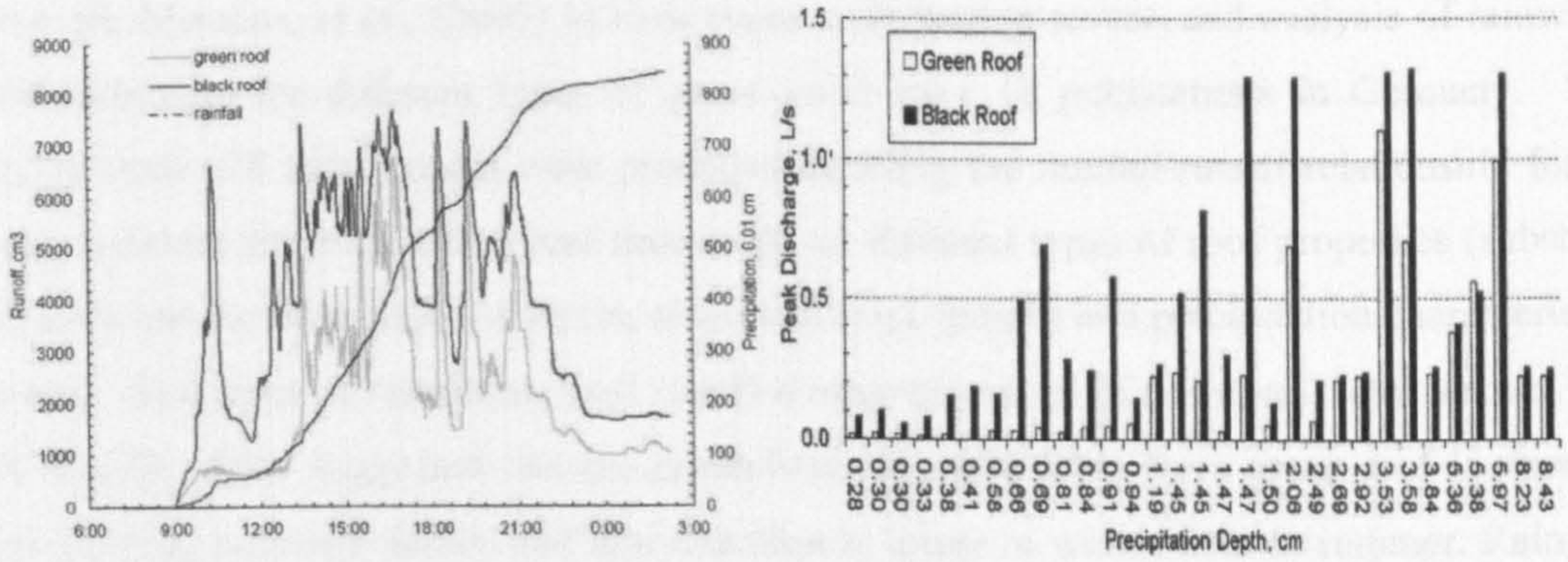


(a) (b)

Figure 2.10: (a) Cumulative precipitation depth and runoff volumes from plots for a storm on September 27, 2004; (b) Green roof and black roof peak discharge rates as a function of precipitation depth (Source: Carter & Rasmussen, 2006)

Fassman, (2008) in a study from the University of Auckland, New Zealand carried out an investigation into the influence of bed depth, roof slope, vegetation, and initial moisture content on the runoff flow rate. It mainly researched the effects of roof slopes (5° and 15°) and substrate depths (100 mm, 150 mm and 200 mm) on hydrological performances. The runoff was measured every 1 to 3 minutes during the test after synthetic rainfall was applied at constant intensity to the beds. For slope comparison, their results demonstrated that increasing the slope will decrease the runoff rate. Moreover, for substrate depths comparison, regardless of slope, runoff rates ranged between 6 and 20% for a short duration event. The 200 mm bed depth had decreased runoff of 55% and 45% compared to the 100 mm depth for the 5° and 15° slopes. The 5° slope and shallower systems produced similar runoff volume to the 15° and 200 mm system for the same rainfall. This study also demonstrated that they can increase the available storage by doubling the bed depth therefore decreasing runoff rate. The increasing of the roof slope from 5° to 15° showed no effect on peak flow. The runoff was generated slightly faster by the 200mm bed at 15° slope compared to the 5° slope, but less than for the 100mm. Initial moisture condition (IMC) is the volume after initial runoff occurs after the onset of rainfall; and the study reported that the ranges of initial moisture condition for vegetated roofs were 22-31% by mass for 5° and 15-26% for 15° tests. For lag time, they reported having insufficient data to interpret the effects of timing as the equipment enabled testing only at a very high intensity. The roof plots can still effectively reduce runoff up to 70 to 90% during larger storms or in near saturated conditions for all tested conditions.

Above all; Mentens, *et al.*, (2005) in their paper undertook a review and analysis of rainwater runoff reduction for different types of green roofs over 18 publications in Germany. The analyses from 628 data records were produced detailing the rainfall-runoff relationship for an annual, seasonal and rainstorm event time scale on different types of roof properties (substrate type, substrate depth, number of layers, slope and slope length) and precipitation characteristics (intensity, time span of rainstorm, total runoff during time span of rainstorm, total amount and peak runoff). They suggested that the rainfall-runoff relationship for a green roof is strongly determined by substrate depths and that retention is lower in winter than in summer. Rainfall-retention capability on a yearly basis may range from 75% for intensive green roofs (median substrate depth: 150 mm) to 45% for extensive roofs (median substrate depth: 100 mm) (Table 2.4).

Table 2.4: Substrate layer depth (mm) and runoff (% of total annual precipitation) characteristics of the literature data set on an annual level (Source: Mentens *et al.*, 2005)

| | Intensive green roof (n=11) | Extensive green roof (n=121) | Gravel-covered roof (n=8) | Non-greened roof (n=5) |
|---|---|---|---|---|
| Substrate layer Depth (mm) | | | | |
| Minimum | 150 | 30 | 50 | / |
| Maximum | 350 | 140 | 50 | / |
| Median | 150 | 100 | 50 | / |
| Average | 210 | 100 | 50 | / |
| Runoff (%) | | | | |
| Minimum | 15 | 19 | 68 | 62 |
| Maximum | 35 | 73 | 86 | 91 |
| Median | 25 | 55 | 75 | 85 |
| Average | 25 | 50 | 76 | 81 |

Runoff (percentage) was significantly different between all seasons; 30% for warm season, 51% for the cool and 67% for the cold seasons. Annual analysis has reduced the retention where higher annual precipitations interfere with a higher amount of extreme events, whereas seasonal variations in the rainfall play a clear role in the retention of runoff. The differences in results may be due to evapotranspiration and rainfall distribution. They also reviewed several ranges of thickness and different slopes that had been used in Germany ranging between 0 and 500 mm and $0^0$ and $84^0$, respectively (Table 2.5). Overall, the reviews and analyses determined that green roof performance improved storm water management in the area, and also the performance of the combined sewer system that served the surrounding area. However, green

roofing alone can never fully solve the urban runoff problem as it needs to be combined with other runoff reduction structures.

Monitoring results in Germany have characterized the rainfall-runoff processes from 18 green roof constructions with different slopes and layer types (Uhl & Schiedt, 2008). Standard materials selected for monitoring were gravel, roof tiles and proofing membrane; and were differentiated by the following types: rectangular roof segments, triangular segments, slopes of 0%, 1.7% and 26.8%, extensive and intensive vegetation, 1- layer and 2-layers system, 5 – 35cm in height. The analysis for this study was undertaken based on runoff coefficient. The runoff coefficient is defined as the ratio between the sums of runoff and rainfall. The seasonal analysis clarifies the influence of different meteorological conditions, where higher runoff coefficients in cool and cold seasons were due to lower evapotranspiration rates while evapotranspiration rates must have been sufficient for a quick drying of the substrates resulting in high retention capacities. The annual runoff coefficients also depend on the seasonal distribution of rainfall and evapotranspiration where annual runoffs are relatively low, due to the fact that 2/3 of the precipitation during the 48 months of observation fell in the summer. They also concluded that storage capacity is a linear function of pore volume and depth of the substrate and the drainage layer where after every rainfall high evapotranspiration rates lead to a fast attainment of high or full storage capacities of roofs. In cold seasons, low evapotranspiration has an effect on low retention because of antecedent rainfalls. They also report that runoff production is influenced by the water content at the beginning of a new rainfall event; a thin layer of construction can still reduce peak flow substantially. Therefore they also agreed that soil moisture and retention is mainly influenced by evapotranspiration and the sequence of rainy and dry periods.

Table 2.5: Summary with some basic characteristics of reviewed publications on water retention from green roofs (Source: Mentens *et al.*, 2005)

| Author (year) | No. of roofs | Substrate (mm) | Roof slope (%) | Location | Yearly Precipitation | No. of years | Seasonal Data | Rainstorm intensity ($mmh^{-1}$) |
|---|---|---|---|---|---|---|---|---|
| Kaufmann (1999) | 8 | 100 | 2 | Burgdorf | 920-1347 | 4 | Yes | 80-130 |
| Kolb (1987) | 3 | 60-120 | 0 | n.r | - | - | - | 208-222 |
| Kolb (1998) | 13 | 0-500 | 0-58 | n.r | - | - | - | 11-350 |
| Kolb (1999a) | 12 | 100 | 2-84 | n.r | - | - | - | 150-300 |
| Kolb (1999b) | 36 | 90 | 2-84 | n.r | - | - | - | 100-300 |
| Kolb (2002) | 9 | 0-100 | 2 | n.r | - | - | - | 200-300 |
| Kolb (2003) | 6 | 20-100 | 27 | n.r | - | - | - | 300 |
| Liesecke (1989) | 8 | 30-180 | 3 | Hannover | 644 | 3 | - | 27.8 |
| Liesecke (1993) | 24 | 70-180 | 2 | Hannover | 554-628 | 5 | Yes | - |
| Liesecke (1994) | 7 | 0-120 | 2 | n.r | - | - | - | 300 |
| Liesecke (1998) | 18 | 0-380 | 2 | Hannover | 644 | - | Yes | 300 |
| Liesecke (1999) | 8 | 0-120 | 0-9 | Tornesch | 712-918 | 3 | - | 300 |
| Liesecke (2002) | 10 | 100 | 2 | Hannover | 533-657 | 4 | Yes | - |
| Mann (2000) | 2 | 150 | 2-27 | Marsberg and | - | - | - | - |
| Mann (2001) | 1 | 100 | 2 | Heilbron | - | - | - | - |
| Mann (2002) | 16 | 100 | 0-2 | Tubingen | 587-930 | - | - | - |
| Mann and Henneberg (1998) | 7 | 0-350 | 0-27 | Throughout Germany | - | - | - | - |
| Mann *et al.* (2000) | 22 | 0-350 | 0-27 | Unknown Krauchenwies-Goggingen | 670 | 1 | Yes | - |

## 2.4.3 Evapotranspiration (ET)

In Section 2.4.1 and 2.4.2, it was demonstrated that the hydrological parameters, as discussed in most green roof studies, can be divided into two main categories; the retention and detention of stormwater management. From the reviews, one key important variable that controlled the retention performance (in providing available storage) for a green roof is evapotranspiration. Evapotranspiration consists of evaporation and transpiration processes and these two main activities relate to the two main parts of green roof; substrate and vegetation. Therefore, in this section we will review the findings of evapotranspiration studies performed on green roofs.

Fassman & Simcock (2008) reported on their development of a new extensive green roof substrate that was suitable for the Auckland, New Zealand climate for new and retrofit construction. In this research, their objectives were to dictate a minimum level of stormwater control while minimizing structural loading to maintain suitability for retrofit. Physical properties work refers to the German FLL *Guidelines for the Planning, Execution, and Upkeep of Green-Roof Sites* (FLL, 2002) procedure with a setting of maximum target; substrate dry bulk density at $\leq 800\ kgm^{-3}$, maximum system weight at $\leq 100\ kgm^{-2}$, and substrate depth at $\leq 100$ mm. A range of potential aggregates and potential organic materials were reviewed and a small number of mixtures tested. Figure 2.11 shows the interpretation breakdown in terms of plant survival, to keep plants alive in a thin extensive green roof, frequent rainfall events are needed. Whilst the 100 mm substrate will likely sustain plants for over a week before reaching stress

point; greater depth will add potential storage. Only three mixtures were selected as they meet the criteria of the field implementation objectives. However after laboratory predictions, based on their physical properties and field performance, only one type of substrate mix was selected. The Field Zeolite is a substrate that consists of 50% pumice (4-10 mm), 30% zeolite (1-8 mm) and 20% composted softwood bark fines. The substrate's physical properties has a 856 kg/m$^2$ dry bulk density, 50% water holding capacity, and 0.07 mm/s permeability (determined according to FLL methodology). Hence, this review describes the possible way of understanding the substrate properties under FLL procedures for our study; therefore the storage availability of the green roof should be investigated.

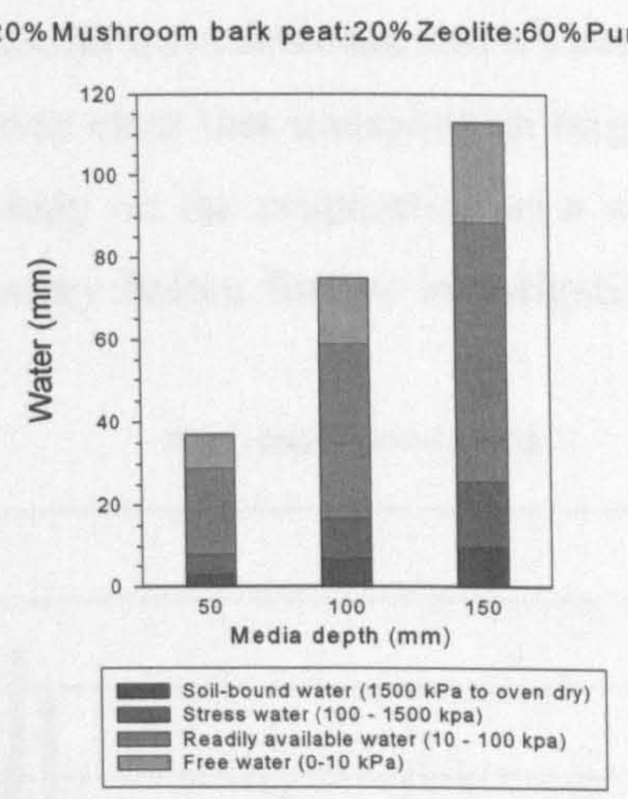


Figure 2.11: Water storage in an extensive green roof substrate (Source: Fassman & Simcock, 2008)

Following the substrate establishment, in their extended green roof study in Fassman *et al.*, (2008), the investigation of the evapotranspiration rates for their green roofs substrate was discussed. In this study, two types of vegetation were analysed; *Sedum mexicanum* (Mexican Stonecrop) and the New Zealand (NZ) *Disphyma australe* (NZ Ice Plant) in their Field Zeolite substrate, to determine their daily and hourly ET rates under unstressed and drought conditions. Seven plastic trays (0.26 m x 0.26 m x 0.12 m) were placed upon PF-1 Bench Platform single beam load cells. An E1310 TCP/IP Network Programmable Indicator was connected to the bench platforms. *Sedum mexicanum* (Mexican Stonecrop) was planted on 3 trays and a further 3 trays were planted with the NZ *Disphyma australe* (NZ Ice Plant), and the remaining tray was not planted to provide the evaporation (E) measurement. Using the load cells, the hourly tray mass was measured and recorded. Water loss by ET is represented by the change in mass for planted trays and E for the bare substrate. The difference between measure ET and E represents

the plant transpiration, T (Figure 2.12). In this study, they reported that the water loss under drought conditions is rapid (up to 3.0 mm/day) for the first 9 to 10 days; and there was consistently greater loss from the planted trays than the unplanted tray. Average total evapotranspiration for *Sedum mexicanum* (Mexican Stonecrop) was 46.8% and 44.2% for the NZ *Disphyma australe* (NZ Ice Plant). Water loss was initially rapid, but then the loss rate pattern became slower and more constant and ET from the planted trays was not significantly different to evaporation from the unplanted trays. ET from the planted trays have also been found to be less than the evaporation from the unplanted tray; as they concluded that water loss from the planted trays had reached a point of water scarcity that was not found in the unplanted tray. Using hourly basis analysis, all trays demonstrated a clear diurnal pattern of ET and E. The comparison was made and it was clear that transpiration might provide more storage capacity for a green roof. Hence the study on the evaporation as a single process following substrate properties assessment is necessary before further investigation with the transpiration process can be undertaken.

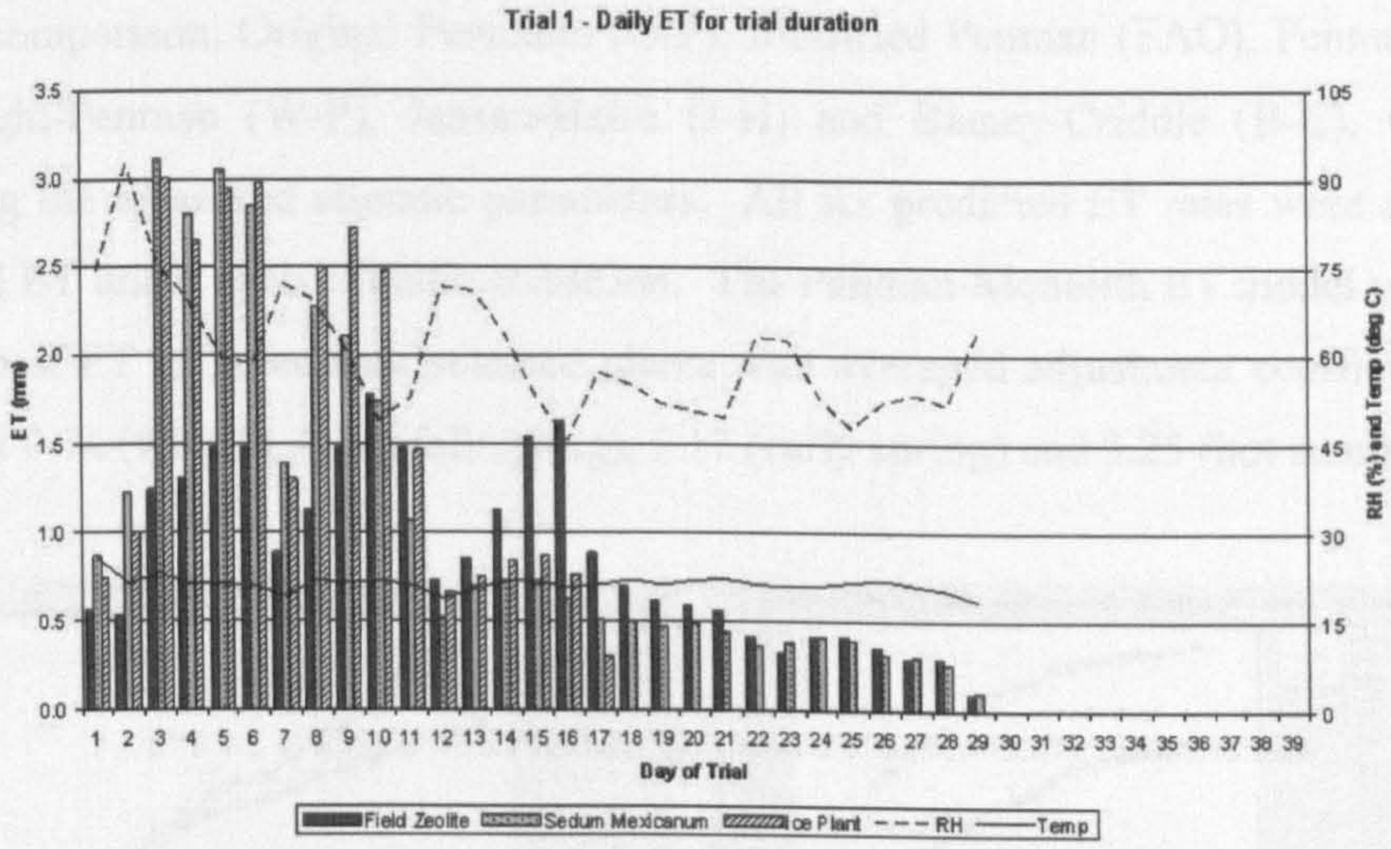


Figure 2.12: Daily evaporation and evapotranspiration over the trial duration (Trial 1) (Source: Fassman *et al*., 2008)

Another similar ET rate measurement and prediction from the green roof was studied by Rezaei & Jarret (2006). In the case of this experiment eight wooden boxes (1.05 m x 0.54 m x 0.10 m) were suspended on Minibem load sensors, LCEB-150. To form the ET treatment, the 1:1 mixture of *Delosperma nubigenum* and *Sedum album* were planted in four boxes; where each box had an 89 mm of expanded clay commercial media with 12 mm thick drainage layer. The other four boxes were unplanted and formed the evaporation treatment. All the boxes were placed in a computer-controlled greenhouse with a heating and ventilation system. This study

differed from that of Fassman *et al*. (2008), in that in this study the greenhouse was built to simulate four seasonal climatic conditions with temperature adjustments for each season. After a particular temperature was established, all the boxes were sprinkle irrigated once every other day until the drainage rate equalled the application rate. The boxes were weighed and averaged every 10 sec after the third wetting, and results reported hourly to a data logger for 21 consecutive days. The weight losses represented the evaporation and ET losses from each treatment. The water loss from the vegetated boxes were averaged for the four seasons and was reported as 0.79 mm/day (winter), 0.97 mm/day (fall/spring), 1.74 mm/day (early summer) and 3.23 mm/day (hot summer) within 21 days. For comparison, the averages of the water loss from the unplanted boxes were 0.58 mm/day (winter), 0.47 mm/day (fall/spring), 1.00 mm/day (early summer) and 2.08 mm/day (hot summer) (Figure 2.13).

While Fassman *et al*., (2008) only reported on the vegetation condition and ET rates performance under ambient condition, Rezaei & Jarret (2006) developed six different ET models for comparison; Original Penmann (O-P), Modified Penman (FAO), Penman-Monteith (P-M), Wright-Penman (W-P), Jensen-Haise (J-H) and Blaney-Criddle (B-C), which were applied using the measured climatic parameters. All six predicted ET rates were compared to the observed ET under each climatic condition. The Penman-Monteith ET model was found to predict the best ET of green roof selected plants with averaged adjustment coefficients for the mixed bed at 0.74 (winter), 0.24 (fall/spring), 1.17 (early spring) and 3.25 (hot summer).

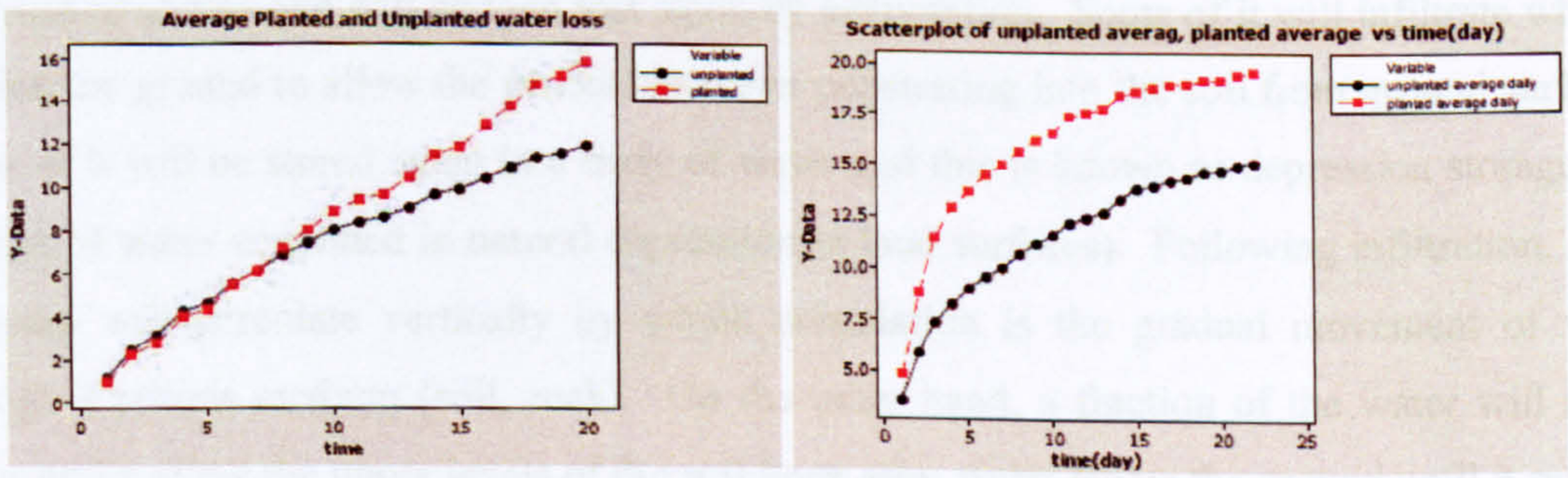


(a) (b)

Figure 2.13: Average water loss in planted and unplanted during (a) winter condition (the wettest month); (b) hot summer (driest month) (Source: Rezaei & Jarret, 2006)

Both studies then had described a feasible way to recognize substrate properties and evaporation rate approaches that could be referred to in our research.

## 2.5 Green Roof Modelling

### 2.5.1 Introduction

Green roof hydrological performance on monitoring site has been reported in previous sections, thus this section will then reviews the studies that modelled the green roofs. Some basic general theories for the model and hydrological green roof relationship are also explained in this section. When rain falls onto a green roof, it will undergo, to a greater or lesser extent, key processes in the hydrological cycle and these processes will also be briefly introduced in this section. It is also important to note that hydrological modelling can be classified into two broad types: data-based (or 'black-box') models and process-based models. An overview of hydrological modelling is provided in section 2.5.2.

#### 2.5.1.1 General Principles of the Hydrological Cycle

The hydrologic cycle as described in Figure 2.14 begins when the sun heats the land, air and water and triggers the evaporation process from rivers, lakes, oceans or any other bodies of water by causing the water to change for a liquid to a gaseous state. Transpiration is the process of water entering the air when plants' breathe during the day time and evapotranspiration is the return of moisture to the atmosphere as a result of evaporation from any surface and transpiration from plants. Precipitation is the process of any of all the forms of water particles (liquid or solid) falling from the atmosphere and reaching the ground (i.e. rain, snow, hail). During precipitation on any catchment, some water will be intercepted or held by foliage, twigs, branches or shrubs and will be then lost again by evaporation. Some of it will infiltrate when it reaches the ground to allow the process of water penetrating into the soil from ground surfaces. Some of it will be stored again in a body of water and this is known as depression storage (the volume of water contained in natural depression in land surfaces). Following infiltration, some of water will percolate vertically by which percolation is the gradual movement of water through a porous medium (soil, rock). On the other hand, a fraction of the water will move horizontally along the upper levels of the soil layer after water enters the ground until it reaches a stream and this is known as interflow process. This whole process is the circulation of the hydrological process, and this approach is replicated in a green roof system (Figure 2.15).

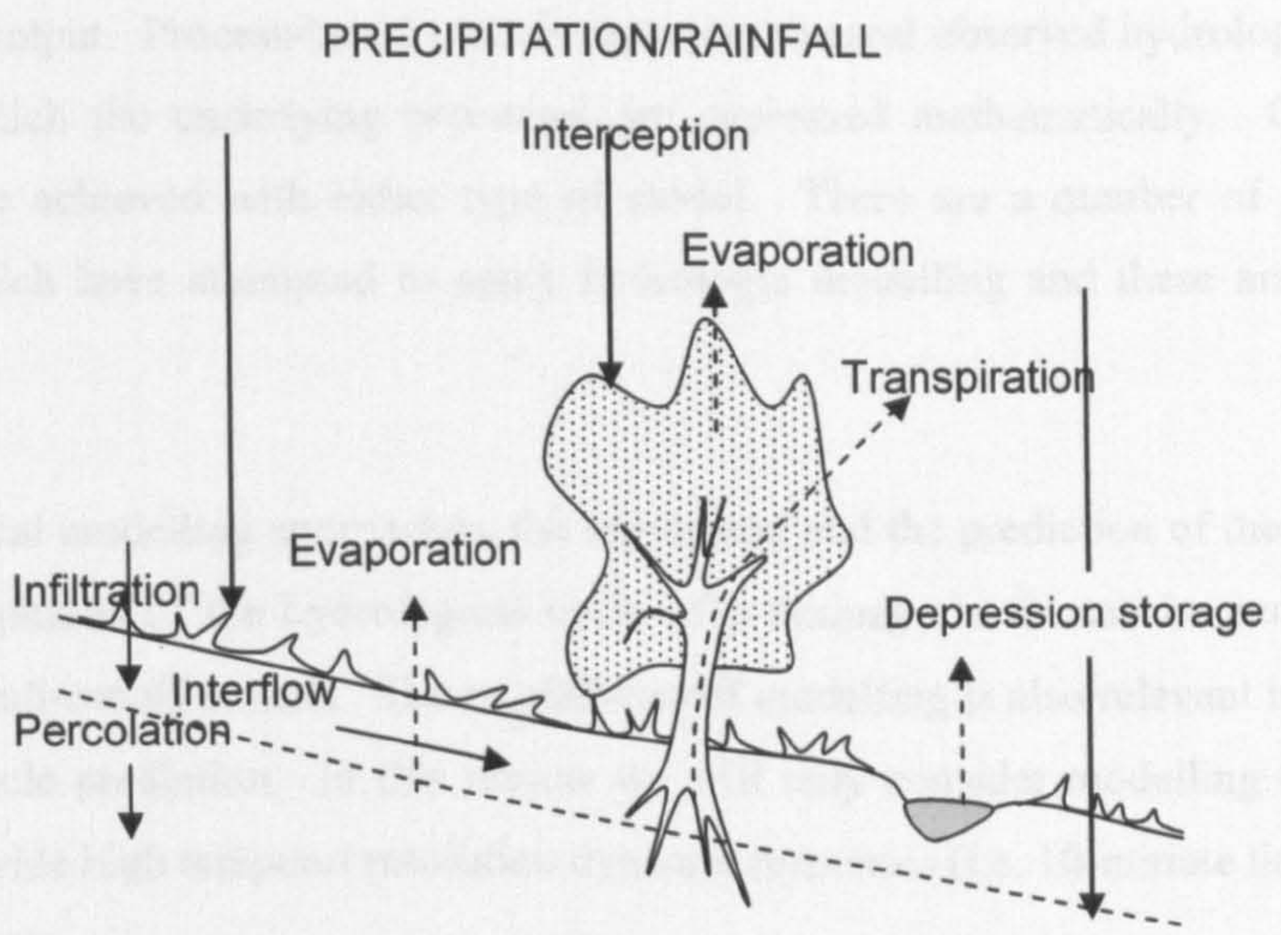


Figure 2.14: A simplified diagram of the hydrologic cycle

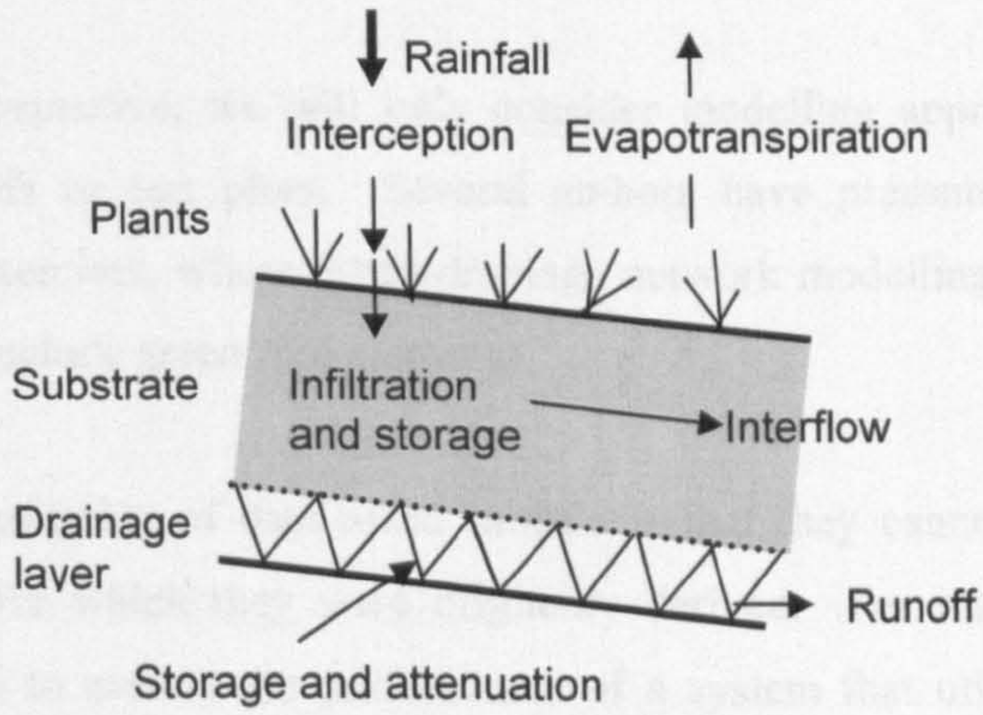


Figure 2.15: Hydrologic cycle in a green roof system

## 2.5.2 Hydrological Modelling

Hydrologists make use of hydrological models to better understand hydrological system behaviour. Models can be used to show fundamental system concepts and processes and to provide predictions of expected performance. There are two types of hydrologic models: data-based models and process-based models (Kirkby *et al*., 1992, Beven, 1988). Data-based models

are, in effect, black-box systems based on data, where all inputted data is transformed by the system to provide output. Process-based models represent the real observed hydrologic process descriptions, in which the underlying processes are expressed mathematically. Green roof modelling could be achieved with either type of model. There are a number of green roof studies applied which have attempted to apply hydrologic modelling and these are reviewed below.

In many hydrological modelling approaches, the movement and the prediction of the amount of water in different phases of the hydrological cycle of a drainage basin can be performed by implementing rainfall-runoff models. The rainfall-runoff modelling is also relevant in the green roof hydrologic cycle prediction. In this review we will only consider modelling approaches that attempt to provide high temporal resolution dynamic responses (i.e. 10-minute time-steps or less) to rainfall events.

There are green roof hydrological models that operate with daily, monthly or annual mass balance approaches, but these are too crude to be compatible with the dynamic network modelling tools used for urban drainage design.

Similarly, from a spatial perspective, we will only consider modelling approaches that are applicable to individual roofs or test plots. Several authors have presented results from catchment-scale modelling exercises, where urban-drainage network modelling packages have been used and/or adapted to include green roof elements.

In general terms, the key limitation of data-based models is that they cannot be utilised in situations other than those for which they were originally derived. For example, it is not feasible to use these models to predict the performance of a system that utilises a different substrate material, because it cannot be assumed that a different substrate will have the same water retention characteristics as the one that the model was developed for.

## 2.5.3 Data-Based Modelling Approaches

### 2.5.3.1 Introduction

In hydrologic engineering designs, the prediction of a discharge hydrograph or peak discharge is needed. In data-based modelling approaches, data from previous storm events is used to develop relationships between rainfall and runoff. Among many rainfall-runoff models, the unit

hydrograph is a basic, conceptual rainfall-runoff model that represents the various time delays by the time distribution of runoff (Beven, 1988). It is used extensively to characterise a catchment's rainfall-runoff response, and it is derived from observed historical records. Unit hydrograph theory is described in section 2.5.3.2.

Villareal and Bengtsson (2005) applied this approach to modelling the rainfall-runoff response of green roofs and their work is described in section 2.5.3.3.

### 2.5.3.2 Unit Hydrograph (UH) Theory

The shape of runoff hydrograph from a period of uniform rainfall for a given catchment is assumed to depend on rainfall's duration, depth, the losses (i.e. evaporation, groundwater flow) and the physical characteristics of the catchment (Mansell, 2003). The physical characteristics of the catchment (i.e. slope, soil types, vegetation) are assumed to remain constant with time, certainly over the short term, while the three factors above (duration, depth and losses) are the main factors to describe the UH theory as they vary with time. A unit hydrograph must be associated with specific units of rainfall depth (i.e. 1 mm or 1cm) and duration (i.e. 1 minute or 1 hour) (Mansell, 2003). Effective rainfall is the net rainfall after deducting all the losses from evaporation, infiltration, interception that are normally used in hydrograph separation methods. Thus, a UH is the hydrograph of direct runoff (excluding base flow or losses) for a storm that produces exactly 1 unit of net rain (the total effective rainfall/total runoff after abstractions) (Viessman & Lewis, 2002).

There are two main principles of UH theory; proportionality (Figure 2.16) and superposition (Figure 2.17). The same proportion of runoff hydrograph will be produced by the same duration of rain with the different intensities (Figure 2.16). For the contiguous and/or isolated periods of uniform-intensity net rainfall, the total hydrograph produced from the three separate storms is the sum of three separate hydrographs (Figure 2.17) (Wilson, 1983). Figure 2.17 applies the superposition principle.

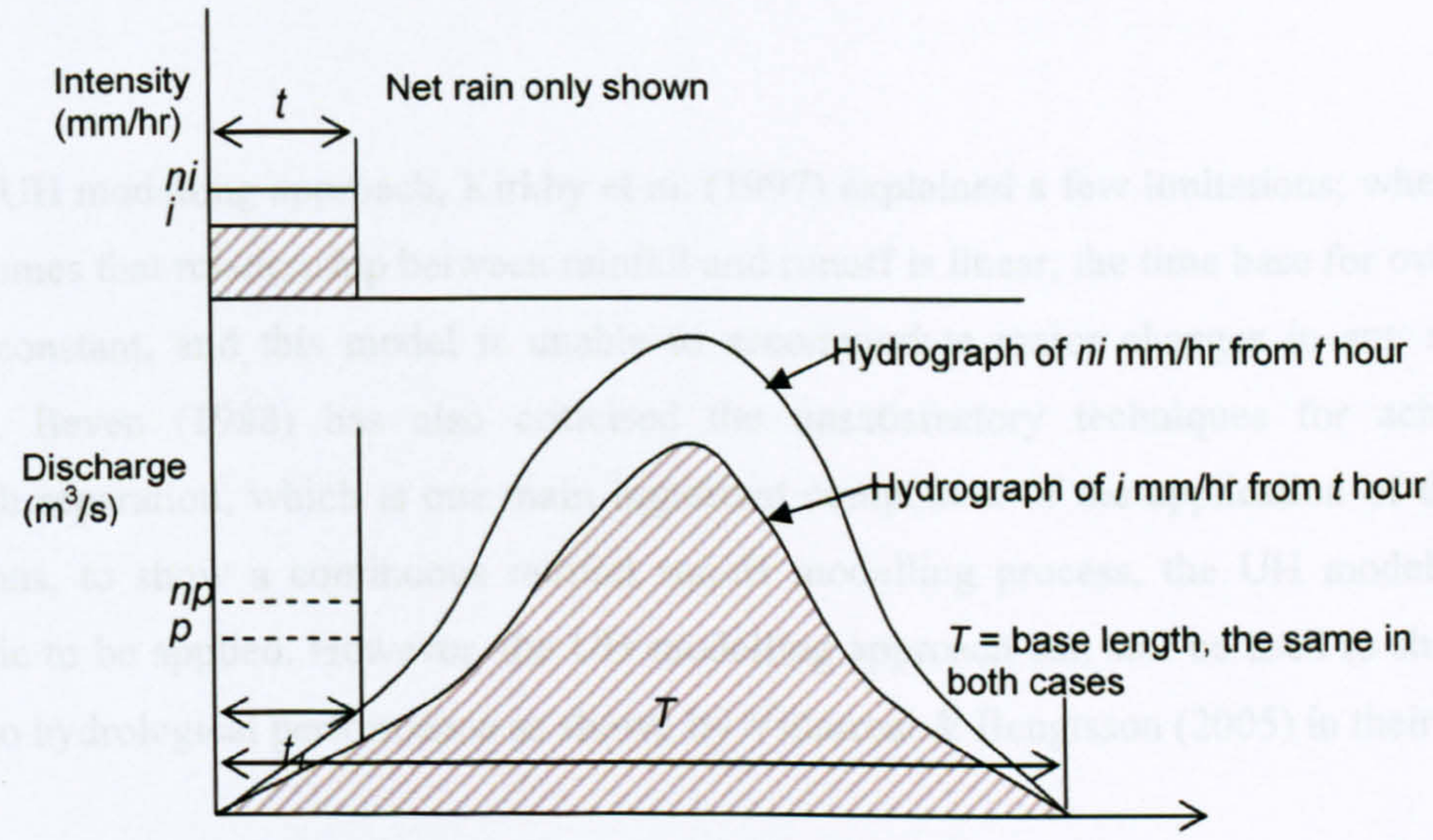


Figure 2.16: Proportionality principle of the unitgraph (Source: Wilson, 1983)

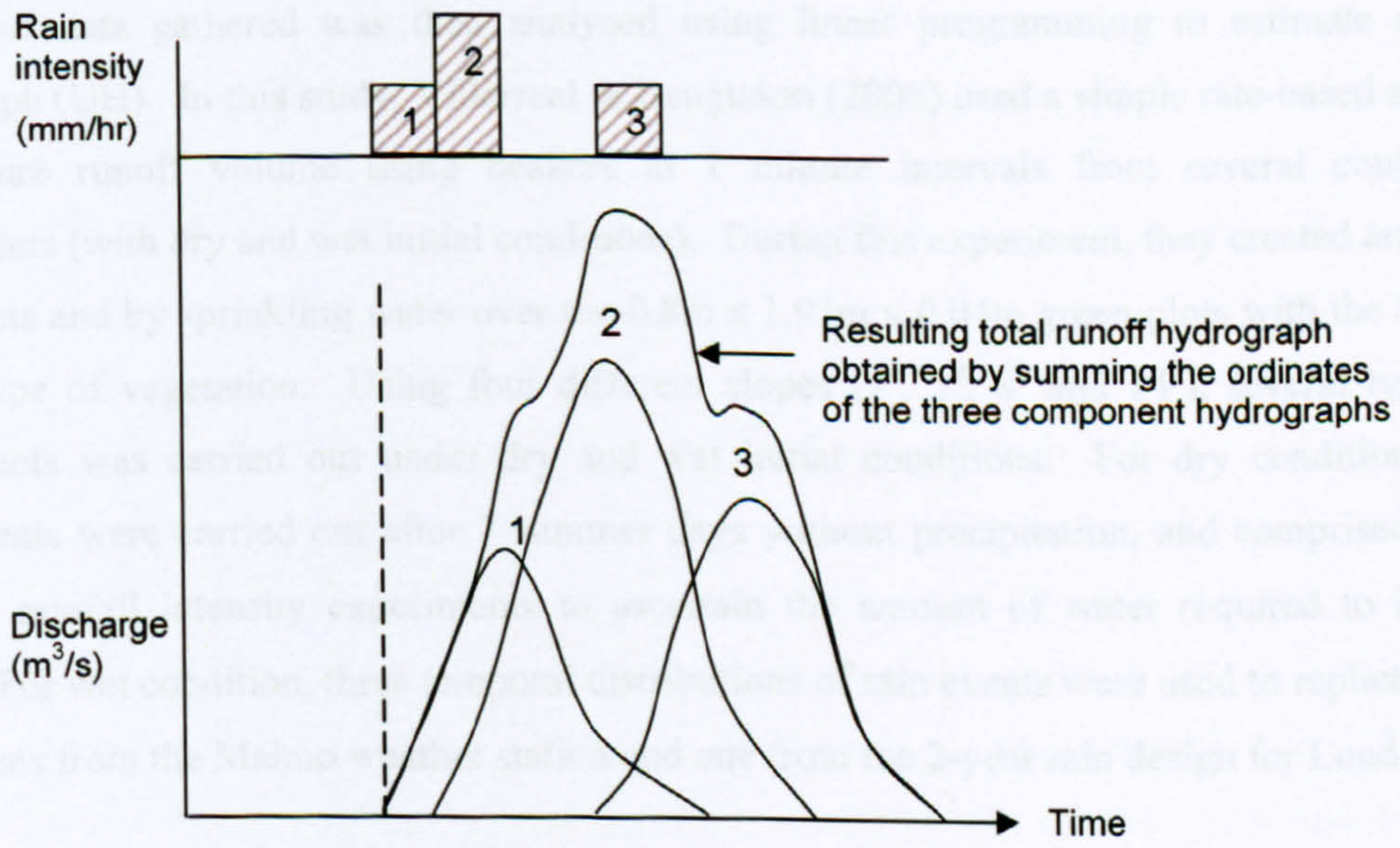


Figure 2.17: Principle of superposition applied to unitgraphs (Source: Wilson, 1983)

Therefore, the basic assumptions of UH theory are: i) the effective rainfall is uniformly distributed within its duration and uniformly distributed over the whole catchment, ii) the base duration of direct runoff hydrograph due to an effective rainfall of unit duration is constant and iii) the ordinates of a UH are 1.0/P times the ordinates of the direct runoff hydrograph for an

equal duration storm with P millimetres of net rain (Chow *et al.*, 1988; Viessman & Lewis, 2002).

Using the UH modelling approach, Kirkby et al. (1997) explained a few limitations; where UH model assumes that relationship between rainfall and runoff is linear, the time base for overflow runoff is constant, and this model is unable to accommodate major changes in any system properties. Beven (1988) has also criticised the unsatisfactory techniques for achieving hydrograph separation, which is one main important component of the application of the UH model. Thus, to show a continuous rainfall runoff modelling process, the UH modelling is rather static to be applied. However, the UH modelling approach can still be used to show the response to hydrological performance as shown by Villarreal & Bengtsson (2005) in their study.

### 2.5.3.3 Unit Hydrograph Theory Applied to Green Roof Performance

Studies carried out at Lund University, Sweden, have aimed to quantify the differences in green roof water retention performance as a function of roof slope and rainfall intensity. The rainfall and runoff data gathered was then analysed using linear programming to estimate a unit hydrograph (UH). In this study, Villarreal & Bengtsson (2005) used a simple rate-based system to measure runoff volume using beakers at 1 minute intervals from several controlled experiments (with dry and wet initial conditions). During this experiment, they created artificial rain events and by sprinkling water over the 0.8m x 1.93m x 0.04m green plots with the *Sedum album* type of vegetation. Using four different slopes ($2^0$, $5^0$, $8^0$ and $14^0$), several types of experiments was carried out under dry and wet initial conditions. For dry conditions, the experiments were carried out after 7 summer days without precipitation, and comprised three constant rainfall intensity experiments to ascertain the amount of water required to initiate runoff. For wet condition, three temporal distributions of rain events were used to replicate two real storms from the Malmo weather station and one from the 2-year rain design for Lund.

Based on their UH model, peak flows and runoff were accurately predicted using direct runoff, Q and effective precipitation relationship;

$$Q_j = U_1R_j + U_2R_{j-1} + \ldots + U_iR_{j-i+1} + \varepsilon_j \qquad 2.1$$

Which j = 1, 2, … n (n being the total number of intervals), i = 1, 2, … m (m being the total number of unit hydrograph ordinates), $U_1$, $U_2$, … $U_m$ are the ordinates of a unit hydrograph of $\Delta t$ duration (for the experiments with the green roof $\Delta t$ = 1 min), $\varepsilon$ is the difference between the

observed runoff hydrograph ordinates, Q and the reconstituted hydrographs ordinates, q. They used the Φ-index as a constant rate (the abstractions) for the hydrograph separation.

Runoff is equated to flow through the soil layer because there was no overland flow observed during the experiment due to the high porosity of the green roof. For the purposes of analysis, effective rainfall, R is defined as the rainfall which infiltrates but is not retained by the green roof and which therefore becomes direct runoff, Q. They used an initial abstract term to define rainfall which infiltrates but was detained beyond the end of the rain event; or at a constant loss rate (Figure 2.18).



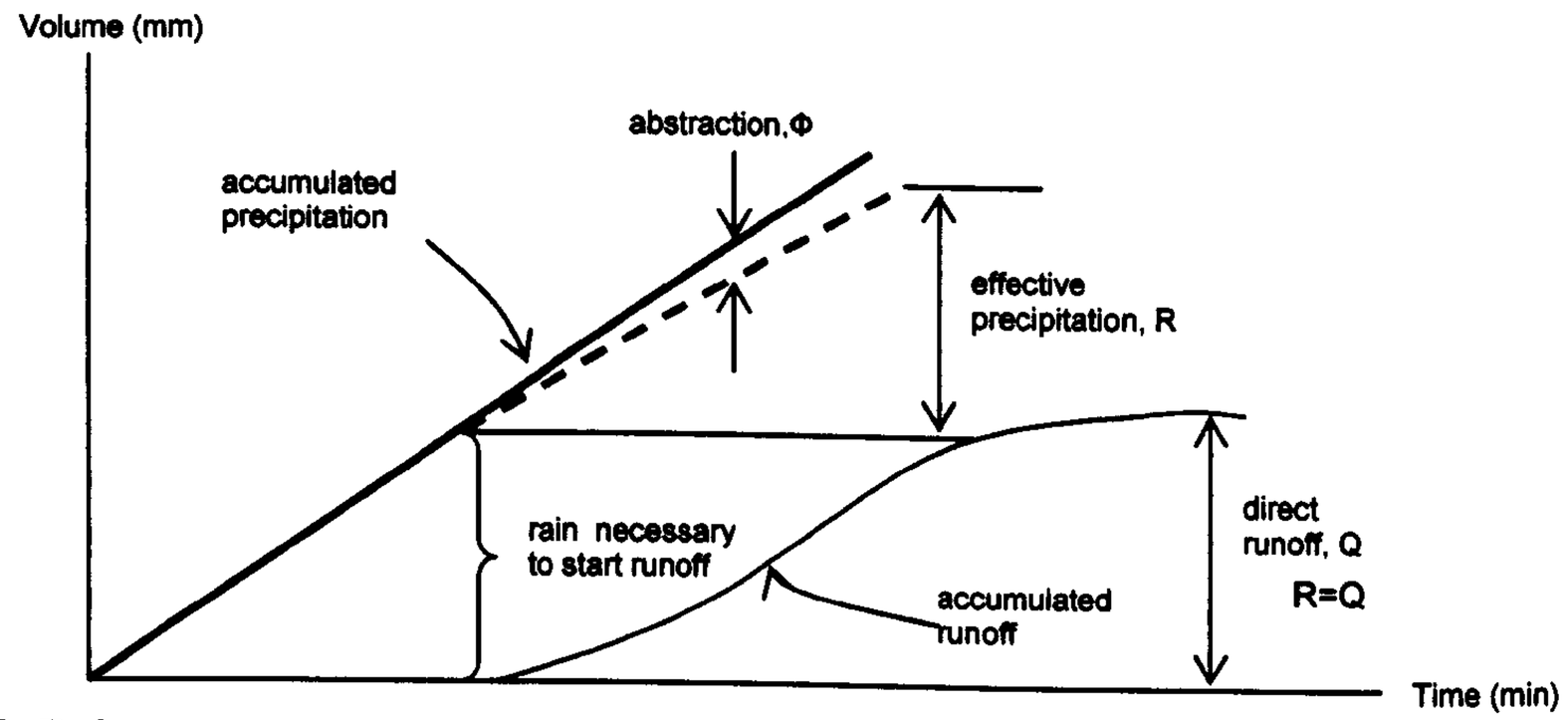


Figure 2.18: Rain necessary to start runoff, abstractions, effective precipitation and direct runoff (Source: Villarreal & Bengtsson, 2005)

Linear programming was used to calculate the relationship between R and Q. A unique UH for each rainfall and slope combination was determined. The UHs obtained were found to be similar for each rain event with some variation for peak flows; so an average UH was calculated to estimate the green roof response of different events for the purpose of comparison with the observed hydrographs. The results from the analysis show that for different slopes, the differences in observed and estimated peak flow and volume values for a given rainfall event are solely due to continuing abstraction which depends on the initial moisture content of the soil, otherwise the hydrograph shows a good fit between the observed and estimated (Figure 2.19). For dry initial conditions, the results show that the runoff required a range of 6-12 mm of precipitation before it starts to appear and that the retention is greater for lower intensity and slopes. Under exceptionally dry initial conditions, a horizontal green roof could retain up to 15 mm of rainfall, and for a sloped roof, the maximum retention was 10 mm (Villarreal & Bengtsson, 2005).

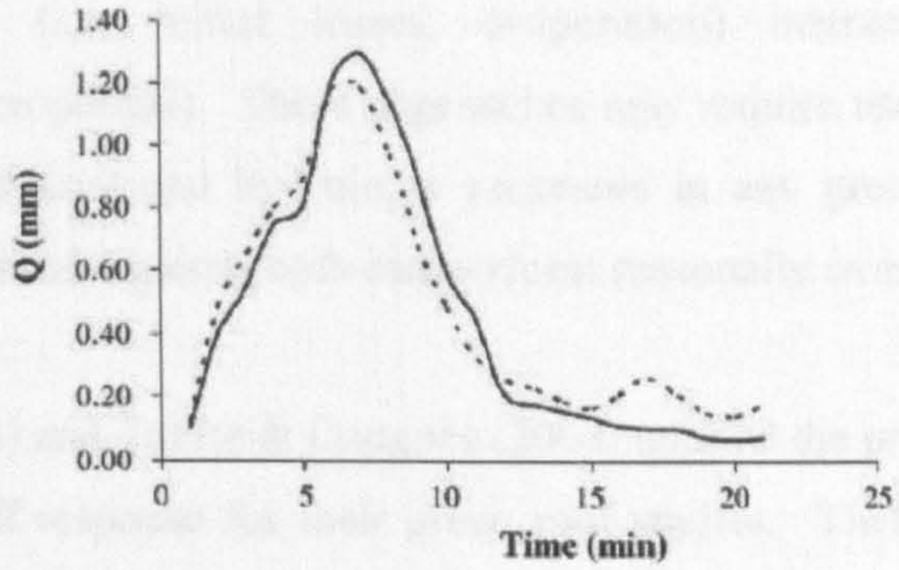


Figure 2.19: An example of a simulated (dashed line) and experimental (continuous line) of direct runoff hydrograph for the rain event on 2 August 2002 (Source: Villarreal & Bengtsson, 2005)

These results show that the UH theory approach can be accurately used to model a green roof to predict the rainfall-runoff relationship. The Villarreal & Bengtsson model provides no information on the expected runoff response from a green roof with a different substrate type or substrate depth and the substrate depth used in this model was very shallow for only 40 mm. They also concluded that the UH averaging that was used to estimate the response of the green roof can only be calculated for experiments with uniform intensity as they showed the least variation between the calculated hydrographs.

Therefore, this UH approach is a data model that the UHs obtained and was only suitable for their specific system and might not be useful if the system was altered or applied in different climatic regions or on different roof sizes. Mansell (2003) and Linsley *et al.* (1988) also described that in most cases, it is very difficult to find suitable, isolated, uniform intensity storms, and other more complex methods may be used to obtain UHs from multiple storms. UH is only a routing model suitable for detention; hence another model is necessary to predict retention (losses). Therefore, this suggests that this model is unsuitable for our purposes, which are to describe a process-based system.

## 2.5.4 Process-Based Modelling Approaches

### 2.5.4.1 Introduction

The UH models do not attempt to model in details the hydrological processes of a catchment system. Therefore the conceptual rainfall-runoff model could be better expressed using process-based or physically-based models, rather than the UH model, to show how the

hydrological processes (i.e. initial losses, evaporation) interact with the catchment characteristics (i.e. soil properties). These approaches may require users to have a quantitative understanding of the physical and hydrologic processes in any green roof system. It is of interest however, to know how green roofs can perform seasonally over the long-term.

Jarret & Berghage (2008) and Taylor & Gangnes (2004) applied the process-based modelling to model the rainfall-runoff response for their green roof studies. Their works are described in section 2.5.4.4. Based on typical physically based runoff models, prediction of initial losses (due to evapotranspiration) and storage-routing is the main approach used in their models. Water balance approach and storage-routing theory are then described in section 2.5.4.2 and 2.5.4.3 to provide more understanding.

### 2.5.4.2 Water Balance Principle

The fundamental water-balance relationship is founded for the physically based models (Mansell, 2003):

$$Q = P - ET - D - \Delta S \qquad 2.2$$

Where Q is the runoff, P is precipitation, ET is evapotranspiration, D is the drainage to the groundwater and $\Delta S$ is the change in water storage in the soil.

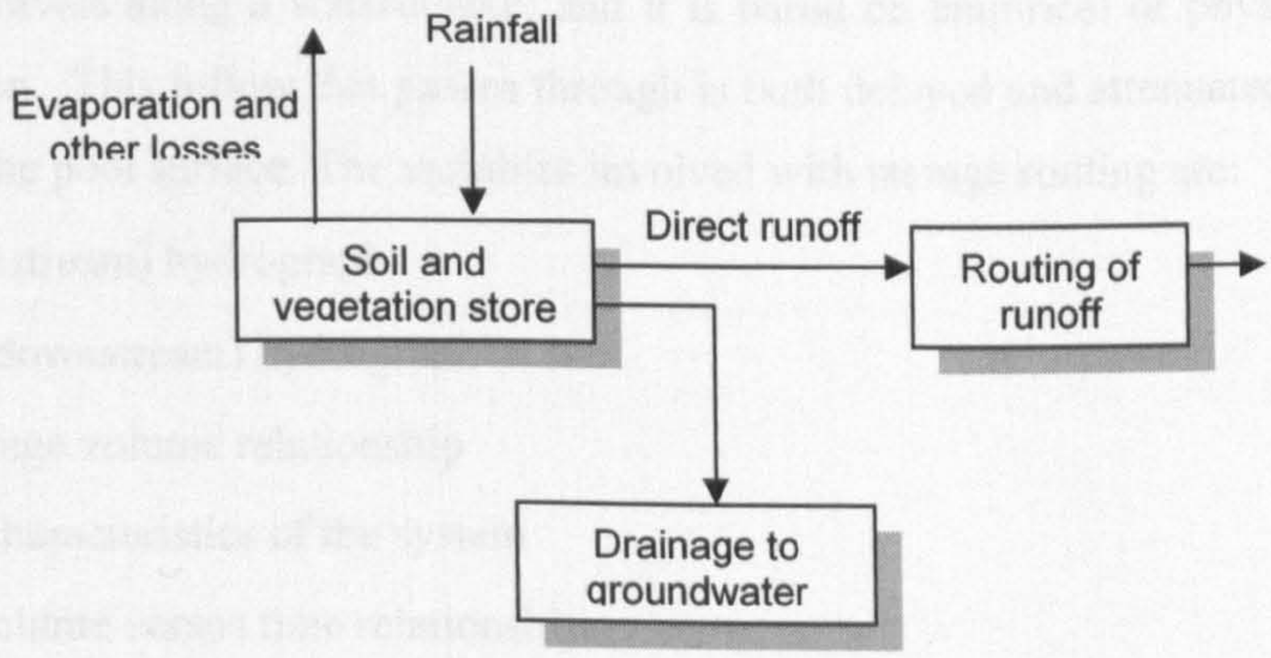


Figure 2.20: The structure of a typical rainfall-runoff model (Source: Mansell, 2003)

Mansell (2003) also explained that to relate the inflows and outflows to the soil store to calculate the runoff, a simple continuity equation will be used together with the water balance equation. In some cases, the outflows from the soil store may be simple overflows (of the excess

flow) when the soil store is full, otherwise they maybe a function of storage (S) of the form; $Q = CS^n$.

Following equation 2.2, the actual evaporation that is largely a function of climatic conditions (i.e. wind speed and radiation) depends on the potential evaporation. The ratio of actual to potential evaporation is usually a function of the volume of water storage (within the soil or on the surface). Further, Mansell (2003) also discussed that evaporation decreases in some models according to linear function; so it will linearly decrease as the contents of the store decrease below a maximum capacity. Whilst others use a negative exponential function; the evaporation falls more rapidly as the store depletes.

### 2.5.4.3 Storage-Routing Theory

Flood routing is the process of calculating the passage of the direct runoff hydrograph through a conveyance system (ISMM, 2007). The flood routing is referred to as; channel (river) routing if it is a channel system, and as storage routing or reservoir routing if the system is a reservoir. It is a technique to compute the effect of system storage and system dynamics on the shape and movement of flow hydrographs along a watercourse (Viessman & Lewis, 2002).

Routing is used to predict the temporal and spatial distribution of hydrographs during excess rainfall as water travels along a watercourse; and it is based on empirical or physical process equations of motion. This inflow that passes through is both delayed and attenuated as it enters and spreads over the pool surface. The variables involved with storage routing are:

- Inflow (upstream) hydrograph
- Outflow (downstream) hydrograph
- Stage-storage volume relationship
- Physical characteristics of the system
- Storage volume versus time relationship
- Depth (stage) – discharge relationship
- Volume and time for extended detention

As described in Section 2.5.4.2, storage routing employs the continuity equation, together with an analytical or an assumed relationship between storage and discharge within a system, in the calculation:

$$\text{Inflow (I)} - \text{Outflow (O)} = \Delta S/\Delta t \qquad 2.3$$

Where, $\Delta S$ is the change in storage during time increment (interval) $\Delta t$. This equation then is approximated, for a time interval, by:

$$\frac{I_n + I_{n+1}}{2}\Delta t + \left(S_n - \frac{O_n}{2}\Delta t\right) = \left(S_{n+1} + \frac{O_{n+1}}{2}\Delta t\right) \qquad 2.4$$

Where the subscripts n and n+1 refer to the flows and storage at the beginning and end of a time interval $\Delta t$ respectively. The attenuation of the hydrograph as flow passes through a reservoir is due to the fact that, as the flow into the reservoir changes, the amount of storage also changes, $\Delta S$ (Mansell, 2003). For given values of the inflow hydrograph, I, the values of the outflow hydrograph, O will be calculated. However, a further relationship is required (equation 2.5) based on the consideration of the hydraulic characteristics of the outflow structure and the topography of the reservoir, since the storage value is also unknown (Mansell, 2003).

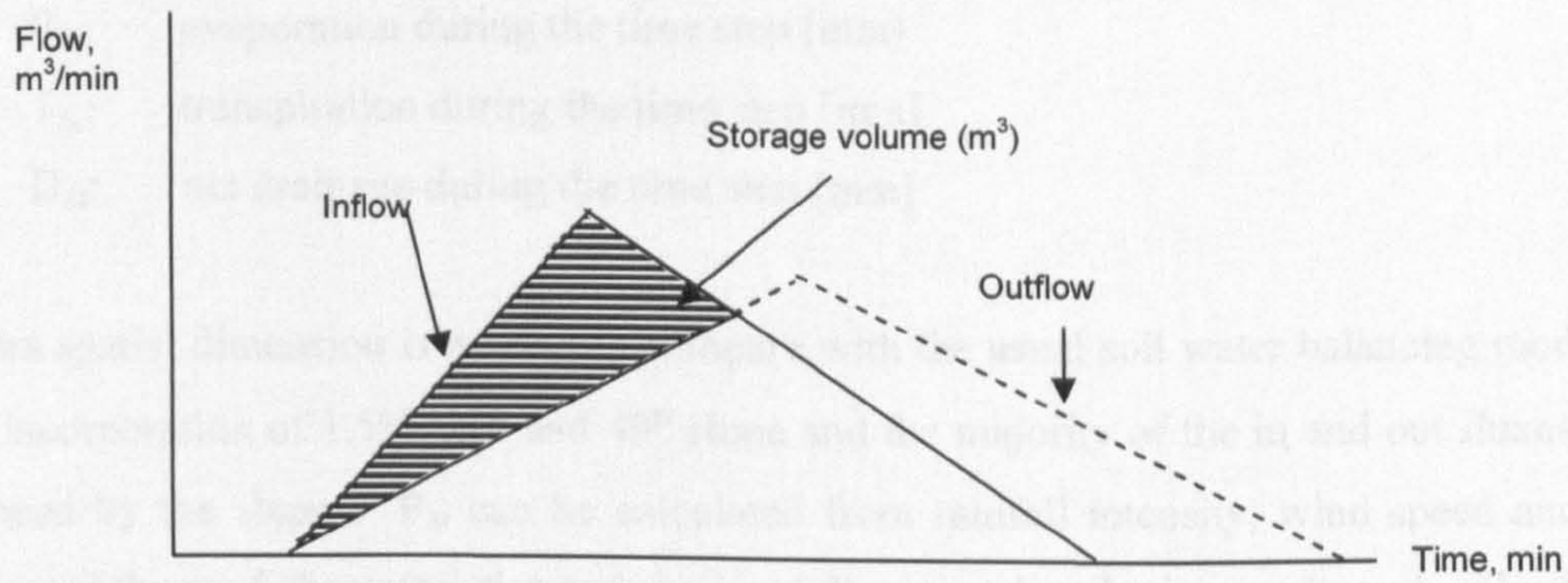


Figure 2.21: Direct estimation of storage volume (Source: Mansell, 2003)

$$Q = kH^n \qquad 2.5$$

Equation 2.5 expresses the relationship between the water level of the reservoir and the outflow from the reservoir that passes over the weir; where Q is the outflow, H is the height of the water level (above the crest of any weir) and k is a constant (incorporating the width and discharge coefficient of the weir) and the coefficient n is normally about 1.5 for weir of typical spillway structure (Mansell, 2003).

### 2.5.4.4 Process-Based Modelling of Green Roof Performance

Water balance has been attempted for use on a physically based model on various types of green roofs and climatic conditions by Mentens *et al.* (2003). The model was also developed for all various slope angles and orientation since they discovered in the study that there was insufficient data for a complete and adequate empirical model of the green roof water balance. Therefore, based on normal water balance of a soil, their model is constructed by dividing the green roof in 78 small lysimeters that receive and release water by a number of different processes:

$$W_{t+\Delta t} = W_t + P_{\Delta t} - RO_{\Delta t} - E_{\Delta t} - T_{\Delta t} - D_{\Delta t} \qquad 2.6$$

Where

- $\Delta t$: time step [s]
- $W_{t+\Delta t}$: water content at the end of the time step [mm]
- $W_t$: water content at the beginning of the time step [mm]
- $P_{\Delta t}$: precipitation during the time step [mm]
- $RO_{\Delta t}$: run off during the time step [mm]
- $E_{\Delta t}$: evaporation during the time step [mm]
- $T_{\Delta t}$: transpiration during the time step [mm]
- $D_{\Delta t}$: net drainage during the time step [mm]

An extra spatial dimension is needed to compare with the usual soil water balancing model due to the incorporation of 1.5%, 20° and 40° slope and the majority of the in and out fluxes being influenced by the slopes. $P_{\Delta t}$ can be calculated from rainfall intensity, wind speed and wind direction; if the roof characteristics and the local drop size distribution are known. The $E_{\Delta t}$ and $T_{\Delta t}$ are different for the different exposure of the roof and also depend on the orientation, slope angle of the roof and their exposure to sunshine. Whilst for $RO_{\Delta t}$ and $D_{\Delta t}$, these depend on the slope angle but not on the orientation.

Mentens *et al.*, (2003) statistically analysed their data using the GLM Repeated Measurement in SPSS and summarised that there is a significant interaction for period*day*orientation. The high interaction between factors can be explained by a significant difference between evaporation for the different orientation but the magnitude of the difference depends on both the period of observation and the day within the period. However in this paper, the author has only provided information on the first stage of their physically-based model, providing information

on their data collection for the water balance model with no further information given on flow detention. They concluded that the process of ET cannot be directly calculated from the FAO Pennmann-Monteith equation, but needs to incorporate further parameters; slope angle, slope orientation, solar radiation, time of year and time of day; and to construct a complete physical model, further research is needed.

On the other hand, Jarret & Berghage (2008), in their extended study in Penn State University (DeNardo *et al.*, 2003), modelled their green roof system using reservoir-routing, the modified Puls routing model. During this study, they developed a stage-storage relationship using the green roof drainage layer and roof media characteristics. The porosity for the drainage layer (12 mm thick) was 78% with a field capacity of 5.2%, where the growth media (89 mm) had a porosity of 55% with a field capacity of 34%. Two independent modelling systems were developed; i) an Annual Green Roof (AGR) model to predict annual roof runoff as the sum of the daily roof runoffs using daily rainfall depths and daily ET; and ii) an Individual Storm Green Roof Response (ISGRR) model to predict the roof's runoff rate and volume using routed individual storm hyetographs. Both models assume that a daily ET can be provided. However, for their rainfall and water storage inputs; the AGR was based on the assumptions of i) availability of a 24 hours rainfall record, and ii) that the roof's maximum water retention and its vegetation is known; whilst the ISGRR was based on i) availability of a storm hyetograph with uniform times steps between 6 and 60 minutes, and ii) that the month of the storm and that the number of days since the last rainfall is known.

Using data reported by Rezaei *et al.* (2005), the influence of water storage in the green roof plants was developed and has been used in Jarret & Berghage (2008) models. For each annual simulation, the daily ET rate was used to reduce the water in the green roof down to field capacity. The ET data was based on results of experimental ET (Rezaei *et al.* 2005) and the number of days since the last rainfall event. The input of the rainfall used was a series of actual uniform rain events and a synthetic rainfall distribution similar to a hydrograph for ungauged development sites (pre and post development runoff hydrograph estimation).

In the AGR model, the depth of available storage is defined as the available pore-space in the drainage layer and roof media below field capacity plus the plants' water holding capacity. The water retention provided by experimental plants was up to 10 mm but then it will decrease as the time between events increased because the plants were reduced in size as the availability of

water decreased (Jarret & Berghage, 2008, Rezaei *et al*. 2005). Whilst for the ISGRR, the stage-storage relationship assumed no runoff until the media and drainage layer was filled with rain to increase the water content to field capacity, and the predicted daily ET rate was used to reduce the water in green roof starting at field capacity prior to each storm simulation.

The AGR model evaluated the 28 years of State College, PA and Raleigh, NC daily rainfall data and shows that the green roof retained 52.8% of the State College annual rainfall depth and 45.4% of Raleigh average rainfall depth. They demonstrated that this model could not only predict retention for the green roof retention storage capacity of 40 mm, but could also predicted variable roof's retention storage capacity in terms of thicker (< 89 mm) and less thick (< 89 mm). They discovered that having a thicker roof did not greatly improve the roof's ability to retain rainwater on the roof, furthermore the 3 mm of retention storage, with addition of one or two layers of a heavy-weight geotextile (no longer a green roof), would cause the roof to retain 25 to 40% of annual rainfall. Figure 2.22 shows the results of the experimental observations and the modelled depth of 28.7 mm storm in June 2, 2003 where the model was able to correctly show the delay of runoff at start and similar total runoff with 22.6 mm from the observed runoff and 20.5 mm from the modelled total runoff (Jarret & Berghage, 2008). The results from the ISGRR model have shown that the detention response of a green roof simulation can be adapted using the modified Puls routing model.

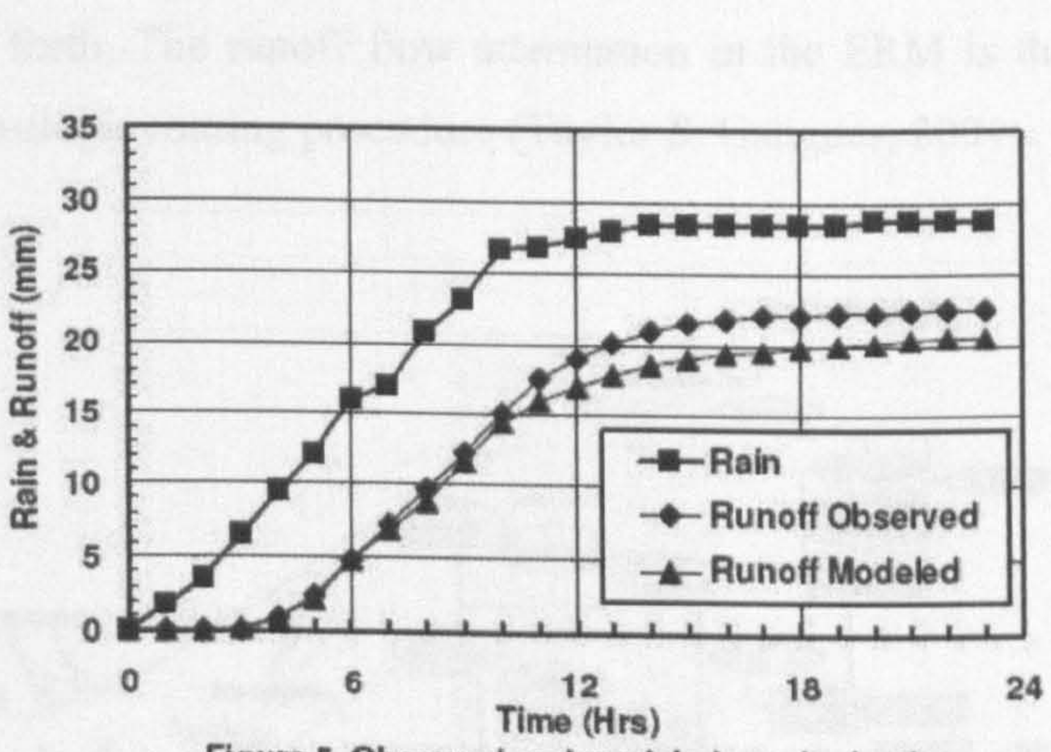

Figure 5. Observed and modeled results for the June 2, 2003 rain.

Figure 2.22: Observed and modelled results for the June 2, 2003 rain (Source: Jarret & Berghage (2008)

Another similar physical process-based model was used by Taylor & Gangnes (2004) to model the eco-roof hydrology processes to facilitate the hydrological analysis and design for Portland.

In this study, the eco-roof is an additional element to their current Santa Barbara Urban Hydrograph (SBUH) catchment hydrologic modelling. The eco-roof runoff model (ERM) is an event-based model developed by Magnusson Klemencic Associated (MKA) which applied two main steps to predict runoff; the instantaneous surface runoff (for each time increment of the design storm) followed by a hydrologic routing (yields the attenuated, design-flow rate at the basin outlet).

The first parameter required in this model (Figure 2.23) is the initial abstraction losses due to evapotranspiration, depression storage and interception (data obtained from professional judgement and other sources). The ERM assumes that the infiltration rate is constant. The infiltration rate is established from testing, observed eco-roofs, and/or the soil media specification where this rate is compared then to the rainfall intensity. In terms of the soil moisture, once the moisture reaches field capacity, subsequent infiltration is held as transient storage in the soil voids. Transient storage is the final component of the moisture storage of the delayed drainable water that flows downward through the eco-roof media. The ultimate retention capacity could be determined by the initial saturation and field capacity of the soil. The storage capacity is determined by the depth and effective porosity of the media; and the attenuation of water flowing through this porous media is then computed, using the hydrologic routing. The water discharge cascades through the layers from the first soil layer at the inflow to the second and so forth. The runoff flow attenuation in the ERM is then computed by the modified Att-Kin hydrologic routing procedure (Taylor & Gangnes, 2004).

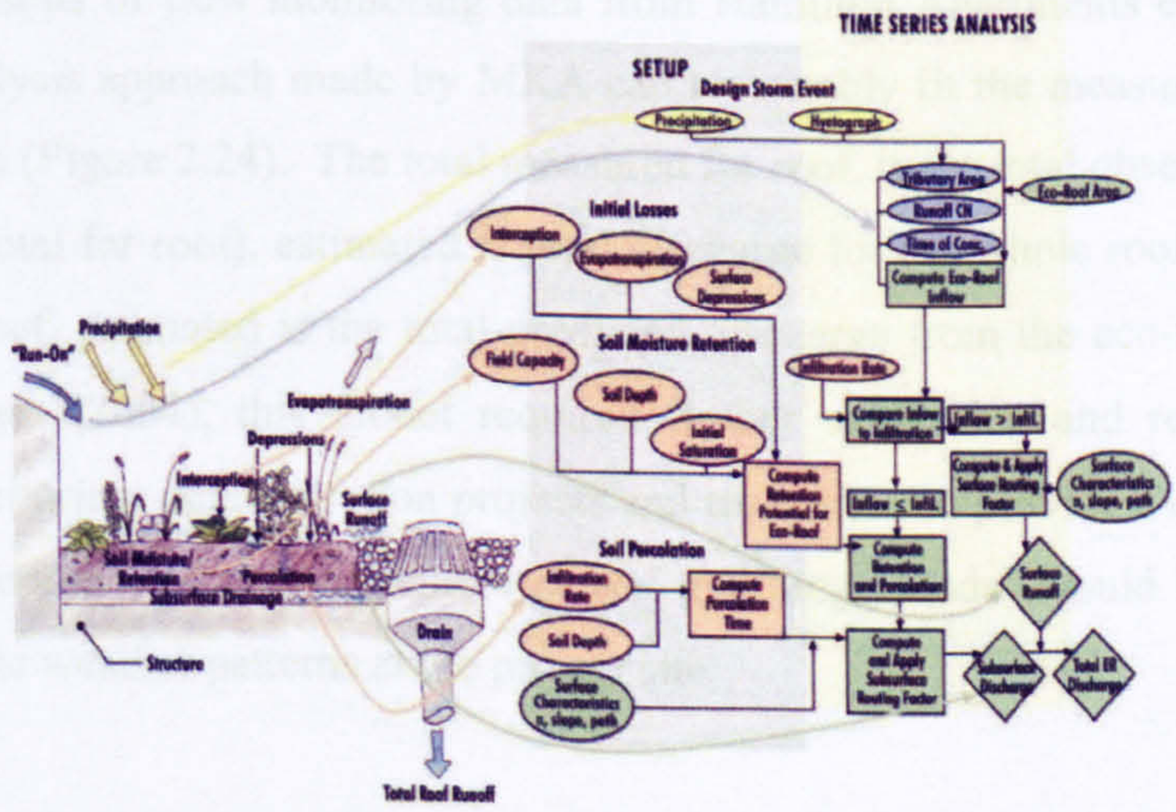


Figure 2.23: Eco-roof Hydrology Model (Source: Taylor & Gangnes, 2004)

A modified Att-Kin routing is used to model transient storage provided in the eco-roof voids (Taylor & Gangnes, 2004). This routing previously accounted for attenuation as flow percolated through the eco-roof. From the original Att-Kin routing method, a relationship between storage (S) and discharge (O) for a basin was used to define the storage coefficient (K):

$$S = K*O \qquad 2.7$$

Analogous to the time of concentration, the equation for the storage coefficient (K) was developed as a function of the depth of the soil media layer, the porosity of the layer and the saturated infiltration rate for the layer:

$$K = D * \frac{neff}{i_{max}}[T] \qquad 2.8$$

Where D is the depth of media layer, neff is the porosity, $i_{max}$ is the maximum infiltration rate and [T] is the generic time dimension. Using this K value, the hydrologic routing coefficient that relates the discharge to the inflow is calculated using this equation:

$$O_2 = O_1 + w\,(I_2 + I_1 - 2O_1) \qquad 2.9$$

Where $O_1$ is the discharge from the previous time interval, $O_2$ is the discharge from the current time interval, $I_1$ is the discharge from the previous time interval, $I_2$ is the discharge from the current time interval, w is the hydrologic routing coefficient ( = (timestep) / (2K + timestep)), timestep is the time interval used for the time series analysis in minutes.

The validation results of flow monitoring data from Hamilton Apartments eco-roof show that the proposed analysis approach made by MKA can reasonably fit the measured roof discharge rates and volumes (Figure 2.24). The total measured for roof, is the total observed discharge for the whole roof (total for roof), estimated is total discharge for the whole roof, predicted by the model and eco-roof, estimated is the total predicted discharge from the eco-roof. As stated by Taylor & Gangnes (2004), this model required further calibration and refinement through having more monitoring, demonstration projects and research. To provide a more sophisticated analysis, a development of a continuous eco-roof hydrology model would be needed to take account of specific weather patterns at the project site.

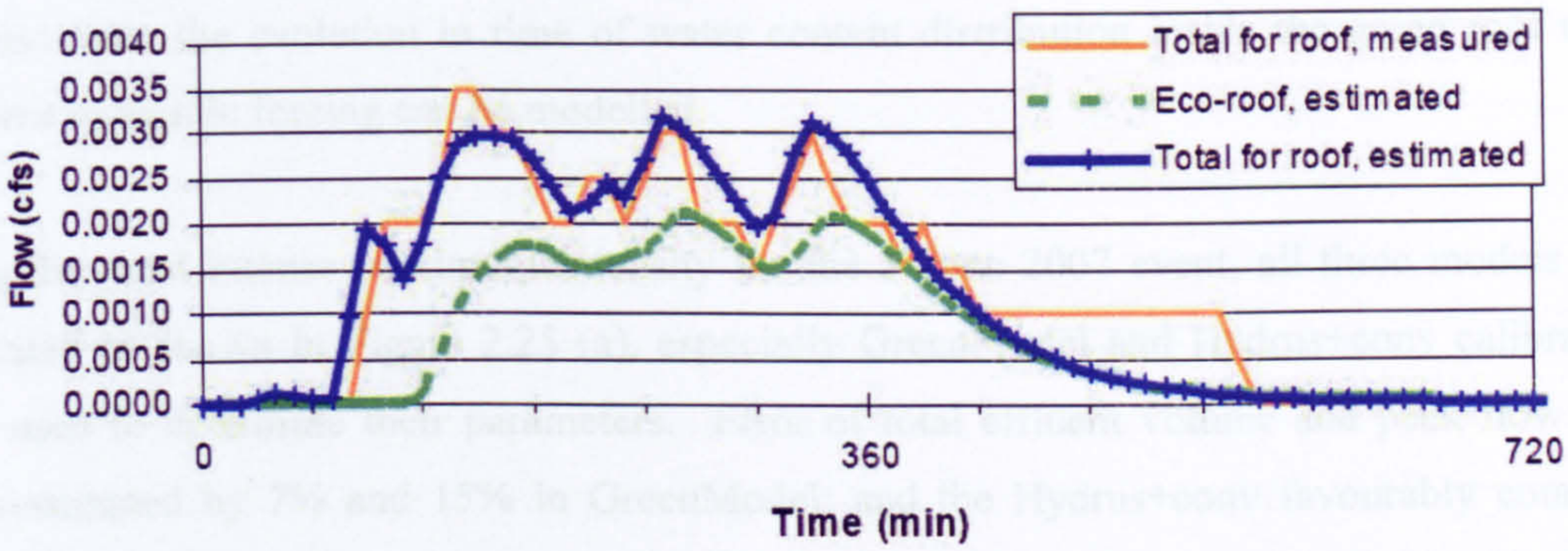


Figure 2.24: Calibrated eco-roof model results for Hamilton Apartments, East Roof, May 17, 2003 (Source: Taylor & Gangnes, 2004)

In Italy, three different models incorporating the numerical model for the impermeable control roof (ImpModel), the conceptual hydrological model for the green roof (GreenModel) and the Hydrus 1-D model for the green roof have been developed (Hydrus+conv) (Palla *et al.*, 2008). The ImpModel was developed for the first phase of the monitoring campaign when the rooftop was only covered with the impermeable layer, while the other two models were developed for the second phase of the monitoring campaign only a day after the completion of the new green roof.

The ImpModel using Soil Conservation Service Curve Number method for the infiltration model and the kinematic wave model was used for the flow routing method. The GreenModel applied the three linear reservoirs model by simulating the green roof system using growing medium infiltration and drainage from the saturated and unsaturated zones (Palla *et al.*, 2008). The total specific flow discharged by the green roof, $q_{GreenModel}$ [L/T] = $\beta.q^{i}_{I} + (1 - \beta).q^{i}_{II}$, is calculated as a linear combination of the effluent from the second ($q^{i}_{I}$) and third ($q^{i}_{II}$) reservoirs. Whilst for Hydrus+conv they employed the Hydrus-1D code to simulate the infiltration process and water content profile in 1D variably saturated media; and the one-dimensional form of the Richards' equation is used as the flow governing equation:

$$\frac{\partial\theta(\psi)}{\partial t} = \frac{\partial}{\partial z}\left[K(\psi).\left(\frac{\partial\psi}{\partial z}+1\right)\right] \qquad 2.10$$

Where $\theta$ is the volumetric water content [$L^3L^{-3}$]; $\psi$ is suction head [L]; K is the unsaturated hydraulic conductivity [$LT^{-1}$]; and they assumed that in the liquid flow movement the air phase is negligible and that the thermal gradients in the water flow were also neglected. Using the

Hydrus+conv, the evolution in time of water content distribution inside the green roof under transient hydraulic forcing can be modelled.

Using the most intense maximum intensity for the 5 June 2007 event, all three models were calibrated as shown in Figure 2.25 (a), especially GreenModel and Hydrus+conv calibrations were used to determine their parameters. Error of total effluent volume and peak flow were underestimated by 7% and 15% in GreenModel; and the Hydrus+conv favourably compares with the measured effluent. While in Figure 2.25 (b), both models were validated using 22-23 Nov event (of one long lasting event – 2870 minutes) with a very good hyetograph shape. The greatest error was found using the GreenModel calibration by underestimating 19% of the peak flow.

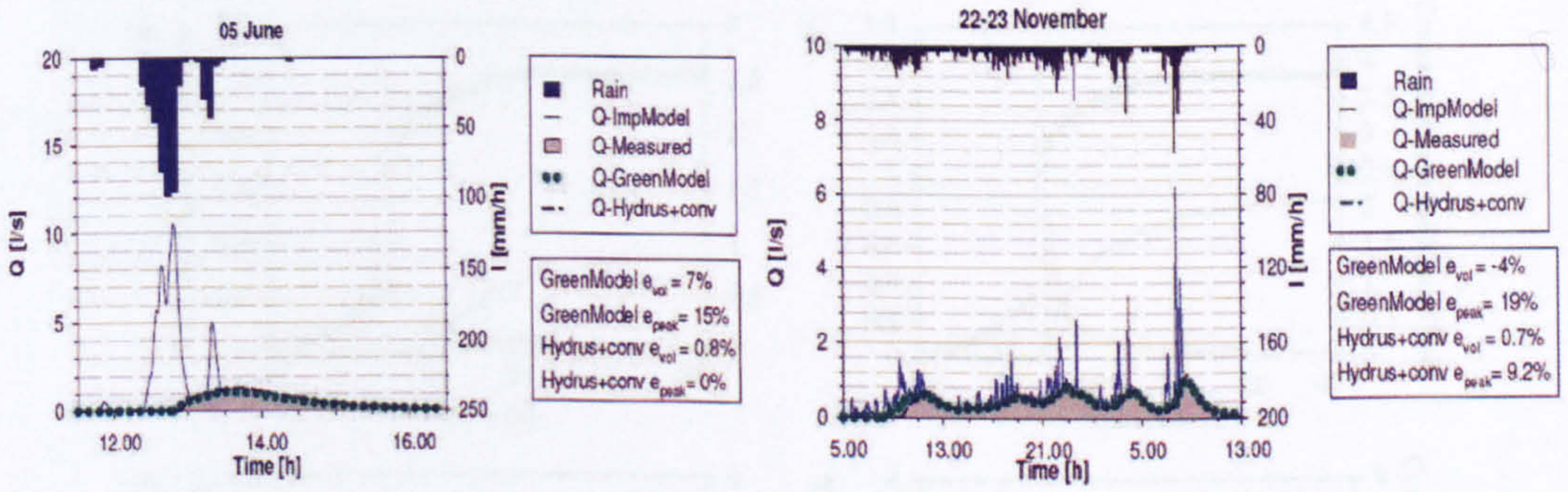


(a) (b)

Figure 2.25: Comparison of the green roof measured and simulated hydrographs and the impermeable roof simulated hydrograph with errors on volume and peak flow operated by GreenModel and by Hydrus+conv model for the (a) 5 June 2007 event; and (b) 22-23 November 2007 event (Palla *et al.*, 2008)

They stated that the main important variables governing the flow regime through the green roof are rainfall forcing (rate, duration); substrate media (type, hydraulic conductivity and degree of saturation) and drying process (ET). During inter-event duration, the role of evapotranspiration must be quantified for each historical event; where the measured meteorological conditions need to be compared with the null conditions for better estimation of initial water content. They also concluded that the conceptual (GreenModel) model predictions are more reasonable and easier to implement than the numerical (ImpModel) though the results of the latter predictions are more accurate (Palla *et al.*, 2008).

The package soil moisture Hydrus-1D runoff model has been used by Hilten *et al.*, (2008) in their study in University of Georgia, US. The performance of a modular block green roof system was evaluated using individual storms with rainfall intensity inputs based on Soil Conservation Service design storms. Hydrus-1D numerically resolves heat and moisture transport for a given soil, and the study system was simulated based on measured or estimated parameters; surface moisture fluxes (ET and rainfall) and soil properties (field capacity, wilting point, density, and sand, silt and clay fractions). The estimation for potential ET in this study has been modelled using the same Hargreaves' method from the previous study at the same green roof site. The runoff model will be validated based on measured runoff, while simulated ET will be verified by water balance-derived ET over one full study month. This is due to the difficulty of measuring small changes soil water content, longer interval are suggested (i.e. 7+ days) to obtain accurate ET values.

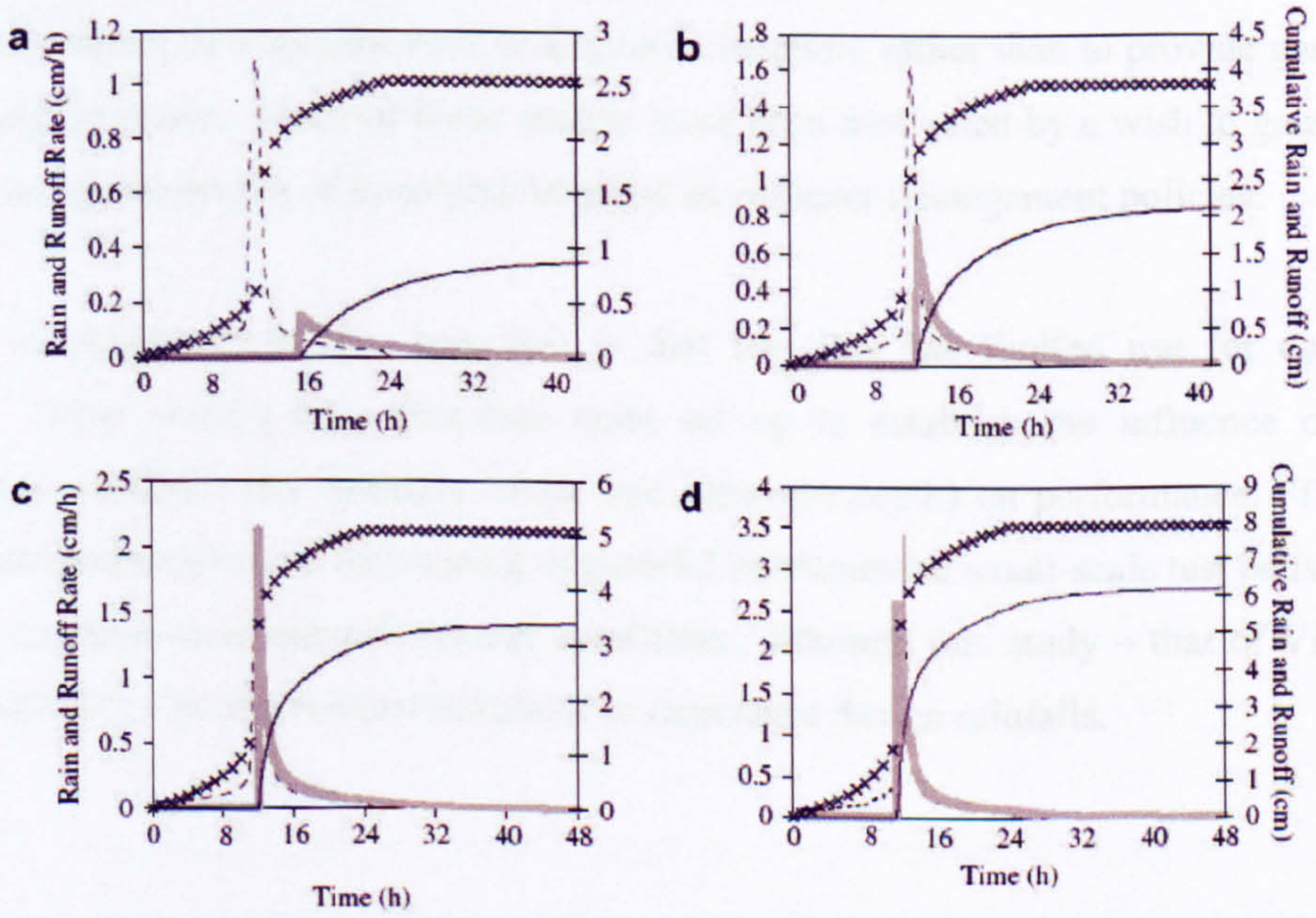


Figure 2.26: Simulated hydrographs including cumulative runoff (solid line), cumulative rainfall (x-symbol), instantaneous runoff (thick shaded line), and instantaneous rainfall (thin dashed line) for rainfall amounts of (a) 2.54 cm, (b) 3.81 cm, (c) 5.08 cm, and (d) 7.93 cm (Hilten *et al.*, 2008)

Figure 2.26 shows the design storm simulation results where for all SCS design storm, both rate and cumulative amount for the greenroofs exhibit some level of reduction. This is mainly due to the fact of the designing of blocks with drain holes 1.0 cm above the base creating a reservoir capable of holding 1.0 cm of moisture. Once the reservoir is filled, runoff commences. Overall

results from this simulation show that the performances of the modular green roof block decreases with increasing rainfall amount; and also exhibits detention for all rainfall amounts approximately by 12-hours detention times compared to detention times for an impervious roof. The model appears to over-predict the larger rainfall quantities, therefore more validation for their model needs to be done for additional large storms.

## 2.6 Discussion

The literature contains a large number of green roof hydrological performance studies. These are summarised in Table 2.6, which provides an updated version of the Mentens *et al.* (2005) overview. However, despite the large number of studies, we do not have a complete understanding of how an unmonitored green roof system will perform in a particular climatic context. This is because the majority of studies have been conducted to gain an overview of the overall performance of a specific roof in a specific location, rather than to provide generic rules to predict performance. Many of these studies have been motivated by a wish to gain evidence to support the development of local planning and stormwater management policies.

The main disadvantage of this approach is that the data has limited use for comparative purposes. Other studies have therefore been set up to establish the influence of specific configuration variables (for example, slope and substrate depth) on performance. These have generally utilised continuous monitoring of parallel instrumented small-scale test beds subjected to short to medium-term natural weather conditions, although one study – that of Villarreal & Bengtsson (2005) – used a rainfall simulator to reproduce design rainfalls.

Table 2.6: Summary with some basic characteristics of reviewed publications on water retention from green roofs (updated version from the literature review)

| Author (year) | No. of roofs | Substrate depth (mm) | Roof slope (%) | Location | Yearly Precipitation (mm) | No. of years | Seasonal Data | Rainstorm intensity ($mmh^{-1}$) |
|---|---|---|---|---|---|---|---|---|
| Full scale | | | | | | | | |
| Kohler *et al.*, (2001) | - | 50-120 | - | Berlin, Germany | 495.7-591.5 | 2 | Yes | - |
| Hutchinson *et al.*, (2003) | 2 | 50.8-114.3 | 2 | Portland, North America | 959.1 | 2 | Yes | 17-93 |
| MacMillan (2004) | 1 | 140 | 10 | Toronto, Canada | 663.8 | | Yes | - |
| Liu & Minor (2005) | 2 | 75-100 | 2 | Toronto, Canada | - | 1 | - | - |
| Moran *et al.*, (2004, 2005) | 1 | 50-100 | 3 | North Carolina | 262-1514 | 2 | Yes | 3-37 |
| Seters *et al.*, (2007) | 2 | 140 | <10 | Toronto, Canada | - | 1-2 | Yes | - |
| Palla *et al.*, (2008) | 3 | 350-430 | 2 | Genoa, Italy | - | 3 | - | 110 |
| Uhl & Schiedt (2008) | 18 | 50-350 | 0, 1.7, 26.8 | Hannover, Germany | - | 1<br>2 | Yes | - |
| Test rig | | | | | | | | |
| DeNardo *et al.*, (2003) | 6 | 76-89 | 8 | Pennsylvania, North America | 1055 | 1 | - | 4.5 |
| Mentens *et al.*, (2003) | 78 | - | 1.5, 20, 40 | Brussels, Belgium<br>Michigan, United States | - | - | - | - |
| Rowe *et al.*, (2003, 2005) | 15 | 25, 40, 60 | 2, 6.5 | Lund, Sweden | - | 2 | - | - |
| Villarreal & Bengtsson (2005) | 1 | 40 | 2, 5, 8, | Athens, Georgia, US | - | 1 | - | 24-78 |
| Carter & Rasmussen (2005, 2006) | 2 | 76.2 | 14 | Chicago, US | 1232 | 1 | - | - |
| LaBerge *et al.*, (2005) | 9 | 38.1 | <2 | Seattle, Washington | - | 2 | - | - |
| Taylor, Gangnes & Ellison (2005) | 5 | 51-102 | 2<br><2 | Michigan, United States | - | <2 | - | - |
| Van Woert *et al.*, (2005) | 3 | 25, 40, 60 | 2, 6.5 | Athens, Georgia, US | - | 1 | - | - |
| Carter & Jackson (2006) | 1 | 76.2 | - | Pennsylvania, North America | 1232 | - | - | - |
| Rezaei & Jarret (2006) | 8 | 100 | - | Pennsylvania, North America<br>Michigan, United States | - | <1 | Yes | - |
| Berghage *et al.*, (2007) | 8 | 100 | 8 | Paris, France | - | - | - | - |
| Getter *et al.*, (2007) | 12 | 60 | 2, 25 | Auckland, New Zealand | - | 1 | Yes | - |
| Baraglioli *et al.*, (2008) | - | Multiple types | | Auckland, New Zealand | - | 30 | Yes | - |
| Fassmann (2008) | 3 | 100, 150, 200 | 5, 15 | Pennsylvania, North America | - | <1 | Yes | 233-249 |
| Fassmann *et al.*, (2008) | 7 | 78 | | | 1024-1084 | <1 | - | - |
| Jarret & Berghage (2008) | 1 | 89 | 8 | | - | - | - | - |

## 2.6.1 Continuous Monitoring

It is clear that local climatic conditions will affect the performance of a green roof, and the main advantage of continuous monitoring is that the roof experiences representative weather for the specific location. If rainfall depths are high, the proportion of the rain that the roof is able to retain will tend to be reduced compared to a climate that experiences smaller rainfall depths. It is less clear from the literature whether rainfall intensity affects performance. Temperature, windspeed and other meteorological factors that affect ET are also relevant. Hotter climates will tend to experience higher ET rates, so the roof's retention capacity will tend to be restored more quickly (shorter ADWP). These relationships are complex, making interpolation from existing research to unmonitored climatic regions difficult. For example, in a warm continental climate affected by heavy convective rainfalls we would expect the ET rates to be high and the roof to generally have high retention capacity available at the start of the event. This will lead to high absolute levels of retention per event, but may still lead to a low overall retention if all storm events depths significantly exceed the storage capacity of the roof. On the other hand, a more temperate maritime climate, with frequent light rains might experience lower ET rates but better overall volumetric control.

The majority of studies report performance data measured over periods of two years' or less. In light of the recognised variability in natural climate, many hydrologists would argue that a far longer record should be collected before meaningful long-term statistical analysis can be undertaken. It is perhaps surprising that few – if any – of the studies reported to date have included rigorous return-period analysis or even an assessment of the extent to which the monitored period was typical of the location's climate.

The majority of authors have stressed the importance of seasonal factors for green roof performance. Climatic factors (i.e. monthly variations in temperature and rainfall) are important, as is the growing season for the green roof vegetation. Again, this suggests that for a continuous monitoring study to generate useful data it should operate for at least two years (two seasonal cycles) and the results should be interpreted with reference to the longer climatic record so that anomalous weather conditions are taken into account.

In addition to the long term retention performance, from a drainage engineering perspective, performance against relevant design storms is of particular use. Design storms may be applied to test beds with controlled levels of antecedent dryness using a synthetic rainfall generator. There is only one study reported in the literature which has attempted to do this, Villarreal and Bengtsson (2005), though using Scandinavian rainfall inputs.

A range of variables are employed to describe hydrological performance. The most commonly cited are: annual or seasonal retention (in mm and %); storm event retention (in mm and %); and detention parameters including time to start of runoff, peak delay and peak attenuation. It should be noted that with real rainfall events there may be some ambiguity associated with how these values are determined. Similarly, some performance data requires careful interpretation. An annual retention performance of 50% does not mean that the roof will retain 50% (or even 15%) of the rain falling during an extreme event. The annual performance figure will include a lot of small events that will be completely retained on the roof.

### 2.6.2 The Influence of Roof Configuration

The use of test beds enables specific variables to be analysed in isolation, under constant climatic inputs. This has proved to be particularly useful for observing the potential impacts of specific configuration variables, such as roof slope and substrate depth. However, in most cases

the processes responsible for differences have been inferred or assumed, rather than measured directly. For example, studies have shown that an increase in substrate depth leads to an increase in retention volume, without necessarily reporting the substrate's moisture holding capacity. Indeed, substrate composition has generally received limited attention in this group of studies, with many simply adopting 'standard' commercial substrates.

### 2.6.3 Conclusion

The complexity of climatic controls, combined with the lack of any medium or long-term continuous performance monitoring data from the UK, suggests that there would be real value in establishing a continuous monitoring facility in the UK. It is accepted that the value of a continuous record of around two years may be quite limited from a statistical perspective. However, it should also be seen that its value may be enhanced significantly if return period analysis is undertaken, and if the specific climatic conditions experienced can be compared with conditions known to be 'typical' of the particular location.

The modelling studies have demonstrated that a generic model will require not only climatic input parameters, but also parameters to describe the roof's (substrate) moisture retention properties. The roof's field capacity describes the maximum level of moisture that it can hold, whilst evapotranspiration rates determine the rate at which the retention capacity of the substrate is restored. Retention is therefore closely linked to the ADWP.

This study will therefore focus on the collection of a continuous UK record of green roof hydrological performance, and link this to the development of a generic rainfall-runoff model based on measurable physical characteristics of the substrate.

# CHAPTER 3

# CONCEPTUAL MODEL

## 3.1 Introduction

In the literature review, Section 2.5, several hydrological modelling approaches that have been used to model green roofs was discussed. Process-based model is chosen to be used to describe the conceptual rainfall-runoff model in green roof, in order to relate this model with the hydrological processes (i.e. initial losses, evaporation), roof's physical characteristics (i.e. soil properties) and local climatic condition. This type of model should enable the rainfall-runoff performance of a system that utilises different substrate materials (Chapter 4) to be predicted. To date, a number of hydrological model of green roof have been developed, including those of Hilten *et al.* (2008) and Palla *et al.* (2008). Both of the models emphasized the importance of soil moisture storage in green roof system. However, these green roof models apply quite complicated soil moisture and subsurface flow equations such as Richard's equation and Darcy's Law equation. Therefore these models may require quite a number of inputs to run the model and it means that the model may be applicable for their own system only. Thus, the aim of this model in this study is to develop a simple and generic conceptual rainfall-runoff model, such as that proposed by Mentens *et al.* (2003) using simple water balance equation and make them related with soil physical properties, so that one transferable model can be developed and can be applied to any green roofs. Hence, this chapter will explain further on the conceptual basis of the model.

This chapter is the main part of the study before further discussion on data collection from the experimental in Chapter 6 and model development in Chapter 7 is undertaken. Great understanding on the relationship between model conceptual and data collected are needed, hence will provided significant analysis between these information for further model development and further experimentation. It is decided to develop a process-based model for our green roof study; therefore studies by Jarret *et al.*, (2006) and Taylor & Gangnes (2004) are used as the main reference because of the similar approach with what we need; the process-

based model incorporating losses parameter and storage-routing method. The substrates characteristics (i.e soil porosity, density, permeability) can be quantified in the laboratory (refer to Section 4.3) with reference to the FLL guidance (as used by Penn State (Berghage *et al.*, 2007)) using the material testing protocols (Appendix 3.1). By using this laboratory quantification and monitored data from green roof rigs, it is expected to be able to relate these physical properties data with the modelling to predict the rainfall-runoff response from the soil properties.

## 3.2 Conceptual Process-Based Model Development

As described in Section 2.2.1, green roof systems typically comprise three main layers, as shown in Figure 3.1(a):

1. The layer of vegetation;
2. The substrate layer to support the growth of the plants. This part of layer is the most significant layer from the stormwater management/moisture retention perspective. The substrate's moisture retention is assumed to be divided into two main compartments (Figure 3.1(b)); transient storage and substrate moisture storage (which also have two main compartments; permanent retention storage (lower part) and potential retention storage (upper part));
3. Drainage layer is assumed to be part of permanently-retained moisture;

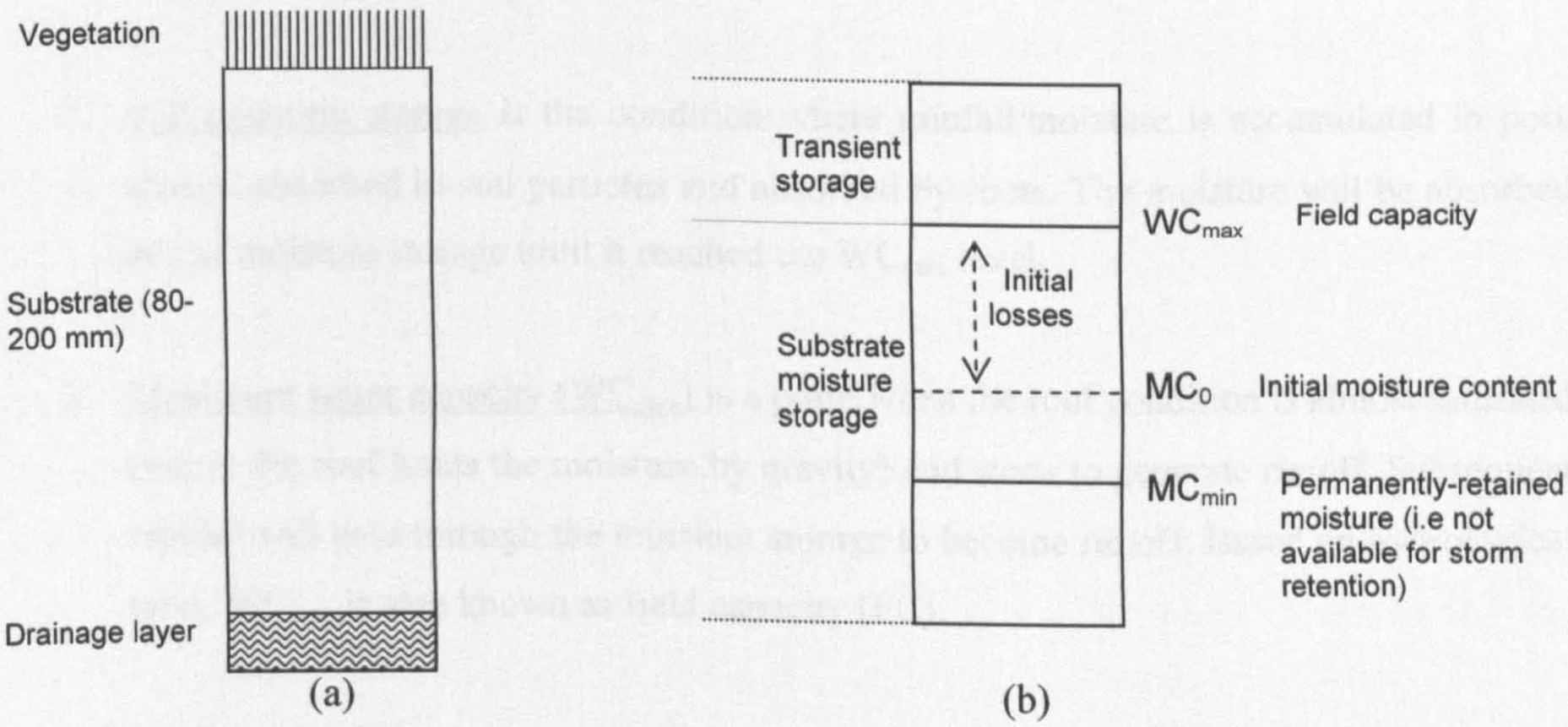


Figure 3.1: (a) Typical vertical structure of a green roof system; (b) Moisture content in the substrate

The model will not initially attempt to account for the hydrological effects of different vegetation types, though their moisture retention and evapotranspiration characteristics are expected to affect the system's hydrological response. Similarly, the drainage layer beneath the substrate is also not going to be assessed in this study.

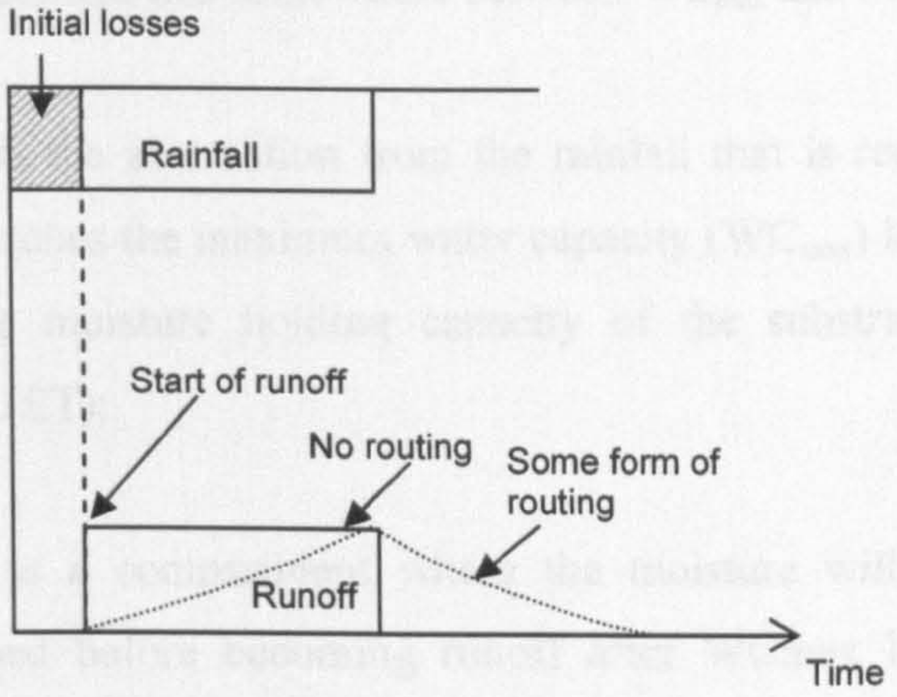


Figure 3.2: Diagram of rainfall separation from the losses and become direct runoff; will be then routed into hydrograph

Figure 3.2 illustrates the timing associated with the movement of rainfall into the substrate's storage compartments. Key definitions are provided below:

1. Rainfall. When rain falls on the roof, it will be initially absorbed by the roof as soil moisture storage;

2. Soil moisture storage is the condition where rainfall/moisture is accumulated in pore spaces, absorbed in soil particles and absorbed by roots. The moisture will be absorbed in soil moisture storage until it reached the $WC_{max}$ level.

3. Maximum water capacity ($WC_{max}$) is a point when the roof condition is almost saturated (where the roof holds the moisture by gravity) and starts to generate runoff. Subsequent rainfall will pass through the transient storage to become runoff. Based on hydrological term, $WC_{max}$ is also known as field capacity (FC).

4. Minimum moisture content ($MC_{min}$) is reached when the roof remains dry for a long period. $MC_{min}$ also known as ambient dry level (ADL). It is also known as maximum available storage. It is expected that the $MC_{min}$ could not be reduced to zero in

temperate climatic regions, as atmospheric moisture levels will be too high, and temperatures too low to remove all moisture.

5. Initial moisture content, $MC_0$. It is assumed that at the start of a rainfall event the substrate moisture content lies somewhere between $WC_{max}$ and $MC_{min}$.

6. Initial losses (IL) is the abstraction from the rainfall that is retained in soil moisture storage before it reaches the maximum water capacity ($WC_{max}$) level. It is assumed that in this model, the moisture holding capacity of the substrate is restored due to evapotranspiration (ET);

7. Transient storage is a compartment where the moisture will pass through and be temporarily detained before becoming runoff after WCmax has been reached. The transient storage process will be modelled using storage reservoir routing.

Based on Figure 3.1(b), it is assumed that the moisture content at a given time t, $MC_t$ will lie somewhere between the maximum water capacity, $WC_{max}$ (i.e. field capacity), and a minimum practical moisture content, $MC_{min}$, which may alter slightly in response to ambient conditions. So, in a rainfall event, substrate will absorb moisture and $MC_t$ will increase up from its initial value, moisture content at time zero, $MC_0$ until the point when $WC_{max}$ (field capacity) is reached. Note that $WC_{max}$ may be quantified in standard laboratory material tests (Section 4.3.1), but that this is currently not the case for $MC_{min}$. It is also important to note that $MC_{min}$ is likely to be significantly higher than zero, as zero moisture content corresponds to oven-dry conditions. $MC_{min}$ may be considered to define the depth of permanently retained moisture. $MC_0$, and the depth of initial losses, IL ($IL = WC_{max} - MC_0$) are assumed to depend on the antecedent conditions. If the event is preceded by a long dry spell, $MC_0$ will be closer to $MC_{min}$ (high initial losses) than when the ADWP is short (small initial losses). Therefore, based on this theoretical assumption, evaporation experiments (as substitute for evapotranspiration) have been undertaken to identify ET rates and the $MC_{min}$ (Section 4.3.2). Rainfall occurring after $WC_{max}$ has been reached will pass into transient storage, where it will be temporarily detained before becoming runoff. This runoff will be modelled using linear reservoir/storage routing.

### 3.2.1 Initial losses and Storage Routing Approaches

In Section 2.5.4.2 and 2.5.4.3, the explanation on the theoretical of both initial losses and storage routing approaches has been undertaken. The intention of this study therefore is to relate both the initial losses estimation and reservoir routing process to fundamental, measurable, physical properties of the system. Therefore, two main approaches have been applied in the model, both on different compartment; initial losses in storage moisture compartment and storage routing in transient storage compartment. Generally, basic water balance for a reservoir for the initial losses estimation is described by equation (2.2): $Q = P - ET - D - \Delta S$ (Mansell, 2003). However, as in the green roof system no drainage to the groundwater is expected, hence the water balance equation for the system will be:

$$Q = P - ET - \Delta S \qquad (3.1)$$

The established test rig physical properties data in Chapter 6 are going to be used to describe characteristic details in the model later in Chapter 7. The relationship of storage routing and water level is described in equation (2.5): $Q = kH^n$. Parameters in both equations are tool equation to describe the timing and runoff storage in the system. Main parameters needed in the modelling as described in equation (3.1) and (2.5) in time dependent are as follows:

Table 3.1: The description of parameters that mainly used for the losses modelling and storage routing

| Model | Parameters | Description |
|---|---|---|
| Initial losses (Potential retention compartment for the volume of runoff) | Known data:<br>Precipitation (P) | As input from monitoring data values. |
| | Known parameter:<br>• WCmax (FLL test)<br><br>Unknown parameter :<br>• $MC_{min}$ (mm)<br>• $MC_0$ (mm)<br>• ET rate (mm/day)<br>= $\frac{WC_{max} - MC_0}{ADWP}$ | To derive the initial losses (assumed due to ET rates) value in substrate will be depended on its ADWP in substrate physical properties. These parameters need to be estimated by experimental work (Chapter 6). Parameters that need to be derived from experimental work before ET rate can be estimated are $WC_{max}$ and $MC_{min}$. While $MC_0$ value which can be derived based on previous substrate ADWP condition also need to be investigated.<br>• $MC_{min}$ (f(substrate properties, climatic variables))<br>• $MC_0$ (f(ADWP, ET)<br>• ET (f(climatic variables, substrate properties, vegetation) |

| | | |
|---|---|---|
| Storage routing (Transient storage compartment for the timing of runoff) | Known variables:<br>• Inflow ($Q = kH^n$)<br><br>Unknown parameter<br>• k<br>• n | Runoff from the potential retention compartment will be used as the input and based on the size of the green roof the inflow will be estimated. Q is predicted outflow based on the previous h, h is the depth of the moisture in the substrate, k and n are routing parameters. The values of k and n parameter are related to the roof's physical properties and to define the amount of lag/attenuation for runoff to begin. The output data (outflow) in routing development will be related to physical properties coefficient k and n. Both the coefficient parameters will be derived from the best fitted modelling back-calculated. |

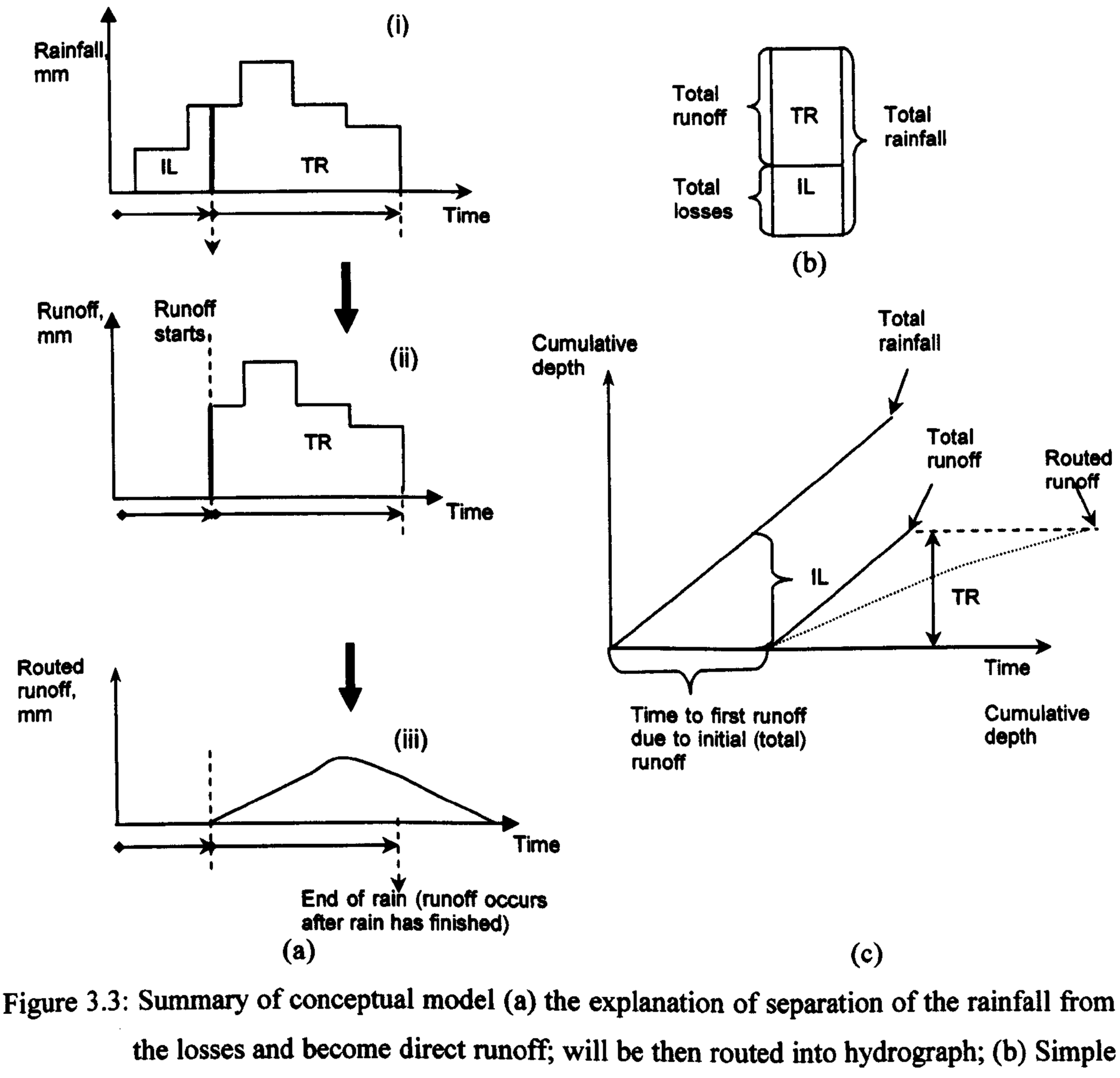


Figure 3.3: Summary of conceptual model (a) the explanation of separation of the rainfall from the losses and become direct runoff; will be then routed into hydrograph; (b) Simple description of the separation, and; (c) Illustration of the whole process in one figure

Figure 3.3 summarizes the details from Figure 3.1, Figure 3.2 and Table 3.1. The initial losses and storage routing models are providing basis for the model development that has been undertaken using the Microsoft Excel spreadsheet (Appendix 3.1).

In this conceptual theory, it is expected that the unknown parameter values will be dependent upon measurable substrate characteristics, such as depth, porosity, water permeability, particle density etc. Therefore, based on the conceptual process-based model (Figure 3.2), the aims of the next chapters (Chapter 5, 6 and 7) will be to identify values from the monitored data and demonstrate the conceptual model can be fitted to monitored data (Chapter 5). Laboratory experiment needs to be undertaken to see whether these parameters vary as a function of substrate types used on the roof under different condition. All these parameters of soil moisture loss rate (ET rate) and minimum moisture content, $MC_{min}$ will be determined in order to establish general relationship to link the parameter values to relevant measureable physical properties characteristics.

# CHAPTER 4

# EXPERIMENTAL SETUP

## 4.1 Introduction

As stated in Chapter 2 (Section 2.4), two types of green roof experimental set-up have been used by many researchers to evaluate the stormwater performance; full-scale roof and small-scale test rigs. In this study, we are concentrating on providing field and experimental data for a green roof numerical model using eleven small-scale test rigs subject to field environmental condition.

The objective of the modelling work will be to generate a high temporal resolution (5 minute) process-based rainfall-runoff model for a green roof. The inputs to such a model should be rainfall, the physical characteristics of the configuration (e.g. substrate depth), and measurable characteristics of the substrate (e.g. evaporation, porosity, hydraulic conductivity). This chapter will cover the data instrumentation setup for the experimental works and is divided into two parts, as follows:

1. Field monitoring setup
2. Substrate tests – experimental setup

## 4.2 Field Monitoring Setup

The aim of the monitoring is to provide field experimental data on hydrological performance that could be used to develop and calibrate the model. Hence, small-scale test rigs equipped with continuous monitoring instrumentation has been developed. Initially, one test rig was installed on a roof of the engineering building in Mappin Street, Sheffield. Another ten test rigs were constructed in 2008 – 2009 by the Green Roof Centre, University of Sheffield (link to: http://www.thegreenroofcentre.co.uk/) on the Sir Robert Hadfield Building. The ten test rig replicated the configuration profile of the main test rig, but with combinations of different substrates (Section 4.2.1) and vegetations. Note that within this thesis only preliminary finding

on the substrates properties characteristics will be reported on within this thesis. The Mappin test rig is the only main rig that has been monitored to gather information about the green roof characteristics and rainfall runoff performance since 2006.

### 4.2.2 Description of the Test Rigs

The 3 m x 1 m main test rig on Mappin Building uses a standard Alumasc extensive green roof profile system (Alumasc, 2004). The design profile for this main green roof is shown in Figure 4.1.

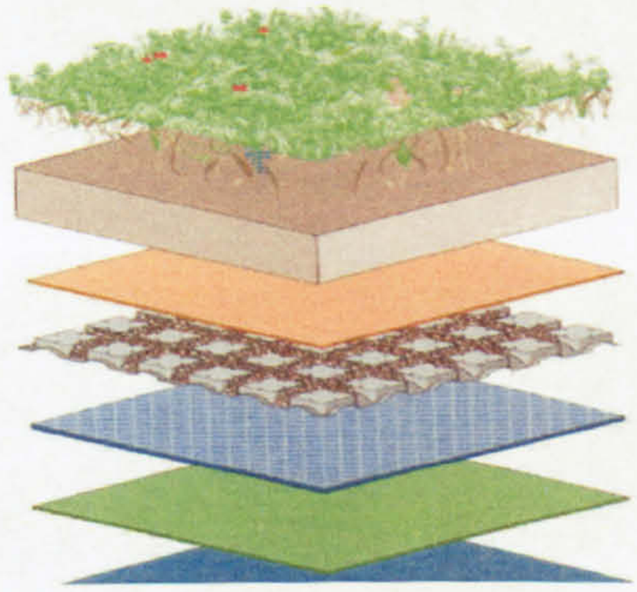

- Sedum mat
- Alumasc extensive green roof substrate
- Filter membrane
- Flora Drain FD25 drainage layer
- No moisture mat is present
- Waterproof membrane
- Base of the test rig

Figure 4.1: Test rig profile

(Source: Alumasc 2004)

The lightweight sedum mat is ideal for minimising the load on the building. Sedum is a robust plant that does not require care and therefore it does not incur high maintenance costs. The Alumasc semi-extensive green roof substrate build-up height is 80 mm and comprises a mixture of 4-15 mm recycled crushed brick (Zincolit) and fines growing media. A fine particle filter membrane separates the substrate from the 25 mm deep Flora Drain FD25 'egg box' drainage layer below which water collects in storage cells. Roots are supplied with both air and water through capillary action. No moisture mat is present in the setup, whereby when present it would usually retain more moisture and nutrients. When wet the weight of the system is approximately 98 kg/m$^2$. The drainage layer alone has a stated retention capacity of 23 l/m$^2$ (Alumasc, 2004).

To allow runoff collection, a storage tank has been positioned under the test rig frame (Figure 4.2(a)) which has been connected to the gutter at the bottom edge of the test rig. The test rig is raised 1 m above from the ground (roof) surface. To direct the water into the gutter, the test rig is set to a slight angle of between 1° and 2°. The structure and the configuration of the existing

test rig have remained constant during monitoring and it has produced a set of results with variables that relate to the rainstorm properties only.

(a) (b)

(c) (d)

Figure 4.2: Stage of test rig construction in Mappin Street, Sheffield (a) Structure of test rig; (b) Drainage layer and gravel ballast; (c) 80 mm of substrate, and; (d) Sedum mat

### 4.2.2 Selection of Parameters to Test

There are some consideration needs to be taken before any roof system can be constructed. As shown in literature reviews, several variables in the test rig configuration could affect retention and the hydrological performance of green roof including substrate type, type of vegetation, slope and drainage layer. For long-term consideration of this study, two variables might be tested; substrate type and type of vegetation. The other two variables; slope and drainage layer need to be excluded due to the following reasons. For the slopes, in order to utilize the flat roof in most urban area; by using the current 2° slopes should be enough to represent the flat area.

Whereas for drainage layer, Flora Drain FD25 'egg box' drainage layer is a commonly used, lightweight and efficient way of storing water, so this drainage layer is the most suitable structure to be used in term of decreasing the green roof load.

The objective in constructing another ten test rigs is to learn about the hydrological response using different types of green roof configuration (i.e. vegetation type, substrate type). However for short-term consideration, in this study, it is expected to initially understand only on the characteristics of different types of substrate for the purpose of model development. Hence the Green Roof Centre is supplied the study with two commercial substrates, Alumasc Heather with Lavender and Alumasc Sedum Carpet type, together with locally-sourced waste substrate products Green Estate (GE) compost and Light Expanded Clay Aggregate (LECA) and loam. These components were blended into a LECA-based mixture: LECA + GE + loam. Note that products from Alumasc use secret recipes; therefore the information quoted for Alumasc product data is nominal and subject to production tolerance. The soil mixtures from Alumasc are normally composed of recycled products with the addition of organic matter. They are regularly tested to comply with the German FLL standards.

Table 4.1: Physical properties for substrate type chosen for the green roof study

| Substrate Type | Physical Properties |
|---|---|
| 1) Alumasc Heather with Lavender (Al-HL);  | As quoted from Alumasc (2005) for both substrate from Alumasc: Heather with Lavender is a growing medium consisting of a specific blend of high quality crushed brick and selected mineral aggregates, enriched with a small amount of mature compost. The product has excellent water permeability, and has high porosity.<br><br>Porosity 64%; pH value 7.8; Dry Weight 940kg/m³; Saturated Weight 1360kg/m³; Maximum water capacity 42%; Air content at maximum water capacity 22%; Water permeability ≥0.064 cm/s |

| | |
|---|---|
| 2) Alumasc Sedum Carpet (Al-Sedum);<br>  | Sedum Carpet substrate is a growing medium consisting of a specific blend of high quality crushed brick and selected mineral aggregates, enriched with a small amount of mature compost. The product has excellent water permeability, and has high porosity.<br><br>Porosity 63%; pH value 7.9;Dry Weight 980kg/m³; Saturated Weight 1240kg/m³; Maximum water capacity 25%; Air content at maximum water capacity 38%; Water permeability ≥0.1 cm/s |
| 3) LECA + GE + Loam (LECA mixtures);<br>LECA<br>  | LECA (Light Expanded Clay Aggregate) are small globes of burnt and puffed clay which provides a lightweight, pH neutral and porous material, which has the ability to store water. They have been used in many hydroculture/hydrophonics application, and blended with other growing media to improve drainage and insulate roots from frost. (Quoted from http://www.specialistaggregates.com/technical-aggregates/hydroleca-pack-p-1368.html) |
| Green-Estate compost<br>  | Green Estate compost is locally-sourced organic compost from waste products. This compost will increase the organic matter content, supplies nutrients and will improve the physical properties of soil to support plant growth. |
| Loam<br>  | Loam is a combination of sand, silt, clay type of soils where it is suitable for plant roof because it could hold moisture but also could drain well (Quoted from http://www.hort.purdue.edu/ext/loam.html)<br><br>The combination of these three types of soil was intended to provide a lightweight green roof substrate with enough nutrients for vegetation and also provide retention for moisture. |

### 4.2.3 Rainfall Monitoring

Continuous rainfall data at 1 minute intervals have been collected for the test rig using a standard ARG100 Tipping Bucket Rain-gauge (Figure 4.3). Inside this rain gauge there are two buckets that tip for every 0.2 mm depth of rain. Every time one of the buckets is filled, it moves to the downside and the other one will take its place to collect the rain. An electric signal is sent to the data logger, for every tipping movement of rain gauge at 0.2 mm resolution.

Figure 4.3: Standard ARG100 Tipping Bucket Rain-gauge is located next to the test rig on the Mappin roof

Rain gauges are easily affected by wind, exposure and height of the gauge (Engineering Manuals, 1994). In order to allow reliable comparable data of rainfall with the quantity of observed runoff, the tipping bucket was placed at the same height as the test rigs (Figure 4.3) and it was free from surrounding obstacles. A real-time display of the rainfall runoff outputs from this system can be found here (link to: http://greenroof.shef.ac.uk/)

### 4.2.4 Runoff Monitoring Instrument, Calibration and Verification

In this project we have eleven storage tanks/barrels and eleven water depth pressure transducers/probes. Laboratory tests have been undertaken to make sure that instrumentation will work accurately on site. Calibration of the pressure transducer and runoff collection barrel on Mappin building was undertaken. To determine the accuracy and the condition of the

instrumentation, calibration analyses for all probes including on Mappin building were done (Table 4.2). The main systems used in this project are summarized below:

Table 4.2: Summary of calibration made for small scale green roof approaches

| Application System | Description | Equipment | Calibration/Validation |
|---|---|---|---|
| • On Mappin Building | • Volume-based<br>• One runoff collection barrel (area varies with depth) | Water level depth<br>• CR1000 logger<br>• Druck PTX 1730 electric current pressure transducer (One piece) | • Runoff barrel<br>• Calibration mV – mm for the transducer |

Flow measurement devices are either volume-based systems which measure water accumulation in a storage tank, rain-barrel or cistern, or rate-based systems which need a specific and calibrated hydraulic devices to establish the rate of flow from water depth at any given instant (Taylor, 2006). Both rate-based and volume-based devices can be used to monitor the runoff characteristics for both small scale test rigs and full scale roofs. Rate-based devices employ primary devices such as a shaped flume, weir or orifice; and secondary devices such as a pressure transducer, probe or gas bubbler to measure water depth (head) (Taylor, 2006). As we are concentrating on small-scale test rig performance a volume-based system was designed. Pressure tranducers/probes are used to collect runoff data, which is stored by a data logger. It was felt that a rate-based system would be unlikely to deliver sufficient sensitivity at low rates of runoff; hence we decided to use a volume-based system for our runoff monitoring.

The principle of volume-based measurement is that the volume of runoff is a function of the depth of water in the collection instrument; rain-barrel. The runoff level in the calibrated barrels is recorded using a secondary device which provides an electric signal unit of voltage, milivolt (mV) to a data logger. The volume in the barrel (as indicated by the measured depth) is then converted into an equivalent runoff depth. The barrel used in the current project has been programmed to empty once per day at 9:00:00, or when it gets full, using a solenoid valve (Refer to Appendix 4.1). The storage barrel on the Mappin Building test rig was profiled into three different zones to provide greatest sensitivity at the start of a runoff event (Figure 4.4).

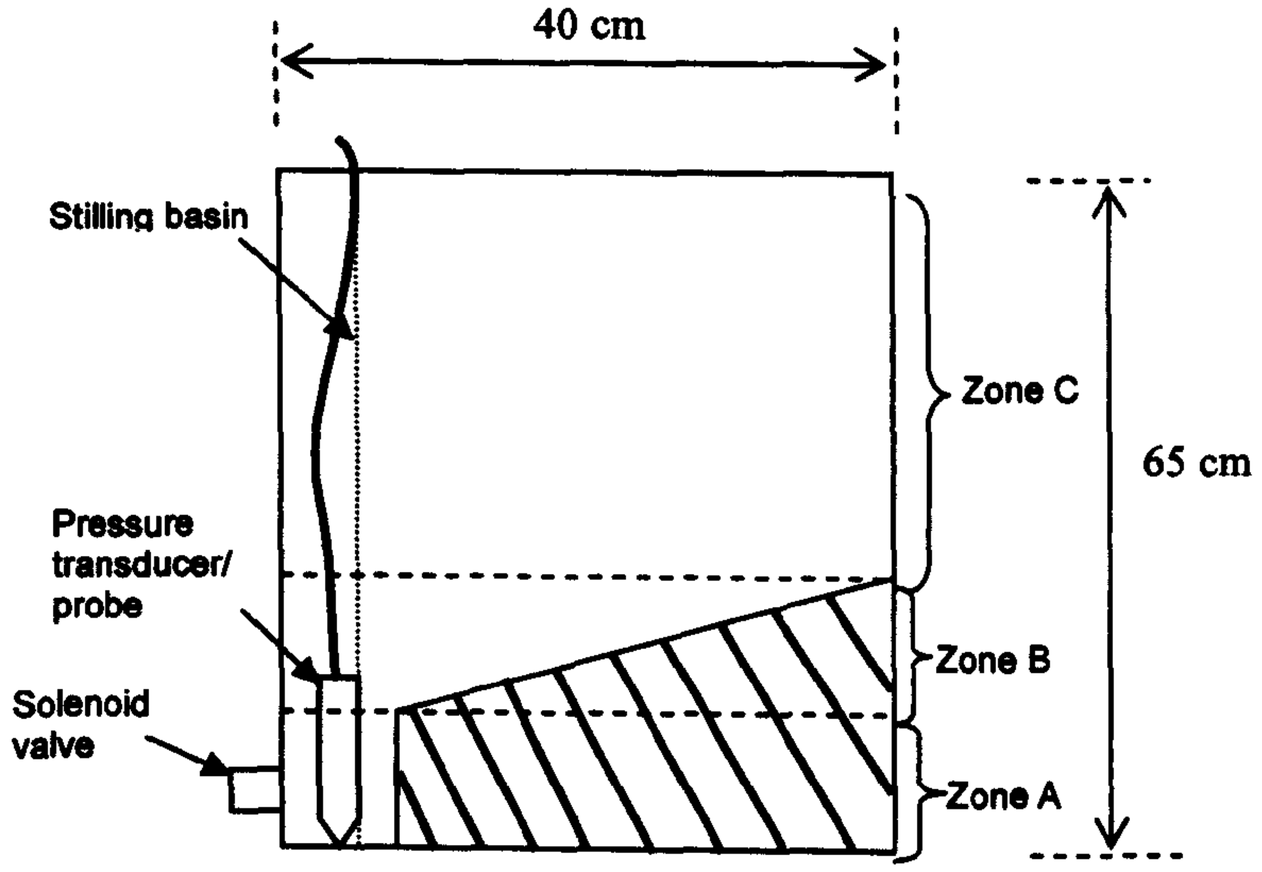


Figure 4.4: Vertical cross-section showing the profile of the storage tank/rain barrel on Mappin Building (Barrel)

### 4.2.4.1 Runoff Instrument Calibration - Relationships between Depth, Volume and Runoff for the Collection Tank

A Campbell Scientific CR1000 data logger is used to monitor and control the single Mappin Building test plot. The logger was programmed to empty the storage tank at 09:00:00 daily or whenever the water reaches a voltage corresponding to the top of the collection tank (Figure 4.5(b)). The test rig was installed with a Druck PTX 1730 electric current pressure transducer/probe. Calibration tests needed to be undertaken before the system could be fully used on site. During the test, the logger was used to collect and store the depth data sent from the probe and at the same time water depth were read manually using a vernier scale (Figure 4.5(a)). A program was produced to allow the logger to read the probe responses automatically (Appendix 4.1). Figure 4.6 shows sample rainfall and runoff data collected by the transducer after resetting the tank datum.

(a)

(b)

(c)

(d)

Figure 4.5: Re-calibration work on the established test rig (a) Water level is measured using the pressure transducer and verified manually using a vernier scale; (b) Solenoid automatically opens the valve when the water level reached its maximum level; (c) CR1000 data logger; and (d) The Druck PTX 1730 electric current pressure transducer

Figure 4.6 – 4.8 show examples of the results collected from the pressure transducer at different times during the monitoring period. They confirm that the test provided confidence in the pressure transducer and logger in combination to be used to read runoff responses. The traces clearly show a steady background reading (around 700 mV), and it can be seen that the barrel empties and returns to this value when it reached its defined 'full' level (around 1800 mV) during runoff events.

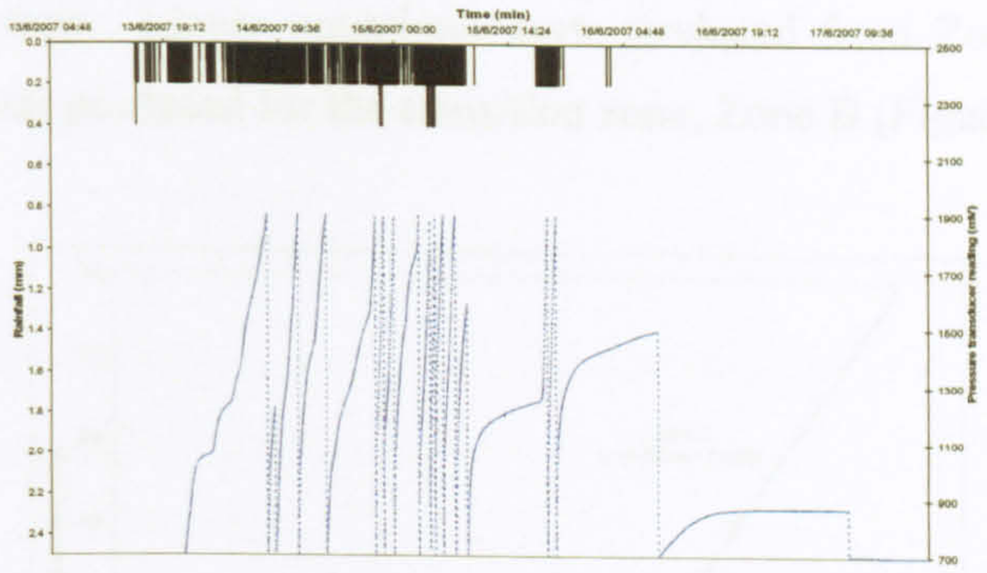


Figure 4.6: An example output for rainfall-runoff from Druck PTX 1730 pressure transducer and tipping bucket in 2007

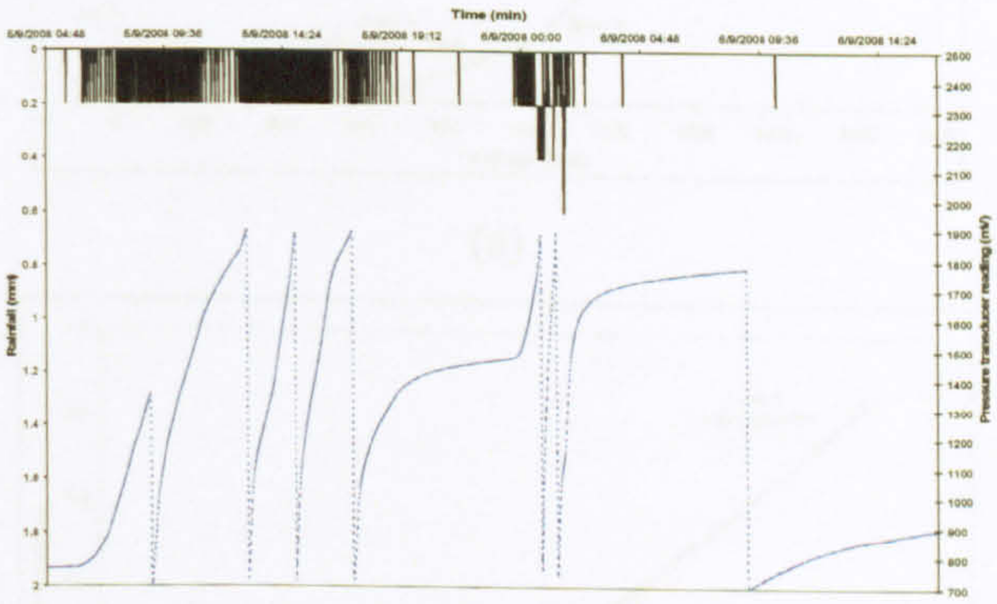


Figure 4.7: An example output for rainfall-runoff from Druck PTX 1730 pressure transducer and tipping bucket in 2008

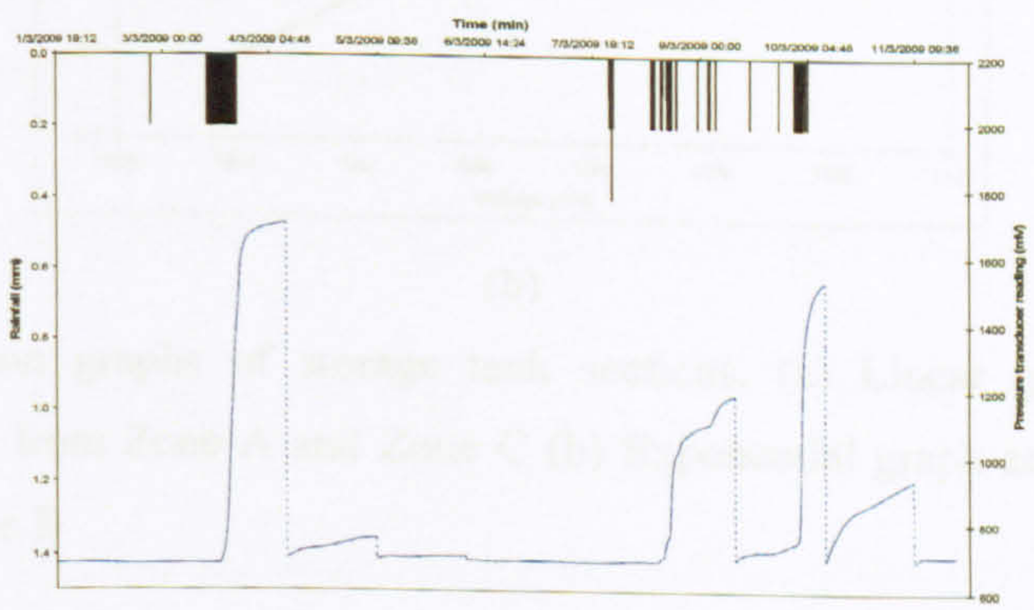


Figure 4.8: An example output for rainfall-runoff from Druck PTX 1730 pressure transducer and tipping bucket in 2009

### 4.2.4.2 The Calibration Graph for Barrel

The calibration graphs for the Mapping Building test rig are shown in Figure 4.9 (a) and Figure 4.9 (b). Figure 4.9 (a) shows a graph of runoff (mm) against the voltage reading from the probe

(mV) for the storage tank. Linear equations were produced from Zone A and C, while an exponential equation was produced for the transition zone, Zone B (Figure 4.9 (b)).

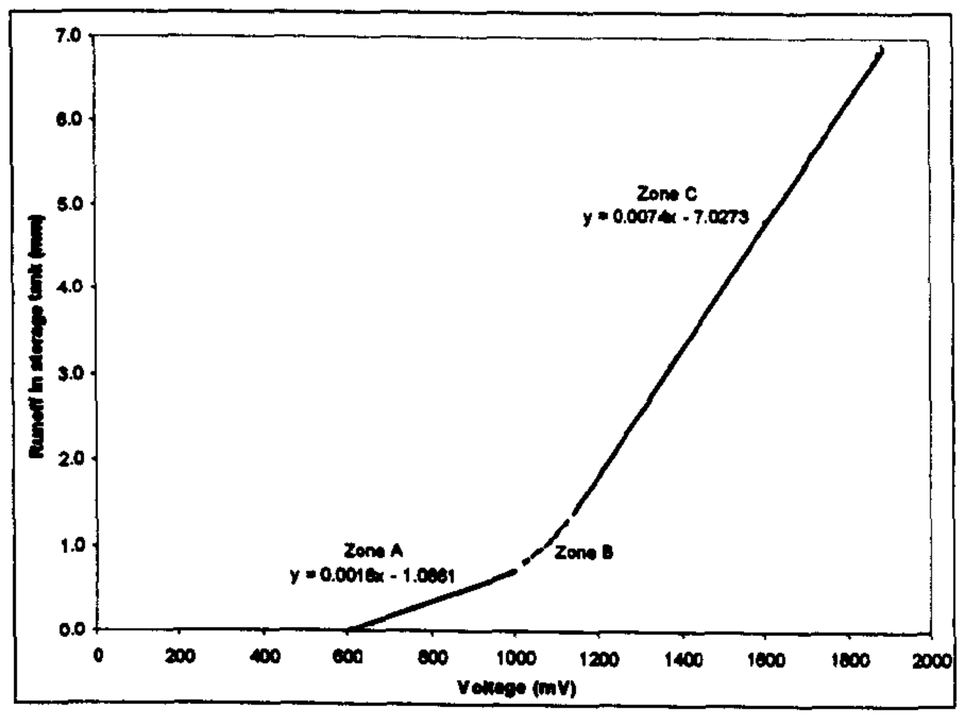


(a)

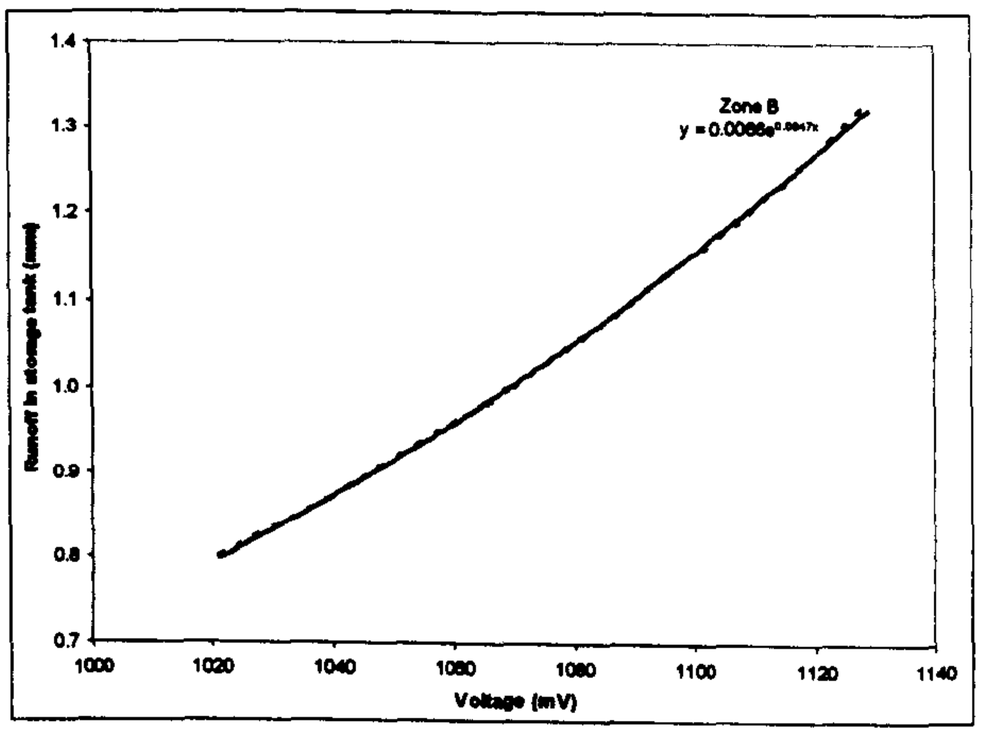


(b)

Figure 4.9: Calibration graphs of storage tank sections. (a) Linear graphs and equations produced from Zone A and Zone C (b) Exponential graph and equation produced from Zone B

The equations produced from these three calibration zones were used to convert voltage data (mV) from the probe into the corresponding runoff depth (mm) in the tank. Runoff volume was calculated from the water discharge ($m^3$) into equivalent runoff depth (mm) over the area of test rig ($m^2$). For every 1 mm of rainfall that fell onto the (3 m × 1 m) test rig the equivalent volume is 0.003 $m^3$ (3 litres). Hence, every 1000 ml of water in the storage tank was equivalent to 0.33 mm of runoff. From these calibration graphs, the conversion equations were derived as follows:

Sensitive response zone (Zone A), voltage < 992.44 mV ; $y = 0.0018(x) - 1.0861$

Transition zone (Zone B), voltage < 1195.99 mV ; $y = 0.0066e^{0.0047x}$

Top zone (Zone C), voltage > 1195.99 mV ; $y = 0.0074(x) - 7.0273$

Where $y$ represents runoff depth in mm, $x$ represents the voltage in mV. It is suggested to do re-calibration for the instruments once a year to provide confidence in data collection.

### 4.2.4.3 Resolution and Storage Capacity for Barrel

This assessment was made to provide information about the probe's resolution, barrel's storage capacity and how these two instruments related each other. The inspection have been made to each barrel and probe to confirm that each of them work within its valid resolution. Barrel represents the set-up on Mappin building.

From the re-calibration test on 1st Oct. 2007 (Figure 4.12(a)), during the daily emptying procedure, the empty water level in the tank corresponded to a voltage response of 697 mV, while the maximum voltage response was found at voltage response 1889 mV. Therefore, the effective range for the barrel was between 697 mV and 1889 mV.

$y = 0.0018(697) - 1.0861 = 0.169$ mm

$y = 0.0074(1889) - 7.0273 = 6.950$ mm

Hence, total volume of storage tank capacity is equivalent to a total rainfall of 6.781 mm

Test bed catchment area = 3000 $mm^2$

Therefore, total volume of storage tank capacity = 6.781 mm x 3000 $mm^2$ = 20343 ml
(During calibration test, 20800 ml of water was poured in and it poured out (due to automatic valve operation) somewhere between 19800 ml and 20800 ml (i.e. 20343 ml).

A similar calculation was also carried out for the sensitive response zone in the tank;

$y = 0.0018(697) - 1.0861 = 0.169$ mm

$y = 0.0018(992.44) - 1.0861 = 0.700$ mm

From this calculation, it shows that the volume capacity within the sensitive zone range in the storage tank has the initial runoff for the first 0.53 mm of a rainfall event.

Using water depth readings, independent checks on the experimental sensitivity were carried out. The linear equation derived in the sensitive zone, $y$ (mm) = 0.0018$x$ (mV) – 1.0861, shows that, every 1 mV variation in pressure indicates a change of 1.9 x $10^{-3}$ mm of runoff in the tank. Similar checks for the top zone of the tank were also done, where 1 mV = 7.2 x $10^{-3}$ mm. Both of these linear resolution responses show they have greater sensitivity than the rain gauge at 2.0 x $10^{-1}$ mm.

### 4.2.4.4 Stability of the Pressure Transducer Readings

The following investigations were undertaken to check on the stability of the transducer readings in response to the small changes in the environment such as temperature, wind, air pressure or other local movement (nearby construction activities, valve activation or building vibration). The analysis of instrument noise was done at three different time scales; long-term fluctuation trend, diurnal fluctuation and short-term fluctuation.

The long-term trend check was done for assuming 5 days dry period (Figure 4.10). The data set shows that the fluctuations from the transducer developed a diurnal pattern. The overall steady decline in Figure 4.11 is thought to be caused by the evaporation of water from the storage tank. This means that the stored water will reduce slowly until a new event of rainfall occurs. This long-term linear decline averaged 0.004 mm of equivalent runoff depth per day.

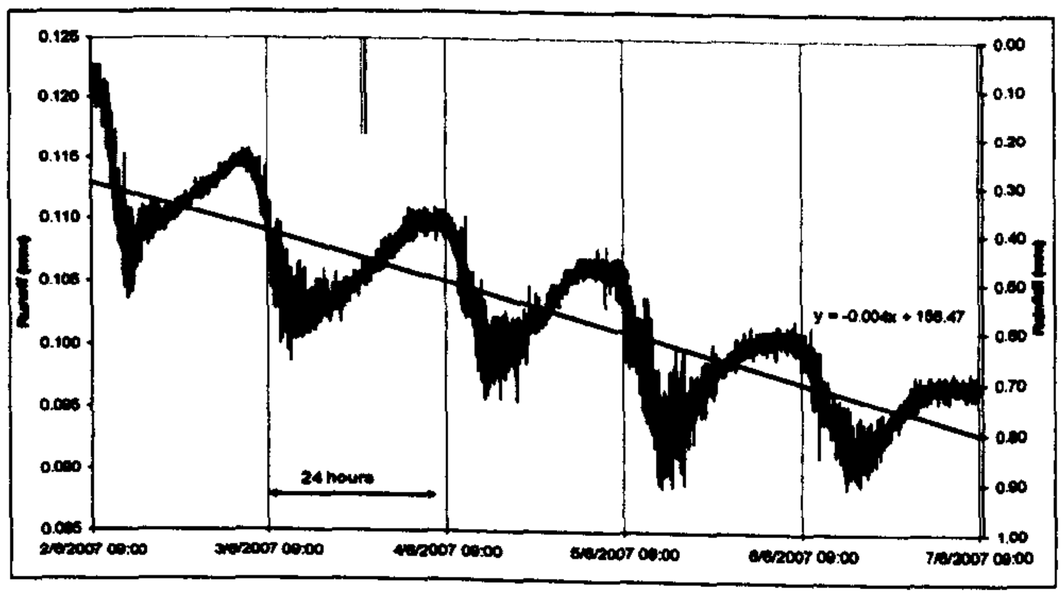


Figure 4.10: Background fluctuation of runoff volume in tank in dry weather period; the 24 hours indicate the 9:00 to 9:00 diurnal cycle

In order to focus on the smaller time-scale diurnal fluctuation, the analysis was carried out from 9:00 to 9:00 (Figure 4.10). From Figure 4.10, the minimum and maximum fluctuation reading

of diurnal range averaged at 0.015 mm of equivalent runoff depth. The comparison between Figure 4.10 and 4.11 shows that the higher variation of fluctuation in Figure 4.11 occurred at the same time as the lower readings in Figure 4.10, at approximately 9:00 to 21:00 (12 hours day time). This higher level of noise suggests that the fluctuation was influenced by daily activities and thermal expansion.

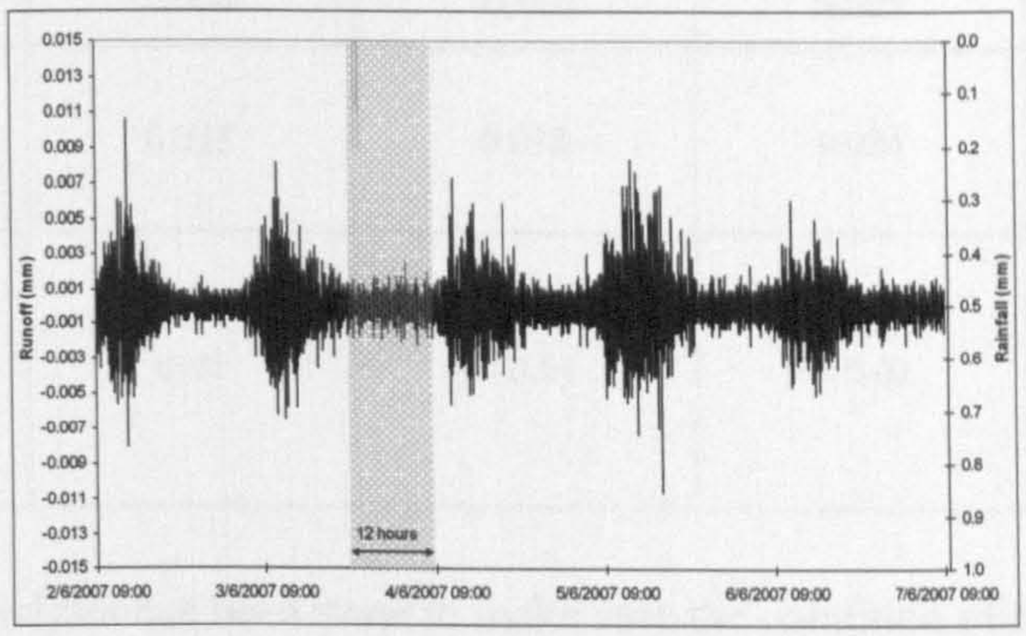


Figure 4.11: A discretised fluctuation of runoff volume from the background fluctuation

Figure 4.10 shows that the pressure transducer recorded the same pattern of noise and trend every 24 hours. The short-term fluctuation shows that the reading in Figure 4.10 started to fall after 7:00 every morning and started to rise back at approximately around 14:00 to 16:00 each day. Based on Figure 4.10, the short-term fluctuations range averaged at 0.01 mm of equivalent runoff depth. This might be due to the day's activities at the test rig surrounding area and also might relate to the temperature as well. The mechanism of fluctuations read by the pressure transducer can be concluded in Table 4.3 where activities in these three phenomena seem to relate with each other.

The quantities of equivalent runoff depth in each phenomenon (Table 4.3) in the data were significantly smaller than the rain gauge resolution at 0.2 mm. This means that these fluctuation errors can be considered to be negligible within most rainfall events.

Table 4.3: Summary of local fluctuations for different phenomenon for June 2007, April 2008 and May 2008

| Phenomenon | Quantity equivalent to runoff depth (mm) June 07 (18.6°C – 11.2°C) | Quantity equivalent to runoff depth (mm), April 08 (11.4°C – 4.4°C) | Quantity equivalent to runoff depth (mm), May 08 (17.5°C – 8.6°C) | Mechanisms |
|---|---|---|---|---|
| Long-term trend (Daily mean) | 0.004 | 0.0003 | 0.005 | Evaporative loss |
| Diurnal range (Maximum in early morning, minimum in midday) | 0.015 | 0.015 | 0.024 | Thermal expansion, probe effect |
| Short-term fluctuations (Maximum in midday, minimum in night day- Figure 4.13) | 0.01 | < 0.01 | < 0.01 | Activity (noise) worse during working hours |

Another sensitivity analysis has been done to make sure the condition of the pressure transducer is still significantly smaller than 0.2 mm rain gauge resolution. The long-term trend line check was done for 3 days (April 08) and 5 days (May 08) of dry day period. As mentioned above high temperature might lead on the thermal expansion and evaporation activities read by pressure transducer fluctuation. It was shown in this long-term fluctuation (Figure 4.12 (a)) where the stored water does not show decreasing in trend line compared to trend line in Figure 4.12 (b) because rainfall event has occurred on previous day before these 3 dry days. The fluctuation in Figure 4.12 (a) has demonstrated the data of dry days in low temperatures. This long term fluctuation (Figure 4.12) averaged 0.0002 mm (April 08) and 0.005 mm (May 08) of equivalent runoff depth.

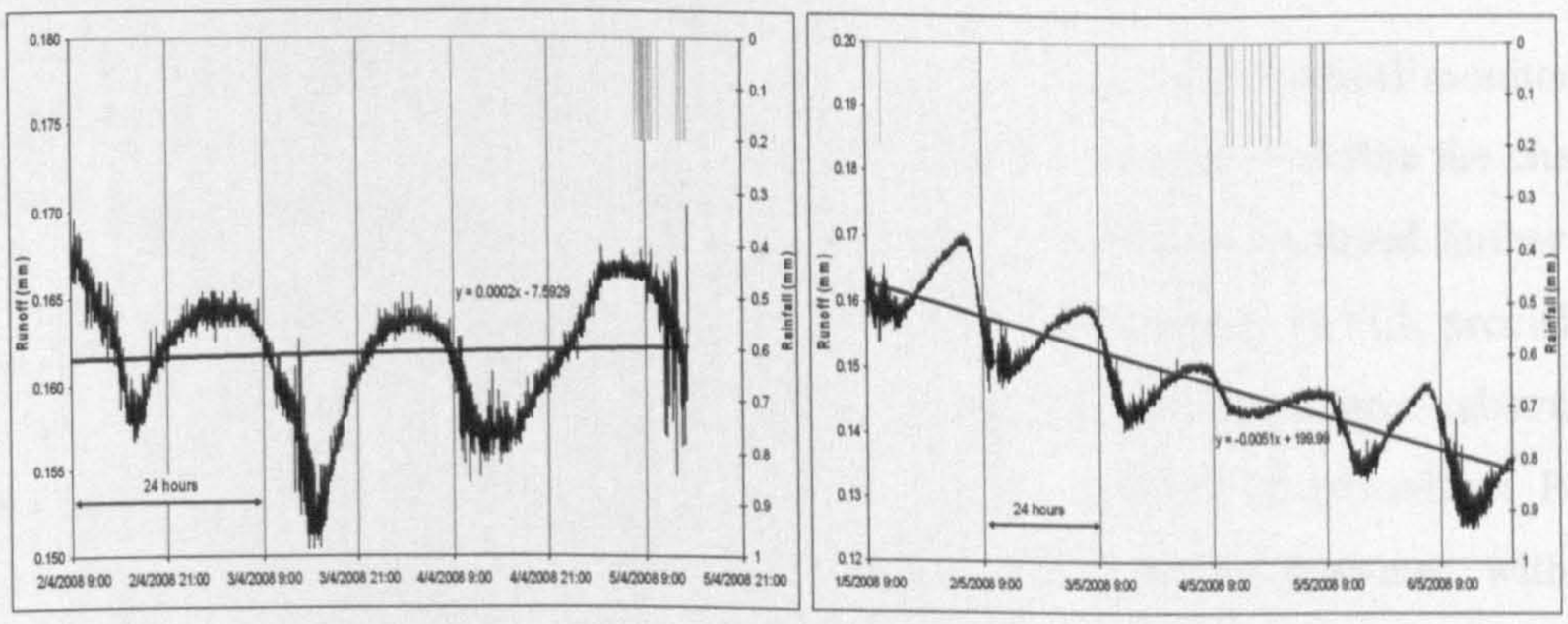


(a) (b)

Figure 4.12: Background fluctuation of runoff volume in tank in dry weather period on (a) April 2008; and (b) May 2008

Diurnal fluctuation checks from Figure 4.12 were carried out for 9:00 to 9:00 (24-hours). The diurnal ranges still within the range of averaged 0.015 mm (April 2008) and 0.024 mm (May 2008) of equivalent runoff depth. Figure 4.13 show that the higher variation of fluctuation and it still recorded the higher fluctuation for less than ± 0.01 mm.

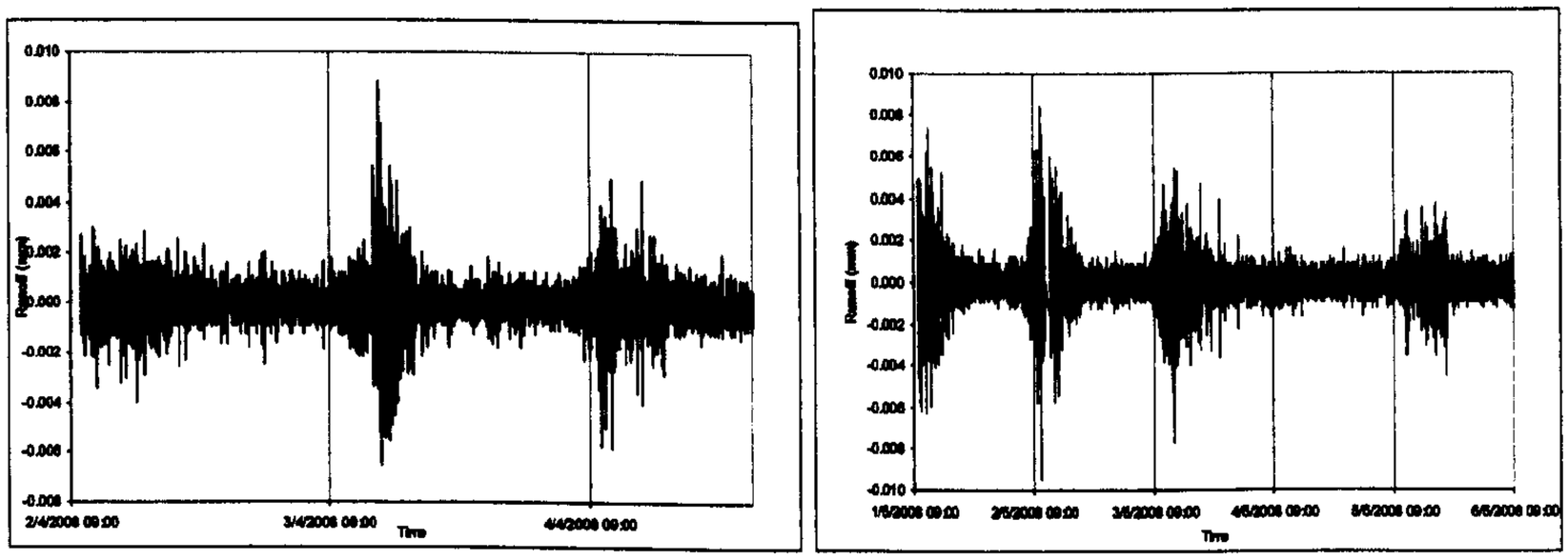


(a) (b)

Figure 4.13: A discretised fluctuation of runoff volume from the background fluctuation in (a) April 2008; and (b) May 2008

For a short-term fluctuation, fluctuations still averaged less than 0.01 mm of equivalent runoff depth for both months, and can be summarized as shown in Table 4.3. The quantities of equivalent runoff depth in each term (Table 4.3) in the data were still significantly smaller than the rain gauge resolution at 0.2 mm and the errors can still be negligible within most rainfall events compared to previous analysis on June 07.

## 4.3 Laboratory Work

The previous sections explained the instrumentation used for rainfall runoff monitoring for the green roof. In this section, the experimental work needed in order to define the characteristics of the substrates will be outlined. The results and analysis will be discussed further in Chapter 6. Two main experimental works have been undertaken including; 1) FLL procedures (FLL, 2002) to determine substrate soil properties; and 2) Evaporation tests on three substrates used on test rigs. These experimental made use of apparatus described in FLL procedure: Permeability cylinder vessels made from metal (165 mm in height, 150 mm in diameter, with perforated metal base, circular metal depth gauge and circular mesh wires (Figure 4.14).

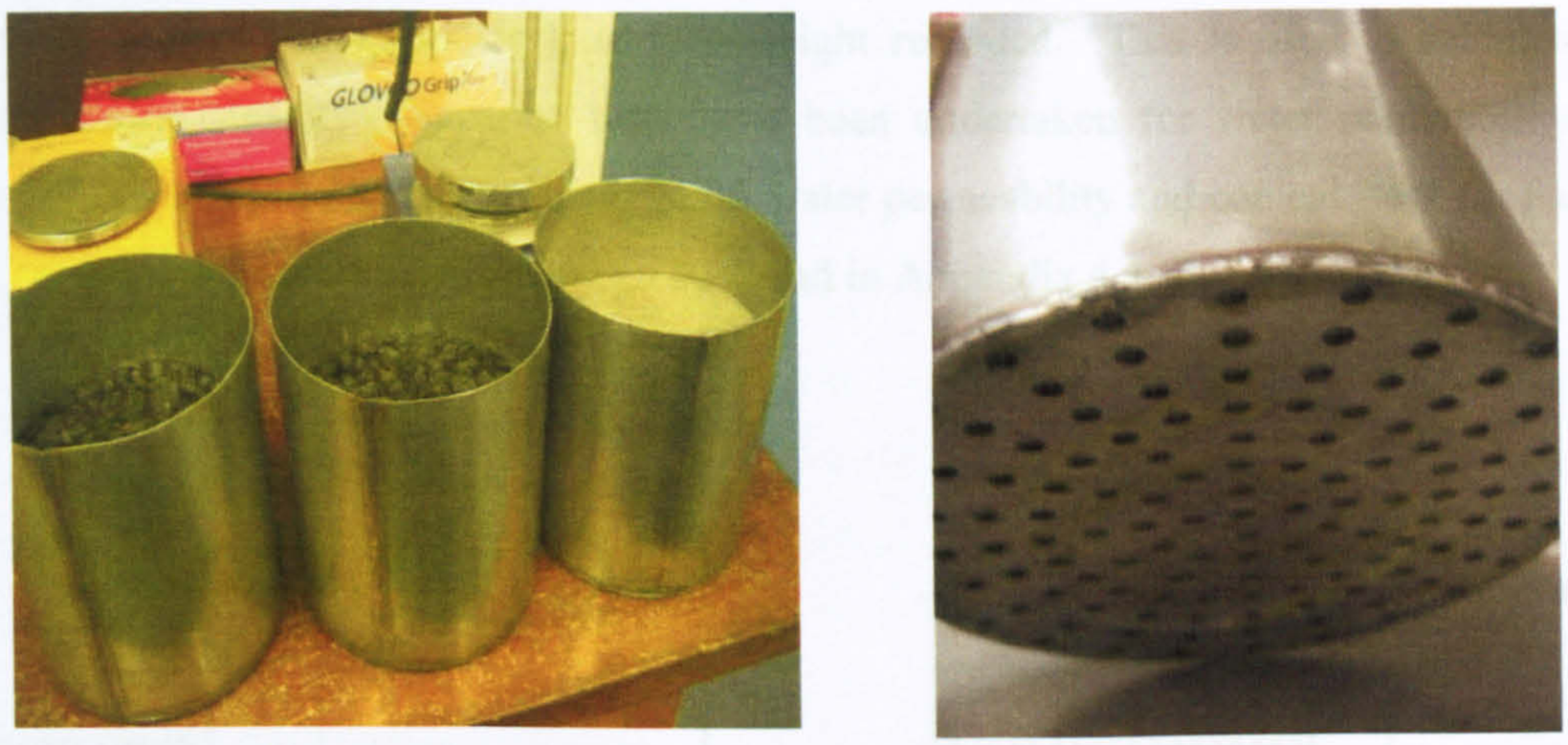

(a) (b)

(c)

Figure 4.14: The cylinder apparatus built as described by FLL; (a) The three permeability vessels; (b) Perforated metal under the vessels to allow water drainage; and (c) Wire mesh on top of the substrate

### 4.3.1 Soil Property Tests

The FLL guidance (FLL, 2002) and/or Penn State material testing protocols (Appendix 4.2), has been utilized to assess substrates properties. As mentioned above (Section 3.2.2), 3 main substrates have been used; 1) Alumasc-HL; 2) Alumasc-Sedum; and 3) LECA-based mixture. The experiments have been undertaken to determine substrate density, maximum water capacity, water permeability, particle density and porosity. The moisture content test is undertaken as follows. A gauze mesh is placed in the base of vessel (Figure 4.15). Substrate is placed within the test vessel, and is compacted using Proctor Hammer. Its weight is recorded, with percentage solids (moisture content) being determined in a separate test. The substrate is immersed in water for 24 hours to ensure full saturation (Figure 4.16). It is then allowed to

drain for two hours (field capacity), and its weight recorded. This is used to calculate the maximum water capacity. Separate tests have been undertaken for water permeability and particle density using the metal depth gauge for water permeability and conical flask for particle density. Full experimental procedures can be found in Appendix 4.2.

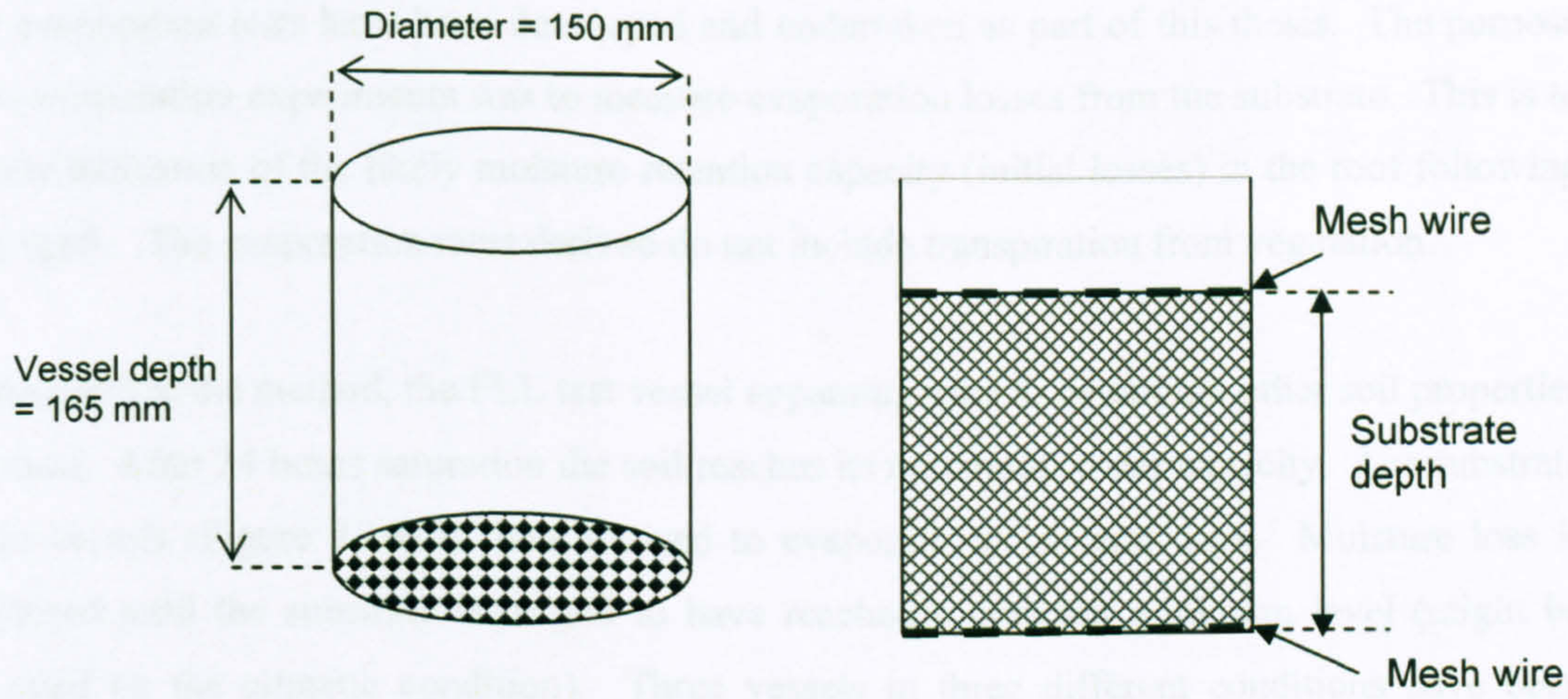


Figure 4.15: (a) Diagram of empty test vessel; (b) Cross section of vessel during experiment

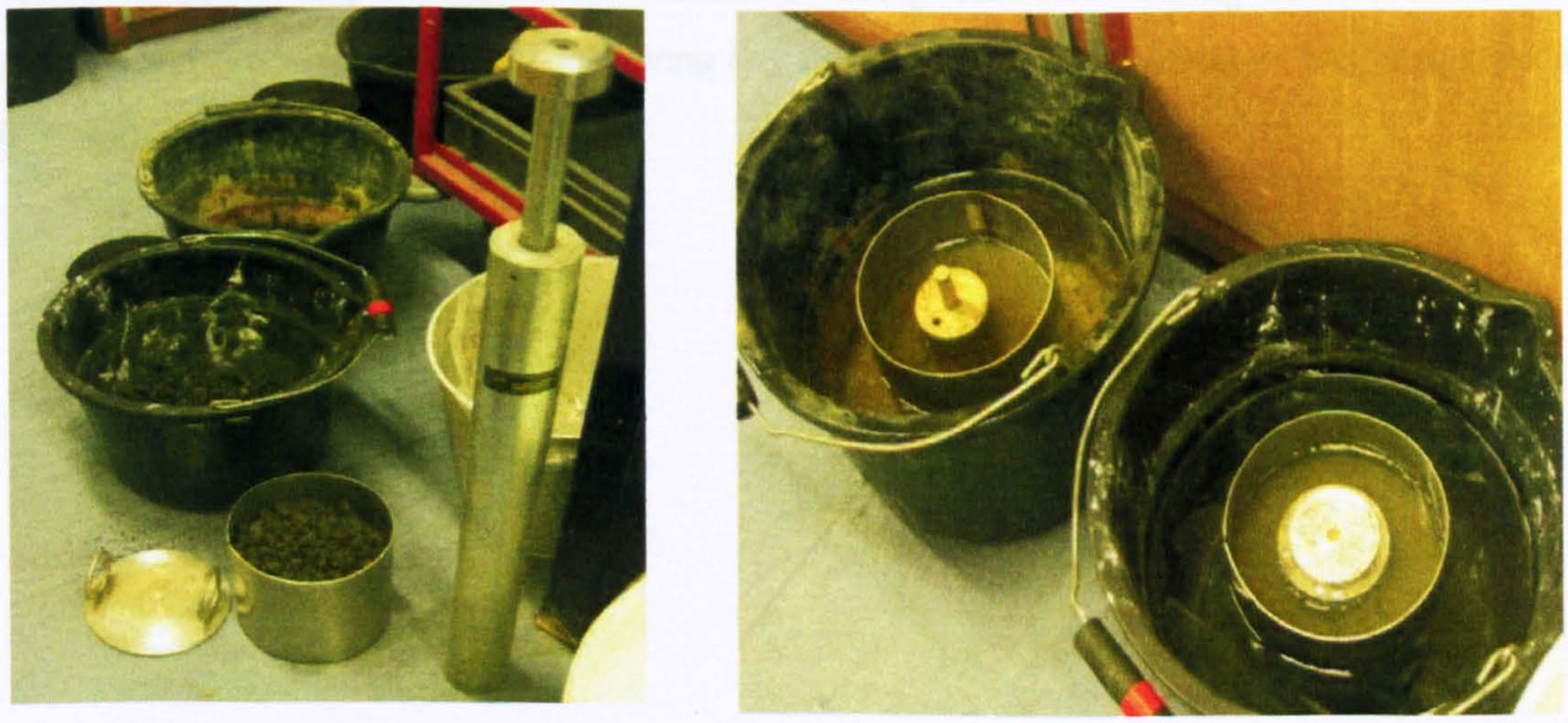

(a) (b)

Figure 4.16: Part of the soil properties experiment (a) Substrate in vessel need to be compacted using Proctor hammer before being submerged; (b) Substrates have been submerged for 24 hours to provide a saturated condition

Example of calculations of the 6 main parameters is shown in Appendix 4.3 for data collection from Alumasc-HL soil properties.

### 4.3.2 Experimental Evaporation Test

New evaporation tests have been developed and undertaken as part of this thesis. The purpose of the evaporation experiments was to measure evaporation losses from the substrate. This is to provide indication of the likely moisture retention capacity (initial losses) in the roof following a dry spell. The evaporation rates derived do not include transpiration from vegetation.

To standardize the method, the FLL test vessel apparatus used to determine other soil properties was used. After 24 hours saturation the soil reaches its maximum water capacity. The substrate in the vessels (Figure 4.16) is then allowed to evaporate for several days. Moisture loss is monitored until the substrate is judged to have reached a constant minimum level (might be depended on the climatic condition). Three vessels in three different conditions have been monitored to see the difference; a) Outside – shaded under the test rig to replicate with the real roof condition but without having more moisture; b) Inside – in room condition; and c) In the oven – using 40°C of temperature (Figure 4.17). The substrate's weight was taken for every condition; after compacted (before saturated); during saturated, during maximum moisture capacity and the weight of every following day until it dry. This experiment has been repeated at least three times; for each substrate.

(a)

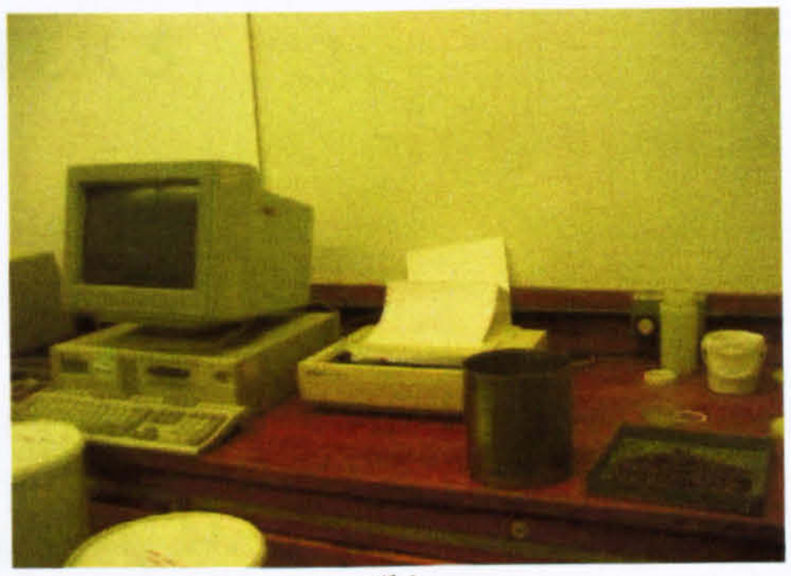

(b)

(c)

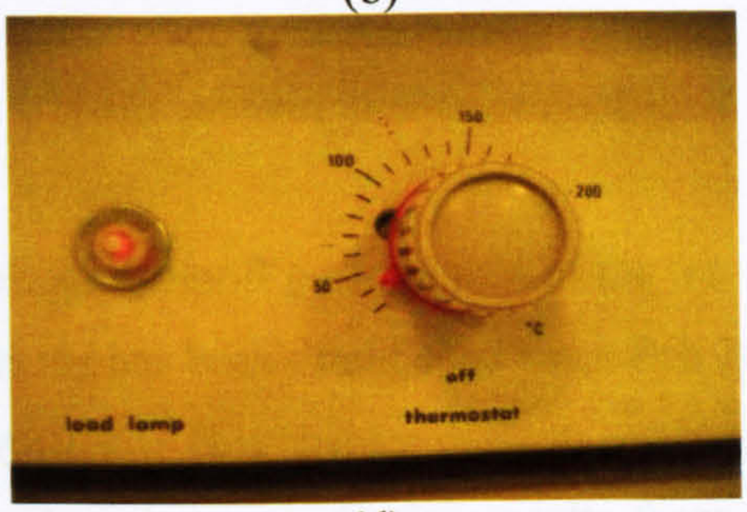


(d)

Figure 4.17: Three vessels in three different conditions; (a) Outside – shaded under the test rig to replicate with the real roof condition; (b) Inside – in room condition; and (c) & (d) In the oven – using 40°C of temperature

# CHAPTER 5

# ANALYSIS OF THE TEST RIG HYDROLOGICAL PERFORMANCE DATA

## 5.1 Introduction

The objective of the monitoring is to evaluate the rainfall-runoff performance of the test rig. As has been discussed in Chapter 4, the green roof test rig has been established since Feb 2006 and has been fully monitored for this project since May 2007. This chapter presents analyses of the test rig's hydrological performance, based on the long-term monitoring results from January 2007 to May 2009. By utilising all the storm events in the data set, regression modelling is used to identify correlations between performance and storm characteristics (Section 5.3). However, as each storm event is unique, it is expected that some specific events might be of interest. The events would require further examination in detail on a storm-by-storm basis (selected on the criteria of the most interesting events; such as extreme flooding, snowing and different types of rainfall intensity). Further discussion on the performance of these events is presented in Sections 5.4 and 5.5.

## 5.2 Description of the Data

The raw voltage data was collected from the data logger in text format. The green roof rainfall-runoff monitoring record contains 29 months' continuous rainfall data from 1 January 2007 to 31 May 2009 at 1 minute temporal resolution. All the conversions and calculations were done manually using Microsoft Office Excel 2003. The calibration graphs of the conversion procedure from transducer voltage response (mV) into the equivalent runoff depth (mm) using the calibration equation were presented in Figure 4.12 and the details are outlined in Appendix 3.1.

The data has been tabulated, converted, discretised and sampled into 5 minute, hourly and daily totals of rainfall and runoff. The sets of data were then separated and are presented in individual events to allow a general statistical analysis to be carried out.

### 5.2.1 Storm Identification

Analysis of the data monitored from Jan 2007 to May 2009 was undertaken for individual rainfall events; although the data collection resolution is in 1 minute intervals, the analysis involved sampling at a 5 minute interval resolution. The hydrological performance of the rig during any rainfall event is illustrated in Figure 5.1. Runoff is expected to be delayed in time (lag), and have reduction/attenuation in the peak flow, time to peak flow and total runoff volume. The main hydrological parameters that were analysed were; initial losses, peak delay in time (Tlag), peak attenuation (PA), time to start runoff (Ta), peak rainfall intensity (Rp), peak runoff intensity (Qp), total rainfall and total runoff.

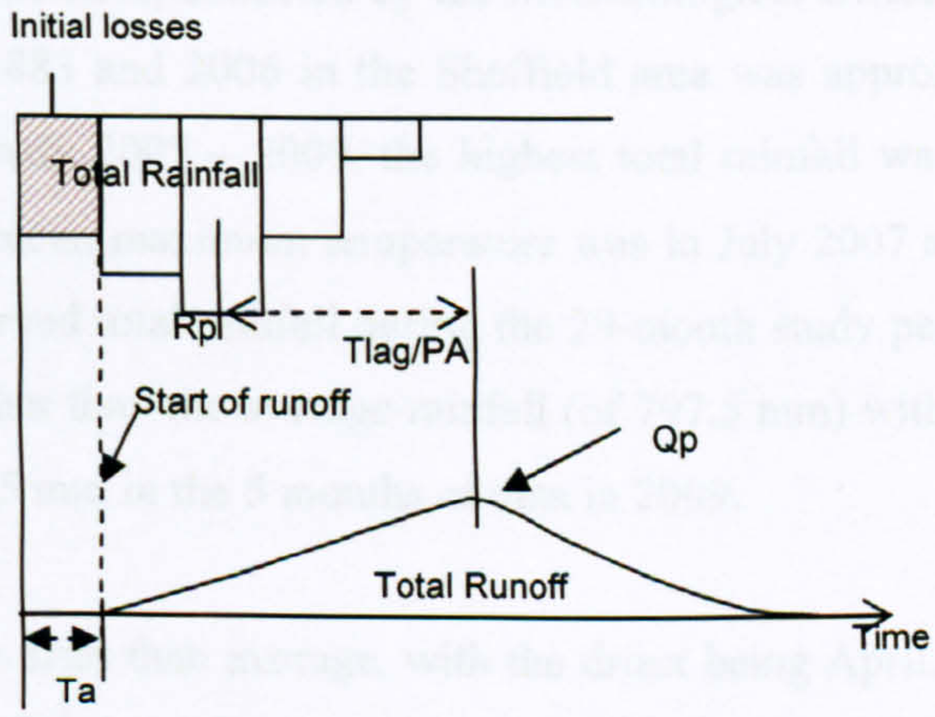


Figure 5.1: Rainfall runoff performances

In order to analyse the rainfall runoff performance, individual events were defined as being separated by continuous dry periods of at least 6 hours. This definition was selected in accordance with Rowe *et al.* (2003) and Getter *et al.* (2007). However, the use of a 6 hour antecedent dry weather period, ADWP is not universal, and many drainage designs are based on an assumed ADWP of 24 hours.

It is apparent that the way in which a storm event is defined will significantly influence any conclusions reached about the overall retention and detention performance of the green roof. For example, if more events are included with short ADWPs this may result in lower average retention than if all the events analysed were preceded by longer ADWPs. Conversely, if the smallest events are completely excluded from analysis, many events with 100% retention will be eliminated, and the average retention percentage per storm event may be reduced as a consequence.

The analyses of some of the storm-based data and some of the overview statistics during the 29-month period were undertaken for runoff retention, runoff delays and ADWP. Runoff retention is the percentage of the runoff being retained and the runoff delay is defined according to the initial appearance of the runoff after the first rainfall. Antecedent dry weather period, ADWP is the period of dry weather prior to a rainfall event. ADWP for this monitoring storm data analysis is referring to as the period of dry days (minimum of 6 hours or more) prior to a rainfall event.

### 5.2.2 Climatic Condition

Based on rainfall data for Sheffield, collected by the Meteorological Office (2010), the average rainfall per year between 1883 and 2006 in the Sheffield area was approximately 797.5 mm. During the period of the study 2007 – 2009, the highest total rainfall was in June 2007 with 285.6 mm and the highest mean maximum temperature was in July 2007 at 20°C (Figure 5.2). The yearly average of observed total rainfall during the 29-month study period (as collected by this study) was slightly higher than the average rainfall (of 797.5 mm) with 948.8 mm in 2007, 970.6 mm in 2008 and 263.5 mm in the 5 months of data in 2009.

In 2007, most months were drier than average, with the driest being April. The wetter months than average were January, February, May and July with June 2007 exhibiting the highest total rainfall (Figure 5.2). Flood events occurred during June 2007 due to this extreme rainfall. 2008 was opposite to 2007, in which most months were wetter than average and wetter than in 2007 with the wettest month being January 2008. February, May, June, November and December 2008 were drier than the average. In 2009, most months were drier than average except May which was slightly wetter.

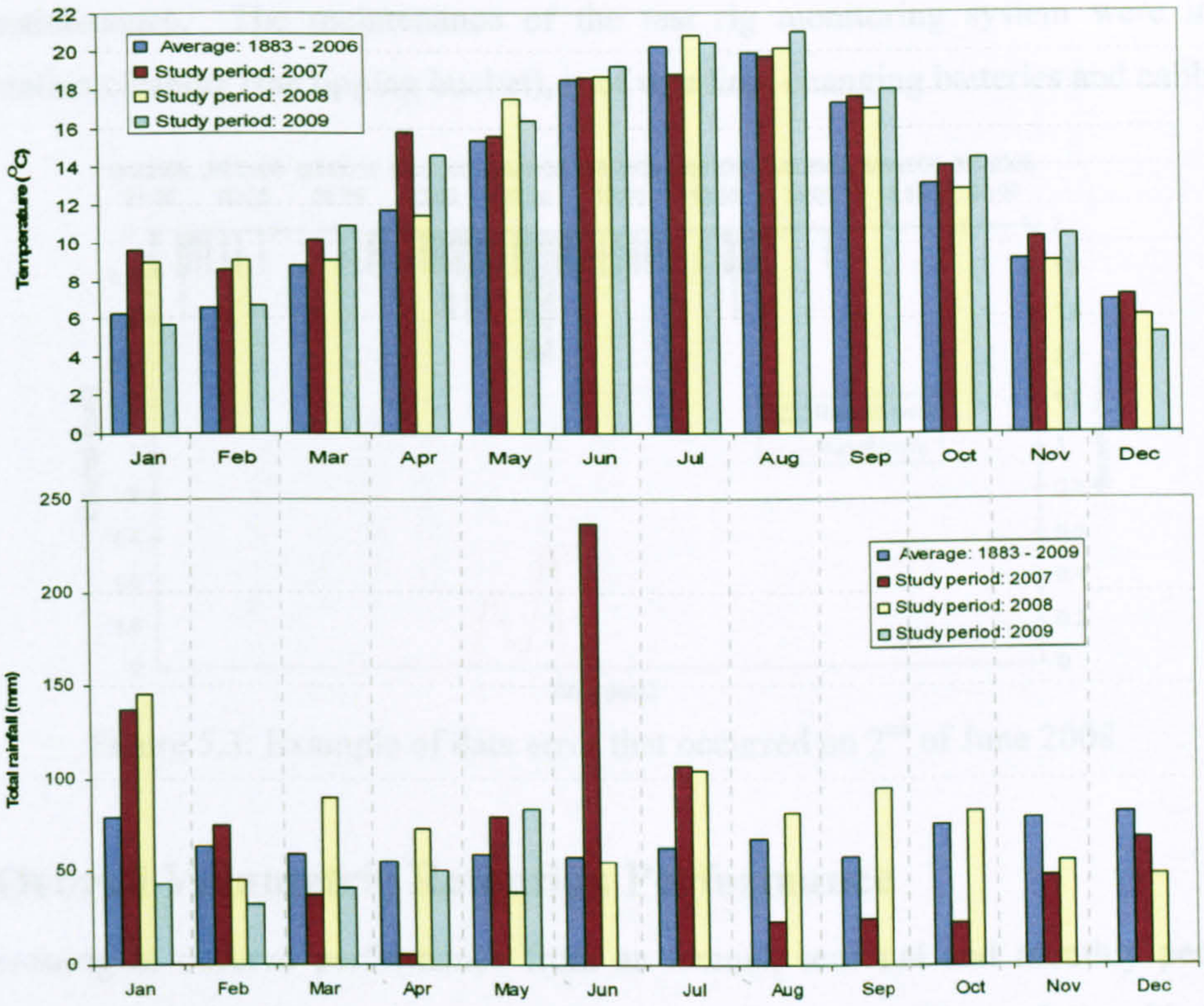


Figure 5.2: Average and study period monthly temperature and total rainfall depth (Source: Met Office, 2010)

### 5.2.3 Data Gaps and Errors

During the monitoring period, a number of issues arose including maintenance of the test rig and problems with the instrumentation. The complete data set for the 29 month period from Jan 2007 to May 2009 is shown in Figures 5.3, 5.8 and 5.10 after sampling according to annual, seasonal and monthly rainfall-runoff performances. It is noted that the runoff data provided between 17th January – 3rd March 2008 and 17th March – 1st April 2008 were corrupt because the batteries for the pressure transducer behaved inconsistently during winter and the gutter lid became dislodged because of the wind, respectively. Some of the storm events were missed (as listed in Appendix 5.1), as on 2/6/2008 (Figure 5.3) when collection did not occur due to instrumentation problems. In the example of case 2/6/2008 data in Figure 5.3, the solenoid valve leaked as a result of small debris becoming stuck in the valve opening on 3/6/2008 at 08:05. As a result, no runoff was reported in the later stages of the event and this is referred to as a data error. However, although this error might affect the volumetric retention analysis, the problem occurred after peak rainfall, therefore the observation data for the lag time and the peak delay could still be used. Extra precautions were taken after the incidents with respect to the

test rig maintenance. The maintenance of the test rig monitoring system were included; instrumentation cleaning (the tipping bucket), roof weeding, changing batteries and calibration.

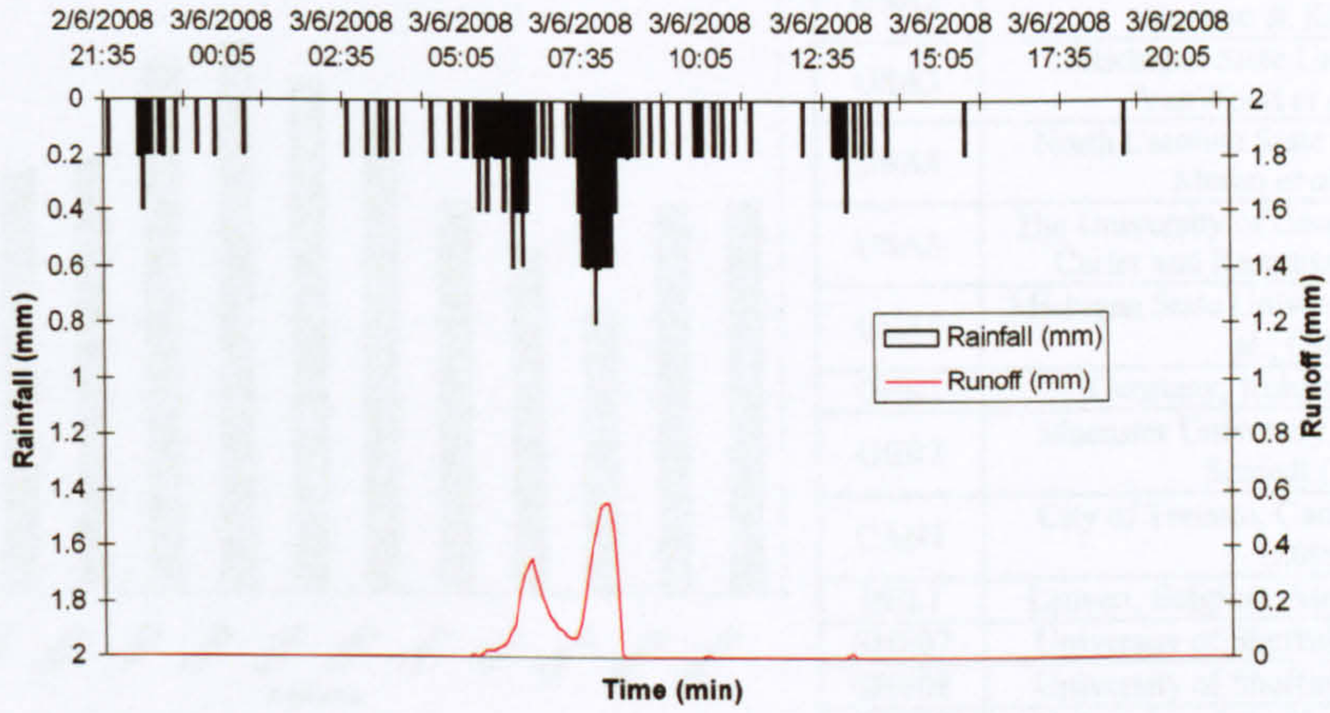


Figure 5.3: Example of data error that occurred on 2nd of June 2008

## 5.2.4 Overall Volumetric Retention Performance

It is interesting to observe performance from an annual, seasonal and monthly perspective. Overall, there were only small variations in annual performance (Figure 5.4), with the mean retention for these 3 years being 51%. Referring to Figure 5.5, the mean retention is similar to the results by Mentens *et al.* (2006) from Belgium and Liu & Minor (2005) from Canada, but slightly lower than results from the USA and Germany, which range from 60 – 80.2%. As discussed in Chapter 2, there are factors which may have contributed to this variation, for instance climatic factors and substrate physical characteristics. However, it is predicted that the detailed analysis on seasonal, monthly and daily data might show greater variation and also suggest some of the factors that might affect runoff performance.

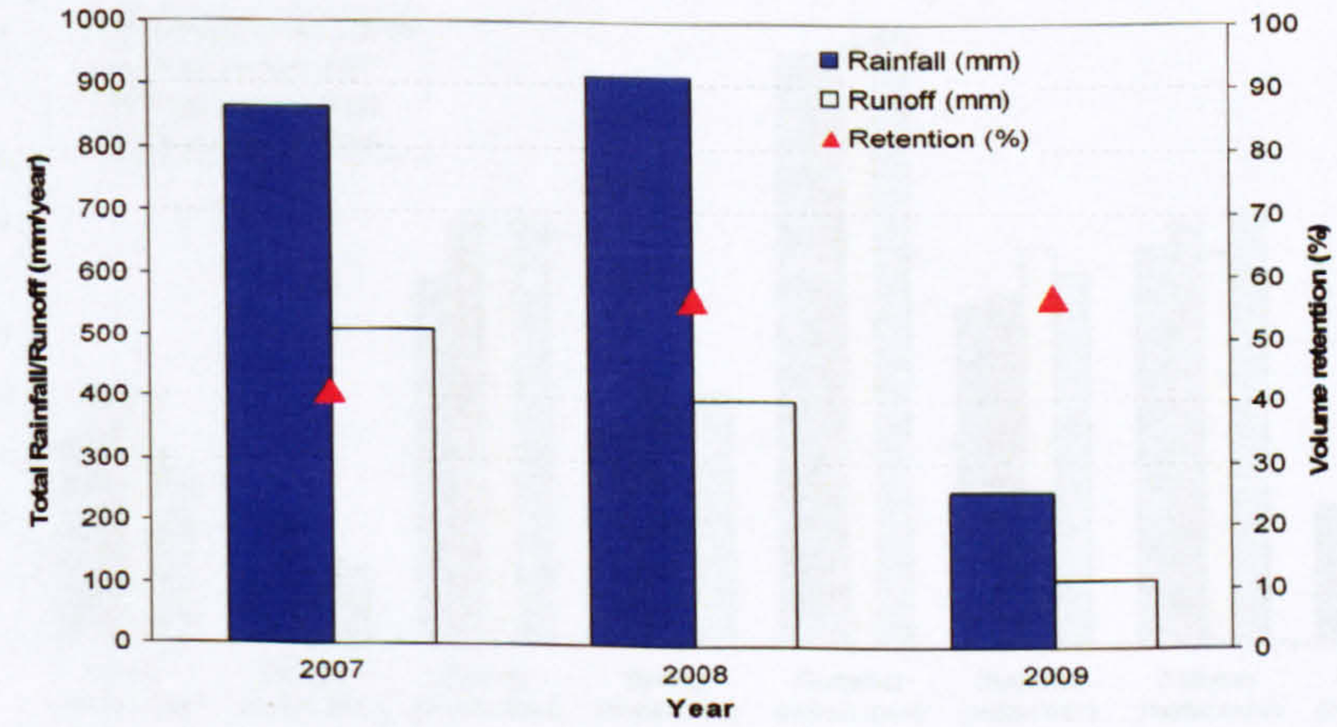


Figure 5.4: Annual total rainfall, runoff and % of volume retention during 2007, 2008 and part of 2009 (January 2007 to May 2009)

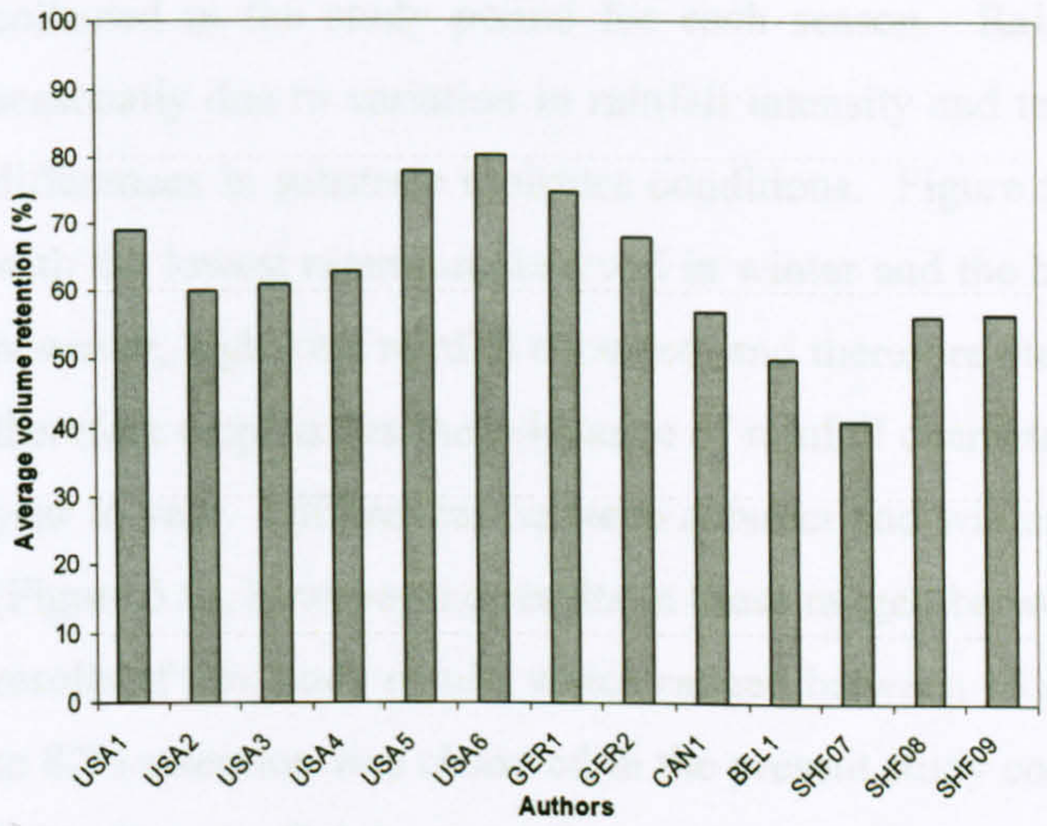


| | |
|---|---|
| USA1 | City of Portland, Oregon, USA, Hutchinson *et al.* (2003) |
| USA2 | Vancouver Regional District, USA, Graham & Kim (2003) |
| USA3 | Michigan State University, USA, VanWoert *et al.*, (2005) |
| USA4 | North Carolina State University, USA, Moran *et al.*(2005) |
| USA5 | The University of Georgia, Athens, USA, Carter and Rasmussen (2005, 2006) |
| USA6 | Michigan State University, USA, Getter et al., (2007) |
| GER1 | Germany, Kohler *et al.*, (2001) |
| GER2 | Muenster University, Germany, Uhl & Schiedt (2008) |
| CAN1 | City of Toronto, Canada, Liu & Minor (2005) |
| BEL1 | Leuven, Belgium, Mentens *et al.* (2006) |
| SHF07 | University of Sheffield, UK- data 2007 |
| SHF08 | University of Sheffield, UK- data 2008 |
| SHF09 | University of Sheffield, UK- data 2009 |

Figure 5.5: Annual volume retention observed from literature reviews compared to Figure 5.4

### 5.2.4.1 Seasonal and Monthly Performance

In Britain winter is normally defined as occurring during the months of December, January and February with mean average temperatures ranging between 1.8 and 6.6°C (Figure 5.6 – average from 1883 - 2006); spring is then from March to May with an average temperature of 7.0 to 12.0°C; followed by summer from June to August with a mean temperature of between 11.3 and 19.5°C; and autumn from September to November with a mean temperature of 4.5 to 13.2°C (Meteorological Office, 2010). During the seasons, the temperature will vary somewhat in terms of mean values in specific months and years; as can be seen in the seasonal pattern shown in Figure 5.6.

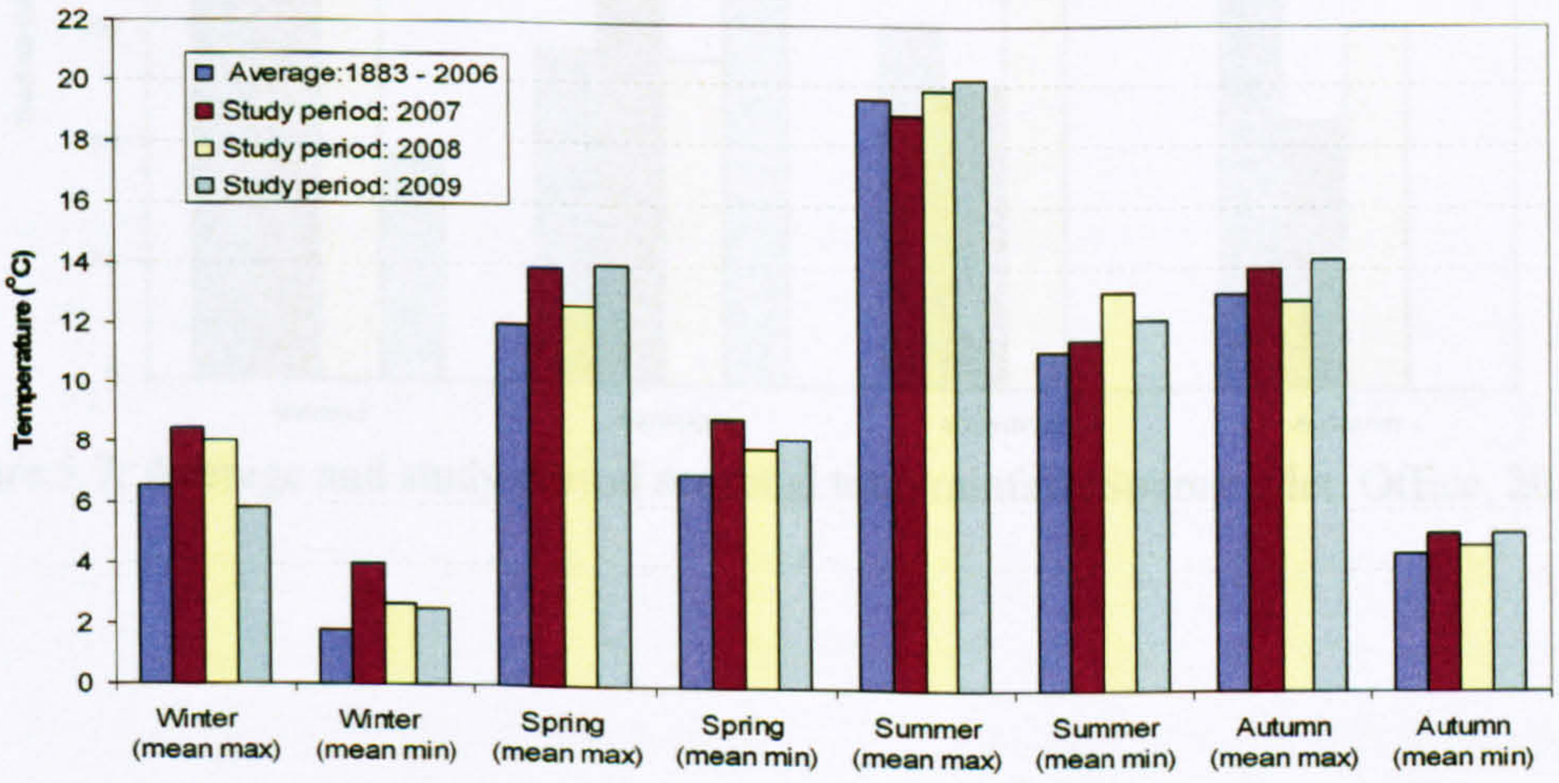


Figure 5.6: Average and study period seasonal temperature (Source: Met. Office, 2010)

Figure 5.7 shows the average total rainfall from 1883–2009 compared with the total rainfall collected in the study period for each season. Rainfall retention may be expected to vary seasonally due to variation in rainfall intensity and temperature (climatic condition) leading to differences in substrate moisture conditions. Figure 5.8 shows a seasonal pattern for retention with the lowest retention observed in winter and the highest in summer. During summer 2007, however, high total rainfall occurred, and therefore the retention was lower than predicted. This therefore emphasizes the relevance of rainfall characteristics on the retention performance from year to year. Differences between summer and winter have also been reported by other studies (Figure 5.9); however the results in these ranged between 33 and 49% in winter compared to the results of this study results which ranged between 15 and 52% (Figure 5.8). During summer 34 to 82% retention was observed in the present study compared to the 70 to 95% monitored in the USA, Canada, Belgium and Germany.

Nevertheless; this is quite impressive when considering that during wet conditions and the low winter temperatures of 2007 with a total rainfall depth of 106.2 mm, the green roof test rig still retained 14.9% of the water volume (Figure 5.8). In summer most of the medium storm events rainfall events were fully retained. Even when a high intense event occurred; i.e. during summer 2007, the test rig still managed to retain 34.2% of total runoff. This also reflects the role of high temperature in providing better water retention capacity due to evapotranspiration.

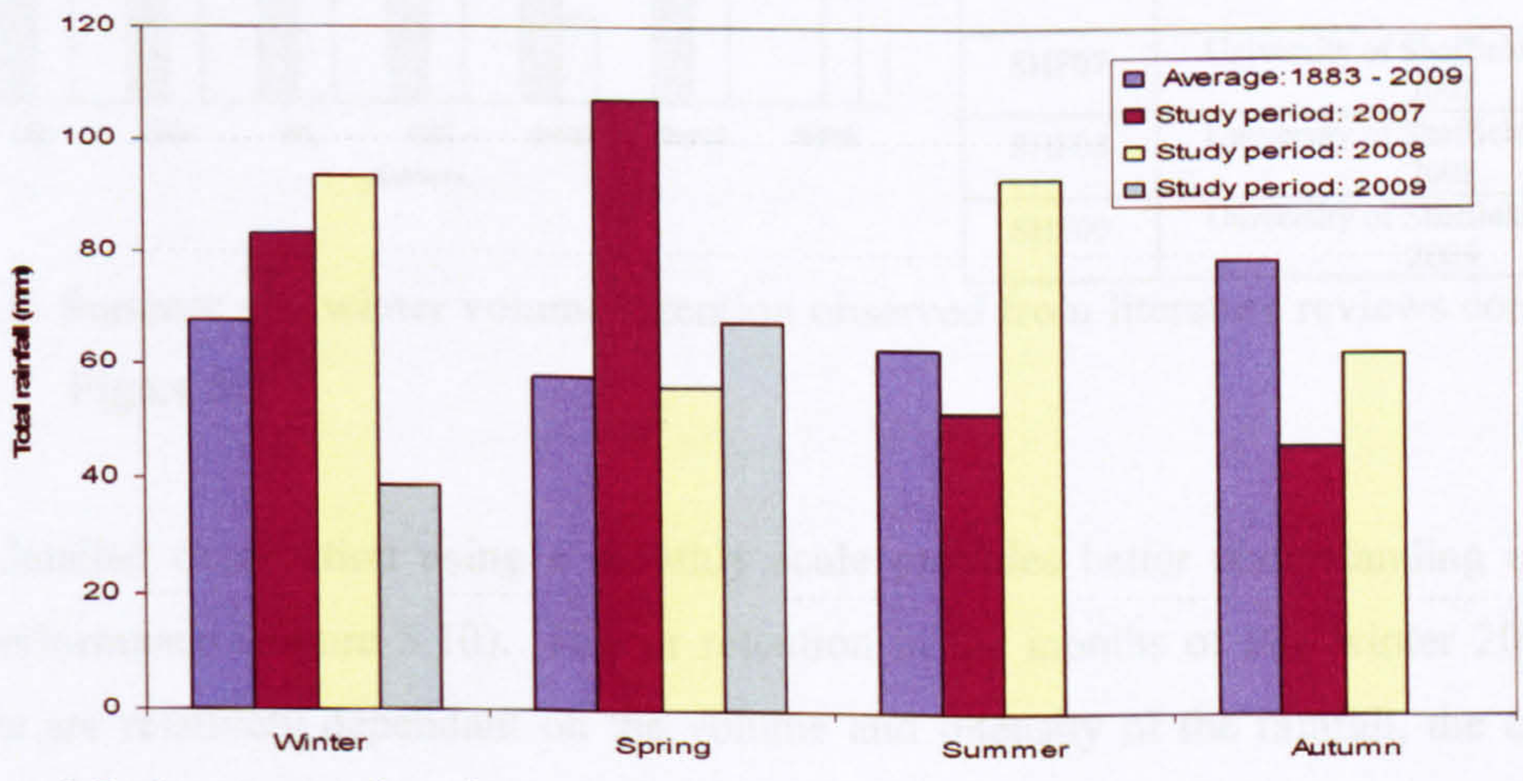


Figure 5.7: Average and study period seasonal total rainfall (Source: Met. Office, 2010)

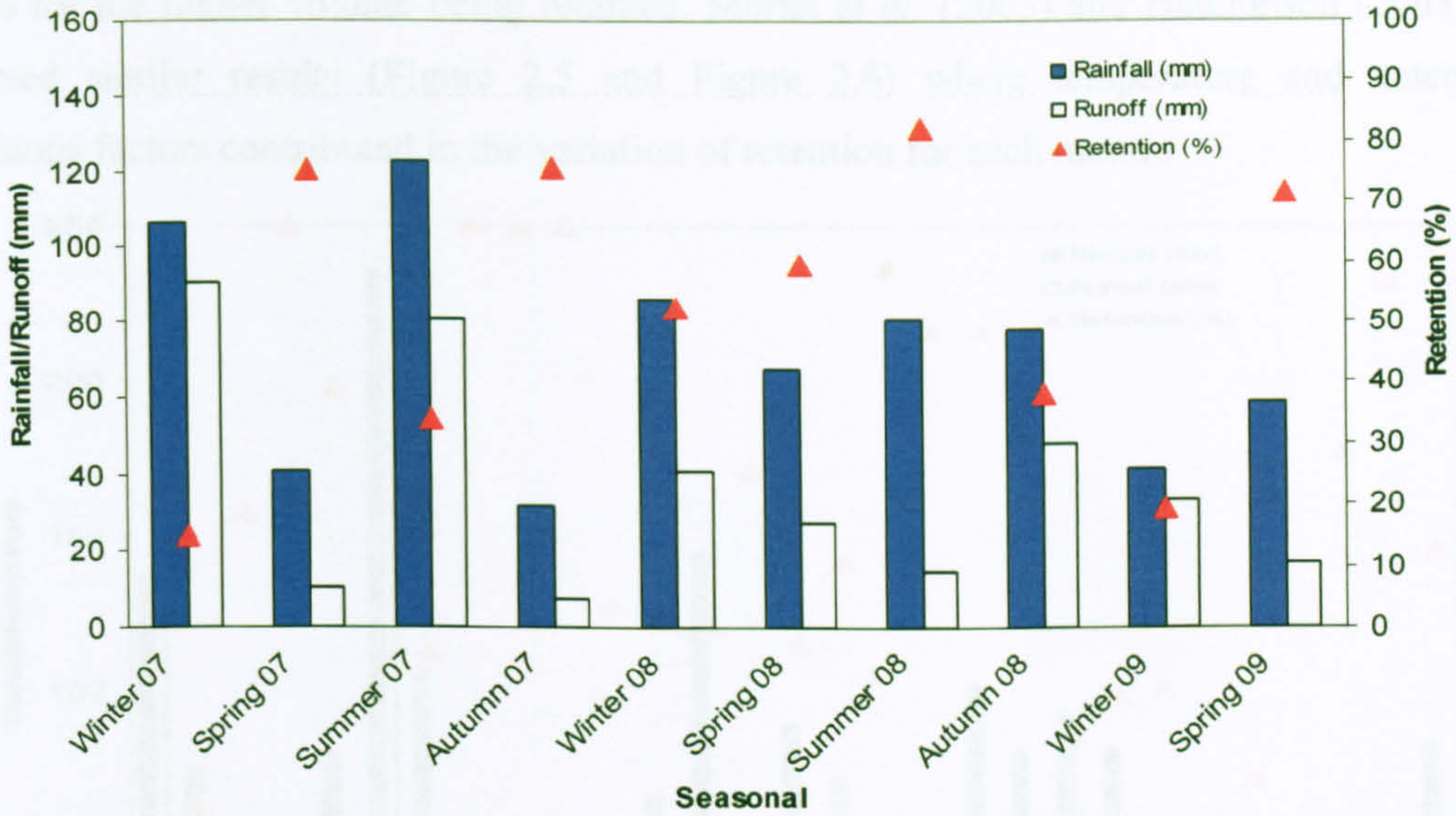


Figure 5.8: Seasonal total rainfall, runoff and % of retention during January 2007 – May 2009

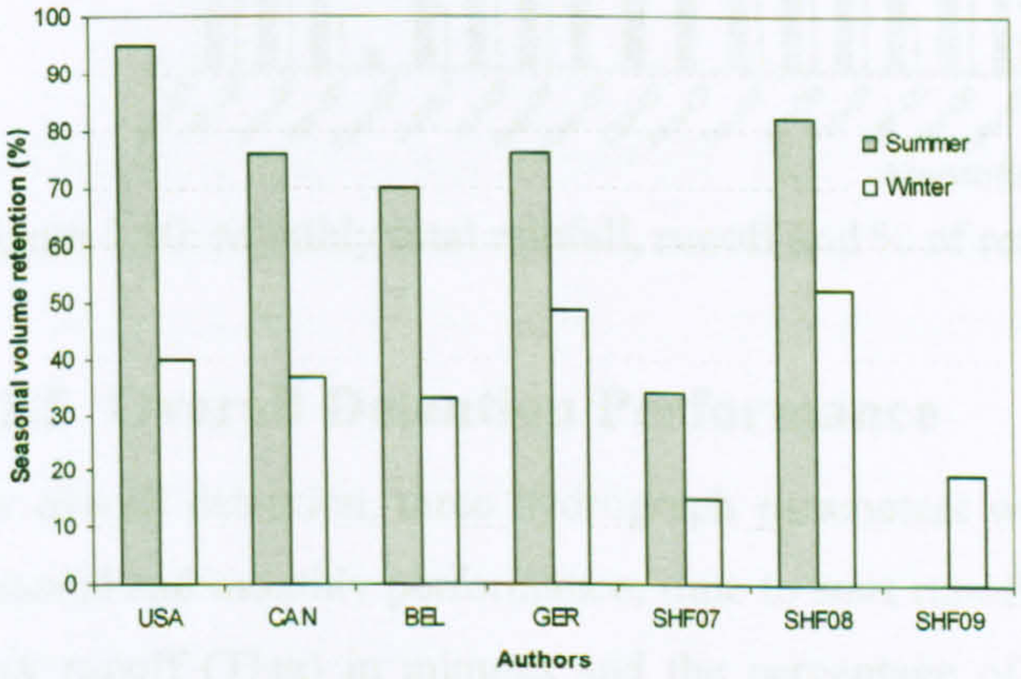


| | |
|---|---|
| USA | City of Portland, Oregon, USA, Hutchinson *et al.* (2003) |
| CAN | York University, Toronto, MacMillan (2004) |
| BEL | Leuven, Belgium, Mentens *et al.* (2006) |
| GER | Muenster University, Germany, Uhl & Schiedt (2008) |
| SHF07 | University of Sheffield, UK- data 2007 |
| SHF08 | University of Sheffield, UK- data 2008 |
| SHF09 | University of Sheffield, UK- data 2009 |

Figure 5.9: Summer and winter volume retention observed from literature reviews compared to Figure 5.8

Further detailed observation using a monthly scale provides better understanding of rainfall runoff performance (Figure 5.10). Higher retention in the months of late winter 2008 shows that these are relatively dependant on the volume and intensity of the rainfall, the antecedent condition and the temperatures (Figure 5.2). Frequent wet days in the early winter months of 2007 and the continuous wet days of the spring months, until winter at the end of 2008 might be the reason of these months tends to have more moisture affecting the low retention ranges between 9 and 40%. However, in late winter of 2007, the high total rainfall in January 2008 meant that the test rig was still able to retain 49% of the total volume. The slightly higher than average temperature of January 2008 (Figure 5.2) and the previous three months could be the

reason for the higher volume being retained. Moran *et al.* (2005) and Hutchinson (2003) also observed similar results (Figure 2.5 and Figure 2.6) where temperature and antecedent conditions factors contributed in the variation of retention for each month.

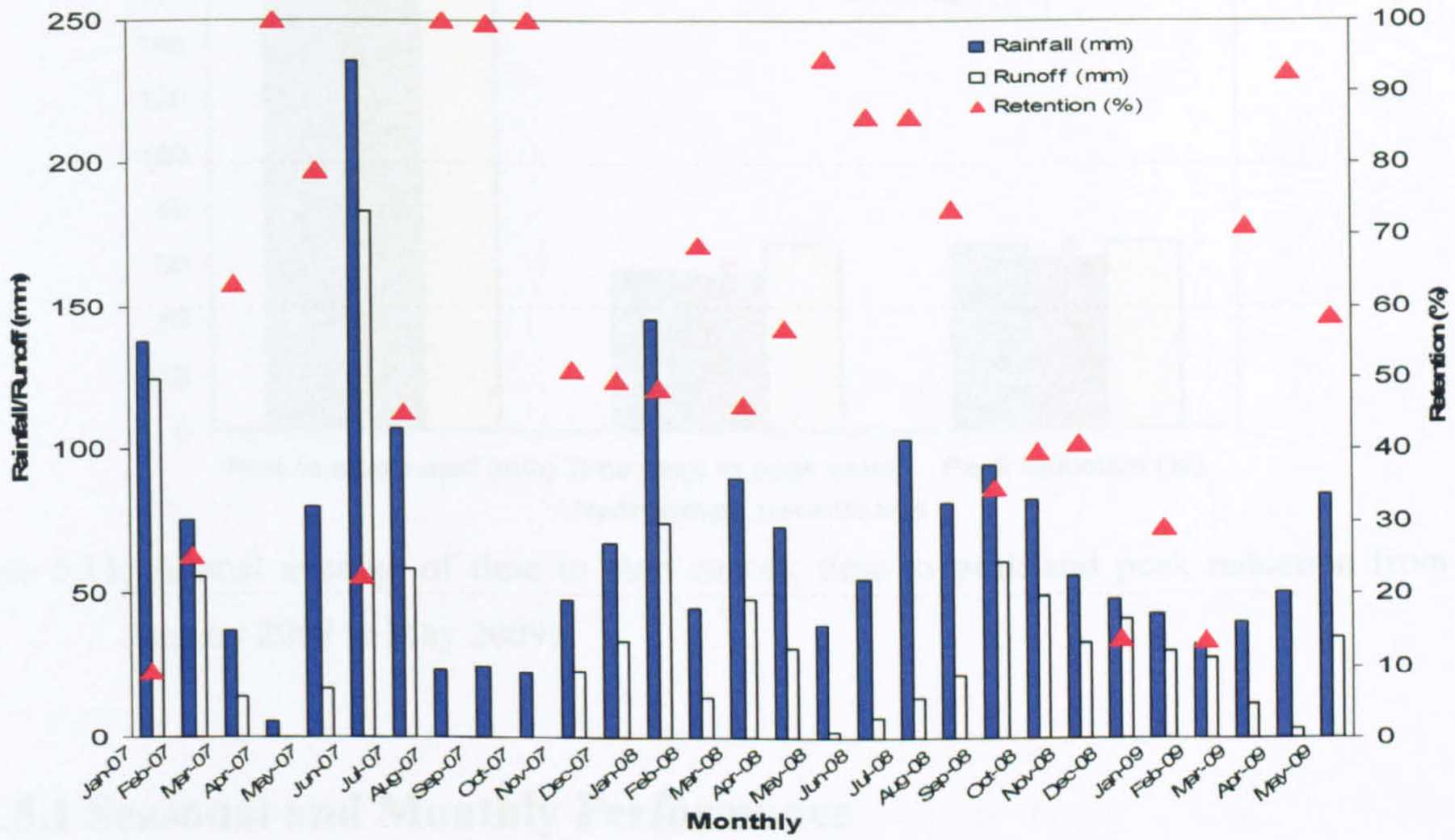


Figure 5.10: Monthly total rainfall, runoff and % of retention during January 2007 – May 2009

### 5.2.5 Overall Detention Performance

For overall detention, three hydrograph parameters were also analysed based on their annual, seasonal and monthly performance; time to start runoff (Ta) in minutes, time of peak rainfall to peak runoff (Tlag) in minutes and the percentage of peak flow reduction (PA) (Figure 5.1). Figure 5.11 presents the average annual performance for all three parameters during the study period. The slightly higher total runoff in 2008 (as presented in Figure 5.5) might explain the slightly lower lag and reduction when compared to 2007 and 2009. However all three periods show a similar time for storm events to reach peak runoff with an average of 60 minutes (1 hour) and 65% of peak reduction. Time to the start of runoff in 2007 and 2009 were slightly higher than 2008, with the average time being 208 minutes (3.5 hours).

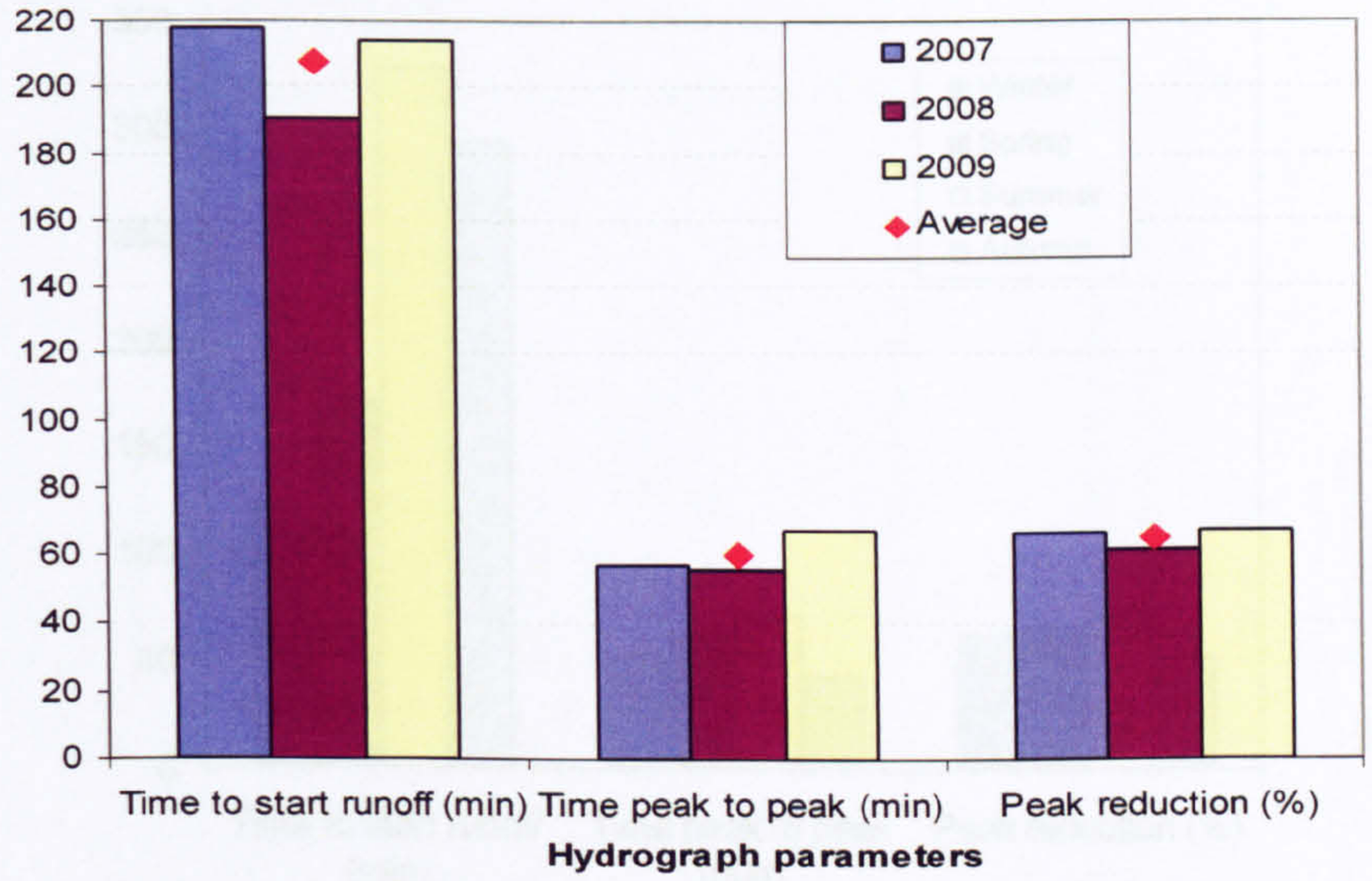


Figure 5.11: Annual average of time to start runoff, time to peak and peak reduction from January 2007 to May 2009)

### 5.2.5.1 Seasonal and Monthly Performance

The fact that the temperature in summer is higher than any other season, could be the reason for the higher lag time and the attenuation that occurs during the summer (Figure 5.12). The higher temperature occurring during dry conditions could provide a quick dry after reaching the substrates maximum storage capacity due to high evapotranspiration. Therefore, the average of time to rainfall to start runoff presented in Figure 5.12 shows the highest time during summer is 326 minutes (5.5 hours) compared to winter with 122 minutes (2 hours). It is expected that during spring time, the time to the start of runoff could be influenced by evapotranspiration more so than during autumn, however the antecedent condition of every storm event should be considered as another factor reducing the capability of the test rig within these two seasons. Time to peak is similar for all seasons because this lag time could be dependent on the depth and intensity of each storm with an average of 58 minutes. Peak reduction for all the seasons observed to be more than 50%; with a high of 71% in summer and a low of 53% during autumn. This suggests that, even in the winter wet season, the green roof managed to reduce the runoff rate by at least 50% (the seasonal average).

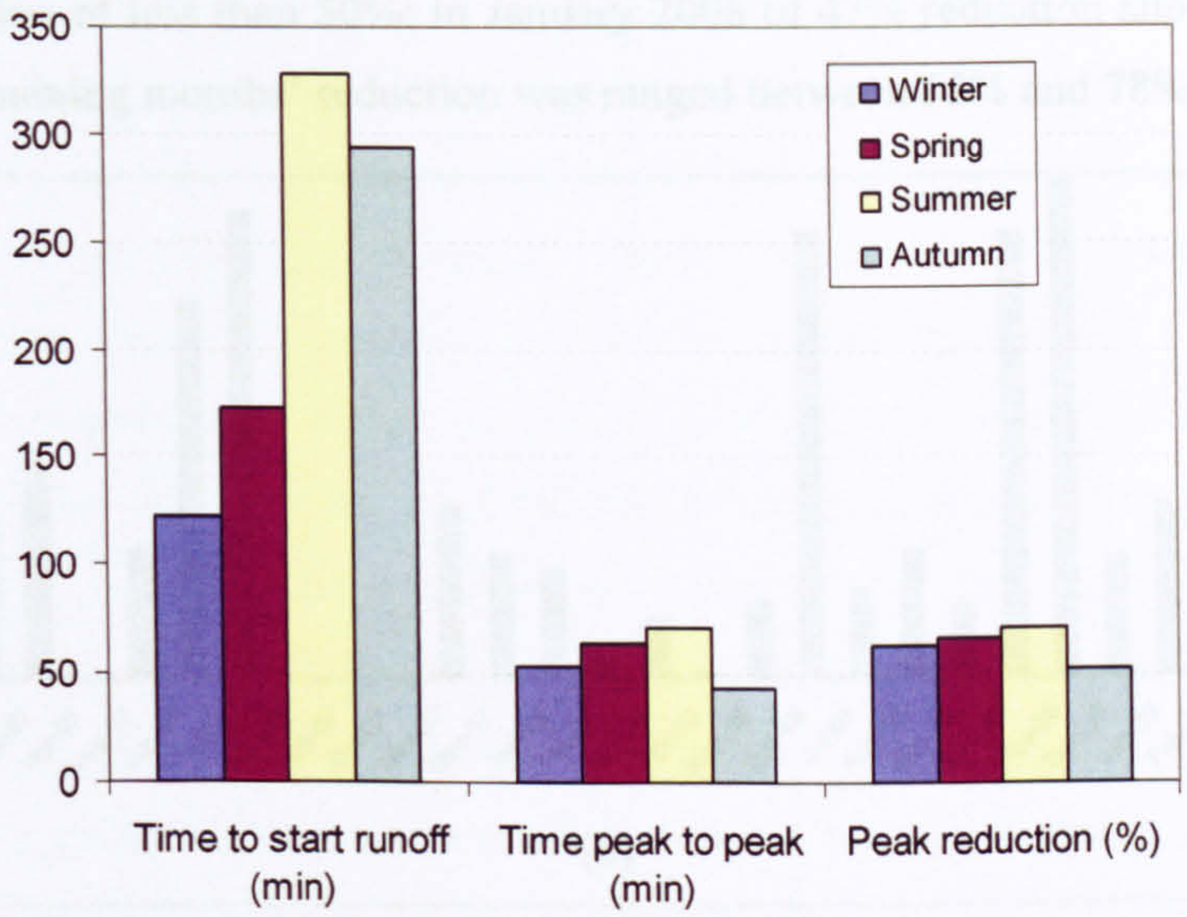


Figure 5.12: Seasonal average of time to start runoff, time to peak and peak reduction from January 2007 to May 2009

Figure 5.13 presents further details of all the three parameters in the monthly average. Note that rainfall events in April 2007 and August 2007 to October 2007 were fully retained; while in February 2009, all storm events that occurred in the early weeks of February were combined as one extreme snow event. Therefore, the snow event in February 2009 will not very precisely describe the performance of detention as similar to the other storm events. Figure 5.13 (a) shows the highest delay in runoff is during November 2008 in 496 minutes (8.3 hours), with a similar delay in July 2007, June 2008, October 2008 of 467 minutes (7.8 hours), 445 minutes (7.4 hours) and 443 minutes (7.4 hours) respectively. The lowest delay was observed in April 2008; this might be due to the intense storm that occurred during this month and this storm should therefore be evaluated further. Overall, the shortest time lag for a storm to prompt runoff is 50 minutes.

The highest average time to peak as presented in Figure 5.13 (b) was observed in June 2008, followed by March 2009 and August 2008 with 145 minutes (2.4 hours), 133 minutes (2.2 hours) and 105 minutes (1.8 hours) respectively. The lowest time for peak rainfall to peak runoff was observed in June 2007 which is the month when the extreme flood occurred.

The highest peak reduction was observed in Figure 5.13 (c) and was 92% in April 2009, followed by April, May, July 2008, with 84%, 86%, 84% respectively. Only two months

recorded a reduction of less than 50%; in January 2008 of 47% reduction and 35% in February 2008. All the remaining months' reduction was ranged between 55% and 78%.

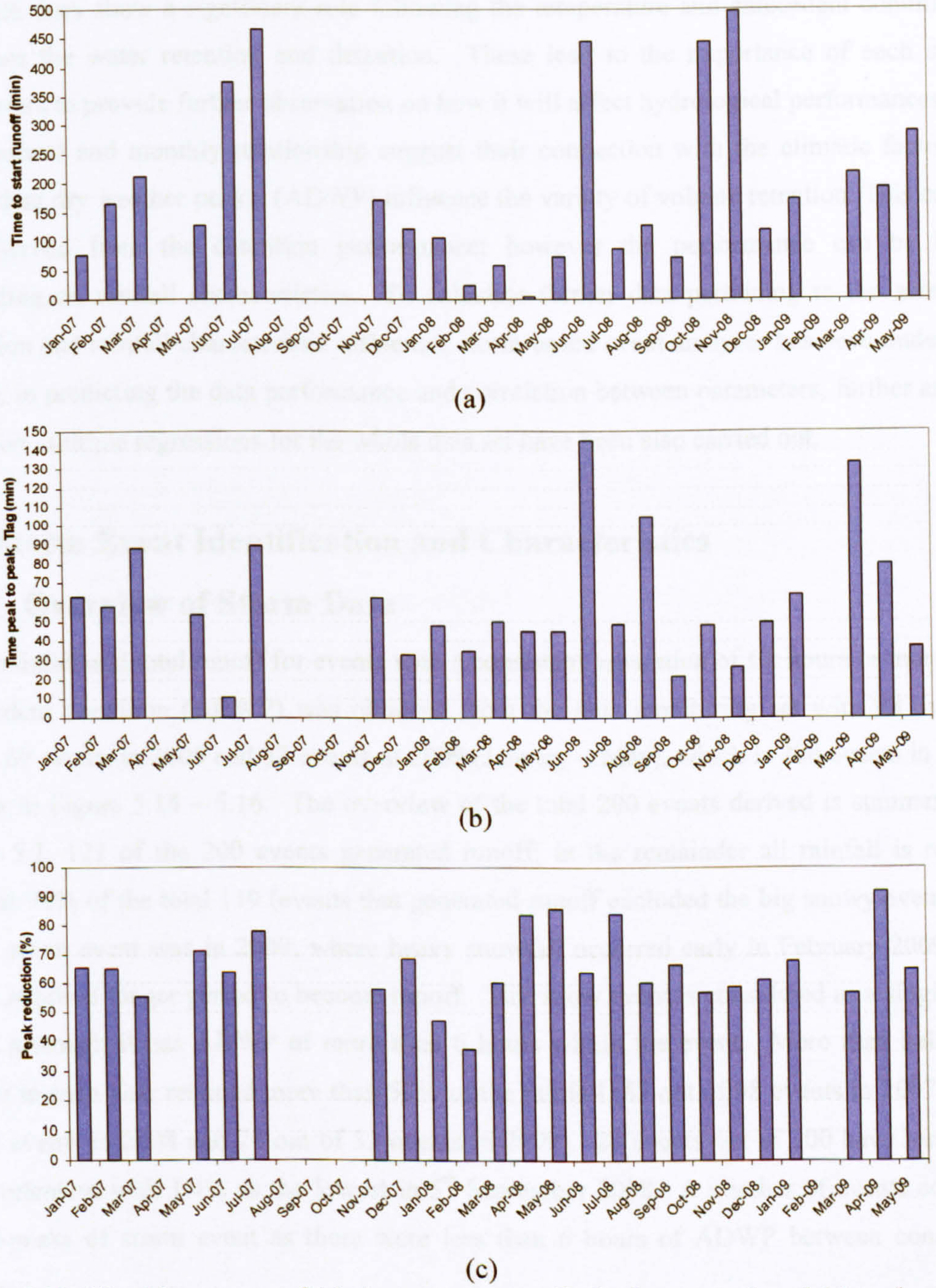


(a)

(b)

(c)

Figure 5.13: Monthly average of (a) time to start runoff, (b) time to peak and (c) peak reduction from January 2007 to May 2009

Overall, the characteristic rainfall factors can be observed from the annual and seasonal data in both the retention and detention performance. Higher resolution of the time series by monthly

performance reveals a better understanding of the rainfall runoff performance as varied with additional climatic factors in each month; where the performance of the storage capacity of the substrate does show a significant role following the temperature and antecedent conditions to influence the water retention and detention. These lead to the importance of each storm's parameters to provide further observation on how it will affect hydrological performances. Both the seasonal and monthly relationship suggest their connection with the climatic factors and antecedent dry weather period (ADWP) influence the variety of volume retention. This can also be observed from the detention performance; however the performance can be limited depending on rainfall characteristics. To calculate further data pertaining to the antecedent condition and rainfall characteristic influence, storm-based event analyses has been undertaken. Hence, in predicting the data performance and correlation between parameters, further analyses based on multiple regressions for the whole data set have been also carried out.

## 5.3 Storm Event Identification and Characteristics

### 5.3.1 Overview of Storm Data

Total rainfall and total runoff for events with a consistent separation of six hours or more of the antecedent condition (ADWP) was obtained from the data monitoring set with 98 events in 2007, 69 events in 2008 and 33 events in 2009 (January – May), which is 200 events in total as shown in Figure 5.14 – 5.16. The overview of the total 200 events derived is summarized in Table 5.1, 121 of the 200 events generated runoff; in the remainder all rainfall is retained. Almost 70% of the total 119 (events that generated runoff excluded the big snowy event). The snow storm event was in 2009; where heavy snowfall occurred early in February 2009. This event required longer period to become runoff. This snow event is considered as a single storm event although it has ADWP of more than 6 hours within the event. More than half of the events in each year retained more than 50% of the rainfall (67 out of 98 events in 2007, 49 out of 69 events in 2008 and 24 out of 33 events in 2009). 20 events out of 200 have less than a 20% retention with 1.4% as the lowest in 5$^{th}$ September 2008. A number of events contained multi-peaks of storm event as there were less than 6 hours of ADWP between consecutive storms.

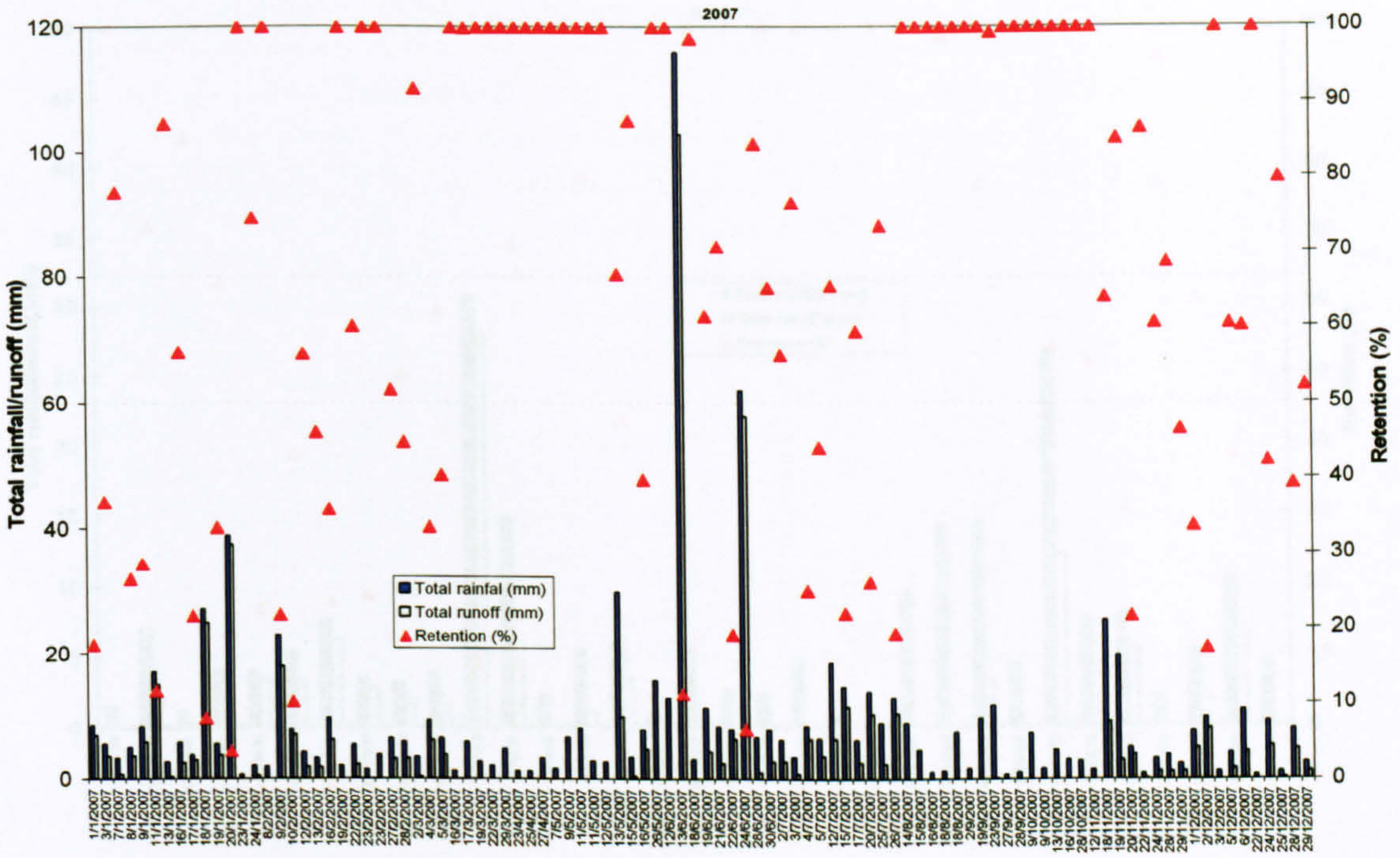


Figure 5.14: Storm by storm total rainfall, runoff and % of retention in 2007

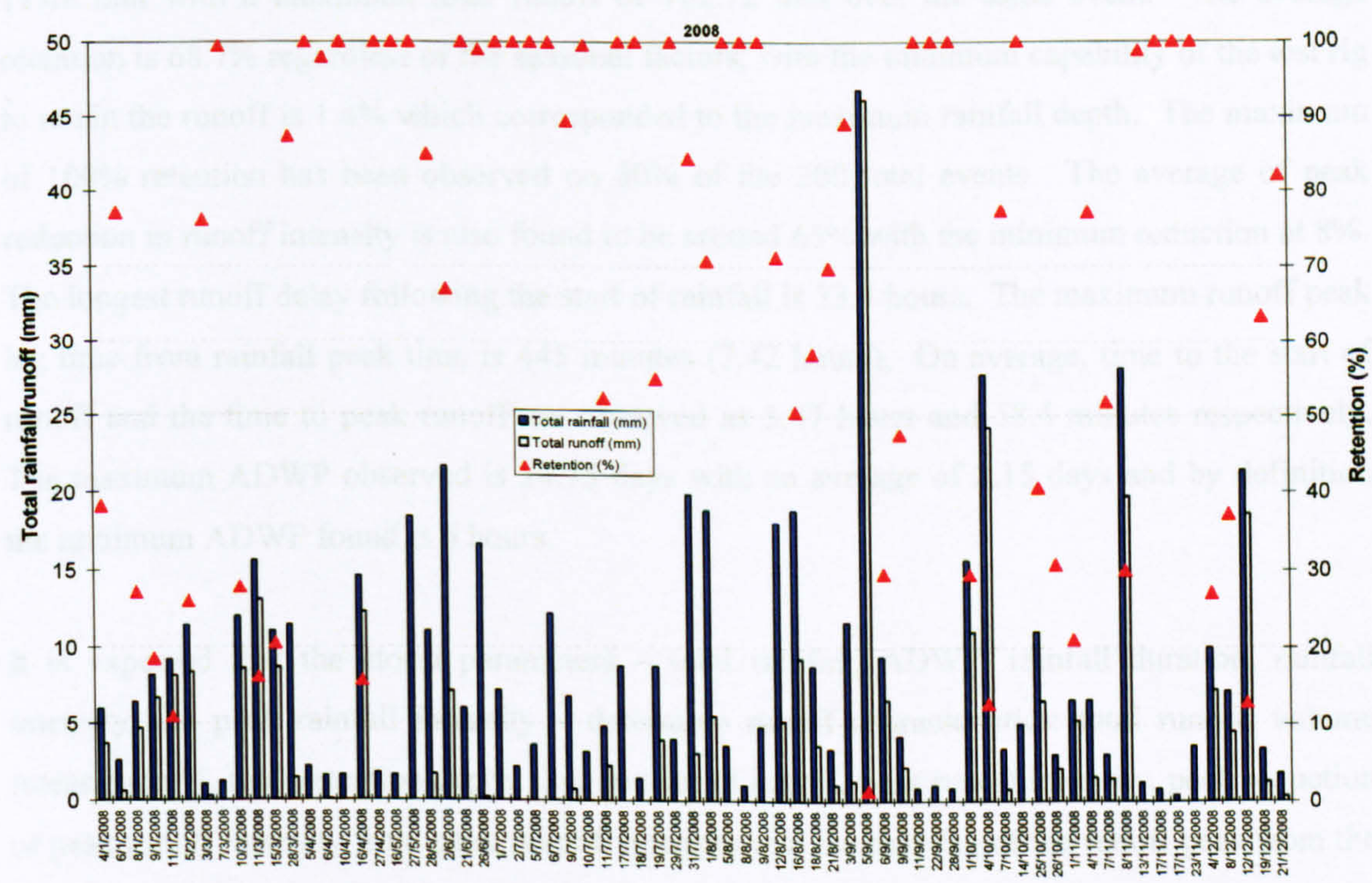


Figure 5.15: Storm by storm total rainfall, runoff and % of retention in 2008

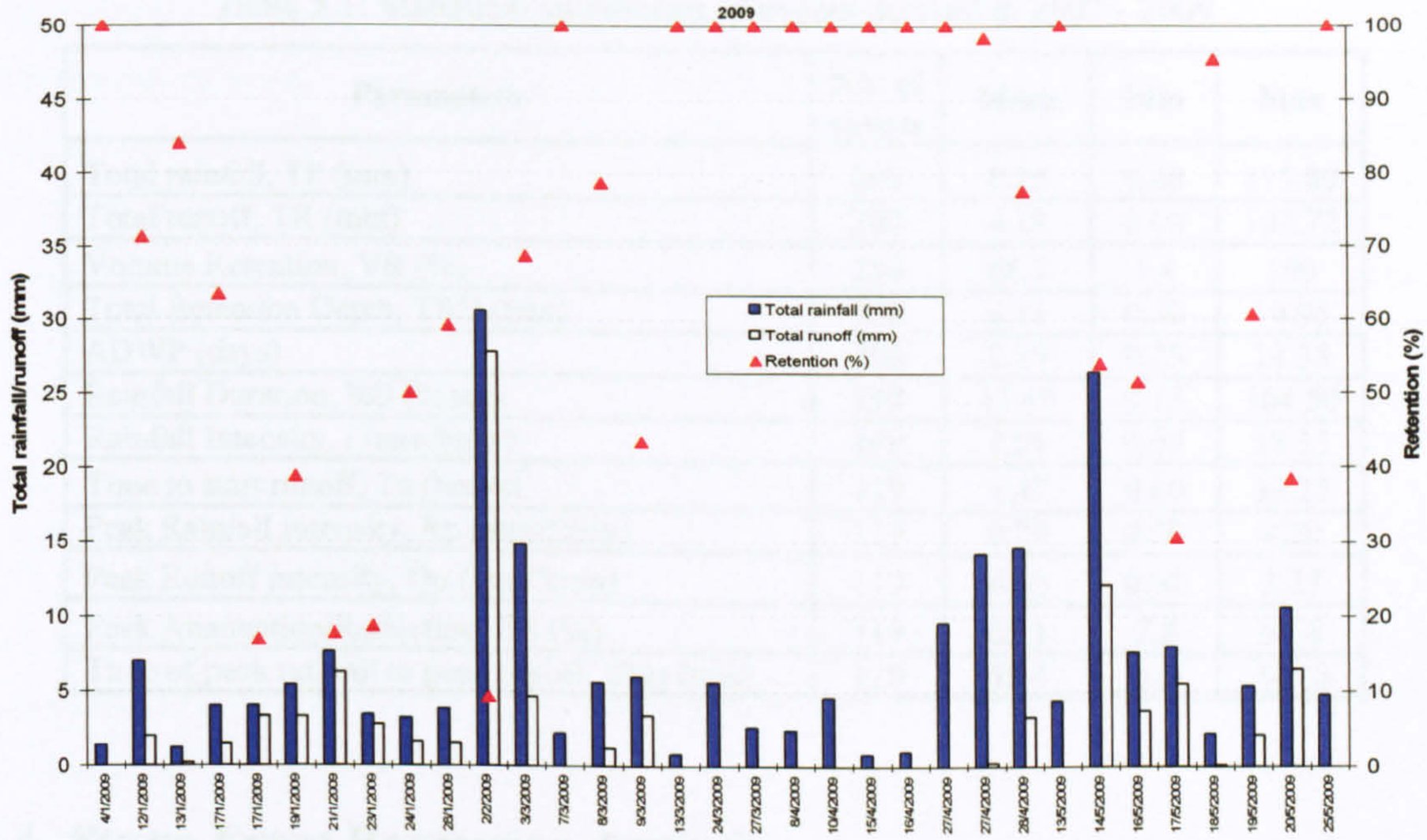


Figure 5.16: Storm by storm total rainfall, runoff and % of retention in 2009

As summarized in Table 5.1, within this 29-month data set, the maximum total rainfall depth is 115.8 mm with a maximum total runoff of 102.72 mm over the same event. The average retention is 68.7% regardless of the seasonal factors; with the minimum capability of the test rig to retain the runoff is 1.4% which corresponded to the maximum rainfall depth. The maximum of 100% retention has been observed on 30% of the 200 total events. The average of peak reduction in runoff intensity is also found to be around 65% with the minimum reduction at 8%. The longest runoff delay following the start of rainfall is 33.3 hours. The maximum runoff peak lag time from rainfall peak time is 445 minutes (7.42 hours). On average, time to the start of runoff and the time to peak runoff are observed as 3.47 hours and 58.4 minutes respectively. The maximum ADWP observed is 24.35 days with an average of 2.15 days and by definition the minimum ADWP found is 6 hours.

It is expected that the storm parameters – total rainfall, ADWP, rainfall duration, rainfall intensity and peak rainfall intensity – determine runoff characteristics: total runoff, volume retention in %, total retention depth, time to start of runoff, peak runoff intensity, peak reduction of peak runoff intensity from peak rainfall intensity and the time lag of the runoff peak from the rainfall peak. The next section will therefore apply regression analysis to explore the potential to develop simple predictive relationships for runoff/retention performance.

Table 5.1: Statistical summaries of events derived in 2007 - 2009

| Parameters | No of events | Mean | Min | Max |
|---|---|---|---|---|
| Total rainfall, TP (mm) | 200 | 8.29 | 0.40 | 115.80 |
| Total runoff, TR (mm) | 200 | 4.18 | 0.00 | 102.72 |
| Volume Retention, VR (%) | 200 | 68.7 | 1.4 | 100 |
| Total Retention Depth, TRD (mm) | 200 | 4.11 | 0.40 | 19.95 |
| ADWP (days) | 200 | 2.19 | 0.25 | 24.35 |
| Rainfall Duration, RD (hours) | 199 | 12.19 | 0.15 | 104.50 |
| Rainfall Intensity, i (mm/hour) | 199 | 1.01 | 0.09 | 18.55 |
| Time to start runoff, Ta (hours) | 119 | 3.47 | 0.00 | 33.25 |
| Peak Rainfall Intensity, Rp (mm/5min) | 119 | 0.73 | 0.20 | 4.20 |
| Peak Runoff Intensity, Qp (mm/5min) | 119 | 0.23 | 0.01 | 2.27 |
| Peak Attenuation/Reduction, PA (%) | 119 | 65.1 | 7.8 | 97.6 |
| Time of peak rainfall to peak runoff, Tlag (min) | 119 | 58.4 | 0.0 | 445.0 |

## 5.4 Storm Event Regression Analysis

### 5.4.1 Introduction

This section presents some preliminary analysis aimed at understanding the extent to which the hydrological performance indicators (total runoff, volume retention, total retention, time to start of runoff, peak runoff intensity, peak reduction and the time lag) are controlled by storm event characteristics (total rainfall, duration, intensity, ADWP, peak rainfall intensity, temperature/season). All 200 storm events are included in the regression analysis but for peak rainfall and peak runoff, only those storm events that generated runoff are included.

Regression analysis is used to predict the relationship of a single dependent variable to one or more independent variables. Statistically, this relationship can be used to improve the level of understanding of the hydrological performance of the test rig. Therefore, the analysis begins with the individual regression of parameters by each parameter and is followed by multiple regressions with combinations of parameters. As the temperature/season might result in some differences in the analyses, for the multiple regression all the events were analysed separately by season.

In regression modelling, the interpretation of the regression output relationship is important to determine whether the regression analysis is significant or not. Hence, the regression analysis will be significant if; i) the coefficient of determination, $R^2$ is within $0 < R^2 \leq 1$, and ii) the t-statistics and their associated 2 tailed p-values is less than 0.05. The coefficient of

determination, $R^2$ indicates the strength of model fit between variables; describes the proportion of response variation 'explained' by the regressors in the model. Its range of $0 < R^2 \leq 1$ indicates that the values that are closer to 1 are a better fit, whilst $R^2 = 0$ indicates that there is no linear relationship between the response variables and the regressors (Montgomery & Runger, 1999). In engineering, a value of less than 0.6 would be considered low (Faraway, 2005).

## 5.4.2 Performance of Retention Parameters

### 5.4.2.1 Runoff Depth

Before looking further into the interrelationships between parameters, Figure 5.17 shows the general relationship between (a) total rainfall and total runoff; and (b) total runoff as a function of total rainfall and ADWP characteristics. As reported by Stovin *et al.*, 2007, there were different rainfall/runoff relationships between ADWPs of less and more than 2. Hence, all events were divided into two categories: events with less than 2 dry days (< 2 days) and events with more than 2 dry days (> 2 days) (Figure 5.17 (b)). These analyses show that there is a correlation between them; Figure 5.17 (b) shows the correlation between < 2 days and > 2 days ADWP, with the total runoff positively correlated with total runoff. As expected, retention is reduced when the ADWP is short. This relationships suggest that the prediction of total runoff are influenced by several parameters, hence multiple regression with selected additional parameters was undertaken and the results shown in Table 5.2.

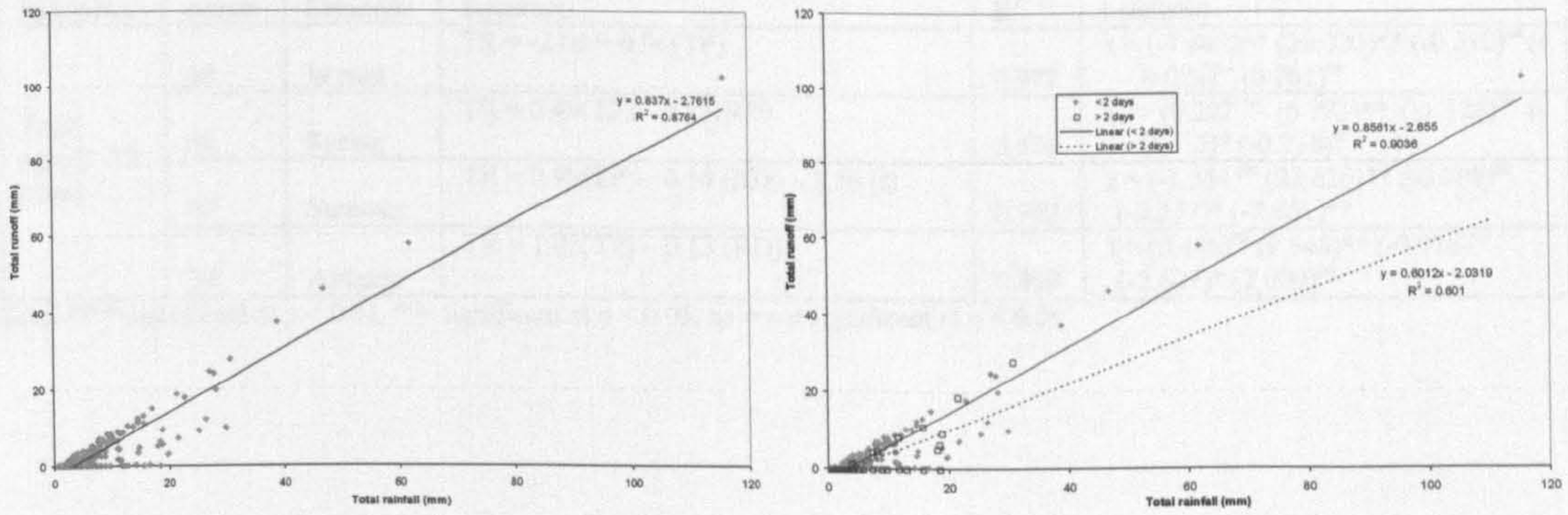


Figure 5.17: Linear regression of (a) total runoff as a function of total rainfall; (b) total runoff as a function of total rainfall of different ADWP

Table 5.2 shows the multiple regressions for total runoff with four parameters that may have some potential influence; total rainfall (TP), ADWP, rainfall duration (RD) and rainfall intensity

(I). By definition, rainfall intensity is a measure of the quantity of rain falling in a given time (i.e. mm per hour (Wilson, 1986)). The t-statistic values in Table 5.2 are written following the sequence of these parameters after the constant coefficient value. Note that the analysis has been undertaken for all four parameters but only significant parameter results are presented in Table 5.2. The analysis was separated seasonally and it reveals that in every season the total rainfall variable influenced the total runoff. The ADWP appears not to have a significant influence on TR over any season while the other two parameters; rainfall duration which affects the total runoff except in winter; and the intensity variable that is only an influence on runoff during the summer time. All the correlations between variables to predict runoff were explained; 0.98 in winter, 0.96 in summer, and 0.86 in autumn and a lower variable for correlation during spring of 0.58 of $R^2$. These findings are consistent with the relatively strong linear relationship between TR and TP demonstrated in Figure 5.17. Correlations between measured and modelled total runoff are shown in Figure 5.18. Data plotted in winter, summer and autumn (Figure 5.18 (a), (c) and (d)) confirm the good fit between the predicted values from the regression analysis and the measured total runoff ($R^2$>0.7). However, as predicted in $R^2$ by the correlation of 0.58 in Table 5.2, the predicted total runoff could not be fitted as effectively as the values to the 1:1 line in spring time (Figure 5.18 (b)). Also note there are no large rainfall events in the spring months.

Table 5.2: Seasonal multiple regression for total runoff prediction for 200 events

| Parameter | No of events | Seasonal | Equation | $R^2$ | t-statistic |
|---|---|---|---|---|---|
| Total runoff, TR (mm) | 58 | Winter | TR = -2.02 + 0.96(TP) | 0.977 | t = (-7.843)** (39.020)** (-0.590)$^{ns}$ (-0.024)$^{ns}$ (0.961)$^{ns}$ |
| | 56 | Spring | TR = 0.49(TP) – 0.11(RD) | 0.576 | t = (0.202)$^{ns}$ (6.773)** (-1.126)$^{ns}$ (-2.155)* (-0.738)$^{ns}$ |
| | 47 | Summer | TR = 0.99(TP) – 0.14 (RD) – 1.74 (I) | 0.962 | t = (-1.384)$^{ns}$ (23.620)** (-0.798)$^{ns}$ (-2.337)* (-3.851)** |
| | 39 | Autumn | TR = 1.03(TP) – 0.13 (RD) | 0.859 | t = (0.486)$^{ns}$ (9.548)** (-0.916)$^{ns}$ (-2.627)* (2.000)$^{ns}$ |

Where; ** = significant at $p < 0.01$, * = significant at $p < 0.05$, ns = not significant at $p < 0.05$

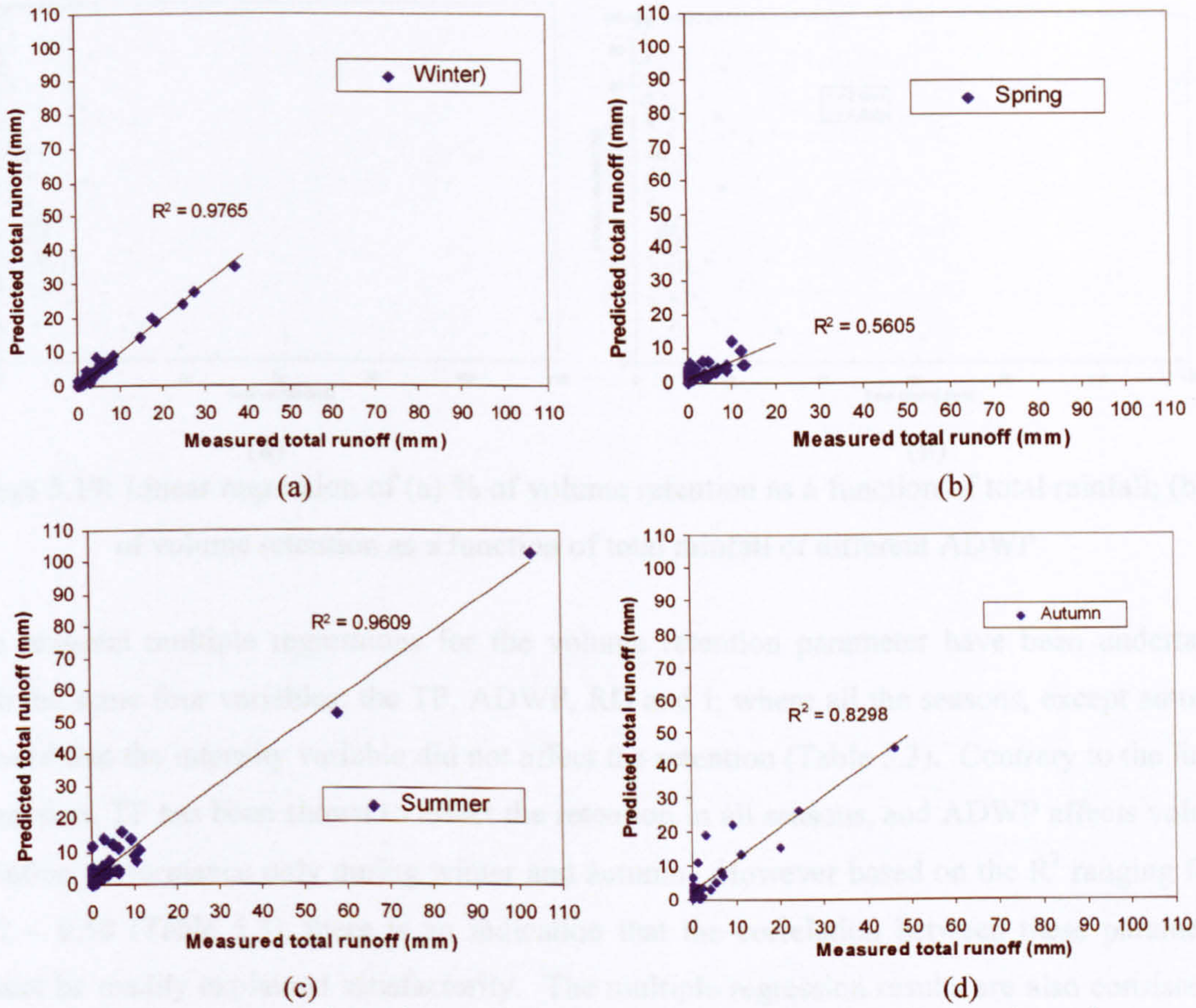


Figure 5.18: The measured total runoff versus predicted total runoff; based on the seasonal prediction equation from Table 5.2 for (a) winter, (b) spring, (c) summer, and (d) autumn

### 5.4.2.2 Volume of Retention

Contrary to the results of total runoff, linear regression does not however show any significant correlation between percentage of volume retention parameter with total rainfall and ADWP variables as shown in Figure 5.19 (a) and (b). This shows that the volume of retention is not dependant on total rainfall. Some rainfall events of less than 10 mm resulted in a retention of less than 15%; whilst for some events with more than a 20 mm depth, the retention was more than 50%. However, other variables could be influenced by the retention variation; hence multiple regression analysis has also been carried out.

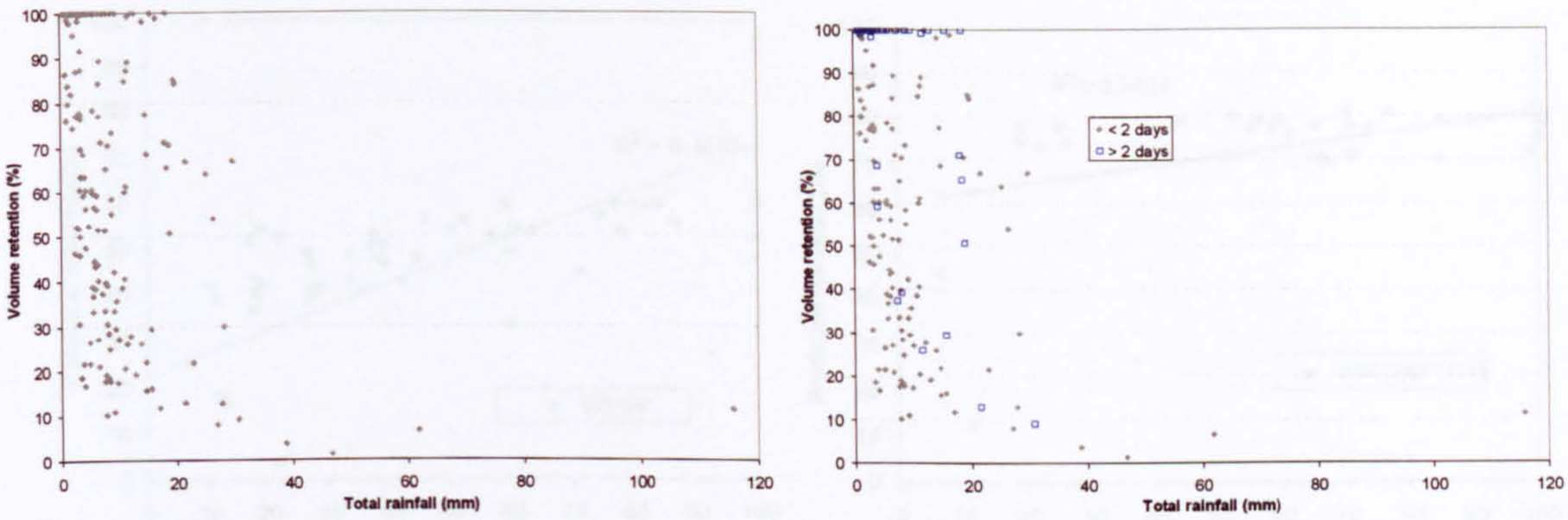


(a) (b)

Figure 5.19: Linear regression of (a) % of volume retention as a function of total rainfall; (b) % of volume retention as a function of total rainfall of different ADWP

The seasonal multiple regressions for the volume retention parameter have been undertaken with the same four variables; the TP, ADWP, RD and I; where all the seasons, except autumn, showed that the intensity variable did not affect the retention (Table 5.3). Contrary to the linear regression, TP has been shown to affect the retention in all seasons, and ADWP affects volume retention performance only during winter and autumn. However based on the $R^2$ ranging from 0.32 – 0.50 (Table 5.3), there is an indication that the correlation between these parameters cannot be readily explained satisfactorily. The multiple regression results are also consistently related to the result of linear regression in Figure 5.19. Following Figure 5.17 (b) with $R^2$ of 0.56 fitted for the spring season presented a weak correlation between parameters, therefore for the percentage of volume retention relationship only data fitted in winter and summer is presented (this is an example of poor prediction) in Figure 5.20. The other season of spring and autumn relationship is not present as their fitted correlation was $R^2 < 0.5$.

Table 5.3: Seasonal multiple regression for % of volume retention prediction for 200 events

| Parameter | No of events | Seasonal | Equation | $R^2$ | t-statistic |
|---|---|---|---|---|---|
| Volume Retention, VR (%) | 58 | Winter | VR = 61.35 - 2.60(TP) + 2.77(ADWP) | 0.487 | t = (12.103)** (-5.380)** (2.724)** $(0.402)^{ns}$ $(0.524)^{ns}$ |
| | 56 | Spring | VR = 88.32 – 2.43(TP) | 0.317 | t = (15.304)** (-3.440)** $(1.781)^{ns}$ $(1.113)^{ns}$ $(0.472)^{ns}$ |
| | 47 | Summer | VR = 83.50 - 0.61(TP) | 0.349 | t = (10.522)** (-2.035)* $(1.550)^{ns}$ $(-1.140)^{ns}$ $(-0.190)^{ns}$ |
| | 39 | Autumn | VR = 64.69 – 2.84(TP) + 2.62(ADWP) + 24.41(i) | 0.499 | t = (6.678)** (-3.825)** (2.531)* $(1.161)^{ns}$ (2.073)* |

Where; ** = significant at $p < 0.01$, * = significant at $p < 0.05$, ns = not significant at $p < 0.05$

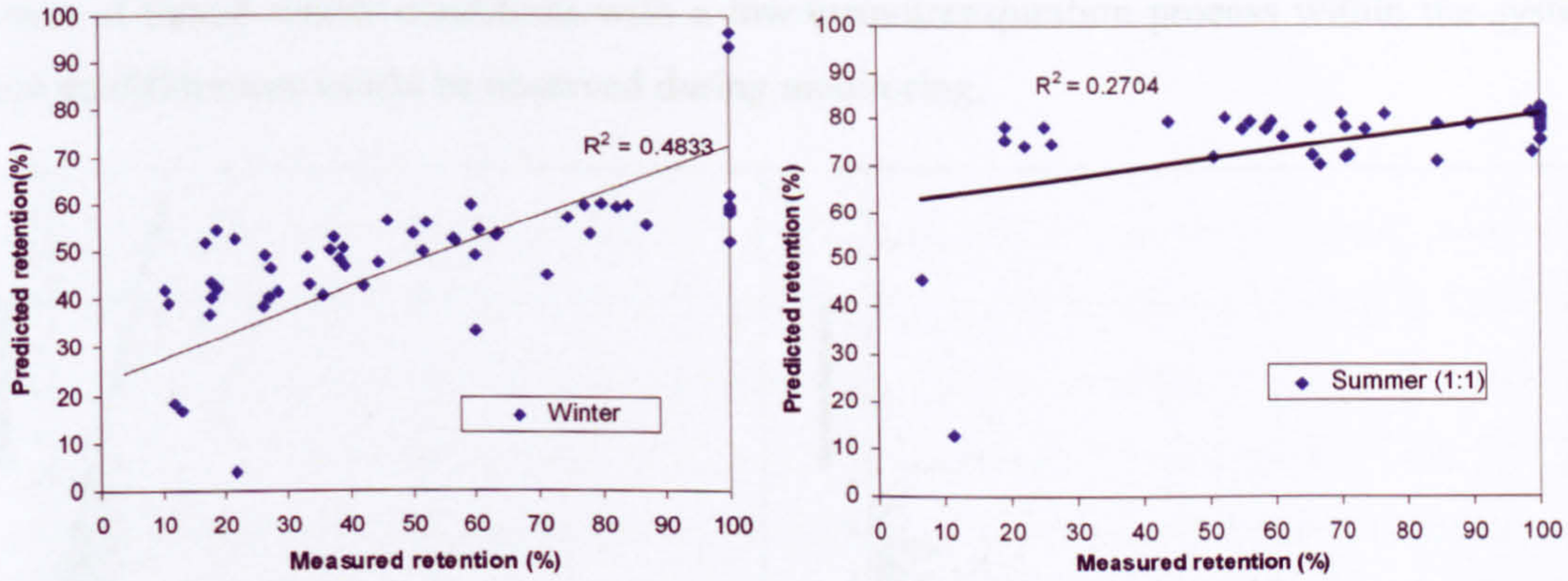


Figure 5.20: The measured total runoff versus predicted total runoff; based on the seasonal prediction equation from Table 5.3 for (a) winter, and (b) summer

### 5.4.2.3 Total Retention Depth/Initial losses

Results concerning the retention depth show that some data correlated a linear relationship between the total rainfall and ADWP, as shown in Figure 5.21 (a). This relationship might suggest the contribution of storage capacity within the test rig where the retention is varied (depending on its ADWP and the moisture balance of substrate) but the maximum taken should be dependent on the total volume of rainfall events. For a larger rainfall (i.e. ≥ 20 mm), the maximum retention observed is 20 mm (which is equivalent to 25% of the 80 mm substrate depth) or at least more than 10 mm of retention (as shown in Figure 5.21 (a) by storm event of > 100 mm).

It is expected that a long ADWP would tend to result in higher levels of retention; however Figure 5.21 (b) does not reveal a strong correlation between these two variables and this is supported by the multiple regressions in Table 5.4. The regression relationship suggests that total rainfall, TP and rainfall duration, RD contribute significantly to the total retention depth, TRD prediction in spring season, with an overall $R^2$ value of 0.74 (Figure 5.22 (a)). The RD is also observed to contribute to the retention depth variation in summer and autumn, following the impact of rainfall intensity variable in summer; where all these seasons have been fitted with very limited correlations ($R^2 \leq 0.42$). Figure 5.22 (b) represents an example of poor predicted retention depth versus measured retention depth in summer based on highly scattered data fitted between both the measured and predicted retention depth. However during winter, the regression identifies no variables as contributing to the TRD performance. This might occur as

a result of humid winter conditions with a low evapotranspiration process within the system, hence no differences would be observed during monitoring.

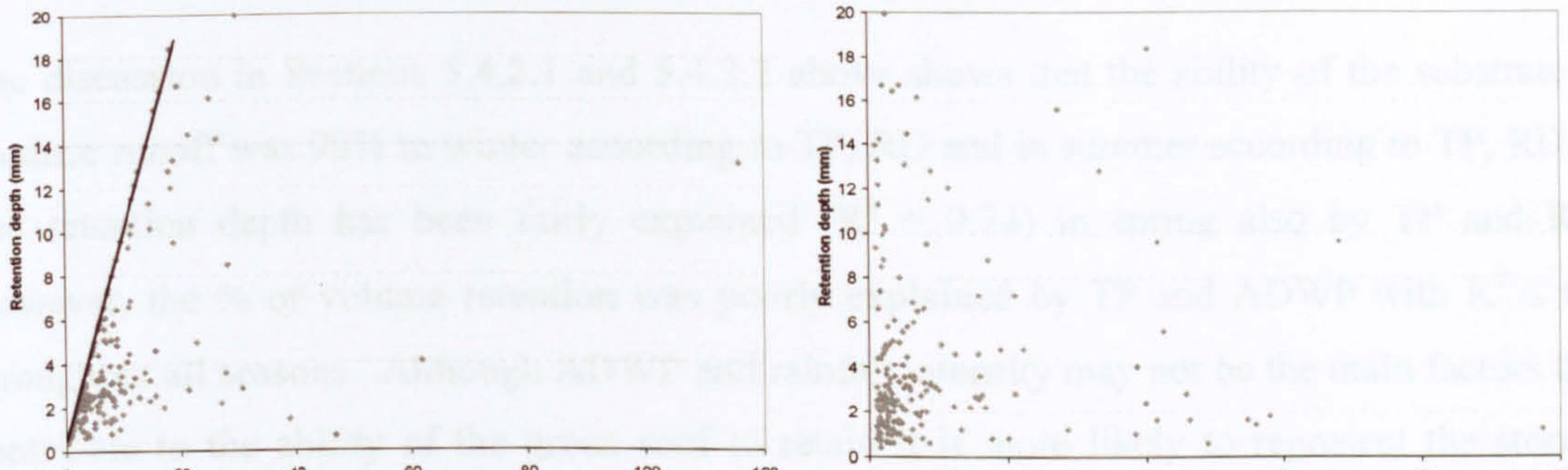


(a) (b)

Figure 5.21: Linear regression of (a) retention in depth as a function of total rainfall; and (b) retention in depth as function of ADWP

Table 5.4: Seasonal multiple regression for total retention in depth prediction for 200 events

| Parameter | No of events | Seasonal | Equation | $R^2$ | t-statistic |
|---|---|---|---|---|---|
| Total Retention Depth, TRD (mm) | 58 | Winter | TRD = 2.02 | 0.101 | t = $(7.84)^{**}$ $(1.751)^{ns}$ $(-0.590)^{ns}$ $(0.024)^{ns}$ $(-0.961)^{ns}$ |
| | 56 | Spring | TRD = 0.51(TP) + 0.11(RD) | 0.737 | t = $(-0.202)^{ns}$ $(6.928)^{**}$ $(1.126)^{ns}$ $(2.155)^{*}$ $(0.738)^{ns}$ |
| | 47 | Summer | TRD = + 0.14(RD) + 1.74(i) | 0.424 | t = $(1.384)^{ns}$ $(0.170)^{ns}$ $(0.798)^{ns}$ $(2.337)^{*}$ $(3.850)^{**}$ |
| | 39 | Autumn | TRD = + 0.13(RD) | 0.364 | t = $(-0.486)^{ns}$ $(-0.251)^{ns}$ $(0.916)^{ns}$ $(2.626)^{*}$ $(2.000)^{ns}$ |

Where; ** = significant at $p < 0.01$, * = significant at $p < 0.05$, ns = not significant at $p < 0.05$

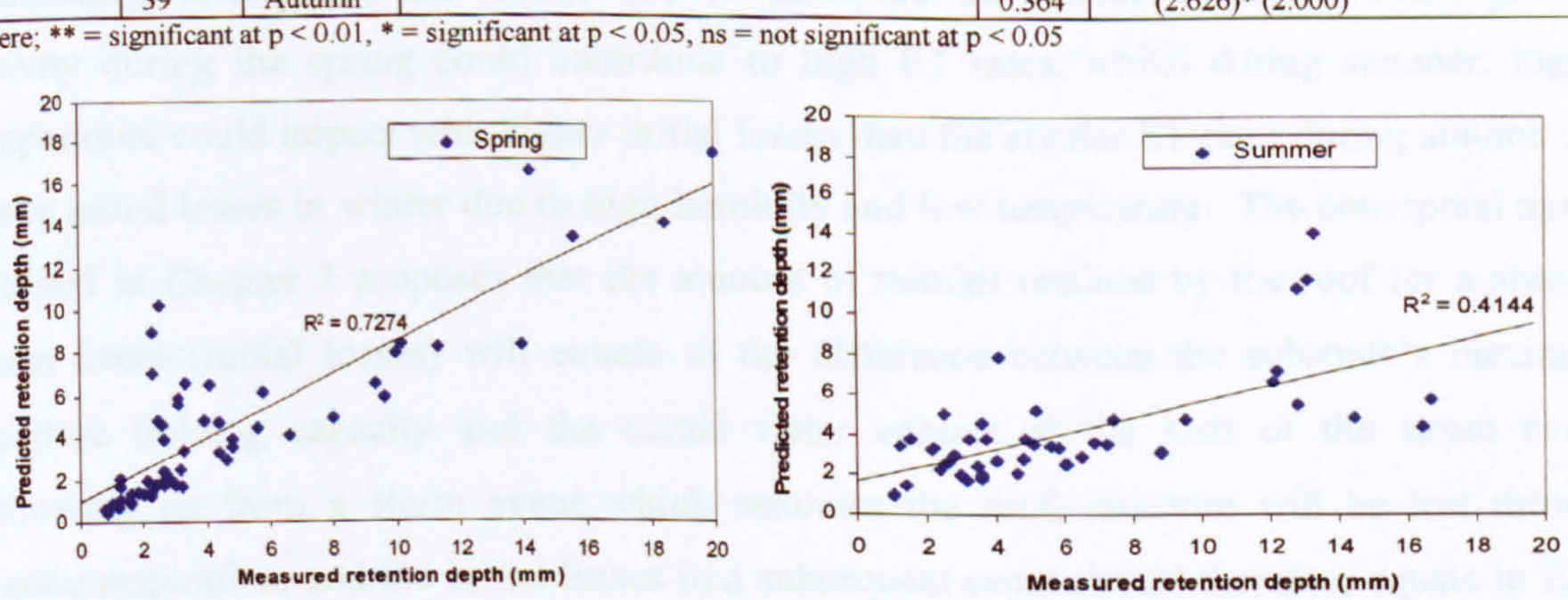


(a) (b)

Figure 5.22: The measured retention depth versus predicted retention depth based on seasonal prediction equation from Table 5.4 of (a) spring; and (b) summer

From all the retention parameters discussed above, it can be observed that the initial losses (total retention depth) could be one essential variable that need to be highlighted (Figure 5.4) and that it is just important to control the retention storage in the substrate. Although the linear and multiple regressions did not statistically reveal the storage conditions based on the ADWP, the

RD parameter, rainfall duration however has an impact on storage moisture capability; based on a moist period of storage.

The discussion in Sections 5.4.2.1 and 5.4.2.2 above shows that the ability of the substrate to produce runoff was 90% in winter according to TP, RD and in summer according to TP, RD, I; and retention depth has been fairly explained ($R^2$ = 0.74) in spring also by TP and RD. However, the % of volume retention was poorly explained by TP and ADWP with $R^2 \leq 0.5$ throughout all seasons. Although ADWP and rainfall intensity may not be the main factors that contribute to the ability of the green roof to retain it is more likely to represent the storage availability at the time of rainfall events as a function of soil characteristics; additionally climatic variables (based on season) will critically influence storage performance. Hence more detailed information relating to the substrate moisture deficit due to evapotranspiration (ET) needs to be considered.

Based on a water loss study by Rezaei & Jarret (2006), different seasonal conditions resulted in different ET values. Further analyses were also undertaken using monitored data to provide some quantitative observations from our ET rates. Apparently, ET rates characteristics are related to seasonal variations, so it is expected that throughout the seasons, ET might lead to understandable response rate values. It is assumed that the increased sunshine and vegetative activity during the spring could contribute to high ET rates, whilst during summer; higher temperature could impact with higher initial losses than the similar ET rates during autumn and lower initial losses in winter due to high humidity and low temperature. The conceptual model outlined in Chapter 3 proposes that the amount of rainfall retained by the roof for a specific storm event (initial losses) will equate to the difference between the substrate's maximum moisture holding capacity and the actual water content at the start of the storm event. Following on from a storm event which saturates the roof, moisture will be lost through evapotranspiration, and the initial losses in a subsequent event should therefore equate to ET x ADWP (Antecedent Dry Weather Period (days)).

Figure 5.23 shows the same information as Figure 5.21 (b) but is divided according to seasons and shows the performance of substrate's moisture content as a function of ADWP. The substrate in this case is known to have a $WC_{max}$ (based on Chapter 3) of 50% by volume, which equates to 40 mm depth in the 80 mm test bed substrate. Hence the moisture content values are determined from 40 - (Rainfall - Runoff). The results show the considerable scatter evident

based on each storm characteristic. The definition of a 'storm event' and its ADWP are not straightforward for the start and end times of the event, and some of the events do not leave the roof in a fully-saturated condition might explained the scatter.

Figure 5.23(a) is the moisture content (retention) data from all 200 storms monitored with the assumption that the substrate was fully saturated at the end of preceding event. However, in reality the scatter data set plotted might not be fully saturated and thus tends to overestimate the true ET. The result shows that the roof very rarely experiences moisture levels below 25 mm (i.e. minimum moisture content, $MC_{min}$ = 25 mm; is the maximum initial losses = 15 mm). This value is significantly lower than if the maximum initial loss was assumed equal to $WC_{max}$ (i.e. 40 mm in this case). It should be noted that based on Figure 5.23 (a), even in summer, the roof will take over one week to fully regain its maximum moisture retention capacity following saturation.

However, it is also believed that events which did not generate runoff (including that in Figure 5.23(a)) tend to underestimate ET; therefore Figure 5.23(b) has been plotted excluding the 48 storm events which produced runoff and rapid ET rates were observed. It is assumed that during these events, the storage capacity of the substrate is at maximum, hence fully retains the moisture. Therefore, it seems that during very dry conditions, the roof can fully regain its maximum moisture retention capacity within less than 10 days following saturation over all seasons. The indicative ET values for the substrate are determined based on Figure 5.23 (b) as shown in Table 5.5. In order for the rainfall to generate runoff, the maximum of 2 days of ADWP following saturation has been observed with the highest storage capacity the substrate could provide during summer at 11.0 mm and the lowest in winter at 4.5 mm. Hence the chances for rainfall to be fully retained after 2 days of ADWP are higher. This suggests that after the storage, ADWP and seasonal conditions have been fulfilled, the following factors that control the initial losses should be rainfall characteristics which might result in variations in the retention performance.

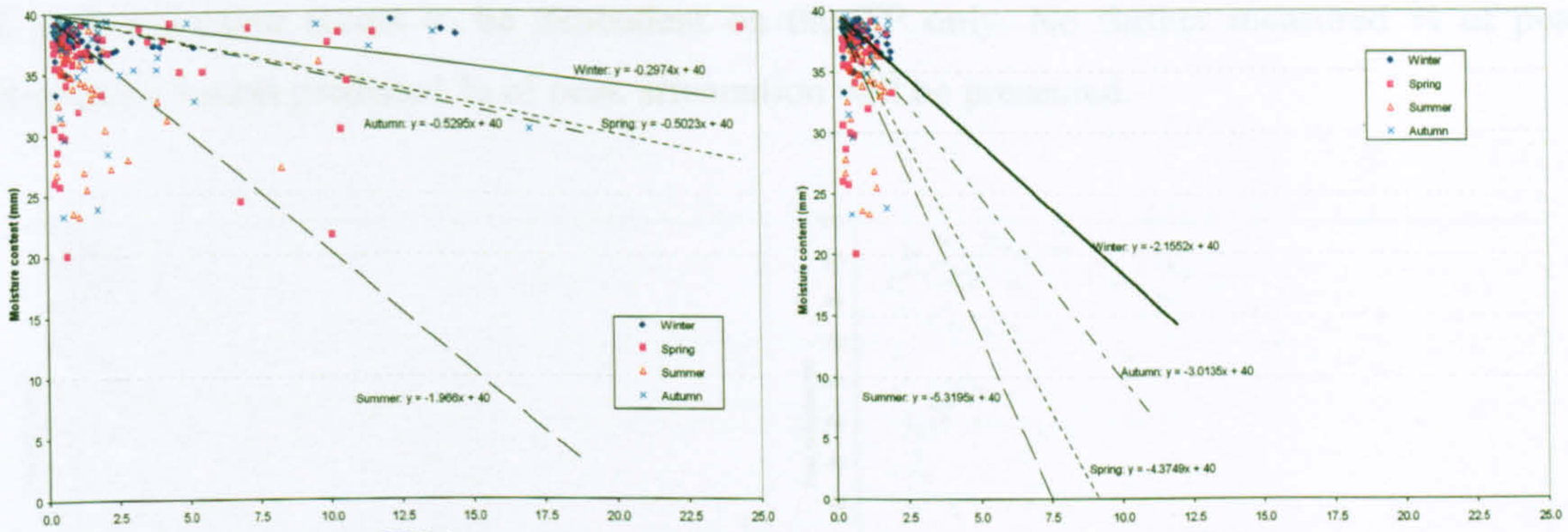


(a) (b)

Figure 5.23: Moisture content of the substrate from storm-based monitoring versus ADWP of (a) rainfall events including the events that produced runoff; and (b) only rainfall that produced no runoff

Table 5.5: ET rates derived from monitored initial losses based on Figure 5.23(b)

| Season | Evapotranspiration rate (mm/day) | Maximum storage to recharge at 2 days of ADWP (mm) |
|---|---|---|
| Winter (Dec, Jan, Feb) | 2.2 | 4.5 |
| Spring (Mar, Apr, May) | 4.4 | 9.0 |
| Summer (Jun, Jul, Aug) | 5.3 | 10.8 |
| Autumn (Sep, Oct, Nov) | 3.0 | 6.2 |

### 5.4.3 Performance of Detention Parameters

#### 5.4.3.1 Peak Attenuation, Delayed Time to Peak and Time to Start Runoff

Figure 5.24 shows the regression analyses with 119 storm events that generated runoff in order to predict the % peak attenuation. The analyses demonstrated poor correlations; with the result for the % of peak reduction as a function of total rainfall fitted in Figure 5.24 (a) and ADWP in Figure 5.24 (b). The % of peak attenuation predicted by the multiple regressions as presented in Table 5.6 also supported the linear regression correlations, where in all seasons it seems that peak reduction is not significantly affected by any of the four variables except for the total rainfall, TP in winter time. This can be observed during winter and autumn which can be explained as $R^2$ at 0.37 and 0.54 respectively. However, during autumn with $R^2$ of 0.74, the %

of peak reduction seems to be dependent on the TP only. No further measured % of peak attenuation versus predicted % of peak attenuation will be presented.

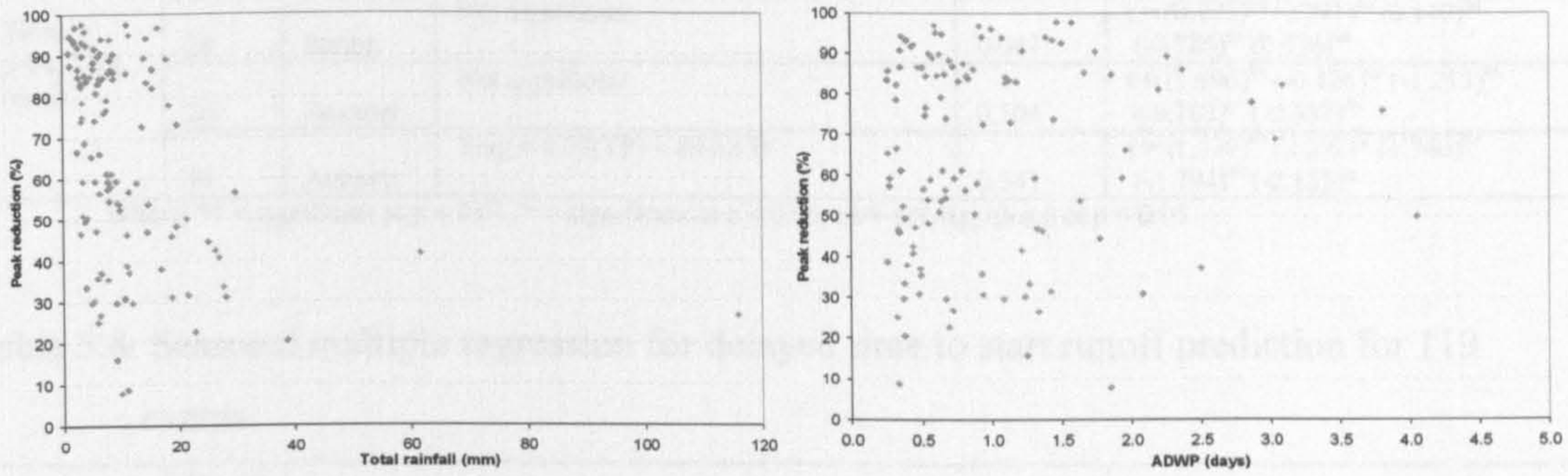


(a) (b)

Figure 5.24: Linear regression of (a) the % of peak attenuation as a function of total rainfall; (b) the % of peak reduction as a function of ADWP

Table 5.6: Seasonal multiple regression for % of peak reduction prediction for 119 events

| Parameter | No of events | Seasonal | Equation | $R^2$ | t statistic |
|---|---|---|---|---|---|
| Peak Attenuation, PA (%) | 49 | Winter | PA = 67.54 - 2.62(TP) | 0.369 | t = $(8.066)^{**}$ $(-4.269)^{**}$ $(1.179)^{ns}$ $(1.258)^{ns}$ $(1.062)^{ns}$ |
| | 24 | Spring | PA = 85.37 | 0.168 | t = $(5.019)^{**}$ $(-0.891)^{ns}$ $(-0.064)^{ns}$ $(1.267)^{ns}$ $(-1.073)^{ns}$ |
| | 28 | Summer | PA = 86.12 | 0.330 | t = $(7.228)^{**}$ $(-1.085)^{ns}$ $(0.525)^{ns}$ $(-0.894)^{ns}$ $(-1.149)^{ns}$ |
| | 19 | Autumn | PA = 49.85 – 3.50(TP) | 0.736 | t = $(4.224)^{**}$ $(-4.308)^{**}$ $(2.046)^{ns}$ $(2.112)^{ns}$ $(1.754)^{ns}$ |

Where; ** = significant at $p < 0.01$, * = significant at $p < 0.05$, ns = not significant at $p < 0.05$

Statistically, for time to peak variable, there is no relationship ($R^2 < 0.1$) between all the variables in spring and summer (Table 5.7) and the variables of TP and intensity; this has led to a weak explanation of the time response to peak in winter and autumn with $R^2$ at 0.14 and 0.34, respectively. Similarly factors apply to the regression relating to time to start runoff during winter and spring ($R^2 < 0.3$) as presented in Figure 5.8; in summer and autumn however, the regression relationships have been explained less fairly by RD and ADWP with only $R^2$ of 0.53 during summer and $R^2$ of 0.69 in autumn. No further analysis of this data is presented.

Table 5.7: Seasonal multiple regression for delayed time to peak prediction for 119 events

| Parameter | No of events | Seasonal | Equation | $R^2$ | t-statistic |
|---|---|---|---|---|---|
| Time to peak, Tlag (min) | 49 | Winter | Tlag = - 3.6(TP) | 0.138 | t = $(1.893)^{ns}$ $(-2.053)^{*}$ $(-0.130)^{ns}$ $(1.774)^{ns}$ $(-0.494)^{ns}$ |
| | 24 | Spring | Not significant | 0.041 | t = $(0.973)^{ns}$ $(0.271)^{ns}$ $(0.140)^{ns}$ $(-0.786)^{ns}$ $(0.626)^{ns}$ |
| | 28 | Summer | Not significant | 0.104 | t = $(1.996)^{ns}$ $(-0.426)^{ns}$ $(-1.213)^{ns}$ $(-0.103)^{ns}$ $(-0.387)^{ns}$ |
| | 19 | Autumn | Tlag = 4.77(TP) – 80.62(I) | 0.341 | t = $(1.830)^{ns}$ $(2.292)^{*}$ $(1.740)^{ns}$ $(-1.794)^{ns}$ $(-2.155)^{*}$ |

Where; ** = significant at $p < 0.01$, * = significant at $p < 0.05$, ns = not significant at $p < 0.05$

Table 5.8: Seasonal multiple regression for delayed time to start runoff prediction for 119 events

| Parameter | No of events | Seasonal | Equation | $R^2$ | t-statistic |
|---|---|---|---|---|---|
| Time to start runoff, Ta (min) | 49 | Winter | Ta = 12.34 (RD) | 0.195 | t = $(-0.314)^{ns}$ $(-0.421)^{ns}$ $(0.260)^{ns}$ $(2.413)^{*}$ $(0.091)^{ns}$ |
| | 24 | Spring | Not significant | 0.303 | t = $(-0.050)^{ns}$ $(0.527)^{ns}$ $(1.521)^{ns}$ $(-0.033)^{ns}$ $(-0.061)^{ns}$ |
| | 28 | Summer | Ta = 351.7(ADWP) + 22.35(RD) | 0.528 | t = $(-1.894)^{ns}$ $(-1.982)^{ns}$ $(3.454)^{**}$ $(2.886)^{**}$ $(0.555)^{ns}$ |
| | 19 | Autumn | Ta = 14.24(RD) | 0.687 | t = $(-0.580)^{ns}$ $(0.900)^{ns}$ $(1.356)^{ns}$ $(2.588)^{*}$ $(-0.795)^{ns}$ |

Where; ** = significant at $p < 0.01$, * = significant at $p < 0.05$, ns = not significant at $p < 0.05$

## 5.4.4 Conclusion

The relationship between the hydrological performance and the characteristics of the storms have been presented and discussed. The most significant influences on both retention and detention parameters performances were observed more clearly in relation to the different seasons; which leads to the conclusion that contribution of total rainfall, TD and rainfall duration, RD (from the multiple regression) are the main variables that explain the total runoff predictions. However, the analysis suggests that the influence of the other variables can be assessed in terms of fair or poor relationships with the parameters investigated. It is expected that the fact of the maximum moisture capacity or ADWP of the substrate might be the main reason for this non-correlating relationship. However, based on linear and multiple regressions it is suggested that there were no simple explanatory relationships between these variables. Further detailed analysis on each storm-by-storm event has been undertaken in the following section to provide a better understanding of the physical processes.

## 5.5 Analysis of Specific Types of Storm Event

### 5.5.1 Introduction

The previous section considered the general relationships controlling the runoff characteristics of retention and detention in the green roof test rig. This section will focus on selected specific events as some of the relationships seem too complex to be easily understood. All the events in this section are selected based on specifically interesting characteristics and are intended to highlight the reasons why some of the relationships cannot be readily explained.

### 5.5.2 Rainfall Intensity

Based on Table 5.1, it has been observed that the highest intensity was 18.6 mm/hour on 15th May 2007, with 3.4 mm of rainfall depth within 11 min (Figure 5.25(a)). A small rainfall depth, with the highest intensity rainfall has shown an initial runoff delay of only 10 min with 15 min of peak flow attenuation. However since it was a small rainfall event and it had followed more than 1 day of ADWP, the test rig managed to reduce the peak flow by 98% with 87% of volume retention. Another example of high intensity observed from the monitored data took place on 1st August 2008 with an intensity of 7.9 mm/hour (Figure 5.25(b)). The rainfall depth of 18.8 mm within 2.4 hours with an ADWP of 8.2 hours generated initial runoff only 5 min after rainfall started. The peak flow reduction is only 46% with a 10 min lag time. The rainfall however was retained by 71% of total volume with 13.3 mm of initial loss. Hence, both of these examples suggest that high intensity rainfall could have less affect on volume retention but more affect on the detention performance. However, rainfall depth still remains as the main influential factor on both performances.

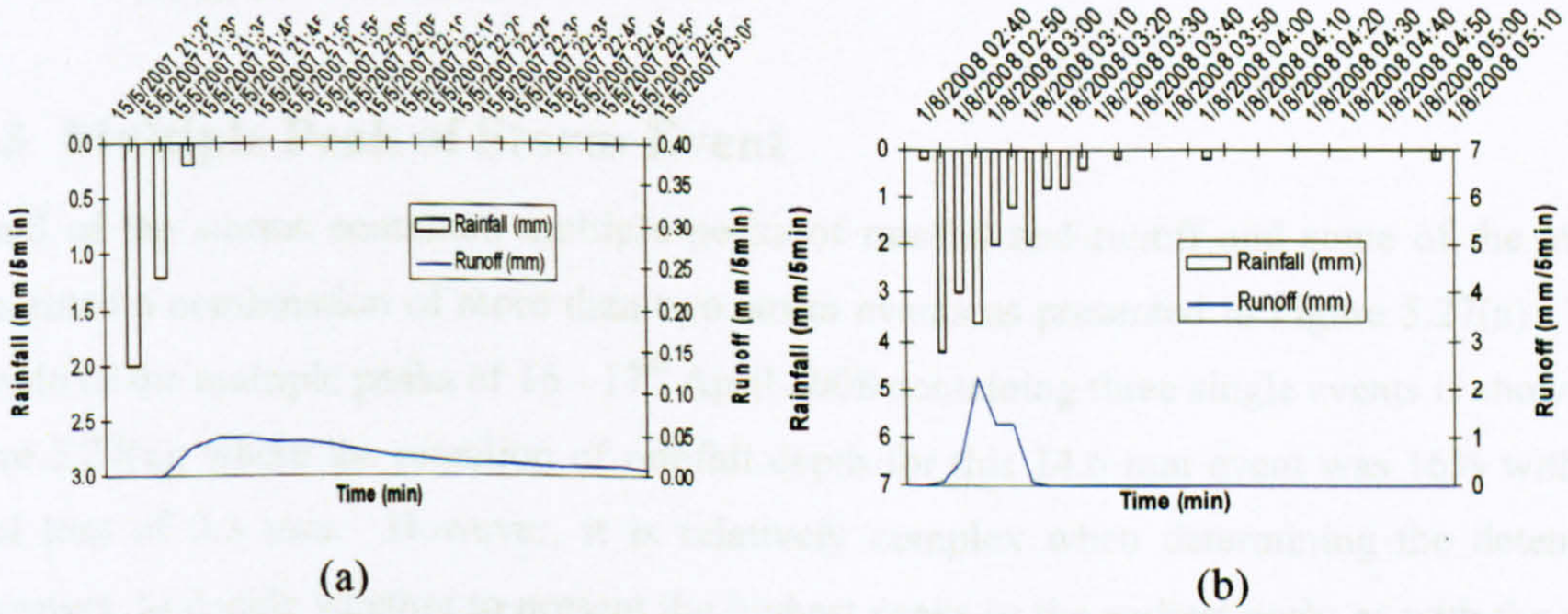


Figure 5.25: Example of high intensity rainfalls on (a) 15th May 2007; and (b) 1st August 2008

Due to our definition of storm events with an ADWP of 6 hours or more, the event on 6th September 2008 has been categorized as fairly low intensity of rainfall at 0.47 mm/hour. This example may point to a complexity in the rainfall parameter description that cannot be revealed by multiple regression analysis as presented in Figure 5.26(a); where this event would be categorized as representing a high intensity of rainfall. Nevertheless, this 9.4 mm rainfall volume was 30% retained by the test rig with a 54% peak flow reduction. There was no initial runoff delay, which might be due to small events occurring following a bulk of high intensity rainfall with only a 5 min peak time lag. While the event on 18th November 2007 is an example of average intensity this example is continuous and shows the same frequency of rainfall from the beginning until the end of the storm (Figure 5.26(b)). Volume retention for this event is 64% from its total 25.2 mm depth has intensity of 0.84 mm/hour. It takes 14.8 hours for runoff to start with 4 hours for peak rainfall (centre of the rainfall rate) to produce peak runoff with 44% peak flow reduction. Overall, it can be concluded that the examples of rainfall rate types cannot be explained by one simple rule; therefore variations in hydrological performance are to be expected.

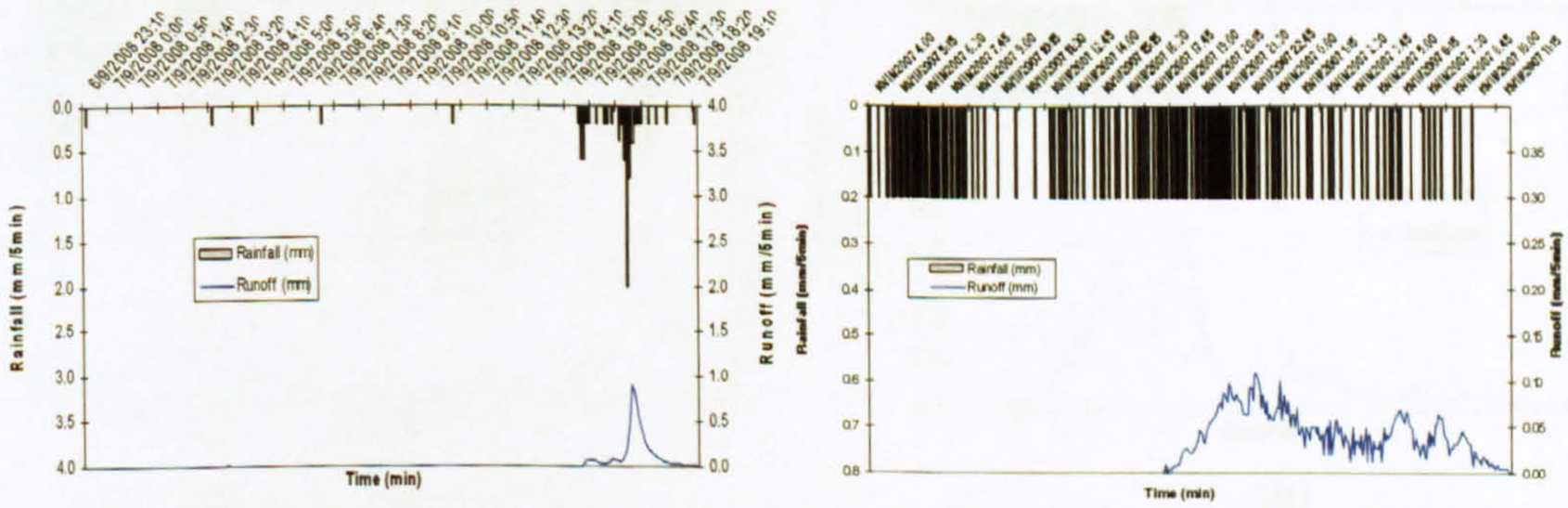


Figure 5.26: The example of low and average intensity rainfall (a) on 6th September 2008; and (b) on 23rd November 2007

## 5.5.3 Multiple Peak of Storm Event

Several of the storms contained multiple peaks of rainfall and runoff and some of the event represented a combination of more than two storm events as presented in Figure 5.27(a). The example of the multiple peaks of 16 - 17th April 2008 containing three single events is shown in Figure 5.27(a); where the retention of rainfall depth for this 14.6 mm event was 16% with an initial loss of 2.3 mm. However, it is relatively complex when determining the detention parameters, to decide whether to present the highest peaks or the earliest peak; as with the next example representing a storm event with two runoff peaks on 4th December 2008, see Figure 5.27(b). All three peaks from the Figure 5.27(a) event have been observed reducing the peak

flow consecutively by 84%, 50% and -11% as the substrate became saturated. Time to the start of runoff for the first peak is 5 min with a peak lag time of 45 min and reducing for the next peak at 25 min and no lag peak time observed for the third peak. The 4th Dec event has been observed in terms of the highest peak flow (which is the second peak) with an 8% of reduction within 25 min of lag time. The initial runoff was observed 1.4 hours after rainfall started (Figure 5.27(b)) with 2.7 mm initial loss from the total of 10 mm rainfall which is equivalent to a 27% volume of retention. This different selection of peak flow reduction and time also demonstrated the complexity of describing the relationship between parameters. The example of multiple peak events also describes the limitation of the storage capacity where in any consecutive rainfall events, especially for larger events, the possibility of runoff production is higher. It seems that for the substrate to recover its retention storage capacity, more ADWP time is required.

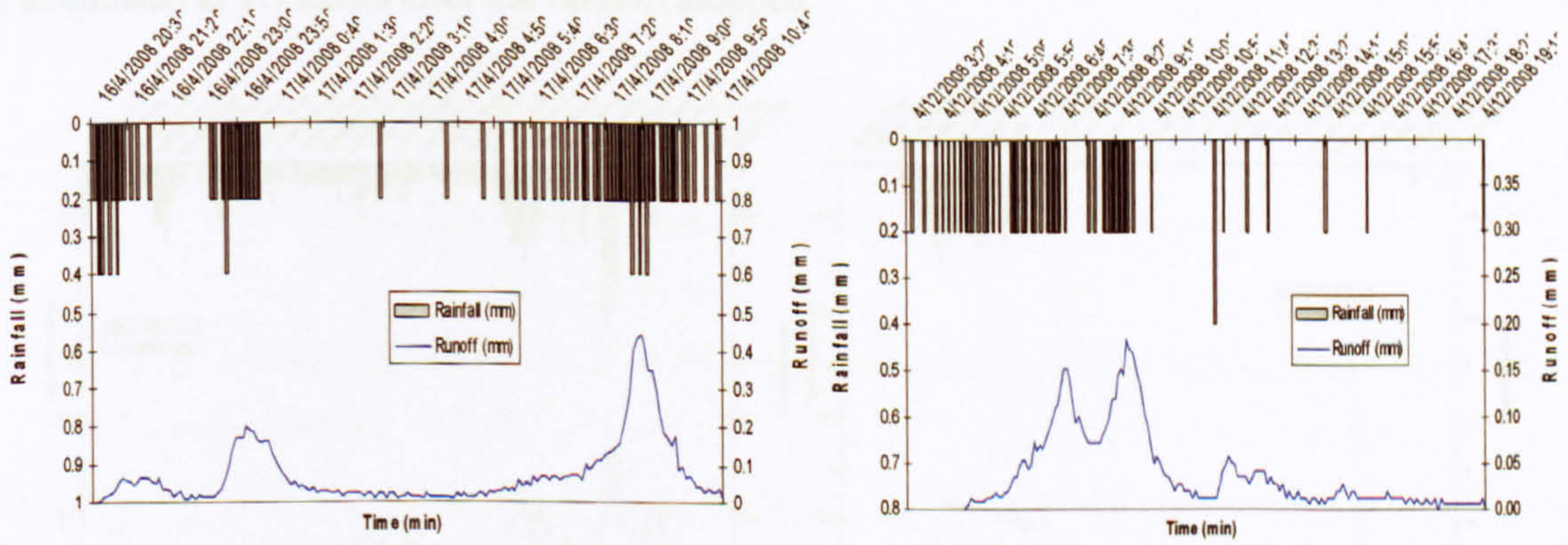


(a) (b)

Figure 5.27: The example of multiple peak flows (a) on 16th April 2008; and (b) on 4th December 2008

## 5.5.4 Extreme Rainfall Event

A continuous 2 day high intense rainfall event occurred in Sheffield between 13th June and 15th June 2007. The test rig collected the highest volume of total rainfall; 115.8 mm for 59.6 hours of rainfall duration (Figure 5.28). Based on the Flood Studies Report (FSR, Volume II: Meteorology) (Wilson, 1990), this 115.8 mm of rainfall event was comparable to a 1 in 100 year event in the Sheffield area; i.e. it was an extreme event. It is however defined as two periods as presented in Figure 5.28(a) and Figure 5.28(b) for the purposes of observing the performance of the subsequent storm following the large event. These events are however defined as one event in terms of the ADWP between events was less than 6 hours apart. From

the total rainfall, the test rig managed to retain 11.3% of the equivalent runoff, with 13.1 mm of initial loss. Although the ADWP for this event is reported as 1 day and 8 hours, the substrate seam still provided quite a high maximum storage capacity of 13.1 mm; as the substrate had experienced almost 17 days of ADWP since the previous 12.8 mm storm event. The dryness and high temperature of June might explain the high initial loss retained for this storm. The runoff delay was also almost 6 hours after the first rainfall occurred although it took only 5 min of peak rainfall to peak runoff with 27% of reduction. This suggests that the peak flow performance is mainly dependent on the characteristics of the rainfall. The final runoff lasting for 3 hours was observed since the rainfall ceased. After 5 hours of ADWP a subsequent rainfall event started (Figure 5.28(b)). It is expected that during this time, the substrate was already saturated; as indicated by the total runoff generated at 15.8 mm from the 16.2 mm of total rainfall with only a 3% retention. However the test rig still managed to delay the initial runoff by 15 min with a peak reduction of 25% with 5 mins of lag time. The subsequent runoff is attenuated at 1.1 hours after the rainfall stopped.

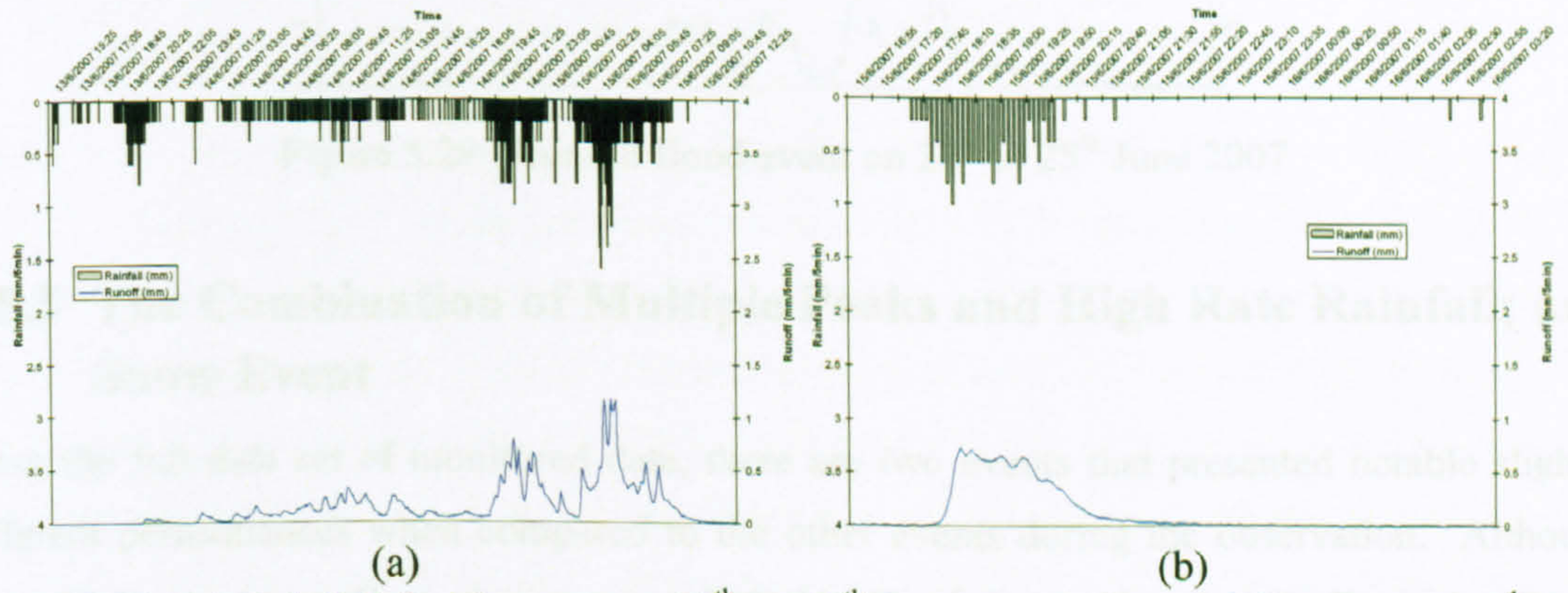


(a) (b)

Figure 5.28: (a) Rainfall flood event on 13th to 15th June 2007; (b) rainfall event on 15th June 2007 following heavy storm on 13th - 15th June 2007

Sheffield experienced a significant flood event on 25th June to 27th June 2007. Figure 5.29 shows that a 62 mm rainfall event occurred on 24th June to 25th June. Based on the Flood Studies Report (FSR, Volume II: Meteorology) (Wilson, 1990), 62 mm falling in 33 hours was comparable to a 1 in 10 year return period rainfall event in the Sheffield area. During this rainfall event, the test rig experienced 7% of retention with an ADWP of 1 day 5 hours was retained 4 mm of the initial losses. It also has been observed that it took 11 hours 9 min to the start of runoff with the final runoff lasting since last rainfall for almost 3 hours with a peak reduction of 60%. This initial runoff delays attenuation performance showing that an initial loss

of 4 mm within an 11 hour delay might be due to the timing of the first early rainfall measured in light intensity and high summer ET. This also suggests that the performance of this event was not affected by the daily rainfall occurring since 19th June and was not even impacted by the very intense rainfall between 13th and 16th June 2007 (Figure 5.28). As long as the substrate has an appropriate time to recover its retention/storage capacity, for example of this 24 – 25th June event there were 29 hours of ADWP, meaning the opportunity for the media to retain and detain the rainfall are higher, especially for small and medium events.

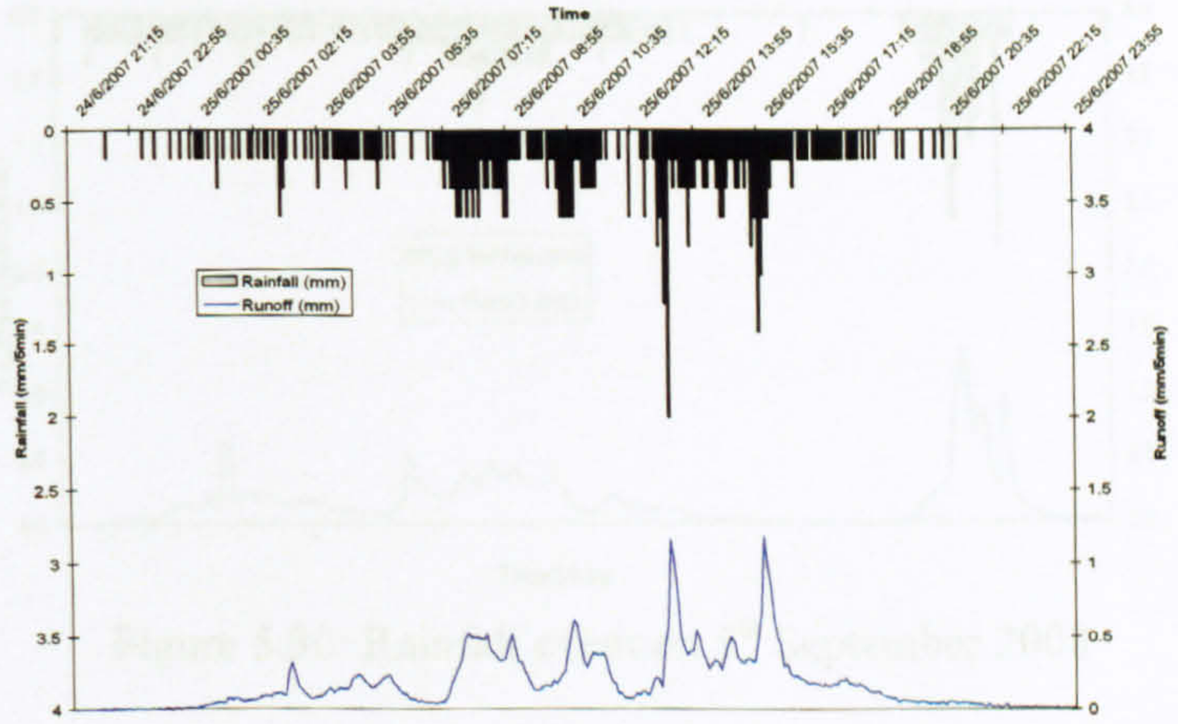


Figure 5.29: Rainfall flood event on 24th to 25th June 2007

### 5.5.5 The Combination of Multiple Peaks and High Rate Rainfall; and Snow Event

From the full data set of monitored data, there are two events that presented notable slightly different performances when compared to the other events during the observation. Although they might not be outliers, they are not individually shown to be statistically insignificant; however with the negative value of peak reduction from the 5th September 2008 event; and a continuous snow storm event for almost two weeks from early February 2009, these rainfalls might be expected to perform differently from the other rainfall events monitored. These events are then presented in Figure 5.30 and Figure 5.31; in order to offer an overview of their performance.

Figure 5.30 demonstrates a combination of multiple peak flows and a high intensity of rainfall. It shows only 1.4% of volume retention with 0.7 mm of initial loss from 47 mm of total rainfall as it has 14.7 hours of ADWP with the combination of the humid conditions of September 2008 (Figure 5.2). This event is however still a bit complicated to comprehend; wherein the first peak rainfall event came after the peak runoff, which may result in 20% at 5.6 hours preceding

the rainfall peak. It has previously been decided that the peak rainfall should be earlier than the peak runoff; therefore, the centre of rainfall before the first peak runoff has resulted in a peak flow reduction of -60% with a 25 minutes peak lag time. However, for single high intense peak flow, a 14% of reduction with a peak delay of 10 min and no initial runoff has been observed. These peak flow parameters have not been used in the multiple regression.

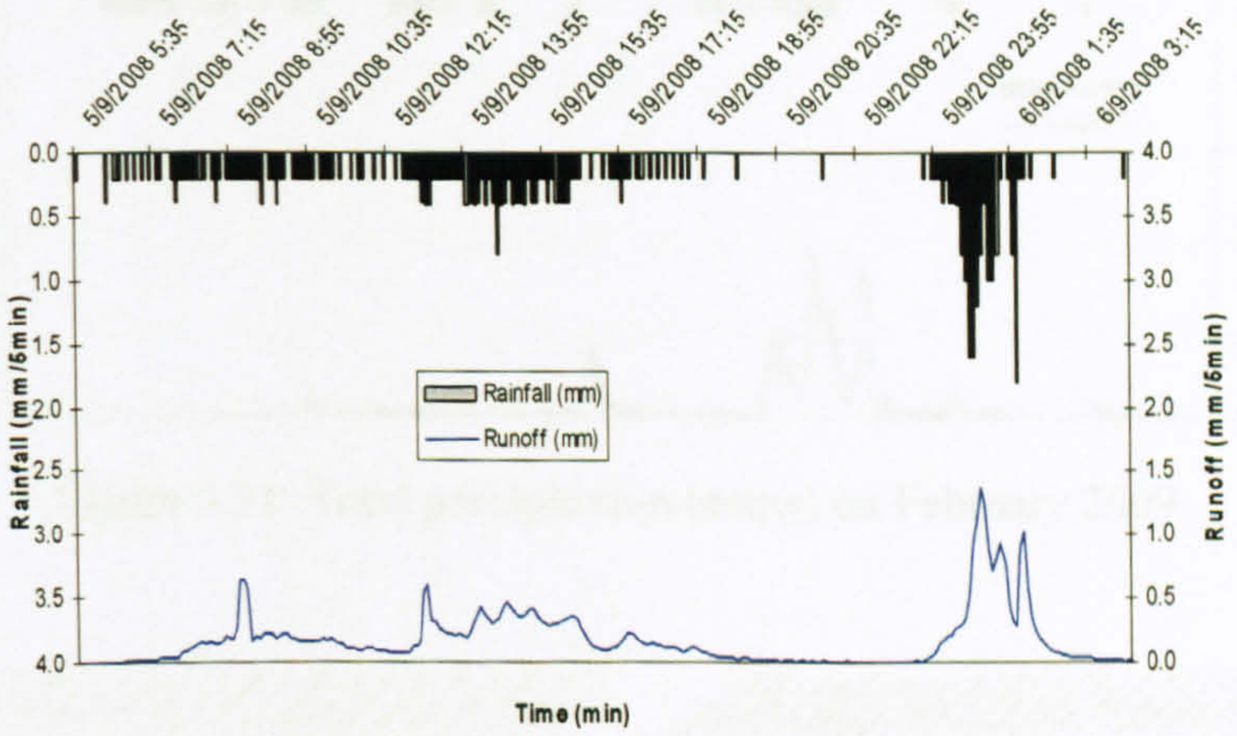


Figure 5.30: Rainfall event on 5th September 2008

Figure 5.31 shows all heavy snow events occurred in the first week of February 2009; on the 2nd and 7th of February 2009 where the collection reading from the rain gauge was 17.6 mm, 5.14 mm of runoff and 10-15 cm of snow thickness. In the second week of February 2009, a mixture of rain, sleet and snow occurred, and the combination of rain and thawing snow might explain the events (with six hours or more ADWP) as shown in Figure 5.32 more runoff was produced than rainfall. Few events have more runoff than the rainfall and these are due to melting snow volumes on 7th, 8th and 11th February 2009, therefore direct analysis for volume retention, peak reduction and attenuation toward the events of ADWP less than 6 hours or more are not made. However, all of the snow events have been combined as one event to simplify the observation of their performance. Overall peak reduction for this February 2009 maximum peak runoff intensity was 37% from 0.2 mm/5min of maximum peak rainfall/snow intensity with 2.5 days of peak attenuation (to the highest peak runoff). Volume retention for this event was 3% with the initial runoff delayed for 2.1 days.

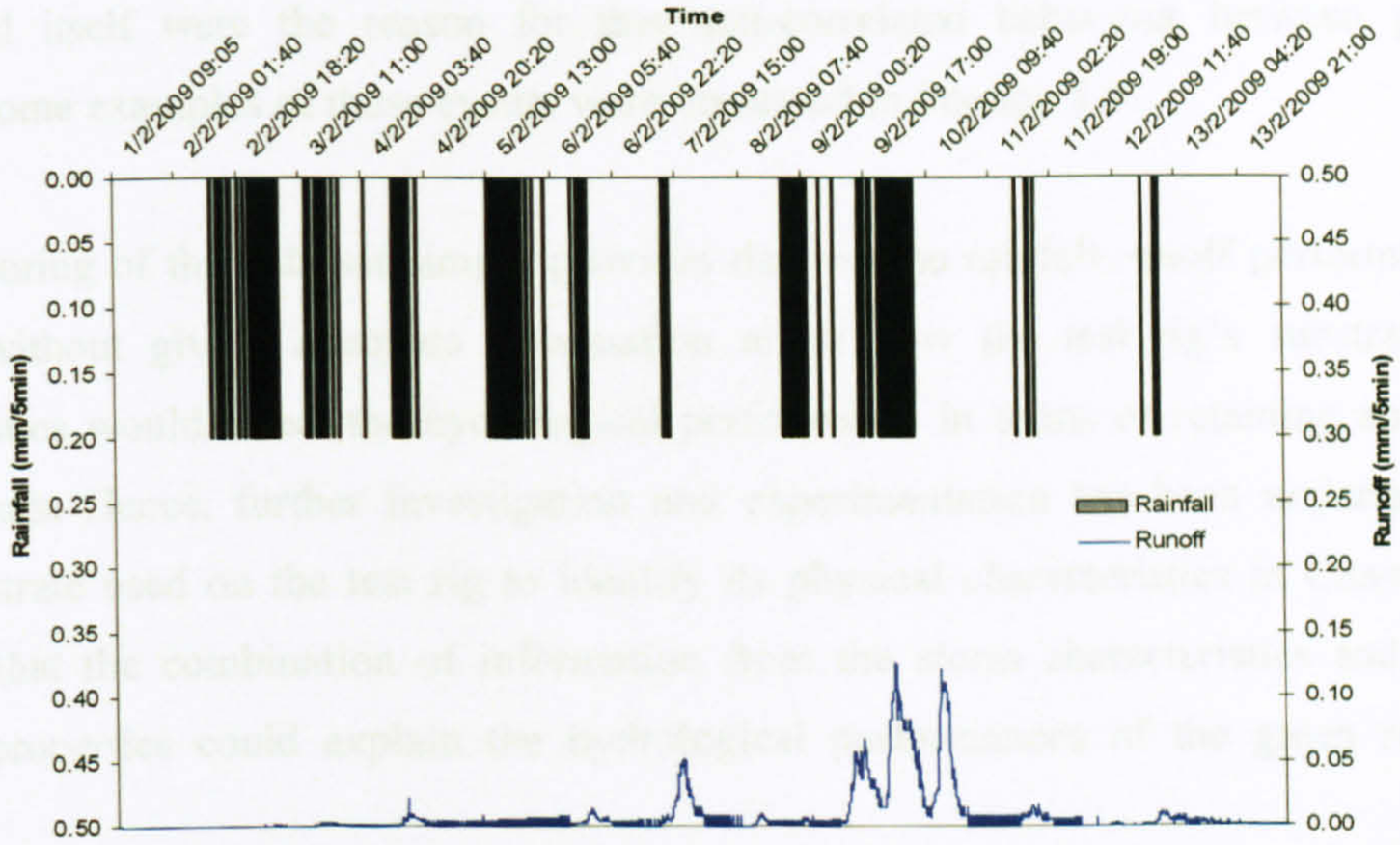


Figure 5.31: Total precipitation (snow) on February 2009

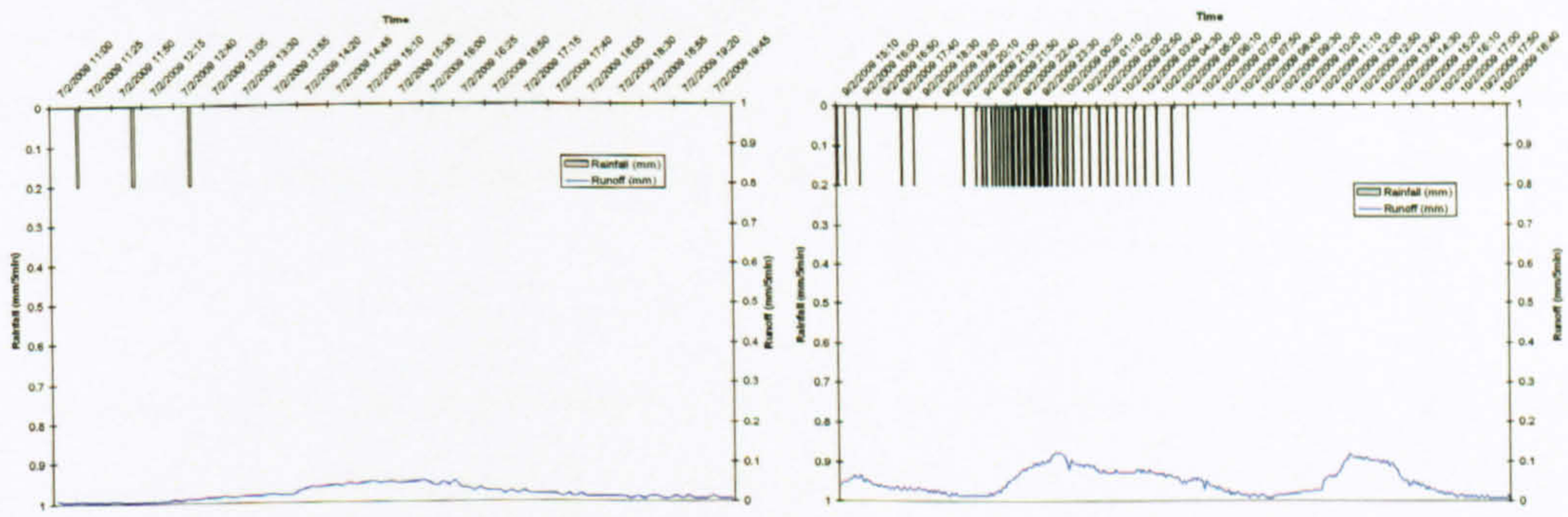

Figure 5.32: Some evidence of the afternoon melting on (a) 7th February 2009, and (b) 8th February 2009

## 5.6 Conclusions

In summation, the data set of monitored storm events from January 2007 to May 2009 has provided interesting and useful details pertaining to the performance of the test rig. Section 5.2 described the overall test rig performance in terms of retaining and detaining the rainfall and the possible parameters that control the performance, while Section 5.3 described the possible parameters that could be observed from the monitoring events. In Section 5.4, these parameters were regressed to assess their possible correlations with each other; however this regression demonstrated that the only parameters that show high significant correlations were total rainfall and rainfall duration in order to predict the total runoff. It is believed that the characteristics of

the rainfall itself were the reason for this non-correlated behaviour between parameters; therefore some examples of these events were discussed in Section 5.5.

The monitoring of the data set simply provides data on the rainfall-runoff performance of the test rig, without giving adequate information about how the test rig's substrate physical characteristics would affect the hydrological performance in terms of retaining and detaining storm events. Hence, further investigation and experimentation has been undertaken on the same substrate used on the test rig to identify its physical characteristics in Chapter 6. It is expected that the combination of information from the storm characteristics and substrate's physical properties could explain the hydrological performances of the green roof test rig further.

# CHAPTER 6

# SUBSTRATE TESTS

## 6.1 Introduction

This chapter follows on from the previous chapter, by presenting further experimentation data. In Chapter 5, the results from the multiple regression analyses for the storm parameters did not reveal clear or simple relationships between roof performance and storm characteristics. This suggested a need for a deeper understanding of the test bed's substrate's physical performance. In Chapters 2 and 3 it was hypothesised that the initial loss (or retention capacity restored due to evapotranspiration following a storm event) is one of the significant parameters for determining the green roof's hydrological performance. This has been observed via event-basis analysis in Section 5.5.

This chapter presents the results from two sets of experiments (Section 4.3) that have been undertaken on the substrates used on the Mappin Building test rig and the Hadfield Building test rigs to provide physical characteristics expected to influence moisture retention and evapotranspiration (ET). The two sets of experiments relate first to substrate physical properties and second to ET rate estimation. It is expected that the hydrological performance (i.e. water retention/soil moisture content) varies as a function of the substrate's physical properties (bulk density, permeability, maximum water capacity, porosity) and that the results from these experiments will support the conceptual green roof model (Chapter 3). Note that during this study, experiments for transpiration were excluded. Therefore only an evaporation experiment was undertaken for evaporation, $E_e$ rate estimation; in term of ET rate. In this study we are aiming to examine the function of the substrate itself rather than the function of the ET. The separation processes data into a single component in order to provide further details of the function of each component; hence this study will initially concentrate on the $E_e$ rate estimation. All the results gathered in this chapter will be utilized as part of the further development of the model presented in Chapter 7.

## 6.2 Substrate Properties – FLL tests

### 6.2.1 Overview of Substrate Properties

In Chapter 4, Section 4.3.1, the FLL standard methods used for determining the substrate's physical properties were presented, and photos of each substrate with descriptions can be found in Section 4.2.2. As required by the FLL guidelines, each experiment was repeated three times, and the averaged results are presented in Table 6.1. The results have been compared with the standards outlined in the FLL guidance. Table 6.1 includes results from the three main substrates used on the test rigs and the experiments for eight parameters have been undertaken for each substrate. All these parameters represent the physical characteristics of the substrate: bulk density; permeability; maximum water capacity and porosity of the substrate; and are related to one another. Thus it is expected that these characteristics can be used to predict the hydrological performance of the substrates. Following Table 6.1, each of these parameters will be described. A comparison of the values measured is presented in Section 6.2.2.

Table 6.1: Averaged values of variables in soil properties tests from three main substrates

| Variables | FLL | Alumasc Heather with Lavender (Al-HL) | Alumasc Sedum (Al-Sedum) | LECA + GE + Loam (LECA mix) | Unit |
|---|---|---|---|---|---|
| Bulk density (dry) Ddry | | 0.809 | 0.990 | 0.401 | $g/cm^3$ |
| Bulk density (moist) Dmoist | | 0.829 | 1.129 | 0.462 | $g/cm^3$ |
| Bulk density (maximum water condition) Dmax | | 1.249 | 1.440 | 0.539 | $g/cm^3$ |
| Particle density, Dp | | 3.962 | 2.123 | 1.050 | $g/cm^3$ |
| Water permeability, mod. Kf | ≥0.0005 | 0.00149 | 0.00557 | 0.0320 | cm/s |
| Maximum water capacity, WCmax | ≥45 | 47.26 | 45.64 | 16.30 | % |
| Total porosity, Tp | | 78.92 | 53.33 | 61.4 | % |
| Air-filled porosity, AFp | ≥10 | 31.66 | 7.69 | 45.10 | % |

#### 6.2.1.1 Bulk Density

Bulk density is calculated from the mass of dry substrate over total volume. The bulk specific gravity of sandy soils with a relatively low volume of pores may be as high as 1.6 $g/cm^3$, whereas that of aggregated loams and clay soils may be below 1.2 $g/cm^3$ (Hillel, 1998). This

parameter is important in calculating the movement of soil moisture in soil profiles, where it will relate to soil porosity. Bulk density is changeable as it is easily affected by the texture and structure of the substrate; by its looseness or degree of compaction, as well as by its swelling and shrinkage characteristics (Hillel, 1998). Bulk density will always be less than particle density as the bulk density calculation of soil volume includes voids.

### 6.2.1.2 Particle Density

Particle density is determined by the dry mass of substrate over the total solids' volume (without pore spaces). This parameter might vary in each sample due to the presence of heavier mineral or lighter organic components (Hillel, 1998). This parameter describes the influence of the mineralogy of each substrate and/or within the substrates. High density minerals may have particle densities closer to 3.0 $g/cm^3$, while substrates with particle densities of 0.9 to 1.4 $g/cm^3$ might contain organic material (Brady and Weil, 1999).

### 6.2.1.3 Porosity

Porosity has been determined indirectly from the bulk density values. It is a measurement of total voids over total volume, and it describes the structural condition of soils. In irregular soil particle composition, the smaller particles tend to fill the voids of larger particles, whereas more regular soil particles tend to be more porous (Wilson, 1969). Therefore, porosity is usually lower when substrate materials are mixed.

### 6.2.1.4 Air-Filled Porosity

Air-filled porosity describes the air-filled pore space volume in a soil structure. This parameter may provide information on soil aeration and its potential for plant root respiration. The air-filled porosity is also an indirect measurement, based on the maximum water capacity, $WC_{max}$.

### 6.2.1.5 Maximum Water Capacity, $WC_{max}$

$WC_{max}$ (field capacity) is reached when the water content in the substrate is at saturation. It is the amount of water held in the soil after excess water has drained away and is primarily controlled by the soil texture and the soil organic matter content (Hillel, 1998). $WC_{max}$ is likely to increase with an increase in organic matter levels in the soil.

### 6.2.1.6 Permeability

Permeability describes the ability of water to move through the substrate. It will generally describe the pore size connectivity in a sample (McCuen, 2004). Permeability is a function of the substrate's porosity and structure (in terms of grain size, shape and distribution).

## 6.2.2 The Substrates

Although there is no specific measurement for soil structure in this study, all the parameters above describe the structure of the substrates. For example, the LECA mix, which has a low particle density value, may explain the presence of organic matter; where the high air-filled porosity for LECA mix describes a limited connection in their particles' composition. Its low WCmax with low water-filled porosity compared to the air-filled porosity and its permeability describes the high movement of water through the LECA mix substrate.

The FLL standard (Table 6.1) does not provide a benchmark for bulk density but, as stated above, bulk densities would normally be low for aggregated loam and clay soils and high for sandy soil types. All three substrates have low bulk densities, with the LECA mixture having a 60% lower bulk density than the two Alumasc substrates. This low particle density of the LECA mix suggests a low mineral content in this substrate mixture, compared with the other two substrates. The Al-HL and Al-Sedum contain high mineral types (brick) that are suitable for plant growth.

The low bulk density is associated with high values of total porosity. Substrate total porosities range from 53% to 79%. A good soil for plantation medium should generally contain 50% solids and 50% pore spaces (Hillel, 1998). The proportion of air-filled porosity and water-filled porosity ($WC_{max}$) of each can be clearly seen from Table 6.1. The LECA mix is less well balanced than the other two, with the air-filled porosity double its $WC_{max}$. However, the Al-Sedum has very low air-filled porosity. It may be less able to drain readily and ensure an air supply to the plant's roots. The Al-HL on the other hand shows a balance between the air-filled porosity and water-filled porosity ($WC_{max}$), demonstrating a good soil medium for growing plants. Both the Alumasc substrates provide greater $WC_{max}$ than the LECA.

The Al-HL also demonstrates a good medium for water retention based on its ability to delay water movement through its water permeability value, as well as Al-Sedum. In contrast, the

water permeability of the LECA suggests that the substrate was close to not retaining any of the water that passed through it as the value was quite high. The LECA mixture has 83% greater water permeability than the Al-Sedum and 98% higher than the FLL standard.

Overall, both the Alumasc substrates indicated good soil properties that would be capable of providing water retention and enough minerals for plantation alongside good for flow drainage (suitable mixture of pore space and solids portion). Meanwhile the LECA mix demonstrates less connection between particle pores (with organic matter) resulting in a $WC_{max}$ 64% lower than FLL standard.

### 6.2.3 Variation between Samples

Section 6.2.2 described the performance of physical characteristics between the three substrates based on the averaged value shown in Table 6.1. This section will examine the 3 tests that have been undertaken for each substrate to observe variation between tests of the same substrate.

#### 6.2.3.1 Bulk Density

Figure 6.1 shows that the variations between tests for Al-HL, Al-Sedum and LECA mix are slightly different within ± 6.7%, ± 2.7% and ± 2% of the mean respectively. The specific reasons for the difference between tests of the same substrate batch are not easy to determine but might be related to the compaction of each sample which can lead to different sample distribution within the particles. It could also be affected by the sub-sampling of the same batch of substrate; as the substrate might not be perfectly mixed. The natural variability or heterogeneity of substrates might be an additional factor causing the variation between tests.

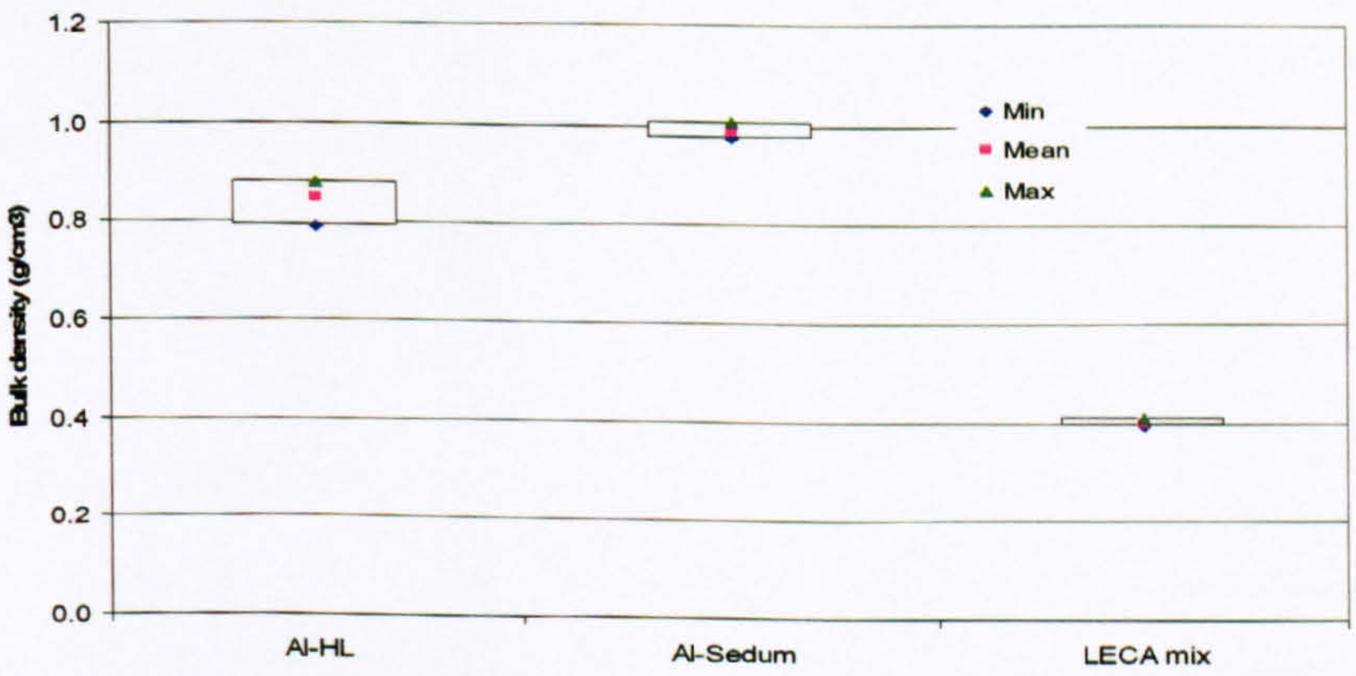


Figure 6.1: The minimum, maximum and mean value of samples for each substrate for bulk density

### 6.2.3.2 Particle Density

Figure 6.2 reveals a high range of maximum and minimum particle density (±28% of mean value) for the Al-HL substrate. This might be caused by the quantity of high mineral particles of the substrate during each test. It is believed that the high value of the particle density could indicate that the substrate contained high minerals. Importantly, during this FLL test, the experiment was repeated wrongly using the same sample batch of substrate. Hence this could reduce the quantity of high mineral content in the substrates during the saturated part of test; thus, the minerals could be washed out during the saturation and drainage process applied to the substrate. This might restructure the proportion of the substrate mixture during the Al-HL tests. There was ± 11% variation between LECA mix tests and just ± 2.1% of the mean of Al-Sedum substrate.

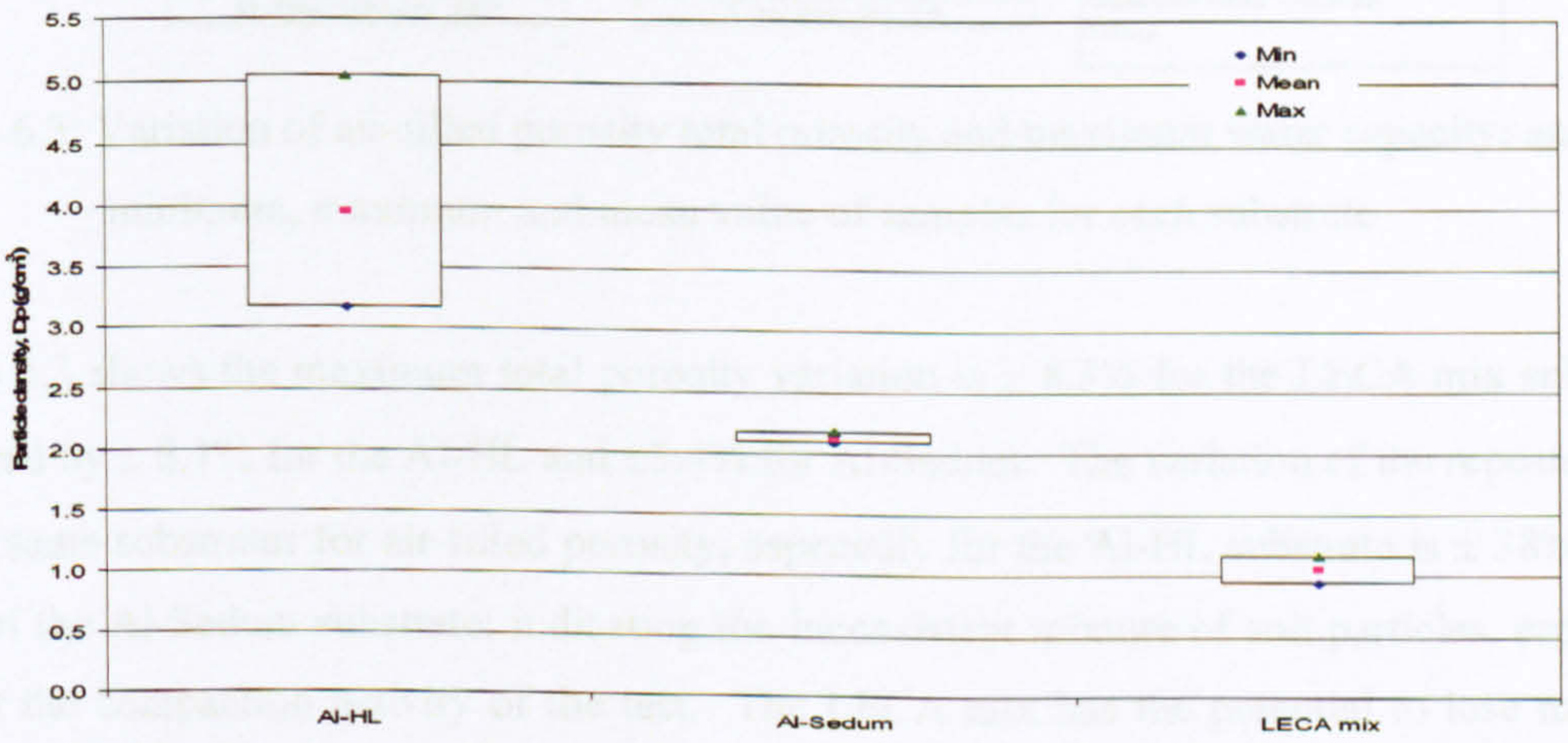


Figure 6.2: The minimum, maximum and mean value of samples for each substrate for particle density

### 6.2.3.3 Air-Filled Porosity, Water-Filled Porosity ($WC_{max}$) and Total Porosity

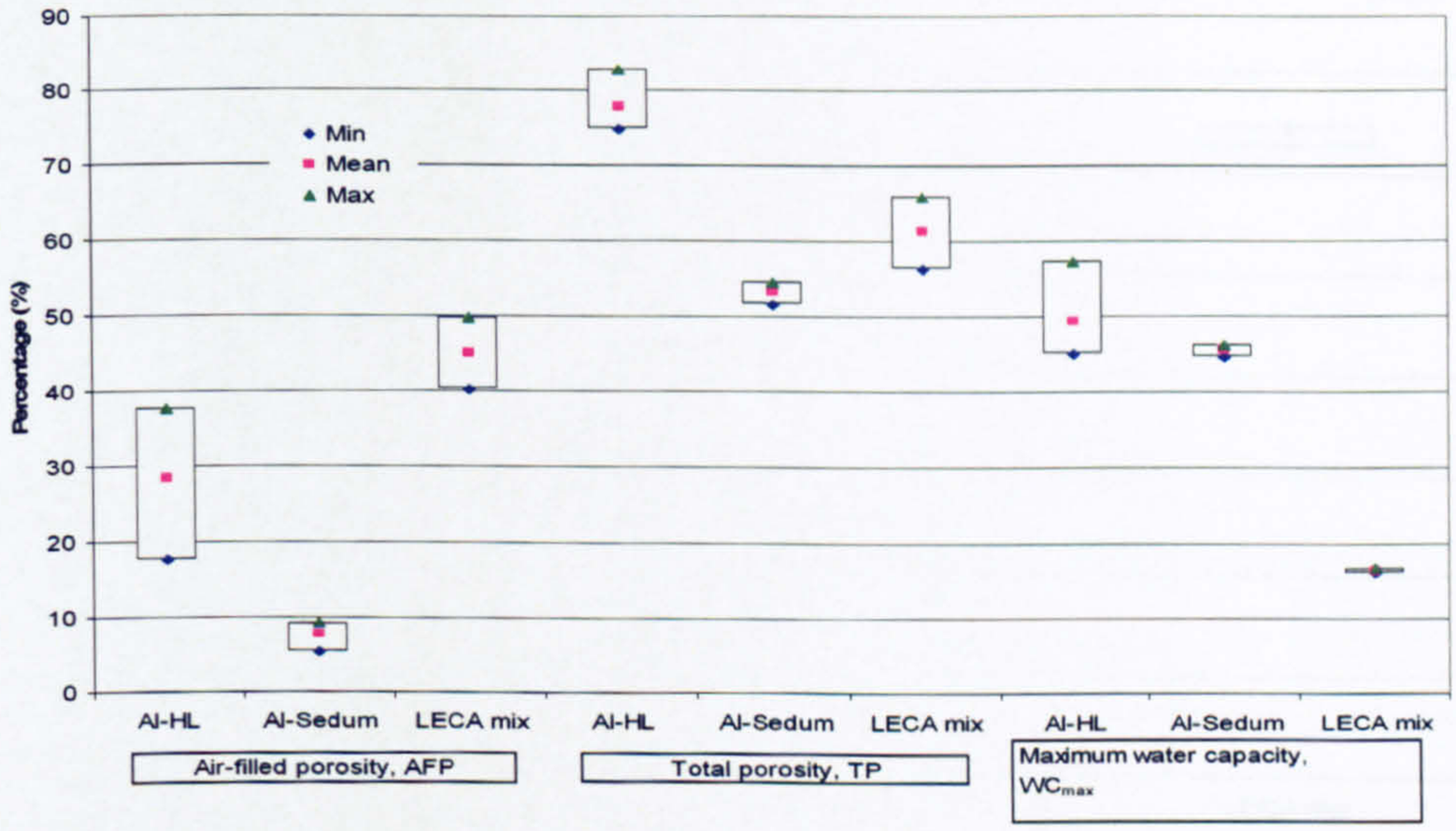


Figure 6.3: Variation of air-filled porosity total porosity and maximum water capacity; and their minimum, maximum and mean value of samples for each substrate

Figure 6.3 shows the maximum total porosity variation is ± 8.3% for the LECA mix substrate, followed by ± 6.1% for the Al-HL and ±3.4% for Al-Sedum. The variation of the repeated tests of the same substrates for air-filled porosity, especially for the Al-HL substrate is ± 38% and ± 32% of the Al-Sedum substrate; indicating the inconsistent mixture of soil particles, especially during the compaction activity of the test. The LECA mix has the potential to lose moisture very quickly and shows little potential for moisture retention with the variation in its air-filled porosity at around ±11% of its mean. It is not surprising to note that the greater variation in density for Al-HL previously recorded is also reflected in the more significant variation in the porosity measurement. The variation is then reflected in the ranges of WCmax where, for Al-HL around ± 6% of its mean value is discovered, compared with only ± 2% and ± 2.2% for both Al-Sedum and LECA mix respectively.

### 6.2.3.4 Permeability

The Al-Sedum in Figure 6.4 shows the maximum range of water permeability variations between the 3 tests, with 91% of their mean. This parameter demonstrates the variety of pore spaces connected in each sample and how it might differ from each test of the high mineral type of substrates, where the LECA mix just has ± 2% variation between tests and ±50% for the Al-

HL. The high variation of Al-Sedum and Al-HL demonstrate that the mixtures cannot show the same proportion uniformly for repeated samples.

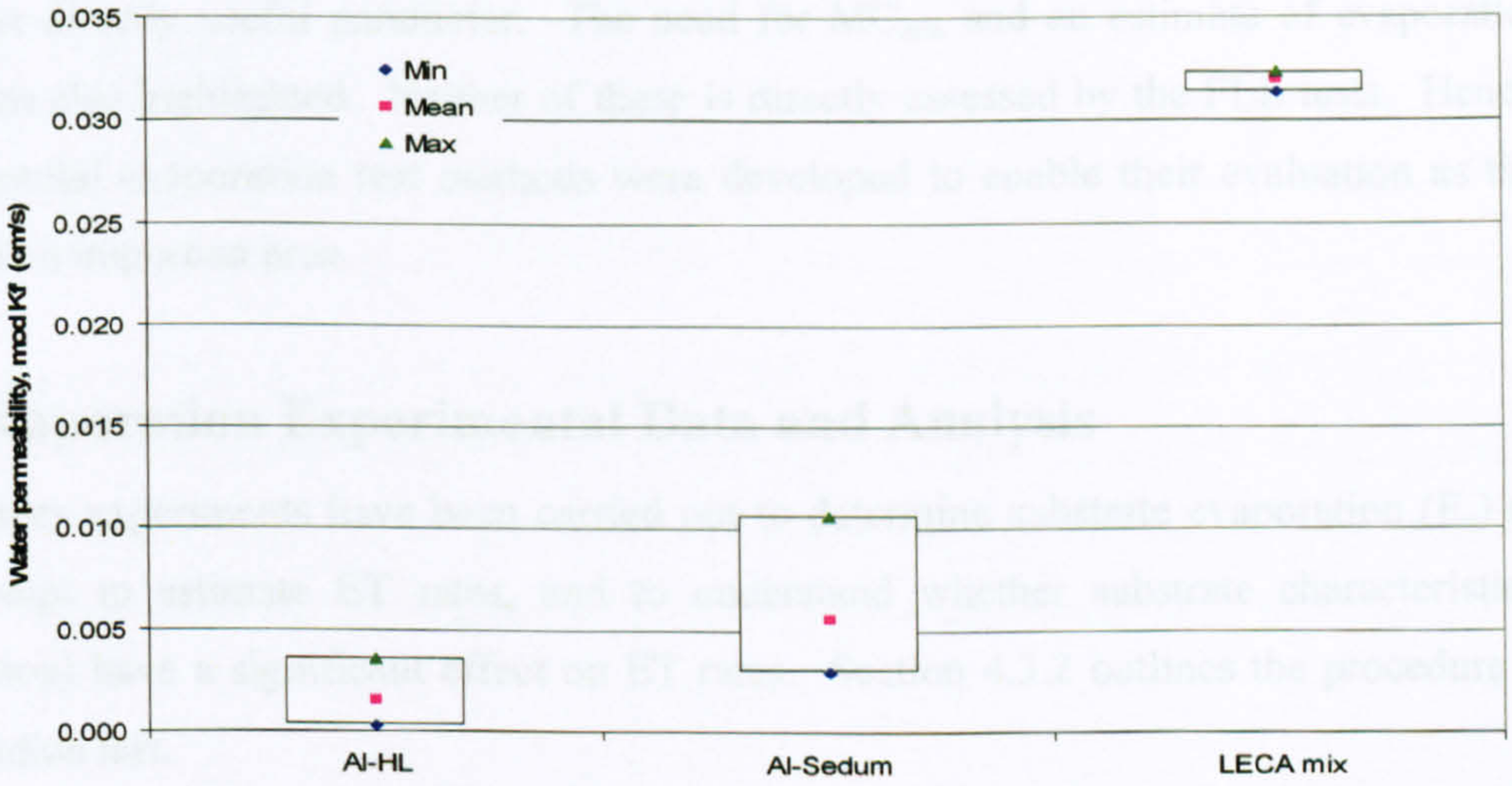


Figure 6.4: The minimum, maximum and mean value for each substrate for water permeability

### 6.2.3.5 Variation Overviews

Table 6.1 provides indicative characteristics for each substrate. However it has been recognized that some significant inconsistencies between repeat tests arise, reflecting the heterogeneous nature of the substrates. This implies that the properties of substrates in subsequent experimental work should be ideally checked on a test–by–test basis.

## 6.2.4 Conclusion

We can conclude that the physical tests have provided information on the characteristic of substrates and the expected ranges of variability between repeat samples. The FLL standard uses a mean value of the three replications. However, it should be noted that the averaged value shown in Table 6.1 is not an absolute value and that replicate tests of same substrate were inconsistent. Therefore, the facts gathered in this experiment suggested that within a particular roof, the physical characteristics of the substrates may vary from those determined experimentally for substrate samples.

It should be noted that the LECA-based mix has a WCmax which is significantly below the minimum level required in the FLL guidance, and that – as a consequence – this would not permit it to be accredited for commercial green roof applications. It does, however, provide a

useful hydrological contrast to the other two samples. All the parameters can be used to predict the substrate's characteristics/behaviour, as the values represent the physical characteristics for each substrate. The conceptual model proposed in Chapter 3 suggested that, of these, $WC_{max}$ is the most directly useful parameter. The need for $MC_{min}$ and an estimate of evaporation loss rates was also highlighted. Neither of these is directly assessed by the FLL tests. Hence, new experimental evaporation test methods were developed to enable their evaluation as this was deemed an important area.

## 6.3 Evaporation Experimental Data and Analysis

Laboratory experiments have been carried out to determine substrate evaporation ($E_e$) rates in an attempt to estimate ET rates, and to understand whether substrate characteristics (and vegetation) have a significant effect on ET rates. Section 4.3.2 outlines the procedure for the evaporation test.

### 6.3.1 Method and Test Programme

The procedure represents a new experimental method which is based on, and intended to complement, the standard FLL physical tests (which utilize a 150 mm diameter test vessel). The experiment begins with a sample of the substrate at field capacity. The weight of the sample is recorded regularly over several days to determine the rate of moisture loss (Figure 4.23) under different conditions: ambient conditions (outside, adjacent to the test rig); under controlled conditions at ±19°C, and ±40°C. Different conditions were used to assess the effects of temperature and climatic conditions for the substrate's experimental evaporation, $E_e$ rates.

The details of the test programme are shown in Table 6.2; Tests 1 to 3 were carried out on the Al-HL substrate only, Test 4 on the LECA mix only, Test 5 on Al-Sedum only, while Tests 6, 7 and 8 were performed on all three substrates. The main limitations on Tests 1 to 5 were the number of vessels; there were only 3 vessels available. Therefore each time the test was run, only one substrate was tested under three different conditions. Since July 2009, more vessels have been built and the evaporation test has been undertaken for all substrates simultaneously.

Table 6.2: Time and substrates tested during evaporation experiments

| Test/substrate | Date | Average local temperature (°C) |
|---|---|---|
| 1/Al-HL only | September 2008 | 16.5 |
| 2/Al-HL only | October – November 2008 | 8.1 |
| 3/Al-HL only | March – April 2009 | 10.4 |
| 4/LECA mix only | May 2009 | 11.4 |
| 5/Al-Sedum only | June 2009 | 15.8 |
| 6/All substrates | July – August 2009 | 18.7 |
| 7/All substrates | August 2009 | 18.0 |
| 8/All substrates | October 2009 | 10.4 |

It was assumed that, over time, the sample would lose moisture due to evaporation. Referring to Figure 4.21, in order to convert the weight loss recorded for each test into an equivalent moisture content loss (in %), the volume of water ($\rho_w$ = 1000 kg/m$^3$) was assumed, and converted into depth by dividing the test vessel's surface area (Figure 4.21 and Equation 6.1).

$$Depth = \left(\frac{Weight}{Density}\right) \Big/ Area \qquad (6.1)$$

Where weight is weight of moisture loss in kg, density is water density, $\rho_w$ = 1000 kg/m$^3$, area is test vessel's surface/plan area ($\pi r^2$) in mm$^2$ and depth is moisture content depth in mm.

It was anticipated that, under ambient conditions, the sample might never reach a moisture level of zero; instead a constant, 'ambient' level of moisture would be attained, reflecting equilibrium with local atmospheric conditions (minimum moisture content, $MC_{min}$ or available moisture storage).

### 6.3.1.1 Determination of Maximum Moisture Capacity, $WC_{max}$

Figure 6.5 shows an example of percentage loss of moisture content from Test 3 of the Al-HL sample under ambient conditions. Note that, as the exact value of $WC_{max}$ is not known at the start of the test, moisture content is expressed in terms of the difference between the initial ($WC_{max}$) condition, and the current state. This is why the values of y-axis are negative (moisture deficit). Moisture deficit of zero is representative of saturation, and a moisture deficit of maximum typically 50% minus 50% represents completely dry substrate. Still referring to Figure 6.5, the absolute level of moisture in the sample at the start of the test ($WC_{max}$) is unknown. However, based on the tests undertaken, it can be estimated/determined in one of three ways; (note that during the test periods, no specific rules were outlined to determine $WC_{max}$):

i) Assume that $WC_{max}$ (%) is as measured in the FLL test (although there may be variation from one sample to the next).

ii) Dry sample at the end of the test; refer to Figure 6.5, the sample in ambient condition will be left in the controlled oven (not more than 80°C – it tends to burn the substrate's compost if the sample dries in 100°C) a month of tests will take place until the weight of the sample becomes consistent.

iii) Damp sample - at the end of each test, some tests were left dried for more than a month, hence the final weight measurement from these tests was used. Therefore the $WC_{max}$ can be estimated based on these damp sample weights. However, given that a moisture content of ~ 15% is typical for damp substrates; this approach will always underestimate the $WC_{max}$ to some degree. This method is not advised for future studies.

Methods (i) and (ii) are preferable because they correspond to fully dry conditions. However, it should be noted that during these experiments, only two samples (Test 3 and Test 8) were analysed using $MC_{min}$ determined as in method (ii), and the remainder of the samples were analysed using method (iii). The tests were repeated using the same batch of substrate (excepted for Test 3 where this test used the new, fresh batch of substrate). It is highly recommended that for the next experiments, or in every new next experiment, a new batch of substrate will always be used to ensure a better result is obtained.

It was also expected that this experiment would show a range values of ambient dry level, $MC_{min}$ or $MC_t$ (moisture content at any time, t) close to the $MC_{min}$ for between different substrate under room and ambient conditions. To estimate the $MC_{min}$ values under these two conditions, the samples will be left until they reach a consistent, stable minimum as these samples will never reach zero moisture content. However, under ± 40°C oven condition temperature, the substrate reaches a consistent, stable minimum dry level and it then reaches its zero moisture content (maximum moisture storage at $WC_{max}$); as it corresponds to oven-dry conditions. The test value is expected to provide high confidence that the $WC_{max}$ value had reached (at zero-dry sample) (Figure 6.5) and a consistent $MC_{min}$ was also reached (at dry sample under ambient condition in Figure 6.6). However, both under the ambient and controlled ± 19°C conditions, the test is expected not to reach their minimum moisture level but may be reached at an ambient dry weight of each sample. Hence, this end stop point (depends on the end time of test run) is known as $MC_t$ and will vary in response to the ambient conditions

prior to storm events while $MC_{min}$ may be considered to define the depth of permanently retained moisture.

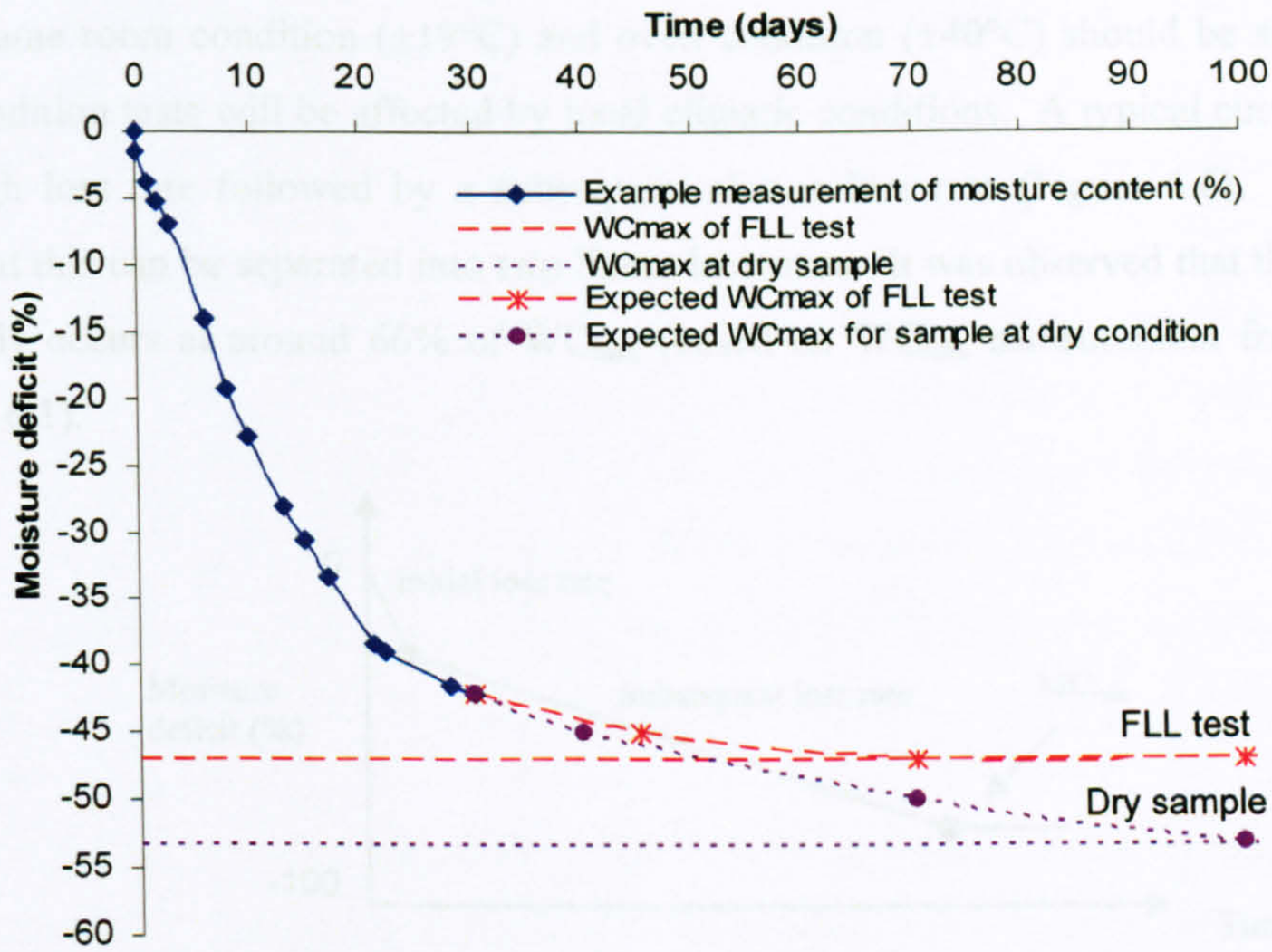


Figure 6.5: Example of the measurement of moisture content loss (by weight measurement) from Al-HL sample under ambient condition in test 3 and the expected loss at $WC_{max}$ (of FLL test and dry sample approaches)

The dry sample is then referred to the maximum measured depth of $WC_{max}$ within the whole tests of ±40°C temperatures (oven dry). Hence, these values provide a range of $WC_{max}$ that might occur for the Alumasc-HL substrate in any temperatures – with the influence of heterogeneous factors demonstrated in Section 6.2 and the same approaches applied for the other substrates. The FLL test value of $WC_{max}$ refers to the $WC_{max}$ derived from the FLL guideline (Table 6.1 mean values). The figure also has been extrapolated to the expected $WC_{max}$ (under oven condition) of the sample; or $MC_{min}$ if it reaches the ambient minimum dry level (only under ambient condition). It suggests that in ambient conditions, it would take more than 3 months for the sample to reach $MC_{min}$. It is expected that if the experimental evaporation, $E_e$ test can be dried further under ambient conditions (following $MC_t$, based on ambient temperatures) until it reaches a consistent weight, the $MC_{min}$ is then reached.

### 6.3.1.2 Determination of Experimental Evaporation, $E_e$ Rates,

It is expected that experimental evaporation, $E_e$ rates for repeat tests with the same substrate under the same room condition (±19°C) and oven condition (±40°C) should be similar. The ambient condition tests will be affected by local climatic conditions. A typical curve shows an initially high loss rate followed by a subsequent slower loss rate (Figure 6.6). It has been assumed that this can be separated into two linear loss rates. It was observed that the change in rate typically occurs at around 66% of $WC_{max}$ (based on $WC_{max}$ measurement from the FLL tests, Table 6.1).

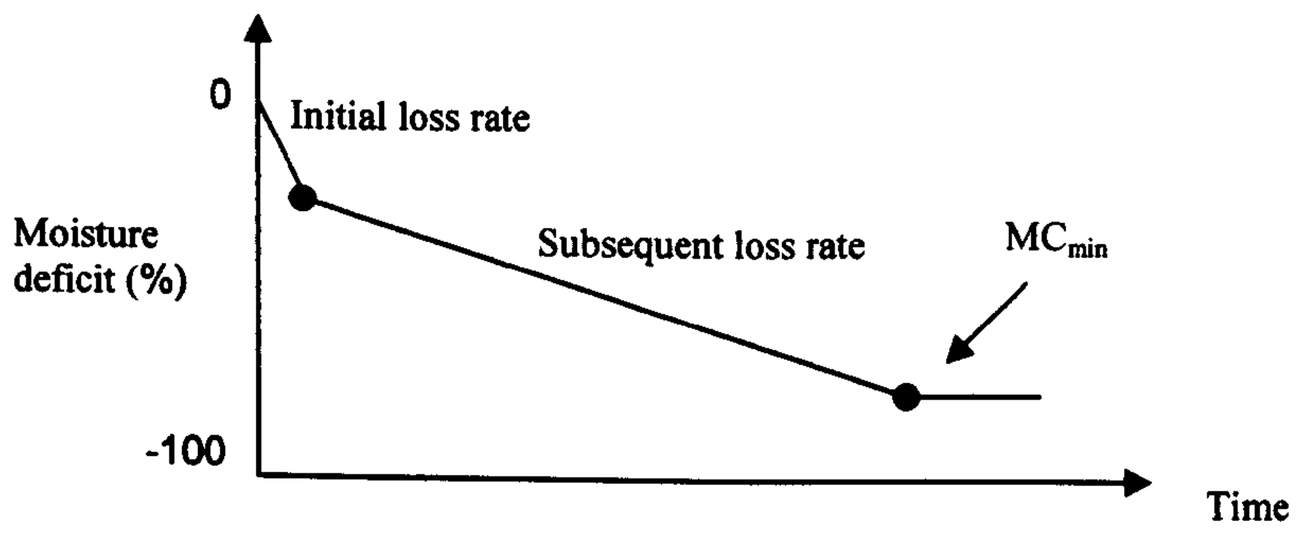


Figure 6.6: Diagram representation of two $E_e$ rates derived from the tests

## 6.3.2 Results of Maximum Moisture Capacity, $WC_{max}$, Minimum Moisture Content, $MC_{min}$ and Experimental Evaporation, $E_e$ rate

### 6.3.2.1 $WC_{max}$ and $MC_{min}$

Following the discussion in Section 6.3.1.1, most of the $WC_{max}$ parameter from Al-HL substrate determined under ambient and controlled ±19°C temperatures was based on method (iii); although for Test 3 and Test 8 it was based on method (ii). Both $WC_{max}$ from these conditions (except for Test 3 and Test 8) was determined using method (iii) and cannot be concluded as a $WC_{max}$ or $MC_{min}$ but as a $MC_t$. Method (ii) was used for the ±40°C temperature samples, and zero moisture content for each test was reached, therefore there is a high confidence that $WC_{max}$ values have been demonstrated under these conditions. Table 6.3 presents the $WC_{max}$ from ±40°C condition to describe the best estimation of $WC_{max}$. The individual sample from the ±40°C condition shows a variation of ±19% between Al-HL samples from the FLL test results (Table 6.3 (b)).

A similar approach was applied for the Al-Sedum under ambient and controlled ±19°C temperatures; except that Test 8 used method (ii). All 4 tests for the Al-Sedum under ±40°C temperatures have been shown to reach a consistent $WC_{max}$, within the test itself but also with the variation ±22% of the FLL results (Table 6.1). The range for the Al-Sedum is between the maximum $WC_{max}$ that was measured using method (ii) and the FLL test from Table 6.1.

$WC_{max}$ was determined using method (ii) for the LECA mix substrate. Based on the LECA mixture characteristics (Table 6.1), the substrate is porous and is water permeable tending to lose all its moisture in a short time, hence all the damped and dried sample test values also show similar weight values. However, the variation of $WC_{max}$ from the LECA-based mix rather than the other substrates of the FLL test result (Table 6.1) is a bit higher, ±36%. The range for the LECA mix is less than the FLL test result from Table 6.1.

Table 6.3: The best estimation of maximum moisture content, $WC_{max}$ for all substrates tests under oven conditions compared to $WC_{max}$ from the FLL test in Table 6.1 (a) in table, and (b) in graph

(a)

| | Maximum moisture content, $WC_{max}$ (%) | | |
|---|---|---|---|
| | Test | ±40°C drying oven | FLL test |
| Alumasc Heather with Lavender substrate (Al-HL) | 1 | 42.0 | 47.3 |
| | 2 | 42.8 | |
| | 3 | 56.4 | |
| | 6 | 38.8 | |
| | 7 | 40.8 | |
| | 8 | 39.6 | |
| Alumasc Sedum substrate (Al-Sedum) | 5 | 36.6 | 45.6 |
| | 6 | 35.4 | |
| | 7 | 36.8 | |
| | 8 | 37.1 | |
| LECA mix substrate | 4 | 12.7 | 16.3 |
| | 6 | 14.2 | |
| | 7 | 13.6 | |
| | 8 | 10.7 | |

(b)

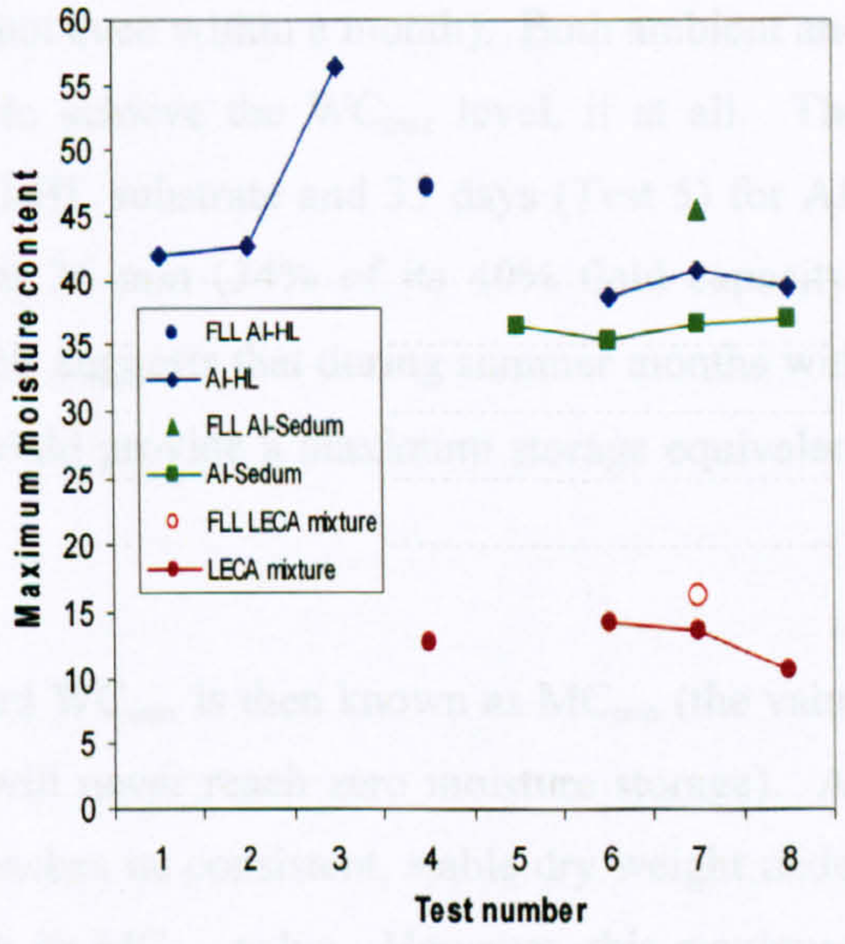


Although there is quite a variation between $WC_{max}$ determined from this analysis activity and $WC_{max}$ derived from FLL tests, both the Alumasc substrates showed a reasonably consistent, similar $WC_{max}$ under ±40°C temperature (except for the Test 3 which used fresh, new Al-HL substrate that might represented the quality of the substrate). This might suggested that this is

the $WC_{max}$ that occurs on the real test rig where on the very first $WC_{max}$ after the substrate on the rig being installed, a value of 56.4% is represented, but after a year or two in position, the capability of its $WC_{max}$ might be reduced within the range describe in Table 6.3. Getter (2007) in their study reported the maturity of their 5 years monitoring substrate had increased the value of the WCmax. However, the difference between this finding and Getter (2007) could be based on the different samples tested as theirs was based on the real test rig's substrate in ambient condition complete with vegetation, while in this study, no vegetation was involved, therefore, no new minerals (that might be developed from vegetation roots) were added. This activity might also suggest that besides the FLL test, the evaporation experiment of green roof substrates can be used to determine the $WC_{max}$ parameter.

All the tests discussed above are plotted in Figure 6.7 – 6.9. The $WC_{max}$ lines from FLL test and oven conditions shown in each figure indicate the potential ambient minimum that moisture should reach with the highest moisture content loss within $WC_{max}$ ranges. All conditions for test 3 using a new batch of Al-HL substrate showed impressive moisture loss even though the temperature of the outside condition was 10.4°C, the performance still exhibited similar high loss patterns in room (±19°C) and oven (±40°C) conditions. In most cases the samples never reached the $WC_{max}$ lines in two weeks of dry days (not even within a month). Both ambient and room conditions could take longer than a month to achieve the $WC_{max}$ level, if at all. The longest times reached were 32 days (Test 2) for Al-HL substrate and 33 days (Test 5) for Al-Sedum substrate; with the highest moisture loss at 36 mm (34% of its 40% field capacity) during Test 2 (under 19°C condition). Therefore, this suggests that during summer months with ADWP longer than a month, Alumasc substrates could provide a maximum storage equivalent to 80-90% of the expected $WC_{max}$.

The 80-90% maximum storage value of the expected $WC_{max}$ is then known as $MC_{min}$ (the value that provides the maximum moisture storage but will never reach zero moisture storage). As mentioned in Section 6.3.1.1, if a drying sample reaches its consistent, stable dry weight under ambient or room conditions, it is expected to reach its $MC_{min}$ value. However, this maximum storage (or minimum moisture content, $MC_{min}$) was not observed during all these ambient and room condition tests, as it the samples was still drying at the end of the tests. Therefore these ambient dry levels could only be known as $MC_t$ or $MC_0$; $MC_0$ and could be best described as the initial moisture content for real test rig conditions prior to a rainfall event.

### 6.3.2.2 $E_e$ rates

This section will assess the experimental evaporation, $E_e$ rate, (in two stages) and the potential minimum moisture content, $MC_t$. All the results from evaporation experiments in all conditions for all substrates are shown in Table 6.4 and Figure 6.7 – 6.9. Based on Figure 6.6, the data has been split into initial rate 1 with 33% of $WC_{max}$ (rapid initial loss) as the change in slower subsequent rate 2 was observed at around 66%.

It is noted that some data was affected by the short duration of the experiment (not less than 2 weeks), therefore some of the initial losses might not experience a moisture loss of more than 33% of $WC_{max}$. Although the cut-off of 33% always needs to be applied, in order to compare all the tests in accordance with the same conditions, the same value of $WC_{max}$ should be used. Hence 33% from the $WC_{max}$ (of FLL test) of moisture content loss equivalent to 17 mm (for Al-HL), 15 mm (for Al-Sedum) and 7 mm (for LECA mixture). Furthermore, some data might not experience a change of rate during the experiment, where samples lose moisture for more than 33%, one straight decay rate was developed for use throughout the tests. Hence, this explains why some missing numbers occur in 'Rate 2' in Table 6.4, whilst for the Test 8 in ±40°C conditions, due to the availability of the oven (sharing oven with other students), all the substrates were removed from the controlled-oven every Tuesday. Therefore, the result from this test might not be helpful to use.

A week of dry days was used to observe the ranges provided by the tests in all conditions; as the shortest length of time achieved in oven ±40°C was within 6 to 7 days. Therefore, the recharge of storage capacity for each substrate at day 7 ($MC_7$) could be assessed. Under dry conditions, all tests from LECA mixture substrates get back to their 100% $WC_{max}$, 91 – 95% of $WC_{max}$ and were observed from Al-Sedum while Al-HL shows variations on their $WC_{max}$ on day 7 with 83 – 96%. At the same time, under room conditions, only 12 – 39% of $WC_{max}$ observed from Al-HL, 19 – 34% from Al-Sedum and 29 – 46% from LECA mixture. Whilst under ambient conditions, Al-HL exhibited 14 – 50% of $WC_{max}$, 32 – 60% from Al-Sedum and 38 – 61% from LECA mixtures; depending on their temperature and climatic conditions.

Figures 6.7 – 6.9 show different evaporation, $E_e$ rates estimation at different temperatures, with rapid initial losses being observed for the ± 40°C oven condition compared with the other 2 conditions. All the substrates reached close to their absolute minimum in a week's time under oven conditions. The Al-HL substrate lost its moisture content between 34% - 52% over 7

days, with 32% - 36% and 12% - 14% for the Al-Sedum and LECA mix substrates respectively. All the substrates experienced rapid changes under oven conditions for both loss rates; the initial loss rate changes at ± 2 days, following the next subsequent rate after day 2 (Figure 6.7 (c), Figure 6.8 (c) and Figure 6.9 (c)). Table 6.4 summarised the initial and subsequent $E_e$ rates from all test conditions.

The $E_e$ loss rate results for room conditions for the Al-HL was slightly rapid for Test 2 and Test 3, but the other tests showed slightly slower Ee rates with moisture content loss ranging in a week from 3% to 20% of Al-HL substrate's moisture content loss (Figure 6.7 (b)). Rapid initial rate for Test 2 and Test 3 might be caused by climatic factors based on the surroundings of where Test 3 was undertaken in March 2009 (10°C) and might be affected by radiation and heat from the room. It took place in the early spring season with a 10°C, heater on for the building. Test 2 was undertaken in October - November 2008 (8.1°C) and might experience similar cool dry days of autumn with radiation, and heat from the heater could contribute to the higher $E_e$ rate. Whilst for the Al-Sedum, all 4 had slow $E_e$ rates with a small range of moisture content loss between 7% - 11% over 7 days. This is where the minimum days for this condition reached their 33% of $WC_{max}$ at day 14 (Figure 6.9 (b)). A similar variation is observed for the LECA mix with 3% to 6% moisture content lost in a week at a slower $E_e$ rate, with the shortest time for the sample to reach 33% of $WC_{max}$ being at day 8.

Table 6.4: Result of evaporation experimental data rates in all substrates in 3 different conditions

| Substrate types | Test | Experimental evaporation data Ee rate (mm/day) | | | | | |
|---|---|---|---|---|---|---|---|
| | | Ambient | | ±19°C | | ±40°C | |
| | | Initial loss rate | Subsequent loss rate | Initial loss rate | Subsequent loss rate | Initial loss rate | Subsequent loss rate |
| Alumasc Heather with Lavender substrate (Al-HL) | 1 | 1.17 | - | 1.00 | - | 8.72 | 2.14 |
| | 2 | 0.50 | - | 2.04 | 0.67 | 10.42 | 3.91 |
| | 3 | 2.32 | 1.22 | 2.89 | 1.63 | 10.53 | 2.94 |
| | 6 | 0.89 | 0.70 | 0.55 | - | 6.80 | 1.41 |
| | 7 | 2.39 | 0.97 | 0.73 | - | 8.38 | 1.80 |
| | 8 | 0.46 | - | 0.52 | - | - | - |
| Alumasc Sedum substrate (Al-Sedum) | 5 | 1.46 | 0.63 | 1.19 | 0.60 | 7.54 | 1.78 |
| | 6 | 1.68 | 0.53 | 0.68 | 0.69 | 7.37 | 1.71 |
| | 7 | 2.54 | 0.97 | 1.21 | - | 7.84 | 3.64 |
| | 8 | 0.58 | 0.51 | 0.67 | 0.55 | - | - |
| LECA mix substrate | 4 | 0.91 | 0.58 | 0.86 | - | 6.41 | 1.27 |
| | 6 | 0.49 | 0.24 | 0.32 | - | 5.08 | 0.51 |
| | 7 | 1.02 | 0.22 | 0.63 | - | 7.43 | 0.95 |
| | 8 | 0.20 | - | 0.33 | 0.18 | - | - |

For the ambient condition, the range of moisture content loss in a week is between 3% and 17% for both initial rates of the Al-HL and Al-Sedum (Figure 6.7 (a) and Figure 6.8 (a)) where this range is similar to Al-HL moisture loss range in room conditions. This suggested that both conditions might experience the same causative factors of evaporation (i.e. similar heat) where in ambient conditions; wind, wet and dry may occur consecutively. Higher initial Ee rates in Test 3 and Test 7 in Figure 6.7 (a) may represent similar factors as those in Test 6 and Test 7 in Figure 6.8 (a) where sunny weather, less rain and strong winds might be contributory factors with a slightly hot temperature as in Test 6 and 7. Only Test 7 of Al-Sedum substrate from Figure 6.8 (b) has reached their 33% of $WC_{max}$ at day 6, Test 3 and 7 from Al-HL substrate reached 33% of $WC_{max}$ at day 7, while the other tests began to lose their 15% moisture content at day 10. The LECA mixture under ambient condition experienced moisture content losses between 3% and 6% in a week, and none of these tests reached their 33% of $WC_{max}$ as yet. However, it is indeed surprising that the LECA mixture in Test 8 had still not reached its 33% of $WC_{max}$ on day 34 as the FLL test proved that the LECA mixture had higher permeability. However; this might suggest that on cold days, around 10.4°C, the LECA mixture could absorb more water within the substrate structure. These figures also demonstrate that almost all tests failed to reach constant minimum moisture content, $MC_{min}$ within 30 days, hence $MC_{min}$ is not evident.

Overall, from the oven dry samples condition all substrates consistently loss 33% of $WC_{max}$ between day 1 and day 4. At the same time, in ambient conditions, depending on their temperatures, substrates under high summer temperatures will lose 33% of their $WC_{max}$ in a week or less, while in autumn, spring and winter low temperatures 33% of their $WC_{max}$ water content loss will take more than a week or even a month. Room conditions could not provide an exact comparison simply based on the temperatures; where during tests period, no high temperature differences were observed but still exhibited variations of moisture content loss as shown in Figure 6.7(b). This may demonstrate that other factors contribute to this variation, such as radiation or thermal energy.

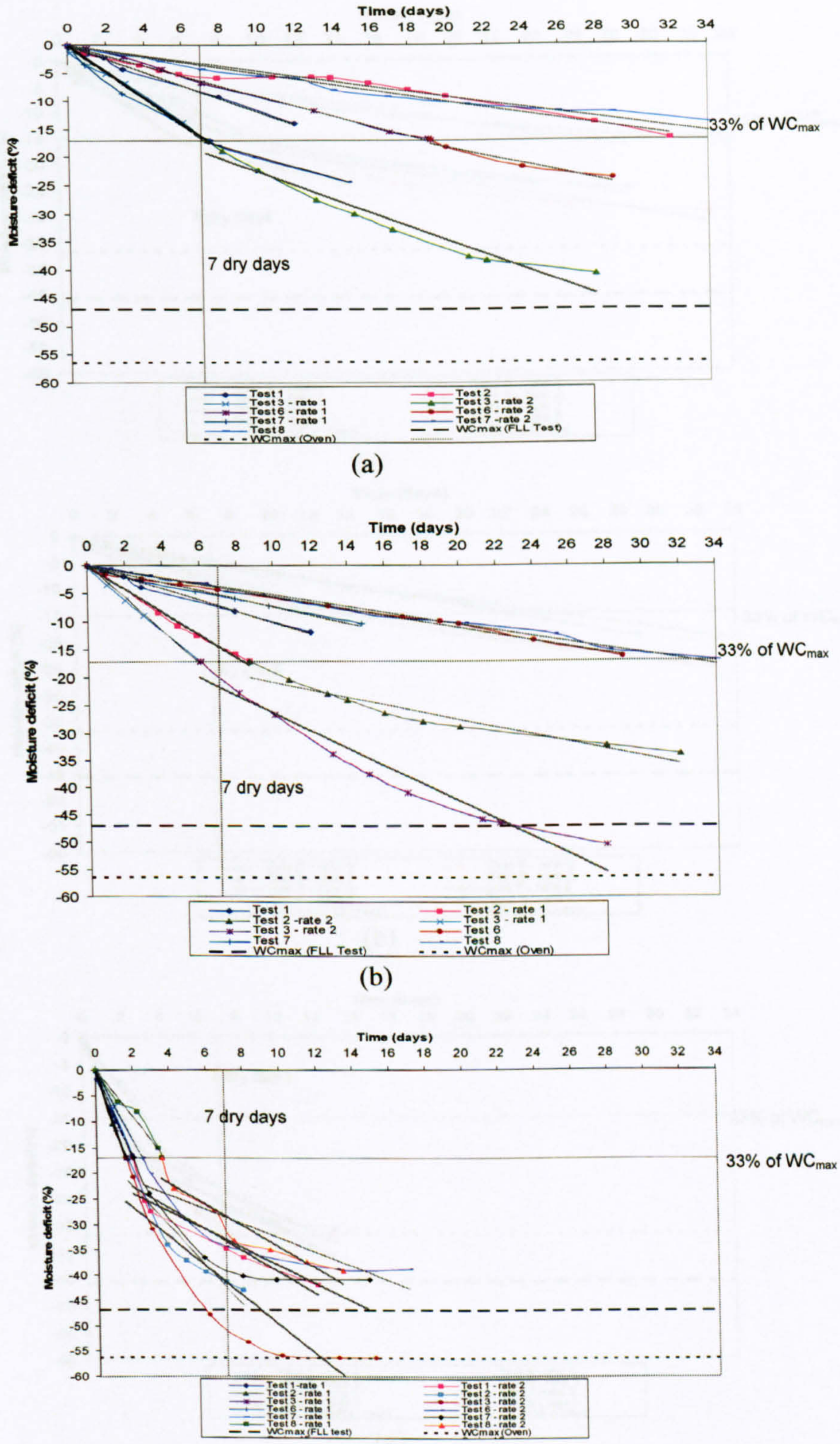


Figure 6.7: The results of experimental evaporation, $E_e$ rate estimation from the Alumasc Heather with Lavender substrate in 3 different conditions; a) Outside – shaded under the test rig to replicate with real roof conditions but without having additional moisture; b) Inside – in room condition ±19°; and c) In the oven – using ± 40°C

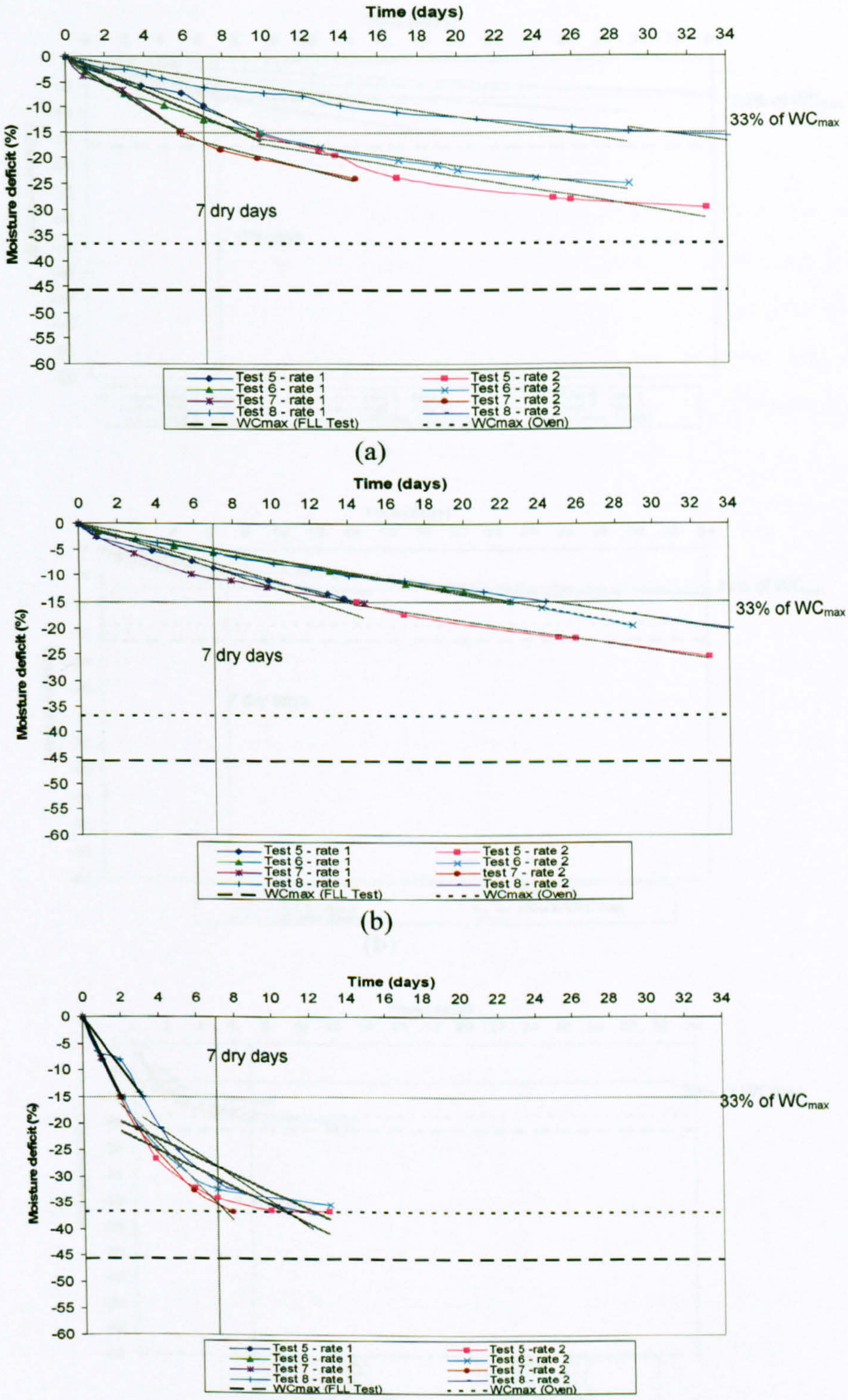


Figure 6.8: The results of experimental evaporation, $E_e$ rate estimation from the Alumasc Sedum substrate in 3 different conditions; a) Outside – shaded under the test rig to replicate with the real roof conditions but without having additional moisture; b) Inside – in room conditions ± 19°; and c) In the oven – using ± 40°C

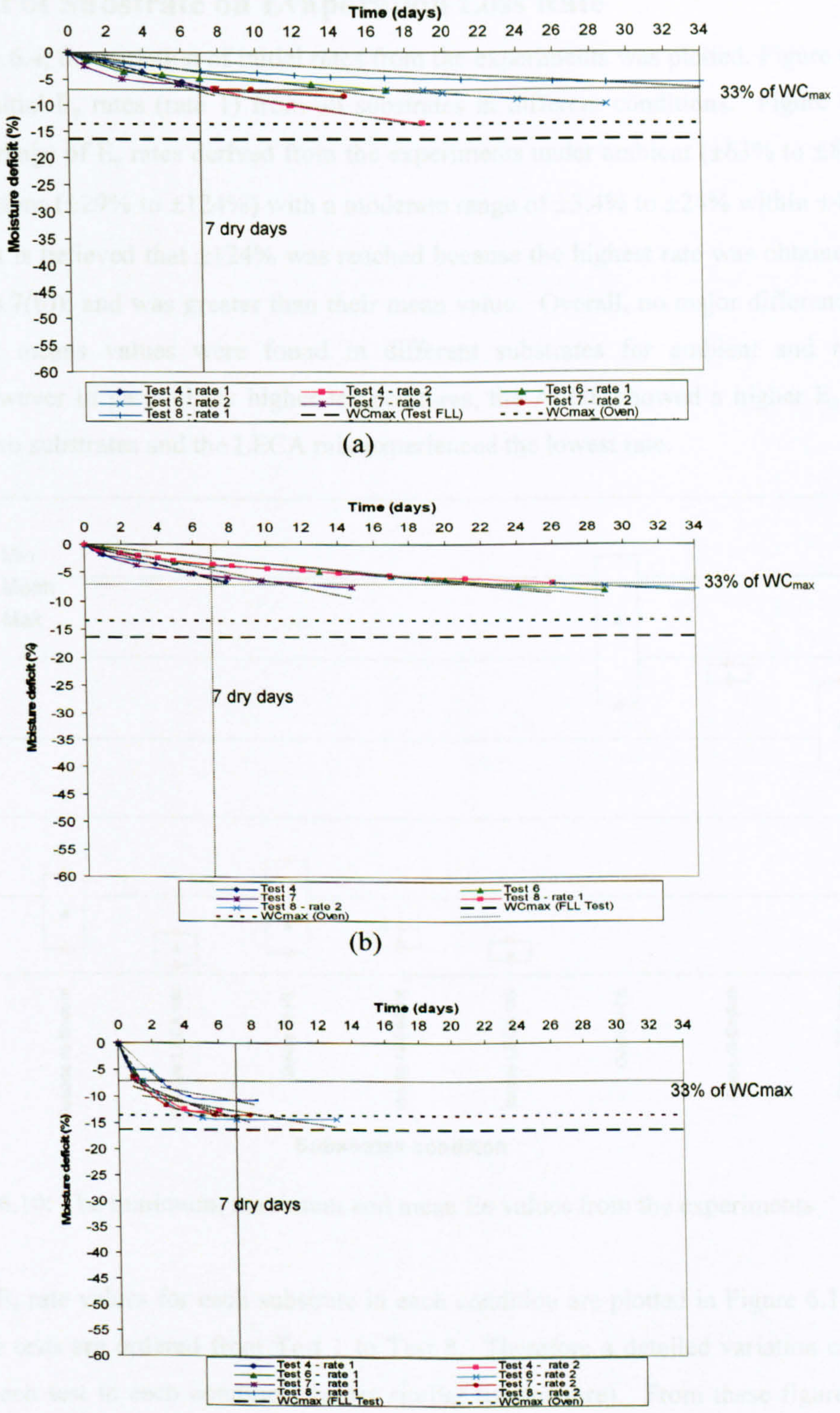


Figure 6.9: The results of experimental evaporation, $E_e$ rate estimation from the LECA mix substrate in 3 different conditions; a) Outside – shaded under the test rig to replicate the real roof condition but without having additional moisture; b) Inside – in room condition ± 19°C; and c) In the oven – using ± 40°C of temperature

### 6.3.2.3 Effect of Substrate on Evaporation Loss Rate

Following Table 6.4, the variation of initial rates from the experiments was plotted. Figure 6.10 illustrates the initial $E_e$ rates (rate 1) from all substrates in different conditions. Figure 6.10 shows the high range of $E_e$ rates derived from the experiments under ambient (±63% to ±85%) and room conditions (±29% to ±124%) with a moderate range of ±3.4% to ±24% within ±40°C temperatures. It is believed that ±124% was reached because the highest rate was obtained in Test 3 (Figure 6.7(b)); and was greater than their mean value. Overall, no major difference in initial Ee rates means values were found in different substrates for ambient and room conditions. However in particularly higher temperatures, the Al-HL showed a higher $E_e$ rate than the other two substrates and the LECA mix experienced the lowest rate.

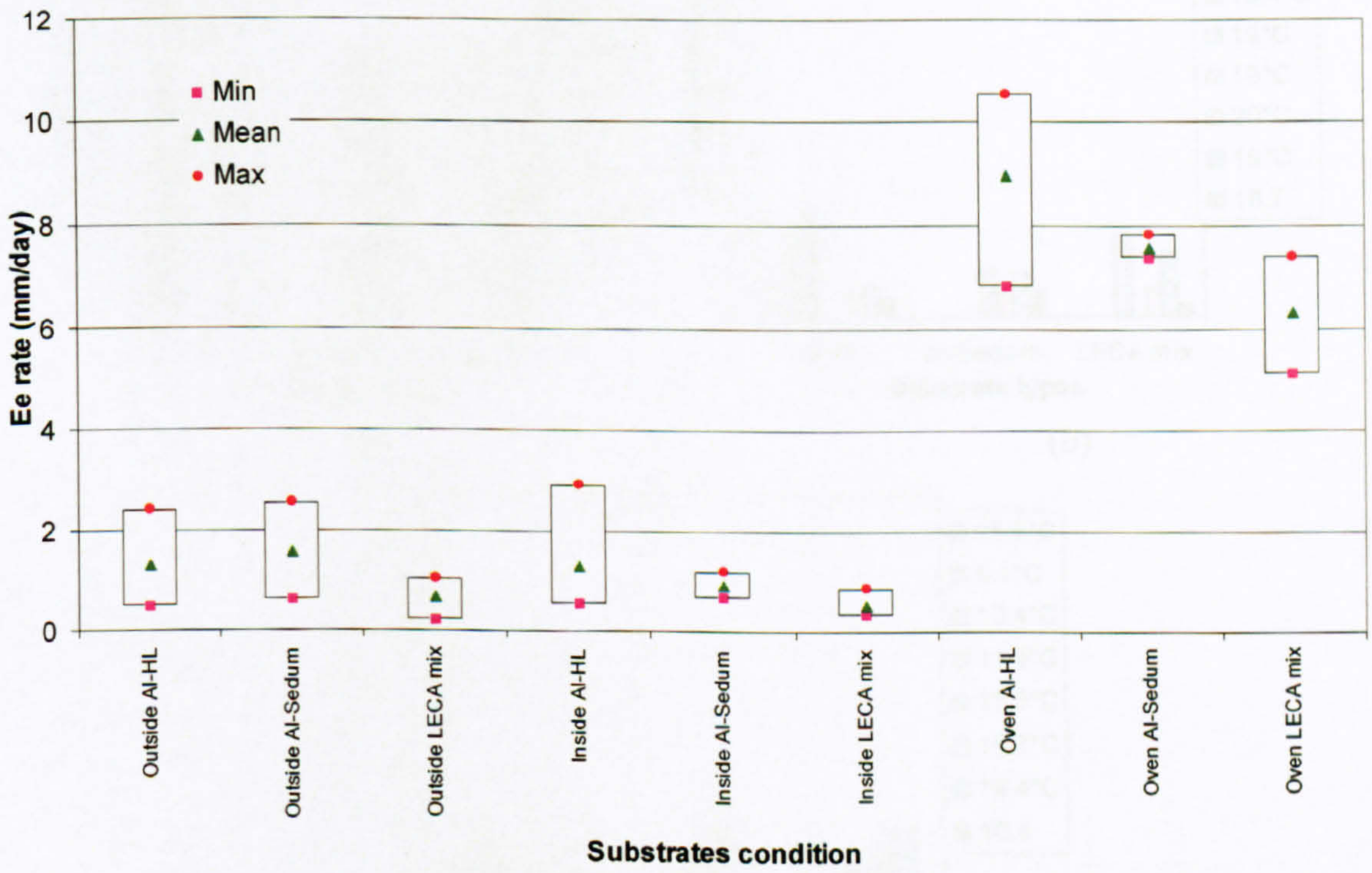


Figure 6.10: The minimum, maximum and mean Ee values from the experiments

Details of the $E_e$ rate values for each substrate in each condition are plotted in Figure 6.11. In each figure the tests are ordered from Test 1 to Test 8. Therefore a detailed variation can be observed for each test in each condition (under similar temperature). From these figures, by comparing the $E_e$ rates between substrates, the values show similar trends of loss rates were observed within different conditions with the same test. A similar trend was observed in Tests 6, 7 and 8 under all conditions with Test 6 showing slower rates than Test 7 with the slowest of

all being Test 8 (except in oven condition). Hence this suggests that the differences in substrates physical properties may not influenced the $E_e$ rates, although it does affect their ability to retain water ($WC_{max}$). Similar trends were also observed between tests under controlled oven and room conditions (Figure 6.11(a) and Figure 6.11(b)) but there was a slightly different trend with tests under ambient conditions (Figure 6.11(c)) for each substrate. It is believed that this demonstrate the tests under ambient conditions having been controlled by natural climatic factors rather than the tests under limited-compact controlled area of oven and room conditions.

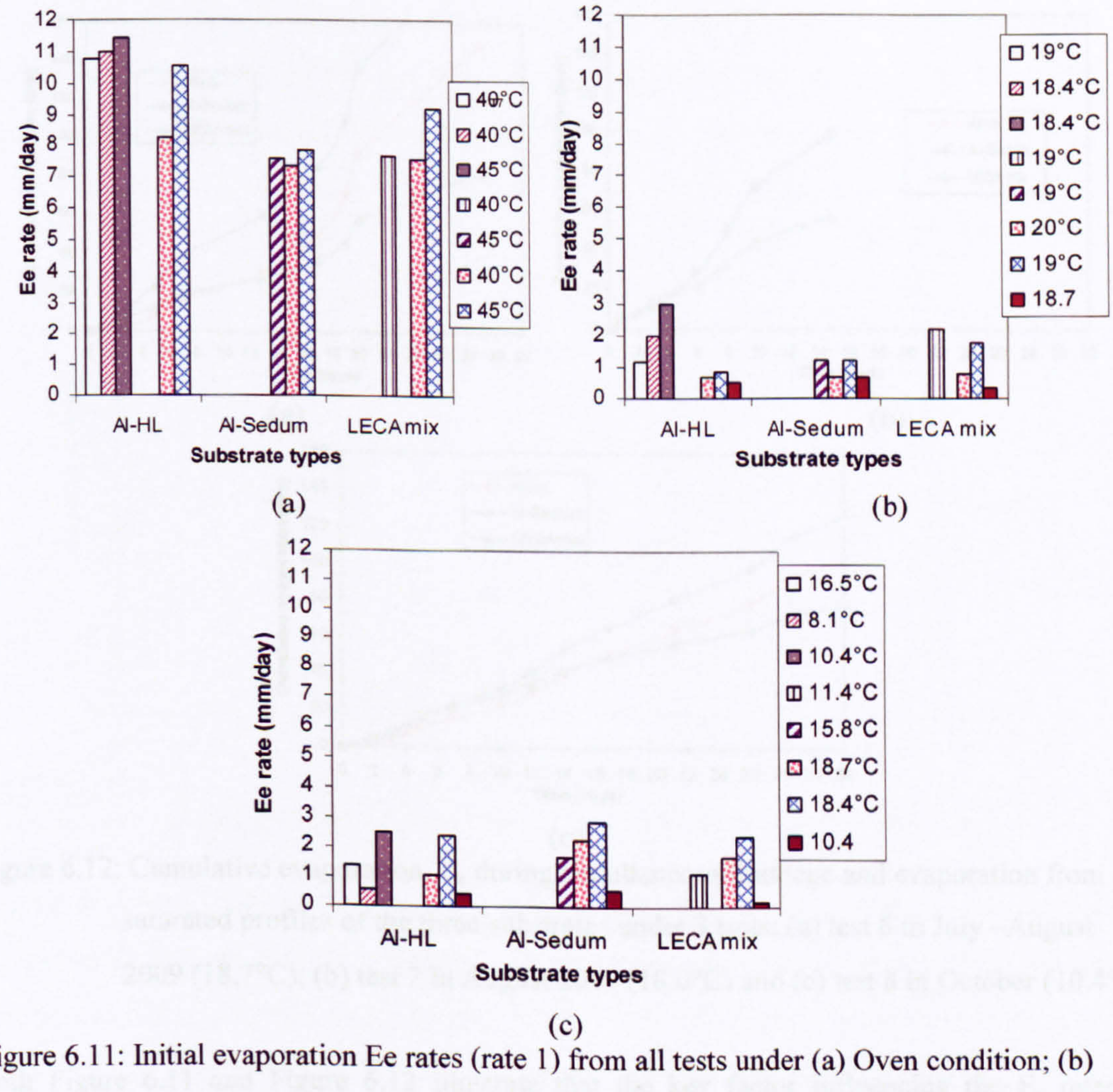


(a) (b)

(c)

Figure 6.11: Initial evaporation Ee rates (rate 1) from all tests under (a) Oven condition; (b) Inside – room condition and (c) Outside – ambient condition

Figure 6.12 then investigates the $E_e$ performance under ambient conditions between each substrate. This showed that cumulative evaporation can be influenced by differences in substrate hydraulic properties as demonstrated by Hillel and van Bavel (1976) in Hillel (1998).

In Tests 6 and 8 with 18.7°C and 10.4°C respectively, both figures show that over time the LECA mixture tends to evaporate the least with Al-Sedum evaporating the most. The LECA mixture and Al-HL also seems to sustain an initial loss rate regarding drying of longer (almost a week) than the Al-Sedum. However, at a slightly lower temperature of 18.0°C than in Test 6, both Alumasc substrates in Test 7 (Figure 6.12 (b)) demonstrate very similar cumulative evaporation. It is not easy to understand this performance but both substrates presented similar soil characteristics as shown in Table 6.1, therefore at certain times, these substrates could produce the same performance.

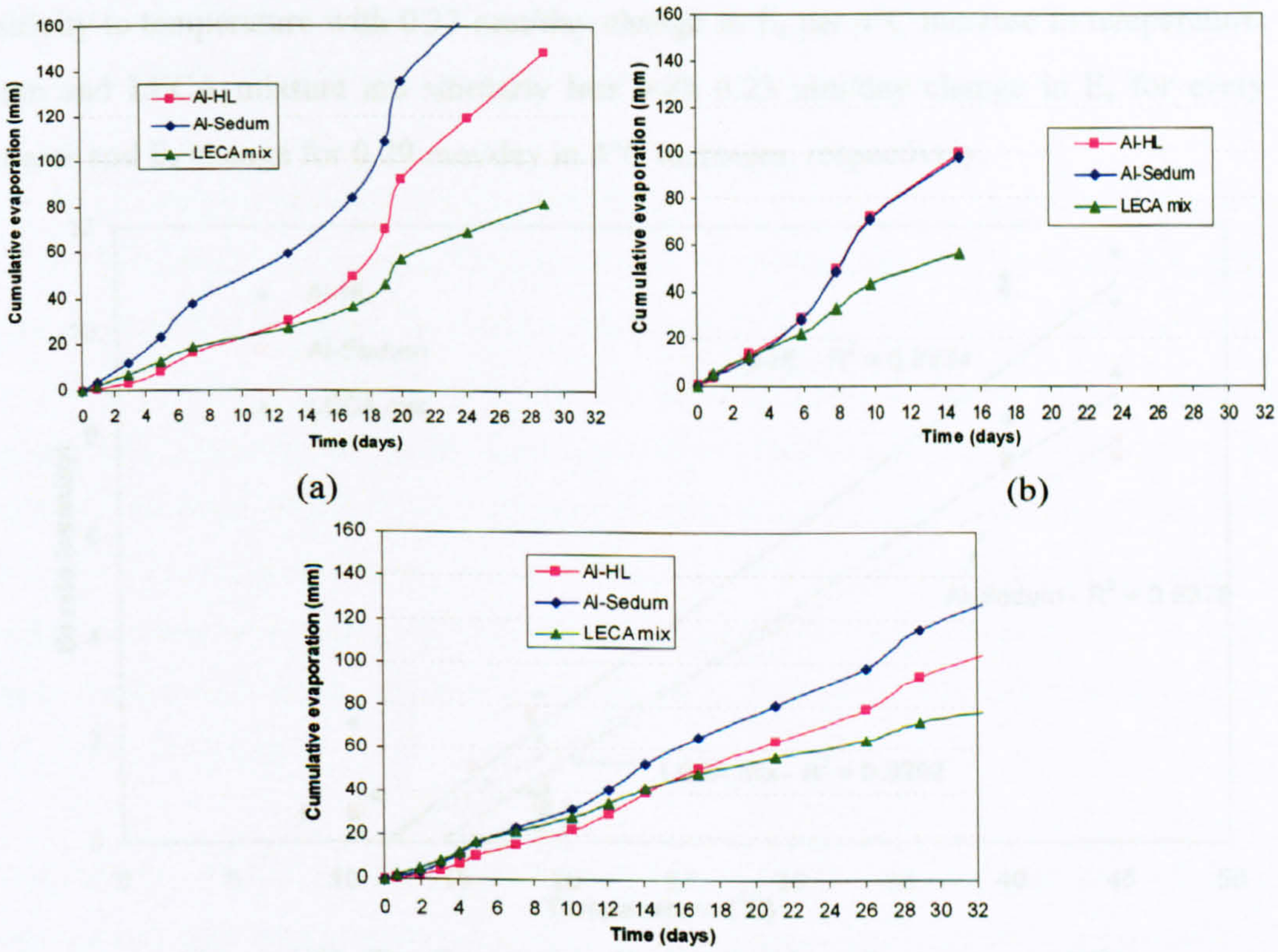


Figure 6.12: Cumulative evaporation, $E_e$ during simultaneous drainage and evaporation from saturated profiles of the three substrates under 3 tests; (a) test 6 in July –August 2009 (18.7°C); (b) test 7 in August 2009 (18.0°C) and (c) test 8 in October (10.4°C)

Both Figure 6.11 and Figure 6.12 illustrate that the key factor influencing the $E_e$ rates is temperature. Therefore the next section will discuss the link between $E_e$ rates and temperature.

### 6.3.2.4 Linking Experiment Evaporation, $E_e$ Rates to Temperature

Figure 6.11 shows different $E_e$ rates at different temperatures in Figure 6.11(a) and Figure 6.11(b), although different $E_e$ rates between the same substrates under similar temperature might be caused by other climatic factors such as thermal energy and wind speed in their surroundings. Figure 6.13 was then plotted using all the test results and it demonstrated a significant relationship of $E_e$ rates as a function of temperature. A clear correlation between moisture loss rate and temperature is evident for all substrates. It also shows that there was no significant difference in $E_e$ rates between the 3 types of substrates. Al-HL shows the greatest sensitivity to temperature with 0.33 mm/day change in $E_e$ per 4°C increase in temperature. Al-Sedum and LECA mixture are similarly less with 0.23 mm/day change in $E_e$ for every 4°C increases and $E_e$ change for 0.29 mm/day in 4°C increases, respectively.

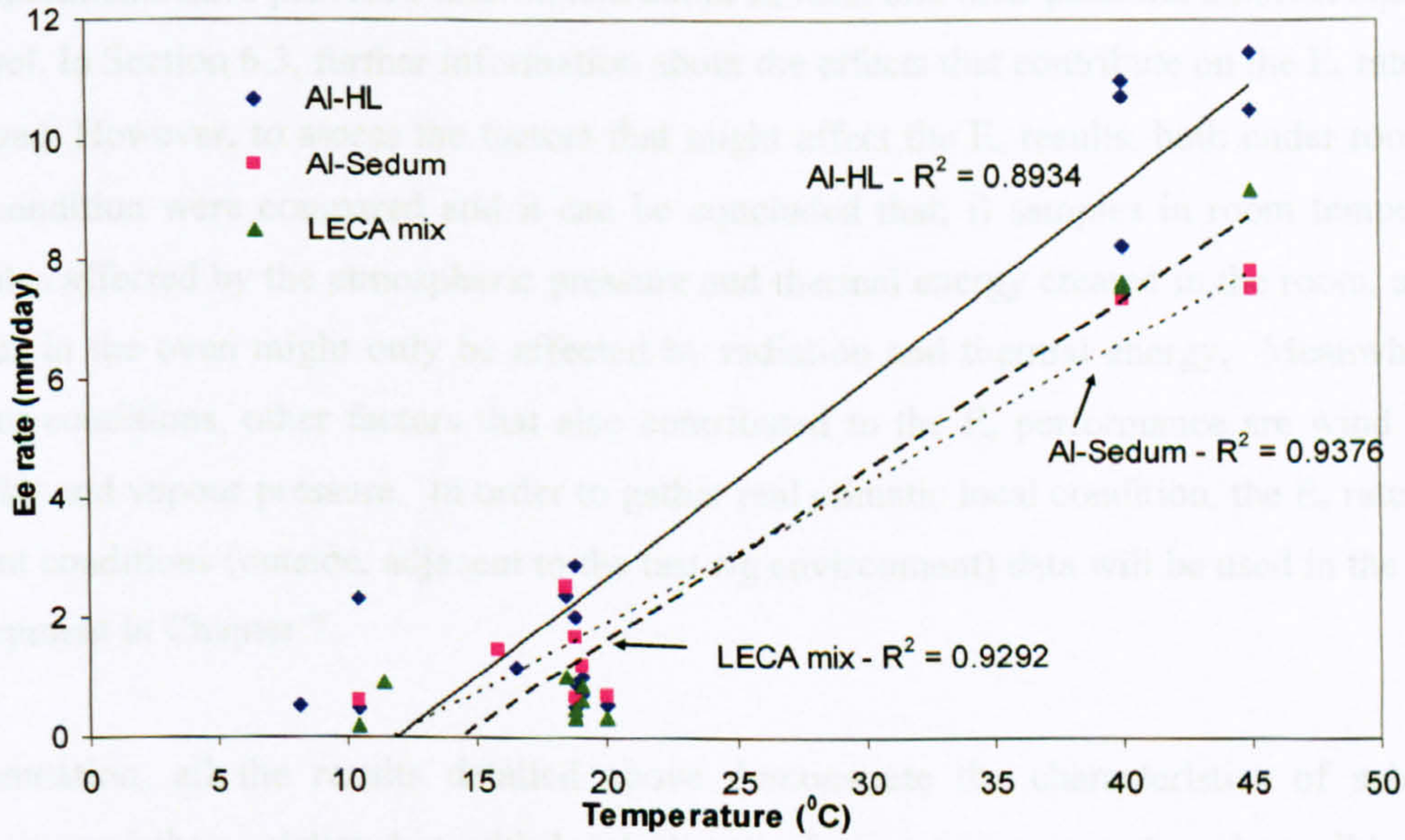


Figure 6.13: The $E_e$ rate (rate 1) as a function of temperature (°C)

Figure 6.13 also suggests that without any contribution of other climatic variables (only temperature), the moisture in substrates may only start to evaporate at ±12°C. However this figure also illustrates that a proportion of the data set showed evaporation below 12°C. Therefore, the contribution of the early evaporation of $E_e$ rates under temperatures of 12°C; might be a combination of the following climatic factors: temperature, humidity, vapour pressure, wind speed, radiation and thermal energy factors (McCuen, 2004).

## 6.4 Conclusion

From the collection of parameter results, it is suggested that besides the FLL test, the experimental evaporation drying at 40°C as a constant also has the potential to yield similar $WC_{max}$ result values as the FLL's. This experiment also provides values for the parameters; $MC_t$ and $E_e$ rate values but no $MC_{min}$ was evident in ambient conditions. It is believed that $MC_t$ is a function of substrate properties (Section 6.2), ADWP and climatic variables (Section 6.3). Figure 6.7 (a) and Figure 6.7 (b) has provided an example of climatic factors, representing another factor that contributes to the variation of the $MC_t$. It is also believed that the $E_e$ rate is a function of substrate properties, climatic variable factors and vegetation; therefore further examination has been undertaken for the Ee rate (without the vegetation factors) in Section 6.3.

The experiments have provided information about $E_e$ rates and their potential ambient minimum dry level. In Section 6.3, further information about the effects that contribute on the $E_e$ rates was discussed. However, to assess the factors that might affect the $E_e$ results, both under room and oven condition were compared and it can be concluded that; i) samples in room temperature were also affected by the atmospheric pressure and thermal energy created in the room, and; ii) samples in the oven might only be affected by radiation and thermal energy. Meanwhile for ambient conditions, other factors that also contributed to the $E_e$ performance are wind speed, humidity and vapour pressure. In order to gather real climatic local condition, the $E_e$ rates from ambient conditions (outside, adjacent to the test rig environment) data will be used in the model development in Chapter 7.

In summation, all the results detailed above demonstrate the characteristics of substrates properties and their relationship with local climatic factors (temperature), and possibly (later) from vegetation characteristics (for transpiration) as key roles in influencing the $WC_{max,}$ $E_e$ rates and $MC_t$ of the substrates. This experiment also proved that in any monitoring green roof test bed or roof, it is possible to provide better understanding and information based on these two main experiments, FLL test and the proposed evaporation experiment. The $WC_{max}$ can always be measured from the substrate hydraulic properties test and the $WC_{max}$ (under ±40°C drying oven) and the $E_e$ rate values from the evaporation test; in order to provide relevant values for the model. The uniformity and density of soils during compaction of the same substrate in different vessels might also contribute to the various $WC_{max}$ results and should be investigated in detail. It can also be concluded that the substrates' physical characteristics may not be the main factor affecting the evaporation rates and the $WC_{max}$. Further detailed research into climatic factors

should be undertaken to investigate the variability in $E_e$ rates, where it seems that temperature alone can be used as a good predictor.

Obtaining information from the $WC_{max}$ and $E_e$ rates in these experiments is useful but could be particular to the samples tested. As we are trying to develop a generic model, we have been aiming to provide comparable and generic methodology and information especially for unmonitored green roof systems. Therefore in next chapter, more generic methods for ET rate estimation will be discussed in Section 7.3.

# CHAPTER 7

# MODEL DEVELOPMENT

## 7.1 The Conceptual Model

In this chapter, further development of the conceptual model discussed in Chapter 3 was undertaken. Restating the conceptual model in Chapter 3, the physically-based model incorporates losses parameters and a storage routing method, as shown in Figure 7.1. Figure 7.1(a) illustrates the main parameters of the substrate moisture storage compartment, whilst Figure 7.1(b) illustrates the timing associated with the movement of rainfall into, and through the substrate's transient storage compartment. Substrate moisture storage and transient storage are modelled using the 'moisture balance' approach (Equation 3.1) and 'reservoir storage routing' (Equation 2.5) respectively.

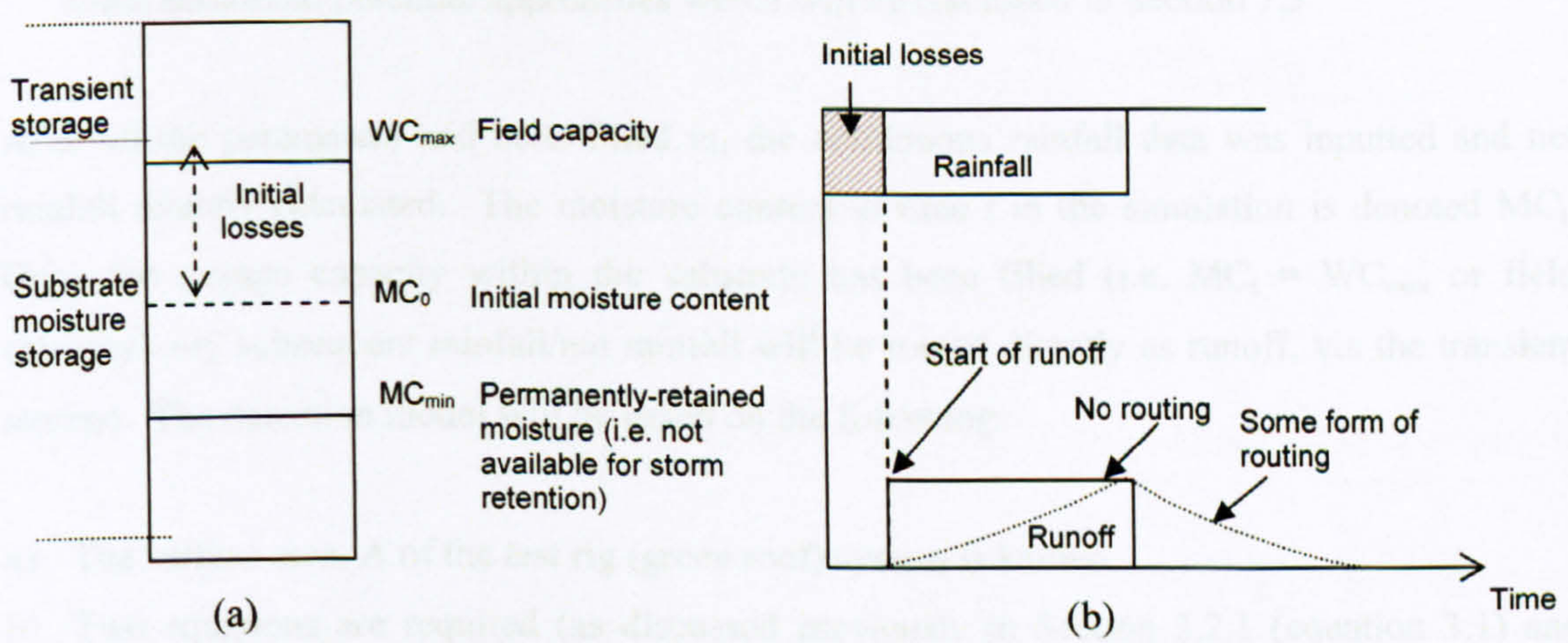


Figure 7.1: (a) Moisture content in the substrate; (b) Diagram of rainfall separation between losses and direct runoff routed into the outflow hydrograph (the attenuation of runoff).

This chapter will describe how the monitored storm data and laboratory data from Chapter 5 and Chapter 6 have been utilised, to provide the parameter values needed in the model. This includes model validation and sensitivity analysis.

### 7.1.1 Model Implementation

With reference to the two main processes discussed in Chapter 2 and Chapter 5, following Figure 7.1, the implementation of the model is based on two processes; retention and detention of the moisture. Retention modelling will require rainfall and rainfall losses (initial losses) inputs and will produce net rainfall as output; whilst detention will require the net rainfall as input and apply routing to model the temporal variation in runoff. All these conceptual green roof model processes have been implemented using Microsoft Office Excel 2003, as shown in Figure 7.2. The temporal values in this model are calculated in 5-minute time steps.

The retention model is based on the following assumptions:

a) The following substrate parameter values can be provided: substrate depth (mm); maximum water capacity - $WC_{max}$ (%); potential minimum moisture content - $MC_{min}$ (%) and initial moisture content - $MC_0$ (%).

b) Loss of moisture from the substrate is due to evapotranspiration (ET). The potential ET can be derived either from the monitored data; from the evaporation, $E_e$, experiment or using some additional potential approaches which will be discussed in Section 7.3.

After all the parameters had been filled in, the continuous rainfall data was inputted and net rainfall directly calculated. The moisture content at time t in the simulation is denoted $MC_t$. Once the storage capacity within the substrate has been filled (i.e. $MC_t = WC_{max}$ or field capacity) any subsequent rainfall/net rainfall will be routed directly as runoff, via the transient storage. The detention model will be based on the following:

a) The surface area, A of the test rig (green roof) system is known.
b) Two equations are required (as discussed previously in Section 3.2.1 (equation 3.1) and Section 2.5.4.3 (equation 2.5) to describe the relationship between the depth (and head, H) of water in the transient storage compartment, and both the rate of runoff and the volume in storage.

An example of runoff conversion and storage routing can be found in Appendix 7.1.

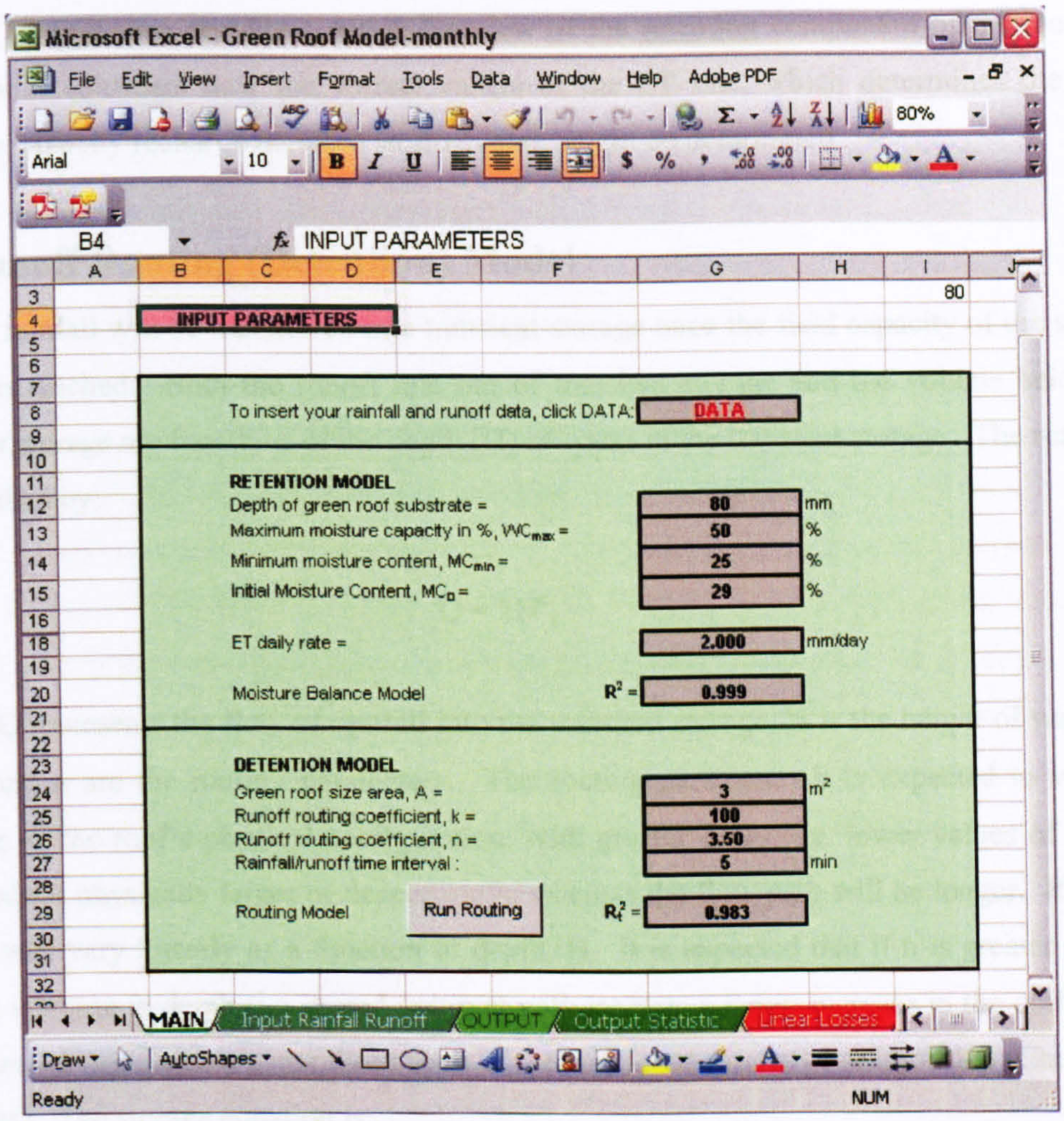


Figure 7.2: Implementation of the green roof model in Microsoft Excel.

It should be noted that the model may be operated in two modes:

a) Storm event mode – Initial moisture content, $MC_0$ parameter is required at the beginning of the simulation of an event.
b) Continuous simulation mode - $MC_0$ is required only at the beginning of the first event. Subsequent storm events, $MC_t$ are calculated internally. The simulation has been undertaken throughout a continuous study period of 29 months.

Initially, a small number of single storm events were used for routing (detention) model development. In this case $MC_0$ was estimated using direct assumed initial losses values, i.e. the difference between the measured total runoff and the measured total rainfall. Section 7.2 explains how the detention (runoff routing) component of the model has been calibrated.

Section 7.3 will then provide a detailed review of the retention component of the model. In particular it considers how the correct values of the ET rate, which determines the rate of retention capacity recharge between storm events, might be determined.

## 7.2 Runoff Routing (Detention) Model

The net rainfall will be transferred into transient storage once the field capacity of the substrate has been reached. Both the runoff rate out of transient storage and the volume held within transient storage are functions of the depth (H) of water in the transient storage. The runoff rate is described by:

$$Q = kH^n, \qquad 7.1$$

Where Q represents the flow of rainfall into the transient storage, H is the height of water level and k and n are the routing parameters. The routing parameter, k is expected to vary as a function of the roof's physical configuration; with greater delay (i.e. lower values of k) being expected for physically larger or deeper roofs; whereas the flow path will be longer. If n is 1.0, then Q will vary linearly as a function of depth, H. It is expected that if n is greater than 1.0, then an increase in depth (i.e. stored volume) will generate a larger increase in the outflow rate. Equation 7.1 represents a generalised form of the weir head-discharge relationship (Chadwick *et al.*, 2004). The storage equation is:

$$S = AH, \qquad 7.2$$

Where S represents the storage volume, H is the depth of water level and A is the surface area of the test rig. At each time step an iterative process (Goal Seek in Microsoft Excel) is used to determine the value of H that obeys the continuity equation (Section 2.5.4.3 - equation 2.4). Based on a measure of goodness of fit for a time series model (a predicted temporal profile p(t) to the measured data m(t)) (Young *et al.*, 1980), a calibration with $R_t^2$ closer to 1 indicates a better fits for the model:

$$R_t^2 = 1 - \left[ \frac{\sum_{t=1}^{n} (M_t - P_t)^2}{\sum_{t=1}^{n} M_t^2} \right]; \; 0 \le R_t^2 \le 1 \qquad 7.3$$

Where $R_t^2$ is r-square, $M_t$ is measured data, $P_t$ is predicted data, n is 1, 2,…n, t is time

### 7.2.1 Calibration of Runoff Routing Parameters

The calibration was undertaken on a selection of storm events that had been chosen based on the variation of total rainfall, season and ADWP. It should be noted that the research to date has only attempted to calibrate and assess model sensitivity to the routing parameters k and n; whilst no attempt has been made to relate the identified values to the physical properties of the substrate or to suggest how the values might differ for other green roof applications.

Using the values of initial available storage, $MC_0$ assumed above, based on the difference between total rainfall and total runoff, the routing parameters, k and n were selected based on the best estimation of $R_t^2$. The calibrations were undertaken on a manual trial-and-error basis. Results of each calibration are shown in Table 7.1. Almost all the calibrations illustrated in Figure 7.3 simulated the observed data very well ($R_t^2 > 0.9$). However, the 27 February 2007 and 13 May 2007 events have $R_t^2 < 0.9$ (Figure 7.4 (b) and (c) respectively). In both of these events the start of the modelled runoff temporal profile was delayed compared with the monitored runoff. This suggests that the assumed value of $MC_0$ may have been lower (i.e. more retention capacity) than in reality. However, once runoff occurs, the fit of the modelled temporal profile is good.

Generally, all events produced the best goodness of fit, $R_t^2$ at k values between 100 and 1000; with n value between 3.5 and 4.0. However in some events, the k and n will go higher or lower, which might be explained by the Q characteristics of each storm and the substrate physical configuration that might change during heavy rainfall or during periods of drought. Therefore further sensitivity analysis has been undertaken, presented in Section 7.2.3 and 7.2.4.

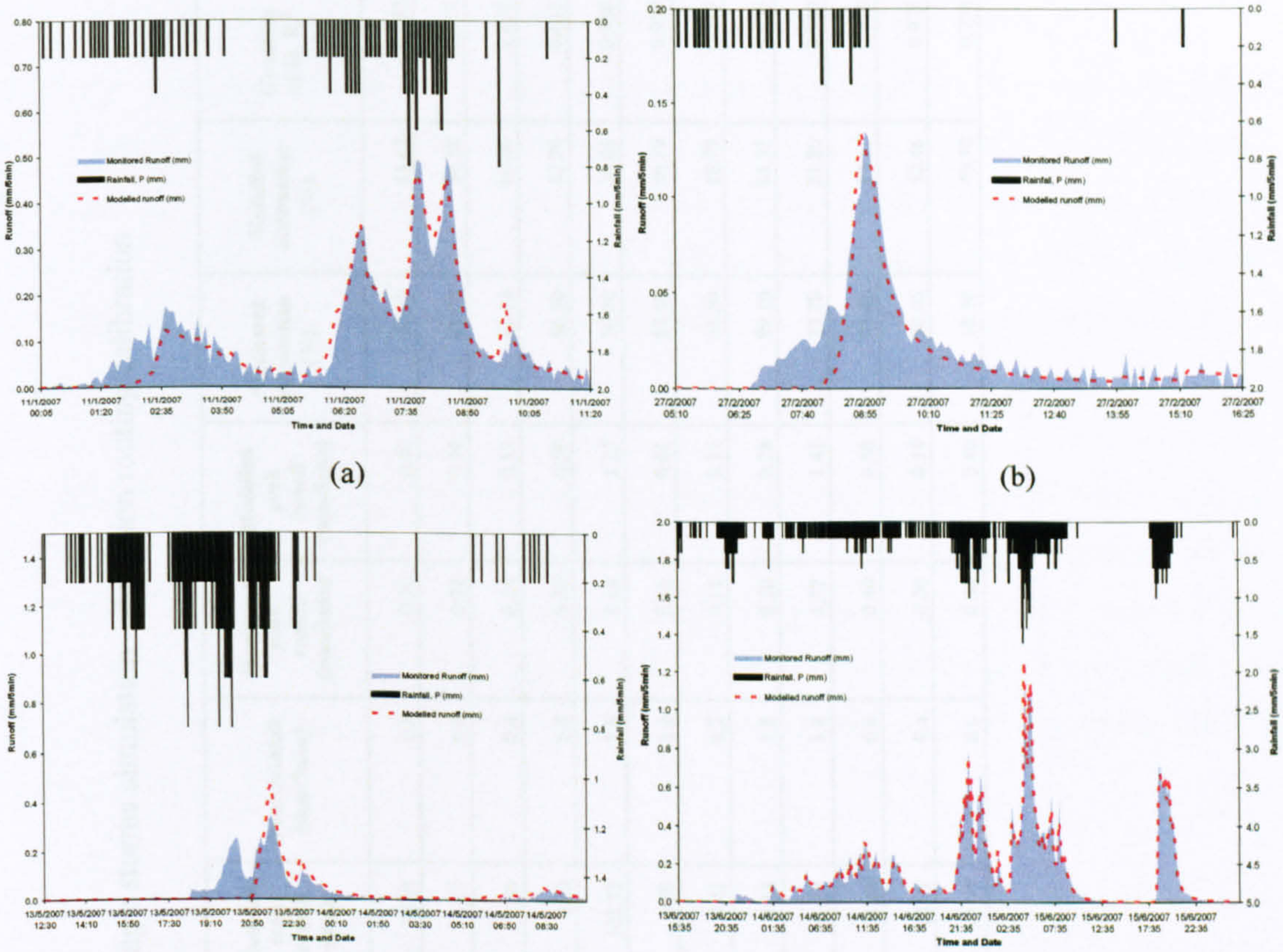


Figure 7.3: Examples of storm events simulated in the model using $MC_0$, k and n (Table 7.1); (a) 11 January 2007 (b) 27 February 2007 (c) 13 May 2007 (d) 13 June 2007 (e) 4 October 2008 and (f) 5 September 2008.

Table 7.1: The details and the results from the single storms simulation – detention routing calibration

| Date | ADWP (hours) | Depth (mm) | | | $MC_0$ (%) | k | n | Modelled total runoff (mm) | Peak rainfall (mm/5min) | Monitored peak runoff (mm/5min) | Modelled peak runoff (mm/5min) | Monitored attenuation (%) | Modelled attenuation (%) | Goodness of fit, $R_t^2$ |
|---|---|---|---|---|---|---|---|---|---|---|---|---|---|---|
| | | Rainfall (P) | Runoff (R) | Initial storage available | | | | | | | | | | |
| 11-Jan-2007 | 9.47 | 17.00 | 15.01 | 1.99 | 47.51 | 200 | 3.5 | 15.01 | 0.8 | 0.50 | 0.47 | 37.10 | 41.67 | 0.952 |
| 17-Jan-2007 | 9.17 | 3.80 | 3.17 | 0.63 | 49.21 | 400 | 3.4 | 3.17 | 0.6 | 0.30 | 0.30 | 49.43 | 50.18 | 0.975 |
| 27-Feb-2007 | 47.10 | 6.00 | 2.89 | 3.11 | 46.11 | 200 | 3.5 | 2.89 | 0.4 | 0.14 | 0.13 | 66.14 | 66.26 | 0.894 |
| 13-May-2007 | 16.08 | 27.60 | 8.77 | 18.83 | 26.46 | 120 | 3.2 | 8.80 | 0.8 | 0.30 | 0.50 | 56.50 | 42.90 | 0.635 |
| 13-Jun-2007 | 31.98 | 115.80 | 102.72 | 13.08 | 33.65 | 100 | 3.5 | 102.72 | 1.6 | 1.18 | 1.27 | 26.00 | 20.45 | 0.988 |
| 19-Jun-2007 | 37.92 | 11.20 | 4.56 | 6.64 | 41.47 | 250 | 3.5 | 4.56 | 1.4 | 0.65 | 0.61 | 53.49 | 56.19 | 0.967 |
| 18-Nov-2007 | 42.62 | 25.20 | 9.41 | 15.79 | 30.26 | 250 | 4.0 | 9.41 | 0.2 | 0.11 | 0.16 | 44.50 | 18.79 | 0.790 |
| 12-Aug-2008 | 54.38 | 18.00 | 5.18 | 12.82 | 33.98 | 2000 | 4.0 | 5.18 | 1.8 | 0.20 | 0.28 | 89.10 | 84.35 | 0.659 |
| 5-Sep-2008 | 14.65 | 46.80 | 46.18 | 0.62 | 49.23 | 100 | 3.5 | 46.18 | 1.8 | 1.37 | 1.41 | 23.78 | 21.86 | 0.940 |
| 4-Oct-2008 | 30.40 | 27.80 | 24.49 | 3.31 | 45.87 | 800 | 4.0 | 24.49 | 0.6 | 0.40 | 0.50 | 33.40 | 17.15 | 0.922 |
| 12-Dec-2008 | 97.22 | 21.40 | 18.91 | 2.49 | 46.88 | 150 | 3.5 | 18.91 | 0.4 | 0.20 | 0.19 | 50.05 | 52.46 | 0.979 |
| 14-May-2009 | 10.47 | 26.20 | 12.77 | 13.43 | 33.20 | 300 | 3.5 | 12.77 | 0.6 | 0.30 | 0.40 | 58.10 | 40.70 | 0.798 |

### 7.2.2 Sensitivity Analysis on Runoff Routing Parameters

From the calibration activities, the analysis demonstrates a variation in k between 100 and 1000; and n between 3.5 and 4.0. The most fitted value for k is 100 and n is 3.5. These may be considered to be the default values for the specific system under consideration. This section will consider the sensitivity of the runoff using these two parameter values, to see how the model prediction fitted when one of the parameters is constant. The coefficients are then validated in Section 7.2.3.

A series of sensitivity analyses have been undertaken for the routed runoff profile to k and n values on a few storm events, selected in Table 7.1 with $R_t^2 > 0.9$ during calibration. Table 7.2 shows examples of k values with a constant n and various n values with a constant k on two events (13th June 2007 and 5th September 2008). These are based on the highest total rainfall and three moderate events (11th January 2007, 4th October 2008 and 12th December 2008) with various total runoffs.

This analysis demonstrates that as k increases (from 100 to 500) the modelled peak attenuation decreases with the best $R_t^2$ observed when k = 100 for almost all events. Figure 7.4 and Figure 7.6 show that for the modelled runoff with smaller k (100) a lower peak flow is observed; Figure 7.4(a) and Figure 7.6(a) than the bigger k (500) (Figure 7.4(c) and Figure 7.5(c) but with more delay as the modelled temporal profile is moving forward with higher peak attenuation than monitored.

Figures 7.5(a) and 7.7(a) show the sensitivity to n with n values getting larger from n = 2.5 to n = 5.0, larger increases in outflow rate are observed. By comparing Figure 7.4(a) with Figure 7.5(a), the usage of n value is smaller than 3.5. This results in reduced runoff production and may suggest that the available moisture depth (i.e. stored volume) is decreased.

Table 7.2: Example of the sensitivity analysis using constant k and constant n value for event-basis

| Date | ADWP (hours) | Depth (mm) | | | MC0 (%) | k | n | Modelled total runoff (mm) | Peak rainfall (mm/5min) | Monitored peak runoff (mm/5min) | Modelled peak runoff (mm/5min) | Monitored attenuation (%) | Modelled attenuation (%) | Goodness of fit, $R_t^2$ |
|---|---|---|---|---|---|---|---|---|---|---|---|---|---|---|
| | | Rainfall, (P) | Runoff, (R) | Initial storage available | | | | | | | | | | |
| 11-Jan-2007 | 9.47 | 17.00 | 15.01 | 1.99 | 47.54 | 100 | 3.5 | 15.01 | 0.8 | 0.5 | 0.50 | 37.10 | 37.93 | 0.938 |
| | | | | | | 200 | | | | | 0.47 | | 41.67 | 0.952 |
| | | | | | | 300 | | | | | 0.48 | | 39.82 | 0.949 |
| | | | | | | 400 | | | | | 0.49 | | 38.70 | 0.945 |
| | | | | | | 500 | | | | | 0.50 | | 37.95 | 0.940 |
| | | | | | | 100 | 2.5 | | | | 0.30 | | 61.94 | 0.704 |
| | | | | | | | 3.0 | | | | 0.41 | | 49.30 | 0.889 |
| | | | | | | | 3.5 | | | | 0.50 | | 37.93 | 0.938 |
| | | | | | | | 4.0 | | | | 0.56 | | 29.60 | 0.894 |
| | | | | | | | 5.0 | | | | 0.60 | | 25.11 | 0.840 |
| 13-Jun-2007 | 31.98 | 115.80 | 102.72 | 13.08 | 33.65 | 100 | 3.5 | 102.72 | 1.6 | 1.2 | 1.2 | 26.00 | 23.7 | 0.988 |
| | | | | | | 200 | | | | | 1.3 | | 21.0 | 0.988 |
| | | | | | | 300 | | | | | 1.3 | | 18.4 | 0.982 |
| | | | | | | 400 | | | | | 1.4 | | 15.1 | 0.977 |
| | | | | | | 500 | | | | | 1.4 | | 12.8 | 0.972 |
| | | | | | | 100 | 2.5 | | | | 0.9 | | 40.9 | 0.870 |
| | | | | | | | 3.0 | | | | 1.1 | | 30.9 | 0.972 |
| | | | | | | | 3.5 | | | | 1.3 | | 20.5 | 0.988 |
| | | | | | | | 4.0 | | | | 1.4 | | 10.0 | 0.968 |
| | | | | | | | 4.5 | | | | 1.6 | | 1.3.0 | 0.937 |
| | | | | | | | 5.0 | | | | 1.6 | | -2.9 | 0.906 |
| 5-Sept-2008 | 14.65 | 46.80 | 46.18 | 0.62 | 49.23 | 100 | 3.5 | 46.18 | 1.8 | 1.37 | 1.41 | 23.78 | 21.86 | 0.940 |
| | | | | | | 200 | | | | | 1.50 | | 16.54 | 0.936 |
| | | | | | | 300 | | | | | 1.54 | | 14.23 | 0.931 |
| | | | | | | 400 | | | | | 1.57 | | 12.88 | 0.927 |
| | | | | | | 500 | | | | | 1.58 | | 11.98 | 0.923 |
| | | | | | | 100 | 2.5 | | | | 0.68 | | 62.18 | 0.712 |
| | | | | | | | 3.0 | | | | 1.11 | | 38.52 | 0.902 |
| | | | | | | | 3.5 | | | | 1.41 | | 21.86 | 0.940 |
| | | | | | | | 4.0 | | | | 1.60 | | 11.32 | 0.921 |
| | | | | | | | 4.5 | | | | 1.66 | | 8.00 | 0.892 |
| | | | | | | | 5.0 | | | | 1.68 | | 6.91 | 0.862 |
| 4-Oct-2008 | 30.40 | 27.80 | 24.49 | 3.31 | 45.87 | 100 | 3.5 | 24.49 | 0.6 | 0.4 | 0.44 | 33.40 | 27.15 | 0.907 |
| | | | | | | 200 | | | | | 0.46 | | 23.93 | 0.901 |
| | | | | | | 300 | | | | | 0.47 | | 22.34 | 0.907 |
| | | | | | | 400 | | | | | 0.47 | | 21.35 | 0.911 |
| | | | | | | 500 | | | | | 0.48 | | 20.66 | 0.913 |
| | | | | | | 100 | 2.5 | | | | 0.29 | | 51.25 | 0.770 |
| | | | | | | | 3.0 | | | | 0.38 | | 37.06 | 0.855 |
| | | | | | | | 3.5 | | | | 0.44 | | 27.15 | 0.890 |
| | | | | | | | 4.0 | | | | 0.48 | | 20.56 | 0.907 |
| | | | | | | | 4.5 | | | | 0.49 | | 17.71 | 0.914 |
| | | | | | | | 5.0 | | | | 0.50 | | 16.75 | 0.916 |
| 12-Dec-2008 | 97.22 | 21.40 | 18.91 | 2.49 | 46.88 | 100 | 3.5 | 18.91 | 0.4 | 0.2 | 0.19 | 50.05 | 53.14 | 0.976 |
| | | | | | | 200 | | | | | 0.19 | | 52.03 | 0.979 |
| | | | | | | 300 | | | | | 0.19 | | 51.50 | 0.979 |
| | | | | | | 400 | | | | | 0.20 | | 51.18 | 0.978 |
| | | | | | | 600 | | | | | 0.20 | | 50.97 | 0.977 |
| | | | | | | 100 | 2.5 | | | | 0.16 | | 60.99 | 0.854 |
| | | | | | | | 3.0 | | | | 0.17 | | 56.71 | 0.951 |
| | | | | | | | 3.5 | | | | 0.19 | | 53.14 | 0.976 |
| | | | | | | | 4.0 | | | | 0.20 | | 51.03 | 0.976 |
| | | | | | | | 4.5 | | | | 0.21 | | 47.49 | 0.965 |
| | | | | | | | 5.0 | | | | 0.24 | | 40.47 | 0.950 |

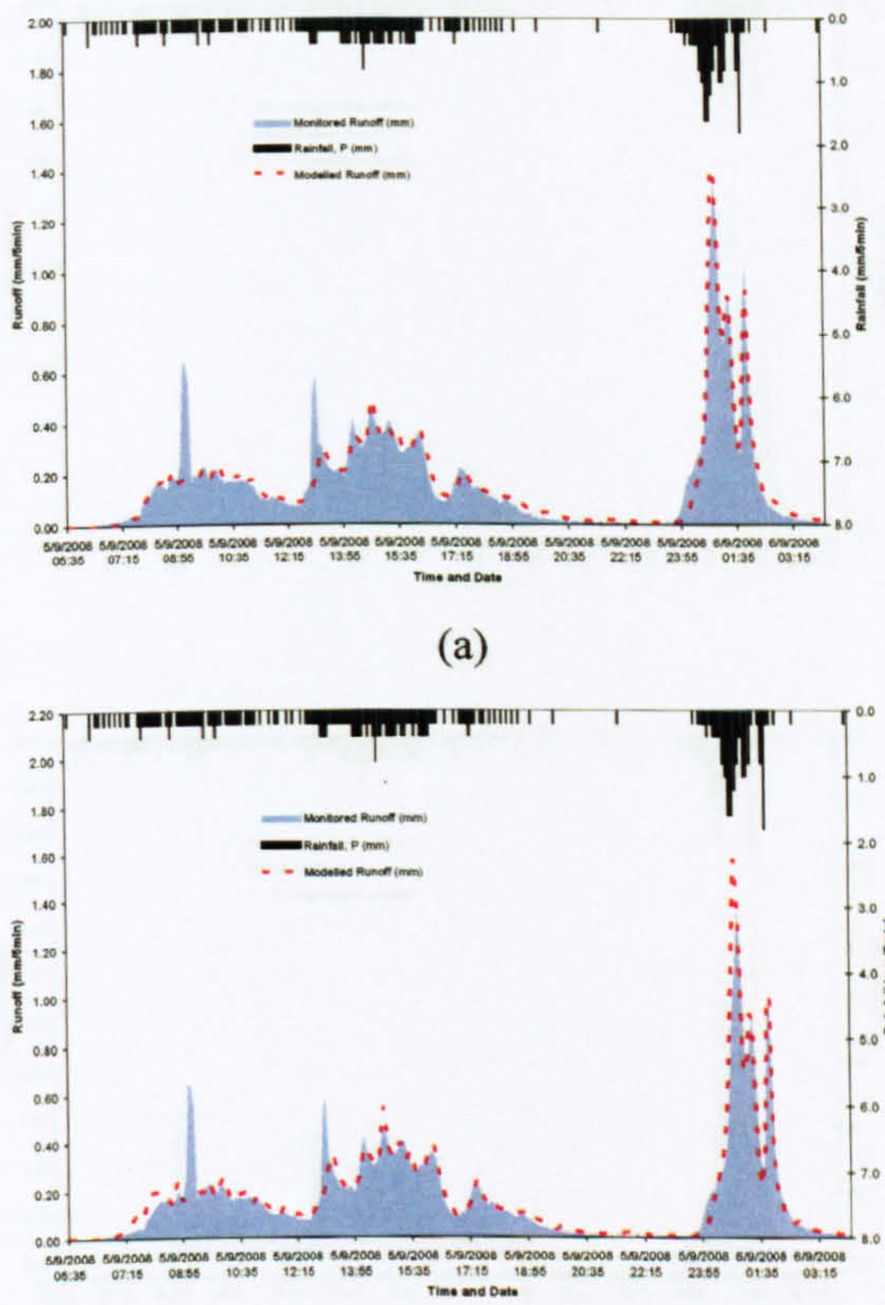


(a)

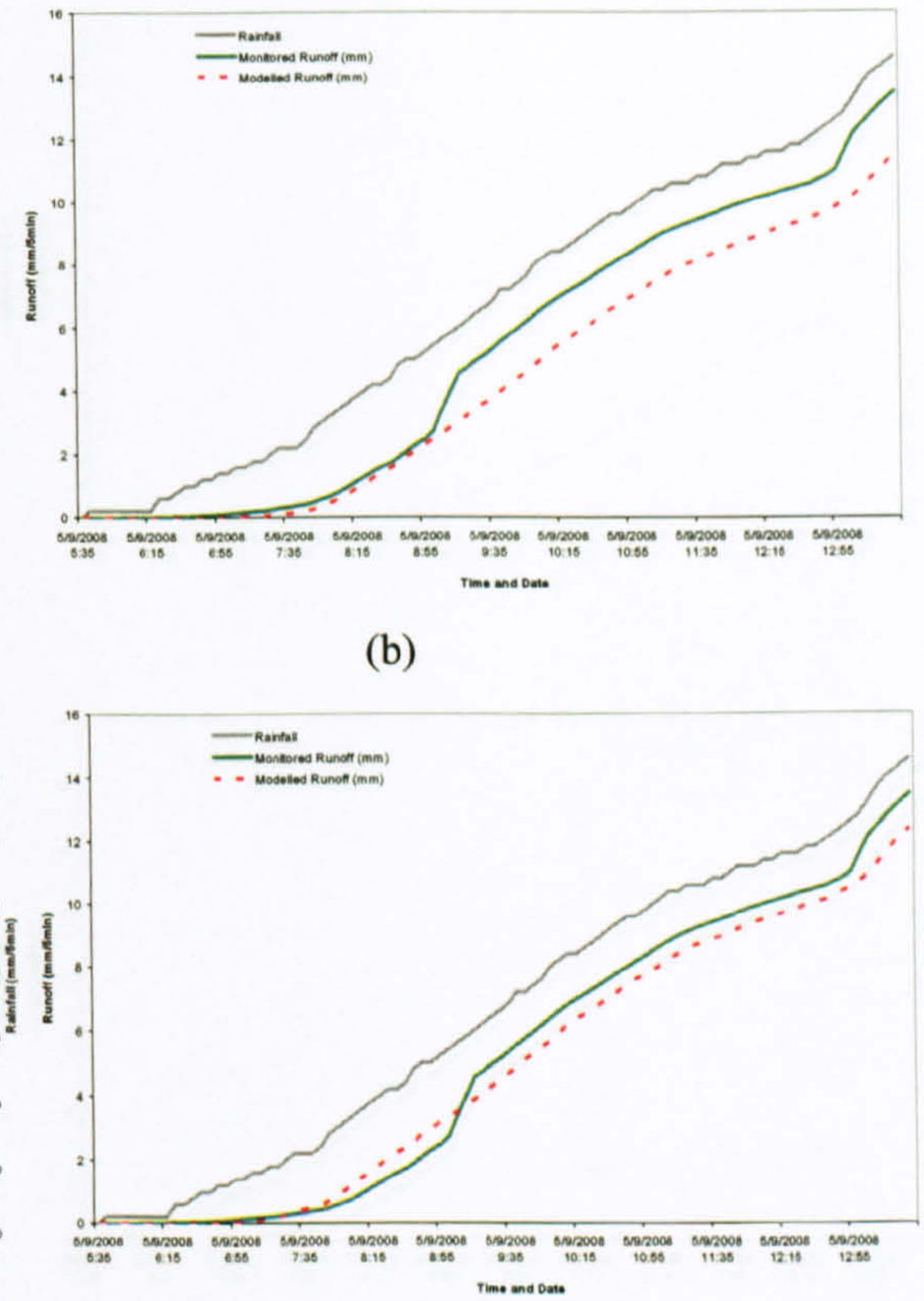


(b)




(c)




(d)

Figure 7.4: Sensitivity analysis for k on 5 September 2008 (a) k = 100, n = 3.5 (b) Cumulative rainfall runoff profiles for (a); (c) k = 500, n = 3.5 (d) Cumulative rainfall runoff profiles for (c)

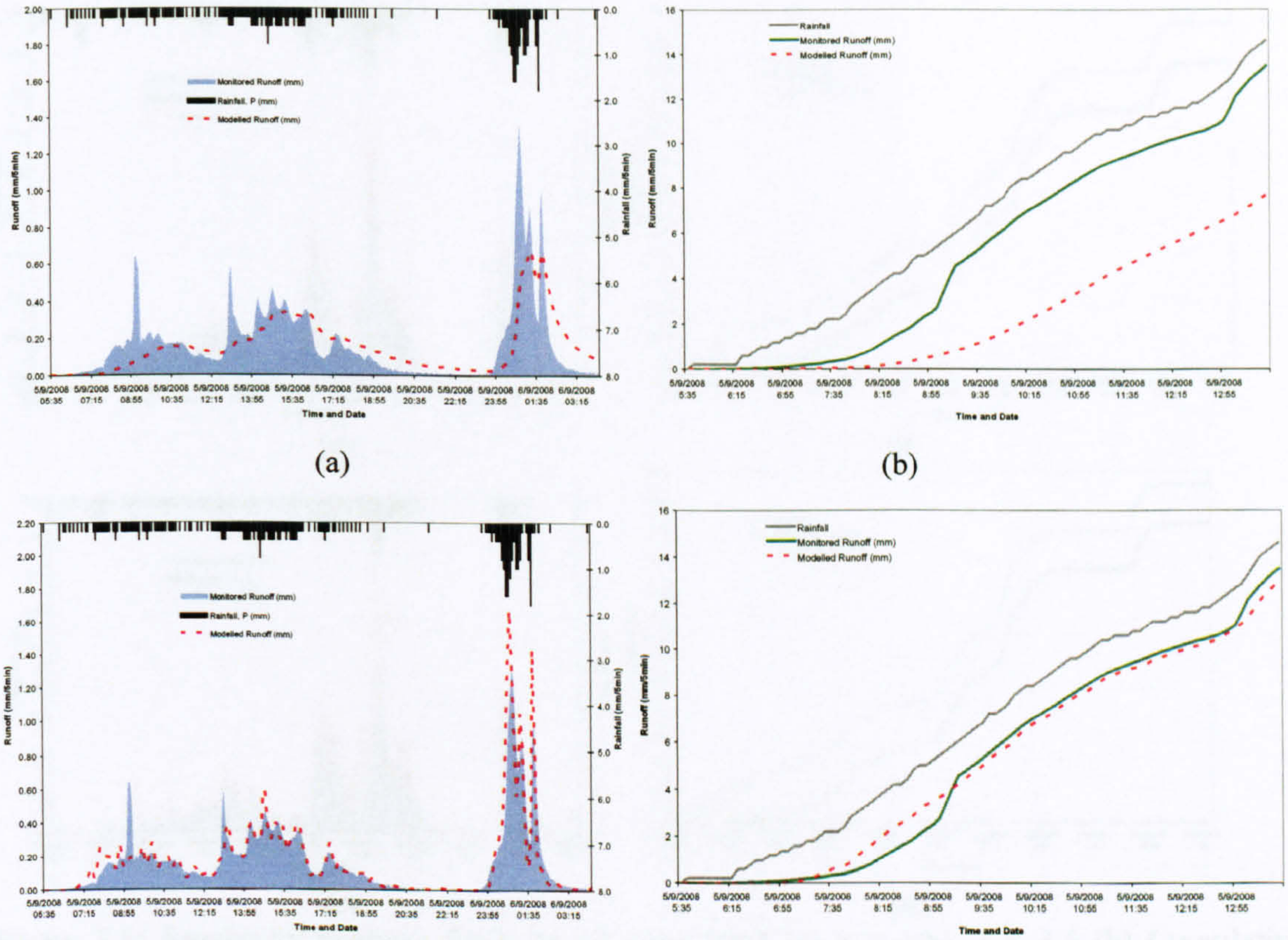


Figure 7.5: Sensitivity analysis for n on 5 September 2008 (a) k = 100, n = 2.5 (b) Cumulative rainfall runoff profiles for (a) ( c) k = 100, n = 5.0 (d) Cumulative rainfall runoff profiles for (c)

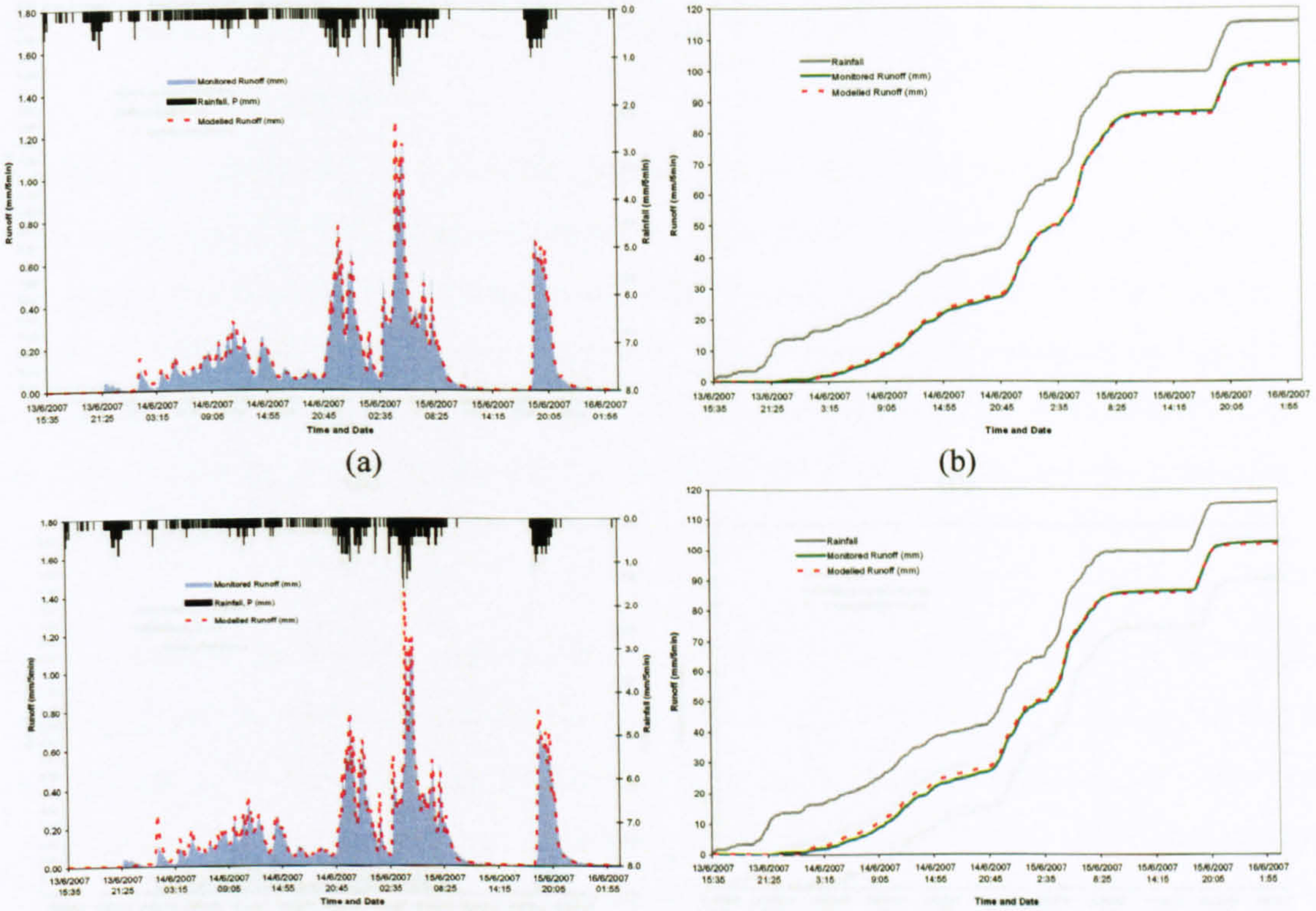


Figure 7.6: Sensitivity analysis for k on 13 June 2007 (a) k = 100, n = 3.5 (b) Cumulative rainfall runoff profiles for (a); (c) k = 500, n = 3.5 (d) Cumulative rainfall runoff profiles for (c)

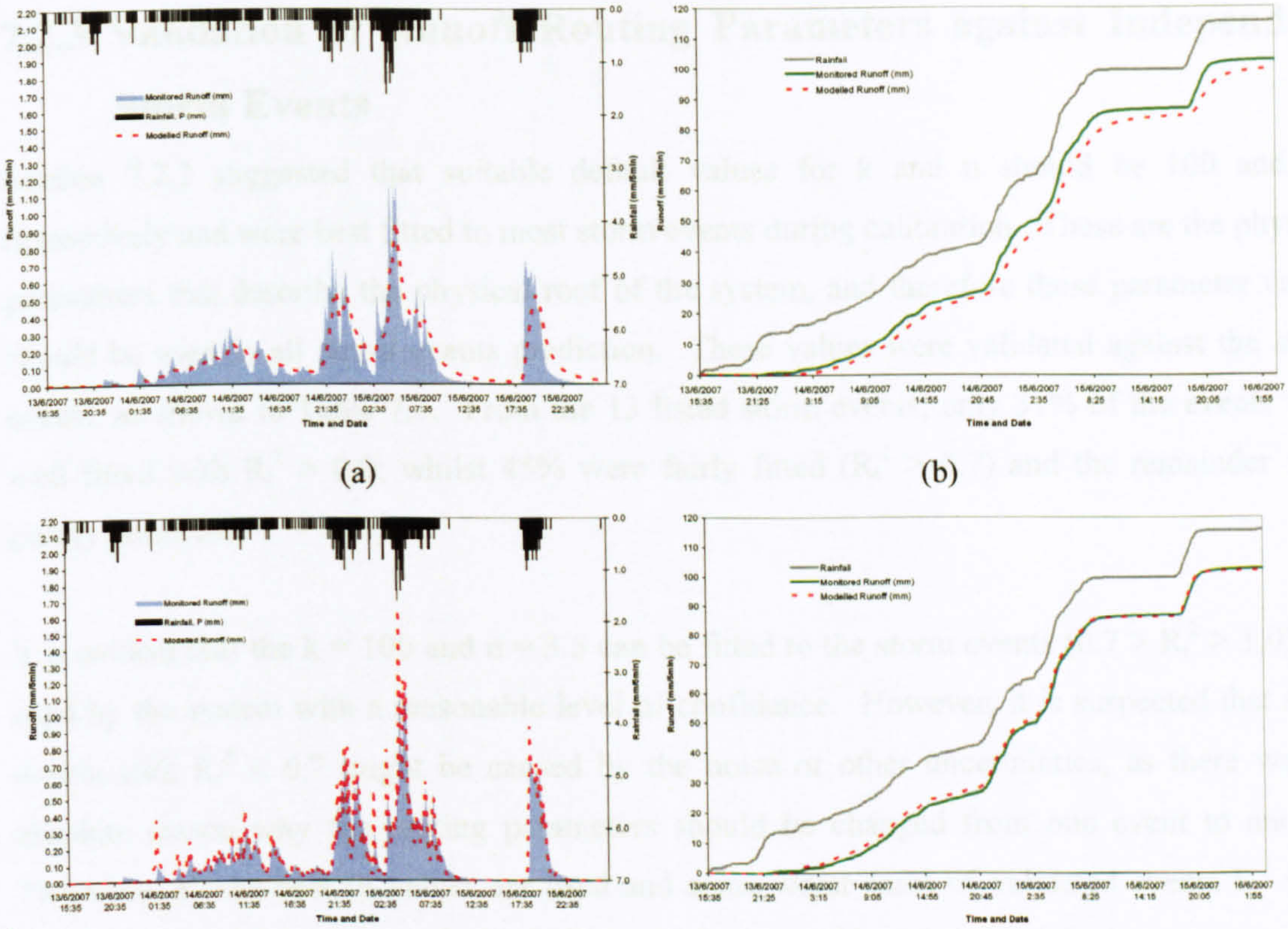


(a) (b)

(c) (d)

Figure 7.7: Sensitivity analysis for n on 13 June 2007 (a) k = 100, n = 2.5 (b) Cumulative rainfall runoff profiles for (a) (c) k = 100, n = 5.0 (d) Cumulative rainfall runoff profiles for (c)

Overall, as observed in both cumulative total modelled profiles in Figure 7.4(b), Figure 7.4(d), Figure 7.6(b) and Figure 7.6 (d) for k; and Figure 7.5(b), Figure 7.5(d), Figure 7.7(b) and Figure 7.6(d) for n both analyses suggests that the model is less sensitive to k then n, within the ranges considered here. The ranges of model response to the n by changing the total modelled runoff from a low value (of a small n = 2.5); than the monitored runoff to a slightly higher total modelled runoff (of a bigger value n = 5.0); whereas the ranges of model were less responsive to the k whether it is 100 or 500. This may be explained by the size of the small scale roof in this study, represented by k, as a result of short distance of the flow; whilst the response of n is most likely a quick response towards the depth of storage structure.

### 7.2.3 Validation of Runoff Routing Parameters against Independent Storm Events

Section 7.2.2 suggested that suitable default values for k and n should be 100 and 3.5 respectively and were best fitted to most storm events during calibration. These are the physical parameters that describe the physical roof of the system, and therefore these parameter values should be used in all storm events prediction. These values were validated against the storm events, as shown in Table 7.3. From the 13 listed storm events, only 31% of the events were well fitted with $R_t^2 > 0.9$; whilst 45% were fairly fitted ($R_t^2 > 0.7$) and the remainder were poorly predicted.

It is evident that the k = 100 and n = 3.5 can be fitted to the storm events ($0.7 > R_t^2 > 1.0$) and used by the system with a reasonable level of confidence. However, it is suspected that some events with $R_t^2 < 0.7$ might be caused by the noise or other uncertainties, as there was no absolute reason why the routing parameters should be changed from one event to another. Therefore, all the best fit values are used and some worst cases of validated events $R_t^2 < 0.7$ using the default k and n are shown in Figure 7.8. It is evident that the default parameters used may not a problem where the plots seem to suggest that the problem might be with the initial losses approach.

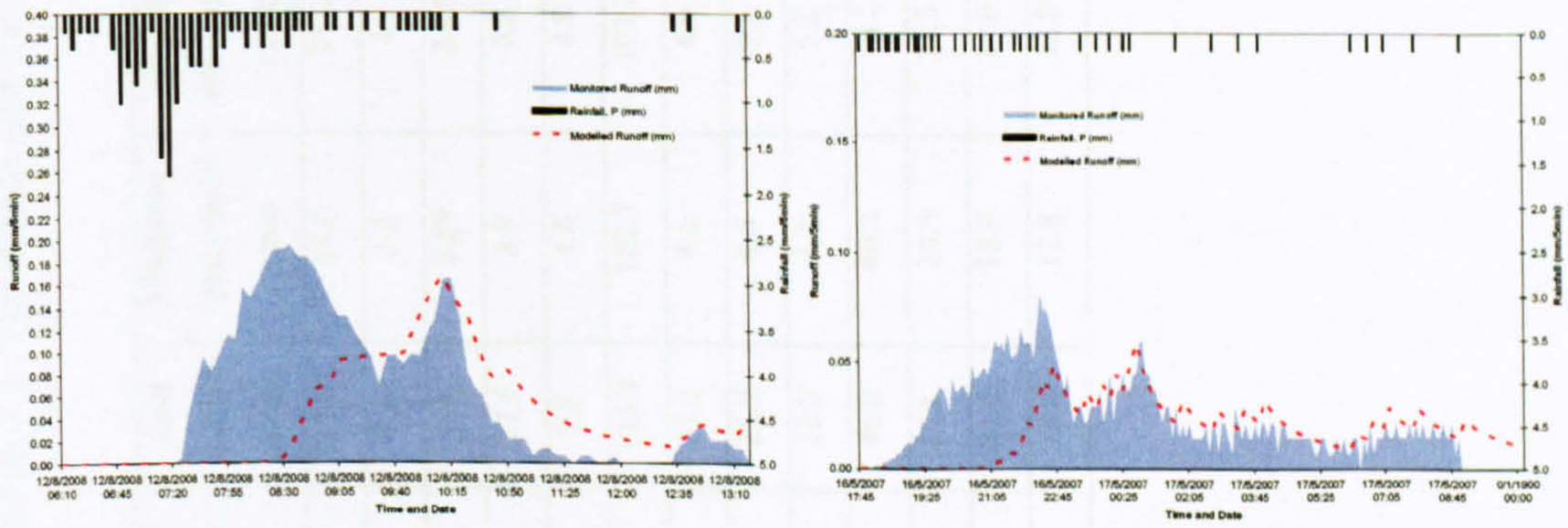


(c) (d)

Figure 7.8: Validation for the worst case events observed from Table 7.3 on (a) 12 August 2008 (b) 16 May 2007

Table 7.3: The details and the results from the validation of single storms simulation; k =100, n = 3.5

| Date | ADWP (hours) | Total rainfall (mm) | Monitored total runoff (mm) | Modelled total runoff (mm) | Monitored Retention (%) | Modelled Retention (%) | Peak rainfall (mm) | Monitored peak runoff (mm/5min) | Modelled peak runoff (mm/5min) | Monitored Attenuation (%) | Modelled Attenuation (%) | Goodness of fit, $R_t^2$ |
|---|---|---|---|---|---|---|---|---|---|---|---|---|
| 11 Jan 07 | 9.5 | 17.0 | 15.0 | 15.0 | 11.7 | 11.7 | 0.8 | 0.50 | 0.45 | 37.1 | 44.3 | 0.946 |
| 17 Jan 07 | 9.2 | 3.8 | 3.2 | 3.2 | 16.6 | 16.6 | 0.6 | 0.30 | 0.20 | 49.4 | 66.8 | 0.832 |
| 27 Feb 07 | 47.1 | 6.0 | 2.89 | 2.89 | 51.8 | 51.8 | 0.4 | 0.14 | 0.10 | 66.1 | 76.1 | 0.848 |
| 13 May 07 | 16.1 | 27.6 | 8.8 | 8.8 | 68.2 | 68.2 | 0.8 | 0.30 | 0.50 | 56.5 | 38.3 | 0.613 |
| 16 May 07 | 6.6 | 7.8 | 4.8 | 4.8 | 39.0 | 39.0 | 0.2 | 0.10 | 0.10 | 59.3 | 71.0 | 0.549 |
| 13 Jun 07 | 32.0 | 115.8 | 102.7 | 102.7 | 11.3 | 11.3 | 1.6 | 1.20 | 1.30 | 26.1 | 20.5 | 0.988 |
| 19 Jun 07 | 37.9 | 11.2 | 4.6 | 4.6 | 59.3 | 59.3 | 1.4 | 0.70 | 0.50 | 53.5 | 67.7 | 0.885 |
| 18 Nov 07 | 42.6 | 25.2 | 9.4 | 9.4 | 62.7 | 62.7 | 0.2 | 0.10 | 0.10 | 44.5 | 45.9 | 0.752 |
| 12 Aug 08 | 54.4 | 18.0 | 5.2 | 5.2 | 71.2 | 71.2 | 1.8 | 0.20 | 0.17 | 89.1 | 90.8 | 0.442 |
| 5 Sep 08 | 14.7 | 46.8 | 46.2 | 46.2 | 1.3 | 1.3 | 1.8 | 1.37 | 1.41 | 23.8 | 21.9 | 0.940 |
| 4 Oct 08 | 30.4 | 27.8 | 24.5 | 24.5 | 11.9 | 11.9 | 0.6 | 0.40 | 0.44 | 33.4 | 27.2 | 0.890 |
| 12 Dec 08 | 97.2 | 21.4 | 18.9 | 18.9 | 11.7 | 11.7 | 0.4 | 0.20 | 0.19 | 50.1 | 53.1 | 0.976 |
| 14 May 09 | 10.5 | 26.4 | 12.8 | 12.8 | 51.2 | 51.2 | 0.6 | 0.30 | 0.30 | 58.1 | 55.2 | 0.774 |

### 7.2.4 Physical Interpretation of Runoff Routing Parameters

The sensitivity analysis shows that lower values of k (e.g. 100) and n (e.g. 1) generate runoff profiles that are far more lagged, attenuated and smooth than the values that best fit the observed data. It should be noted that the monitored roof has a far smaller catchment area and very limited drainage length compared with most full-scale applications. It is recognised that the monitored runoff data, and the routing parameters identified here, may well underestimate the overall impact that a full-scale green roof installation may have on the timing of runoff, with greater lag and attenuation being anticipated at full scale.

As mentioned above, k is expected to vary as a function of the roof's physical configuration; whereas n is expected to be greater than 1.0. A greater increase in depth (i.e. stored volume) will generate a large increase in the outflow rate. Values of n greater than 1.0 might be expected in the green roof system; whereby at below field capacity small quantities of runoff can be stored in the substrate's available pore spaces, and may be expected to move quite slowly. Once the amount of moisture in storage reaches a certain level, and full saturation is approached, gravitational forces will tend to drive the flow through more quickly.

The recommended k = 100 and n = 3.5 from the sensitivity analysis has been shown to produce reasonable predictions. Figure 7.9 describes the relationship between the depth and discharge characteristics of the roof ($Q = kH^n$) using the validated routing parameters. From the monitored rainfall runoff data, the maximum reasonable rainfall observed from the roof was 4.2 mm/5min, with 2.3 mm/5min of typical runoff; hence 13 mm in terms of the temporary storage depth within transient storage (Figure 7.9). This suggests that, the range of runoff rates typically encountered from the green roof, i.e. the depth of moisture in transient storage will rarely exceed a few millimetres. This seems reasonable as substrates selected for green roofs tend to be well drained (high porosity values).

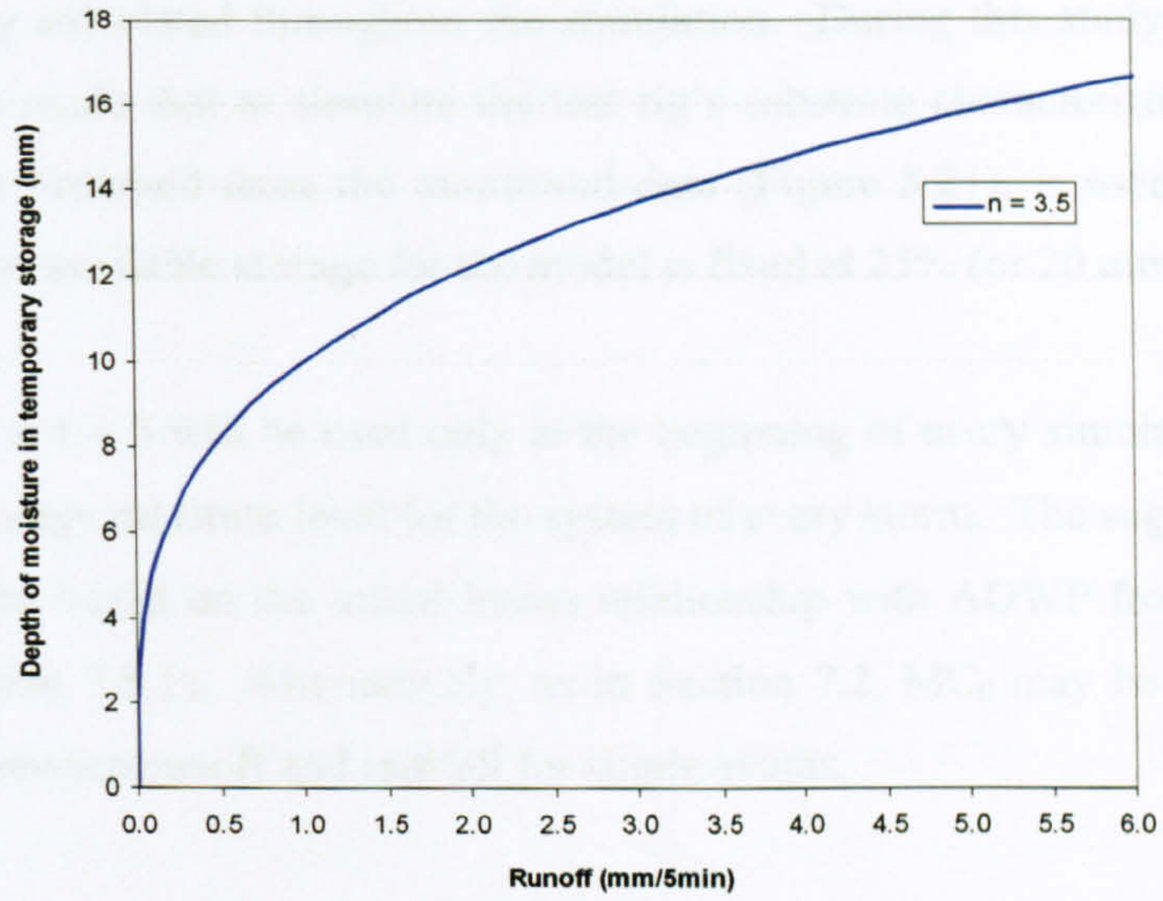


Figure 7.9: The depth-discharge characteristics of the roof based on best fitted routing parameters; k = 100, n = 3.5

## 7.3 Moisture Balance (Retention) Model

Based on the assumptions for the retention model stated in Section 7.1, 3 main input parameters from the substrate properties are required to run the model: the maximum water capacity, $WC_{max}$; minimum moisture content, $MC_{min}$; and initial moisture content, $MC_0$.

a) The determination of $WC_{max}$ has been outlined in Chapter 6: Section 6.3.1.1 and method (i) from the FLL test; or method (ii) oven-dry (less than 80°C) of samples are to be used. This parameter will provide the maximum moisture capacity for the model depending on substrate depth. In this study, the case substrate depth is 80 mm, hence for $WC_{max}$ of 50% (Alumasc HL from FLL test), the maximum moisture capacity is 40 mm.

b) Values for $MC_{min}$ can be derived by one of these estimations:
   (i) Assume the substrate is fully dry – 0% by moisture capacity volume (which is equal to 0 mm).
   (ii) Adopt the maximum retention observed from the monitored data (Section 5.4.2.3) i.e. 20 mm – 25% by volume (which is 50% of $WC_{max}$ equal to 20 mm).
   (iii) From the evaporation, $E_e$ test. During simulation the $MC_{min}$ value will provide maximum available storage for the system. Moisture content at time t, $MC_t$ will then provide the available storage at time t, ($MC_{min} \leq MC_t \leq WC_{max}$) and will be

internally calculated throughout the simulation. During this study, the assumption has been made that to simulate the test rig's substrate characteristic, the maximum retention observed from the monitored data (Figure 5.21), is used. Therefore the maximum available storage for the model is fixed at 25% (or 20 mm).

c) $MC_0$ is $MC_t$ at t = 0 will be used only at the beginning of every simulation to represent the initial storage moisture level for the system of every storm. The suggested values for $MC_0$ could be based on the initial losses relationship with ADWP from the monitored events (Section 7.3.1). Alternatively, as in Section 7.2, $MC_0$ may be estimated as the difference between runoff and rainfall for single events.

### 7.3.1 Estimating $MC_0$ for an Individual Storm Event

If the model is operated on an event-by-event basis, then the critical parameter for the retention model is the initial moisture content, $MC_0$. $MC_0$ is a function of the ADWP and the ET rate, but also depends on the moisture content remaining in the substrate at the end of the preceding event. As has been shown in section 7.2, if a robust estimate of $MC_0$ is available, the model is capable of convincingly reproducing the observed runoff profile.

In Chapter 5, an attempt was made to establish regression relationships between initial losses (i.e. monitored rainfall – monitored runoff) and the ADWP. However, considerable scatter was observed in the data and ADWP alone was not found to provide a good estimate of the storage available for retention at the start of a storm event. For example, Figure 7.10 shows an example of storage available for the event of 13 May 2009. In effect it is assumed that $MC_0$ is initialized to zero following any rainfall event. It shows that the ADWP regression would give 7.4 mm of retention, whereas the model based on continuous simulation, correctly suggests that the storage available was approximately 14 mm. This is because the ADWP of 3 days actually refers to a very tiny rainfall that did not fill up all the storage available.

In Figure 7.10, the monitored runoff data is compared with two different model predictions. Both models provide continuous simulation during the event; the key difference being the way in which the moisture within the green roof substrate has been initialised ($MC_0$ is based on best estimation of total modelled runoff compared with the total monitored runoff). An ET rate of 2 mm/day has been assumed in both cases. In the first case (full continuous

simulation mode) moisture content has been continuously simulated throughout the weeks prior to the event. It can be shown that between 2/5 and 13/5 there were several minor rainfall events that did not result in runoff. The available storage (blue line) drops slightly in response to each of these events, but it does not fall to zero, so no runoff is modelled. It is evident that available storage reached more than half of its total available storage several days before the 13/5 event. During 13/5 and 14/5, sufficient rain falls to exhaust the available storage and runoff are generated. The modelled runoff (red line) is very similar to the monitored runoff response.

If the available storage is initialised based on the ADWP; it must be assumed that no storage was available at the end of the previous event (even though it is evident that the event on 9/5 did not result in any runoff). The ET rate of 2 mm/day means that nearly 8 mm storage (approximately half the correct amount) is available at the start of the event. The result of this is that the modelled runoff starts too soon, and the total simulated runoff is too great.

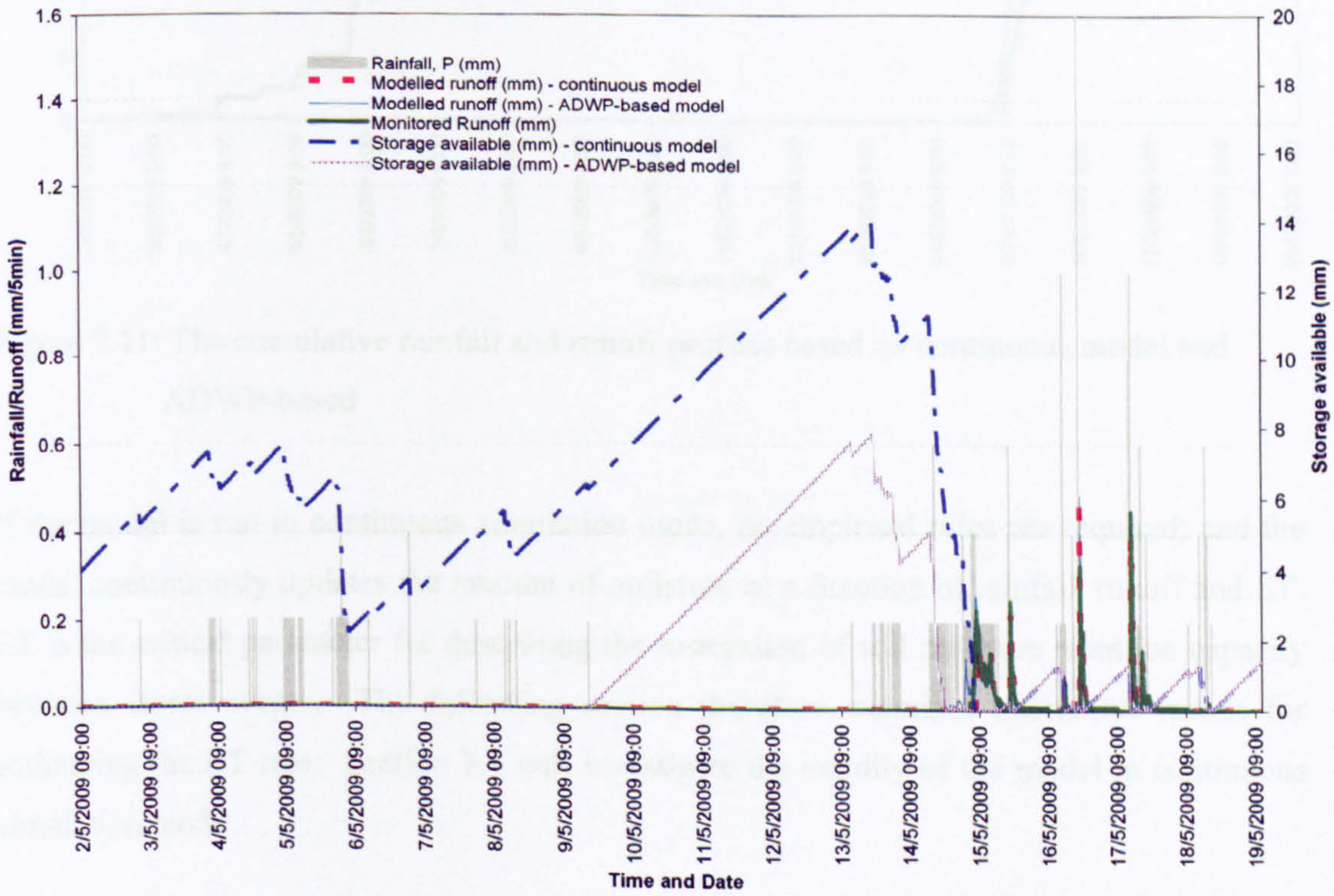


Figure 7.10: The comparison of storage available based on continuous model and ADWP-based model using event of 13 May 2009

Figure 7.11 shows the cumulative rainfall and runoff profiles in each case. This example clearly shows the weaknesses of using the model in storm event mode. The model is heavily reliant on the correct value of available storage, but this cannot reliably be predicted from ADWP alone, as the preceding event may not have resulted in runoff. Hence the remainder of the thesis focuses on continuous simulation.

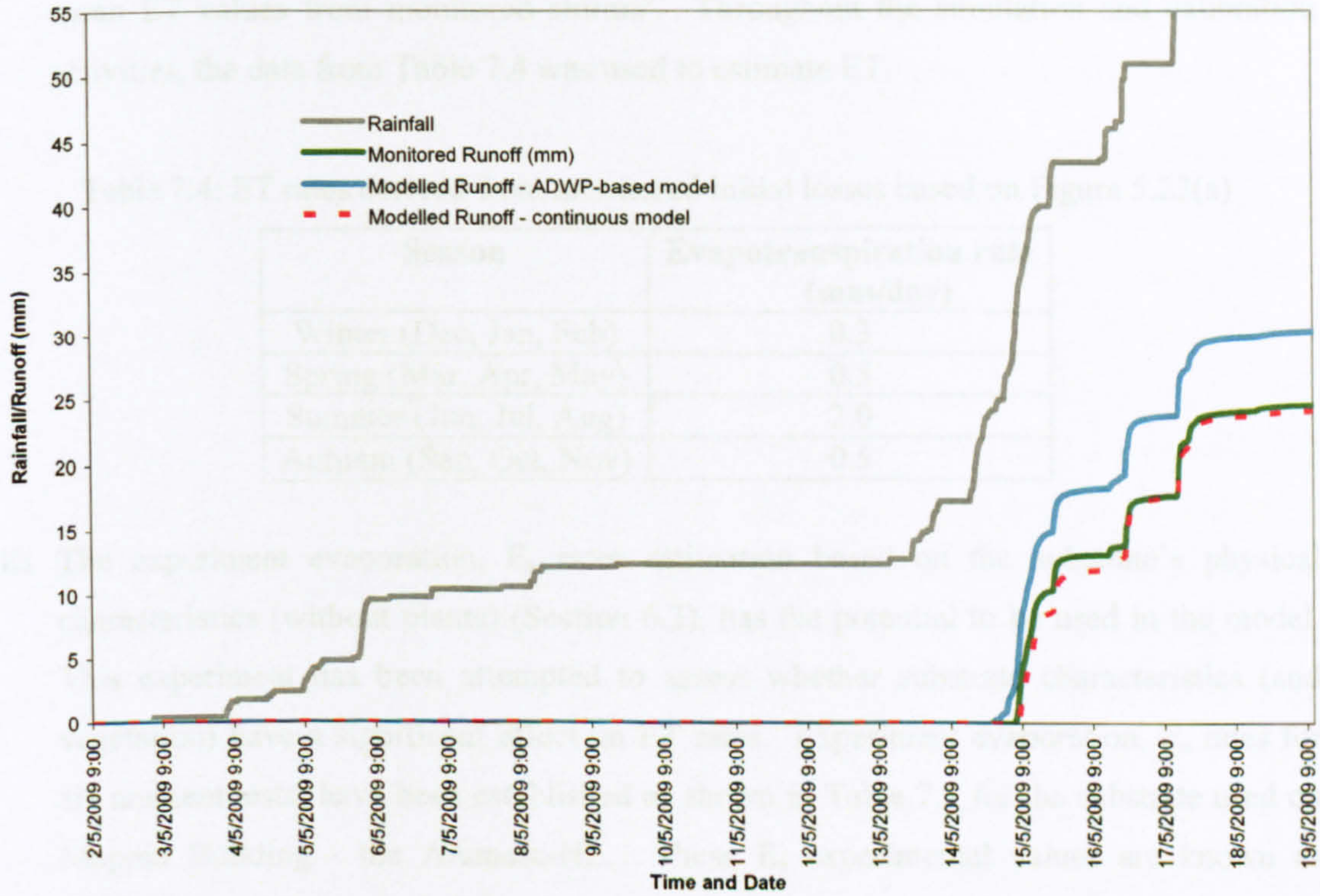


Figure 7.11: The cumulative rainfall and runoff profiles based on continuous model and ADWP-based

If the model is run in continuous simulation mode, no empirical rules are required; and the model continuously updates the amount of moisture as a function of rainfall, runoff and ET. ET is the critical parameter for describing the restoration of soil moisture retention capacity between storm events. The following section therefore examines alternative means for estimating the ET rate. Section 7.4 will investigate the validity of the model in continuous simulation mode.

### 7.3.2 Approaches to the Estimation of Evapotranspiration, ET

Two approaches to ET estimation have been discussed in Chapter 5 and Chapter 6; from the rainfall runoff monitoring data and experimental evaporation work:

i) ET rates derived from observed initial losses as a function of ADWP are shown in Figure 5.23 and Table 5.5. The ET rates from the 200 monitored storm events were divided into seasonal means, and it is expected that these values will represent the ET rates for each season (Table 7.1). This ET rate is plotted in Figure 5.23 as, 'Seasonal mean ET values from monitored storms'. Throughout the simulation and calibration activities, the data from Table 7.4 was used to estimate ET.

Table 7.4: ET rates derived from monitored initial losses based on Figure 5.23(a)

| Season | Evapotranspiration rate (mm/day) |
|---|---|
| Winter (Dec, Jan, Feb) | 0.3 |
| Spring (Mar, Apr, May) | 0.5 |
| Summer (Jun, Jul, Aug) | 2.0 |
| Autumn (Sep, Oct, Nov) | 0.5 |

ii) The experiment evaporation, $E_e$ rates estimation based on the substrate's physical characteristics (without plants) (Section 6.3), has the potential to be used in the model. This experiment has been attempted to assess whether substrate characteristics (and vegetation) have a significant effect on ET rates. Experiment evaporation, $E_e$ rates for six ambient tests; have been established as shown in Table 7.5 for the substrate used on Mappin Building - the Alumasc-HL. These $E_e$ experimental values are known as 'Experimental evaporation data'.

Table 7.5: The $E_e$ rates estimated from the experiment evaporation data

| Month of evaporation test | Average local temperature (°C) | Initial Ee rates (mm/day) |
|---|---|---|
| September 2008 | 16.5 | 1.17 |
| October - November 2008 | 8.1 | 0.50 |
| March – April 2009 | 10.4 | 2.32 |
| July - August 2009 | 18.7 | 0.89 |
| August 2009 | 18.0 | 2.39 |
| October 2009 | 10.4 | 0.46 |

Seasonal ET estimation rates can be estimated from a monitored system and known substrate characteristics, whereas experiment evaporation, $E_e$ is expected to be more useful than other estimations because it does not require the system to be monitored. In order to provide an alternative approach to quantify the initial loss parameter, especially for unmonitored green

roof systems, another two methods for identifying appropriate ET values have been also explored. These are the ET fitted estimations using model calibration (still based on monitored data) and ET estimation based on Thornthwaite formulae (for the unmonitored system). All expected ET estimation approaches have been gathered and compared in Section 7.3.2.3 as shown in Figure 7.13.

### 7.3.2.1 Data-based ET Fitted Estimation using Model Calibration

Another ET estimation from data-based approach uses the process of model calibration to back-calculate suitable ET values. Given that this process utilises the continuous data set, a large number of data points can be utilised, and calibration is feasible on a month-by-month basis.

Two alternative calibration approaches have been adopted. Initially the ET parameter was fitted on the basis that modelled runoff over the month should equate to the total observed runoff. However, in some instances (particularly when runoff totals were low) this approach generated suspiciously high ET values; together with poor correlations between the modelled and observed temporal profiles. As an alternative, the ET values were fitted based on the best fit of the temporal runoff profile. Generally this corresponded to the highest $R_t^2$ value; but in some cases this was further 'tuned' to ensure that runoff was predicted on days when it had been observed. Both methods are shown in Figure 7.13, defined as ET fitted runoff volume and ET fitted temporal profile respectively. The ET values determined from the temporal profile model fit were found to be comparable to those identified from the storm event ADWP analysis, ranging between 0.5 mm/day in winter months up to a maximum of 3.0 mm/day in May 2007. For the temporal profile-based ET estimates, no value has been determined in months where the total runoff fell below 15 mm.

### 7.3.2.2 Empirical Relationship for Generic ET Estimation

The data-based approaches outlined have provided useful indications of ET, but these estimates are not generic. The experiment evaporation analyses in Chapter 6 showed a significant effect from temperatures. Hence, the prediction of ET using existing hydrological formulae is explored. Thornthwaite's formula appears to be one of the simplest approaches, requiring only monthly mean temperature as an input. It is based on US measurements of potential evapotranspiration (PE) from short, close-set vegetation with an

adequate water supply. PE ($ET_{Th}$) for the particular month with average temperature, $t_n$ (°C) is given by (Wilson, 1990):

$$ET_{Th} = PE_x \frac{DT}{360} \text{ mm}; \quad PE_x = 16\left(\frac{10t}{J}\right)^a \text{ mm per month}; \quad J = \sum_{1}^{12} j \text{ (for the 12 months)}; \quad j = \left(\frac{t_n}{5}\right)^{1.514}$$

PE*x* is potential evapotranspiration for any month; D is the number of days in the month; T is the average number of hours between sunrise and sunset in the month; $a = (675 \times 10^{-9})J^3 - (771 \times 10^{-7})J^2 + 179 \times 10^{-4})J + 0.492$; J is the yearly 'heat index'; j is the monthly 'heat index', $t_n$ is the average monthly temperature of the consecutive of the year in °C.

Figure 7.12 compares the values estimated from local temperature data, using Thornthwaite's formula ($ET_{Th}$), with the two sets of fitted values ($ET_f$) derived from the continuous simulation model fits. There is a positive correlation between $ET_{Th}$ and $ET_f$, and this is particularly strong when the $ET_f$ value based on temporal profile is considered. The equation for the regression line suggests that a good estimate of the observed $ET_f$ values corresponds to 0.75 x $ET_{Th}$. This prediction is shown as 'ET modified Thornthwaite' in Figure 7.13.

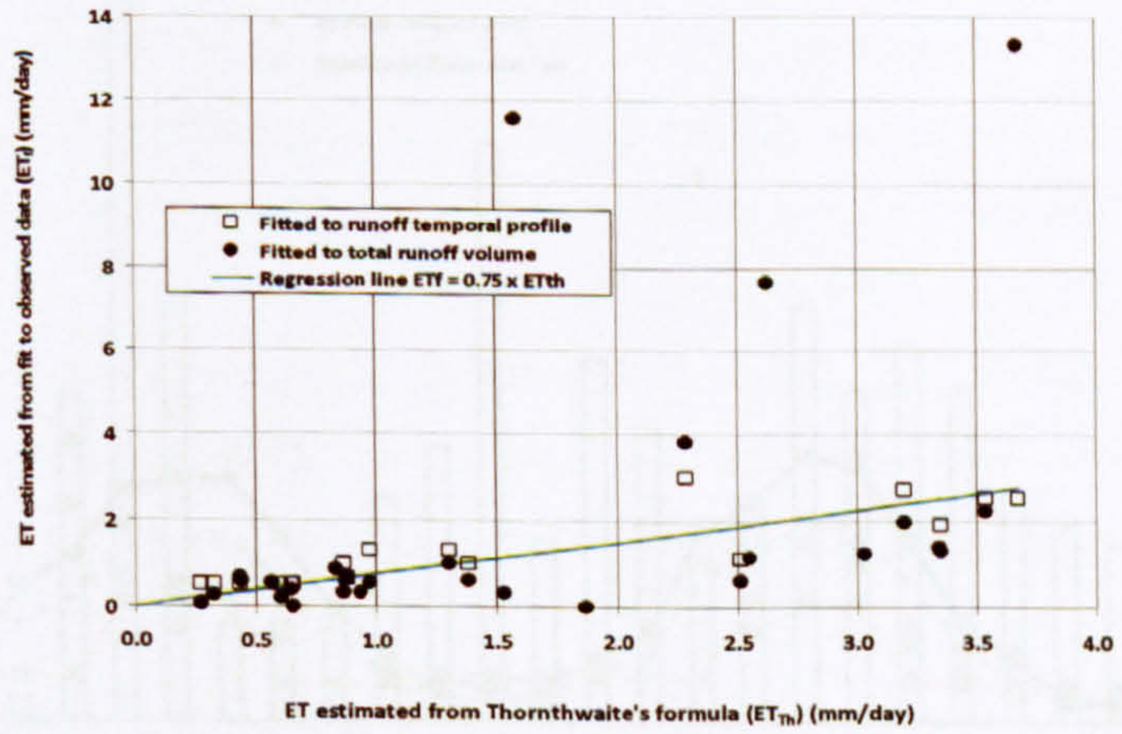


Figure 7.12: Positive correlation between fitted ET estimated from Thornthwaite's formula versus estimated from observed data

Wilson (1990) suggests that the Thornthwaite formula tends to over predict ET, but it would appear that there is potential to use a modified form of the Thornthwaite approach to generate suitable ET values from local climatic data. It is expected that the ET rates would be reduced on the green roof, due to the thin substrate and the low moisture requirements

associated with sedum vegetation. However, we would anticipate that the exact ET rates may require some further modification to account for the specific green roof substrate and vegetation characteristics.

### 7.3.2.3 Comparison of ET Estimation Methods

Figure 7.13 brings together the full set of ET estimations described above; Section 7.1.2, Section 7.3.1 and Section 7.3.2. Overall similar trends in all of the data sets are evident, and it may be concluded that the ET modified by Thornthwaite provides a good initial estimate for modelling purposes. This allows ET to be estimated using only local mean monthly temperature. The ET data determined through model fitting appears to be more consistent with other data sets when temporal profile rather than total runoff is used as the basis for calibration.

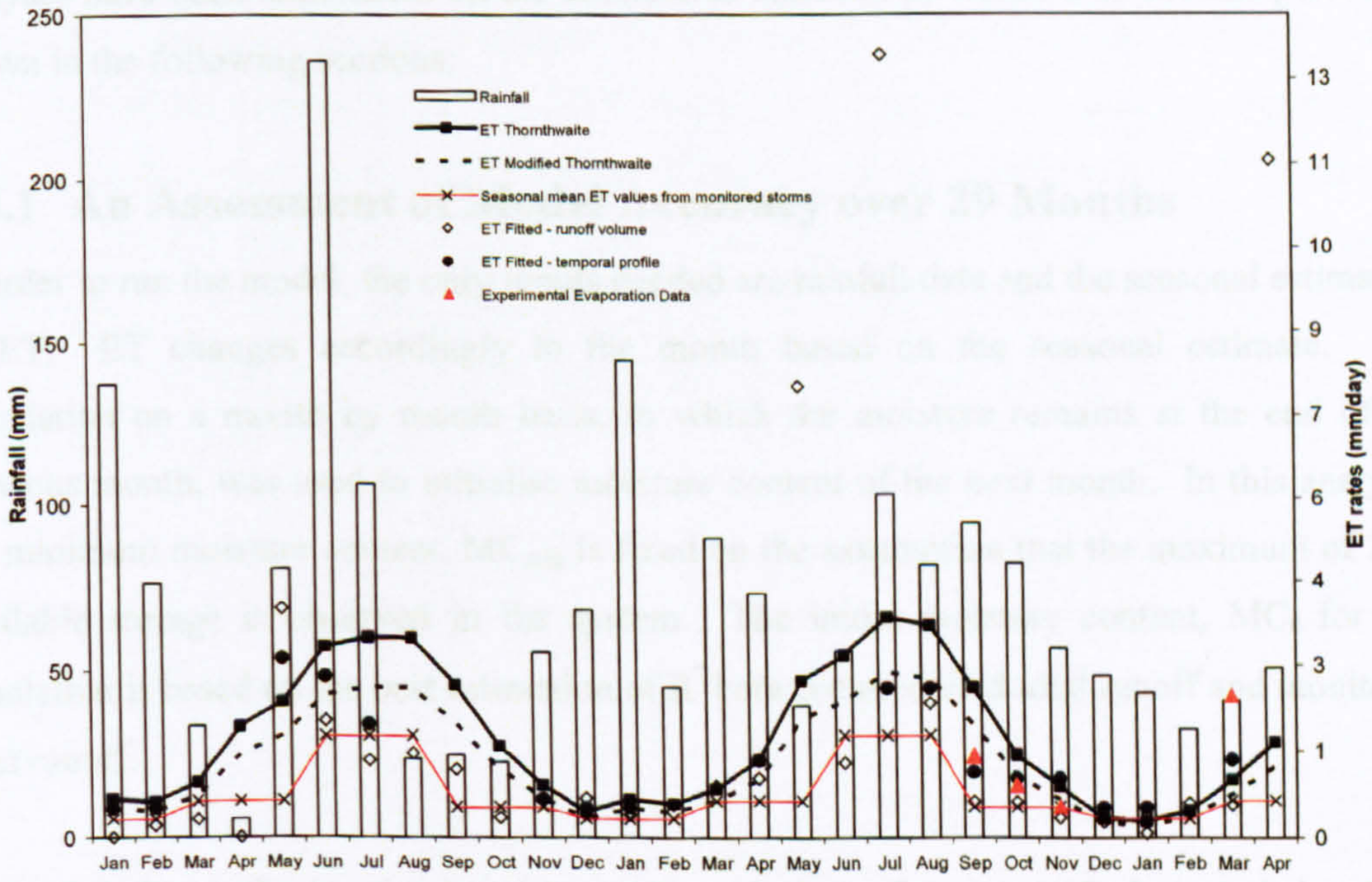


Figure 7.13: The comparison of ET estimation using four different methods

Analysis of long term continuous rainfall-runoff records from a test rig, installed with a commercial extensive green roof system, suggest that ET falls below 1 mm/day for much of the year under UK climatic conditions. The roof may require an antecedent dry weather period and ADWP considerably greater than one week to recover its full capacity.

There appears to be potential to adapt the Thornthwaite ET formula to provide monthly estimates from local temperature data. The development of a standardised laboratory test for ET should be enable differences resulting from substrate characteristics to be quantified, whereas long-term monitoring of test beds will be used to assess the combined effects of vegetation and substrate.

## 7.4 Model Validation – Continuous Simulation Mode

As discussed above, running the model in storm mode will require a value of $MC_0$ for each simulation. In real conditions, the substrate system/storage is expected to have an amount of moisture from the previous storm event, as a function of ET and ADWP. As shown in Figure 7.10, operating a continuous simulation over a long time-series of rainfall runoff events might result in better prediction. In order to test the model, using the default k and n values from storm event monitored data for storage routing coefficient; k = 100 and n = 3.5; analyses have been undertaken on the continuous simulations within a 29 months period, as shown in the following sections:

### 7.4.1 An Assessment of Model Accuracy over 29 Months

In order to run the model, the only inputs needed are rainfall data and the seasonal estimation of ET. ET changes accordingly to the month based on the seasonal estimate. The calculation on a month by month basis, in which the moisture remains at the end of the previous month, was used to initialise moisture content of the next month. In this analysis, the minimum moisture content, $MC_{min}$ is fixed on the assumption that the maximum of 25% available storage is observed in the system. The initial moisture content, $MC_0$ for this simulation is based on the best estimation of $R^2$ between modelled total runoff and monitored total runoff.

Table 7.6 shows the continuous data, as the whole performance of characteristic of the models, against that measured for a 29 month period. The total monitored runoff is 1021 mm and 1440 mm whilst the variation is 30% over 29 months. The $R_{tt}^2$ for the continuous simulation is 0.66 and examples of the simulations are shown in Figure 7.14. Figure 7.15 shows the condition of current storage in the system during simulation and Figure 7.16 shows the cumulative rainfall runoff profiles for the simulation.

The continuous simulation moisture storage is not assessed based on the $MC_0$ values (as used in storm mode) but on the ET rate. Therefore some understanding of characteristics relating to the storage system in each month was investigated further. For example in Table 7.6, a total rainfall of 5.6 mm occurred in April 2007 where it should be assumed with less moisture, the available storage in the system could be increased. However; due to the April weather of low temperature with humid climatic conditions, an ET rate of 0.5 mm/day discovered from the mean seasonal monitored data was used. In real conditions, the ET rate could be higher due to sunny intervals and the early growth of vegetation in spring time. However both thermal and vegetation factors are not going to be investigated in detail in this preliminary model.

Following these expected factors, the moisture reduction in the system during April 2007 exhibited a slow loss rate and the system was left half saturated at the end of the month. The remaining moisture at the end of April 2007 was used to initialise the moisture content for May 2007 simulation (storage available for May 2007). By prediction, with this storage available and the occurrence of May 2007 storm events, runoff production occurred earlier than that monitored (as shown in Figure 7.14(d)). In real conditions, with 11 mm of available storage, the occurrence of rainfall, with much delayed runoff production, again, emphasising the ET rate usage; should be higher. This might also suggest that the seasonal mean ET rates from the monitored data might not be suitable and therefore the monthly mean might be more suitable.

Table 7.6: The 29 months continuous simulation mode; k = 100, n = 3.5 and $MC_{min}$ = 25% by volume

| Date | Rainfall P (mm) | Runoff R (mm) | ET rate (mm/day) | $MC_o$ (%) | Initial available storage (mm) | Modelled total runoff (mm) | Monitored retention (%) | Modelled retention (%) | Goodness of fit, $R_t^2$ |
|---|---|---|---|---|---|---|---|---|---|
| Jan-2007 | 137.2 | 124.7 | 0.3 | 43.00 | 6.0 | 124.5 | 9.1 | 9.3 | 0.946 |
| Feb-2007 | 75.2 | 56.0 | 0.3 | 47.24 | 2.0 | 64.7 | 25.5 | 14.0 | 0.831 |
| Mar-2007 | 37.4 | 13.9 | 0.5 | 49.88 | 0.0 | 23.1 | 63.0 | 38.3 | 0.798 |
| Apr-2007 | 5.6 | 0.0 | 0.5 | 48.42 | 1.0 | 0.0 | 100.0 | 100.0 | 0.000 |
| May-2007 | 80.2 | 16.9 | 0.5 | 36.70 | 11.0 | 55.0 | 78.9 | 31.5 | -2.088 |
| Jun-2007 | 236.2 | 182.8 | 2.0 | 48.88 | 1.0 | 177.6 | 22.6 | 24.8 | 0.984 |
| July-2007 | 106.8 | 58.5 | 2.0 | 49.70 | 0.0 | 55.0 | 45.3 | 48.5 | 0.916 |
| Aug-2007 | 23.6 | 0.0 | 2.0 | 36.95 | 10.0 | 0.0 | 100.0 | 100.0 | 0.000 |
| Sep-2007 | 24.6 | 0.0 | 0.5 | 25.00 | 20.0 | 0.0 | 100.0 | 100.0 | 0.000 |
| Oct-2007 | 22.6 | 0.0 | 0.5 | 46.32 | 3.0 | 8.7 | 100.0 | 61.6 | -21730.1 |
| Nov-2007 | 55.2 | 29.1 | 0.5 | 44.97 | 4.0 | 36.3 | 47.3 | 34.3 | 0.771 |
| Dec-2007 | 67.8 | 32.8 | 0.3 | 49.91 | 0.0 | 58.9 | 51.6 | 13.1 | 0.109 |
| Jan-2008 | 145.0 | 73.5 | 0.3 | 49.50 | 0.0 | 135.3 | 49.3 | 6.7 | 0.337 |
| Feb-2008 | 45.0 | 13.7 | 0.3 | 49.99 | 0.0 | 36.4 | 69.5 | 19.1 | -0.591 |
| Mar-2008 | 90.0 | 47.7 | 0.5 | 48.84 | 1.0 | 73.6 | 47.0 | 18.2 | 0.678 |
| Apr-2008 | 73.0 | 29.7 | 0.5 | 49.95 | 0.0 | 58.2 | 59.3 | 20.2 | 0.588 |
| May-2008 | 39.2 | 1.9 | 0.5 | 49.66 | 0.0 | 24.5 | 95.1 | 37.5 | -26.93 |
| Jun-2008 | 55.4 | 7.4 | 2.0 | 48.67 | 1.0 | 18.0 | 86.6 | 67.5 | 0.514 |
| July-2008 | 103.8 | 13.8 | 2.0 | 37.81 | 10.0 | 32.4 | 86.7 | 68.8 | -1.555 |
| Aug-2008 | 81.8 | 21.8 | 2.0 | 49.61 | 0.0 | 29.2 | 73.4 | 64.4 | 0.763 |
| Sep-2008 | 94.8 | 61.0 | 0.5 | 37.91 | 10.0 | 70.1 | 35.6 | 26.0 | 0.921 |
| Oct-2008 | 82.6 | 48.3 | 0.5 | 50.0 | 0.0 | 67.5 | 41.5 | 19.3 | 0.849 |
| Nov-2008 | 56.2 | 31.1 | 0.5 | 49.47 | 0.0 | 43.9 | 44.6 | 21.8 | 0.693 |
| Dec-2008 | 48.2 | 38.6 | 0.3 | 46.05 | 3.0 | 38.9 | 19.9 | 19.4 | 0.945 |
| Jan-2009 | 43.2 | 30.1 | 0.3 | 46.10 | 3.0 | 32.0 | 30.2 | 25.9 | 0.842 |
| Feb-2009 | 32.4 | 27.9 | 0.3 | 48.44 | 1.0 | 25.9 | 13.7 | 20.2 | 0.177 |
| Mar-2009 | 40.8 | 11.7 | 0.5 | 46.11 | 3.0 | 23.9 | 71.2 | 41.5 | 0.395 |
| Apr-2009 | 27.60 | 8.77 | 0.5 | 47.88 | 2.0 | 34.1 | 92.8 | 32.7 | -3.526 |
| May-2009 | 84.2 | 35.0 | 0.5 | 49.80 | 0.0 | 34.1 | 58.5 | 59.5 | 0.882 |

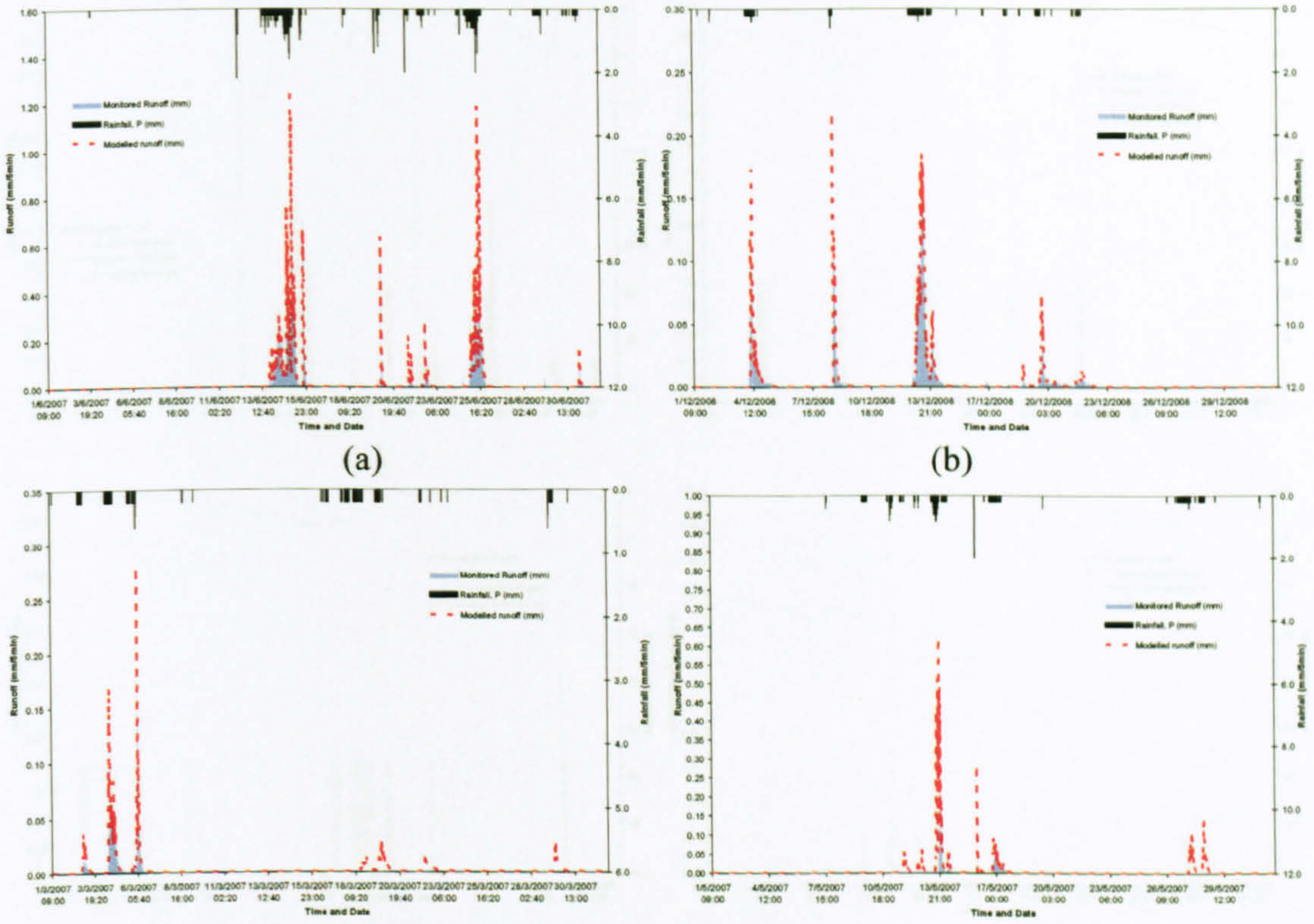


Figure 7.14: The example of longer continuous simulation in (a) June 2007 (b) December 2007 (c) March 2007 (d) May 2007

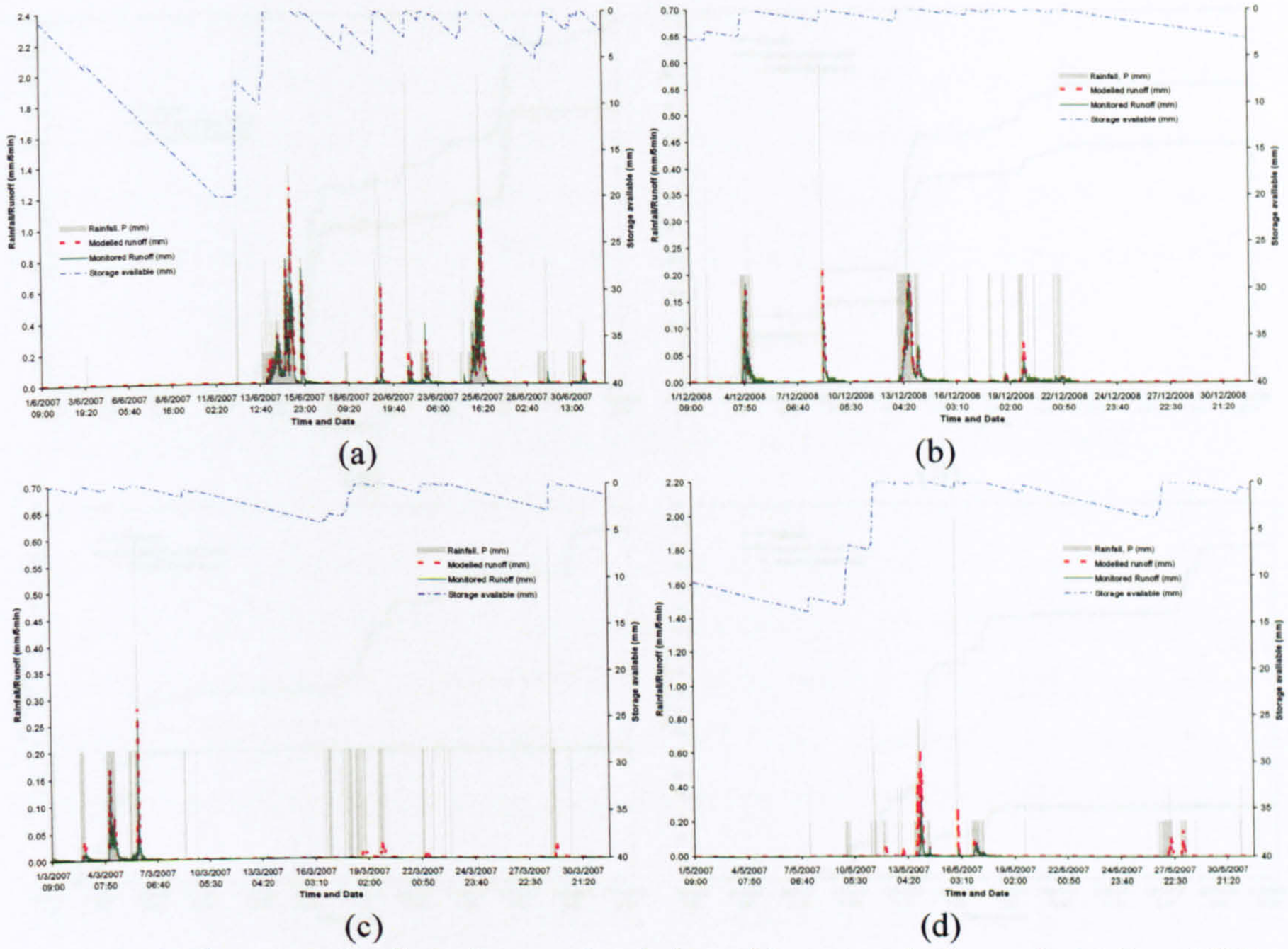


Figure 7.15: The example of continuous simulation with storage indicator in (a) June 2007 (b) December 2007(c) March 2007 (d) May 2007

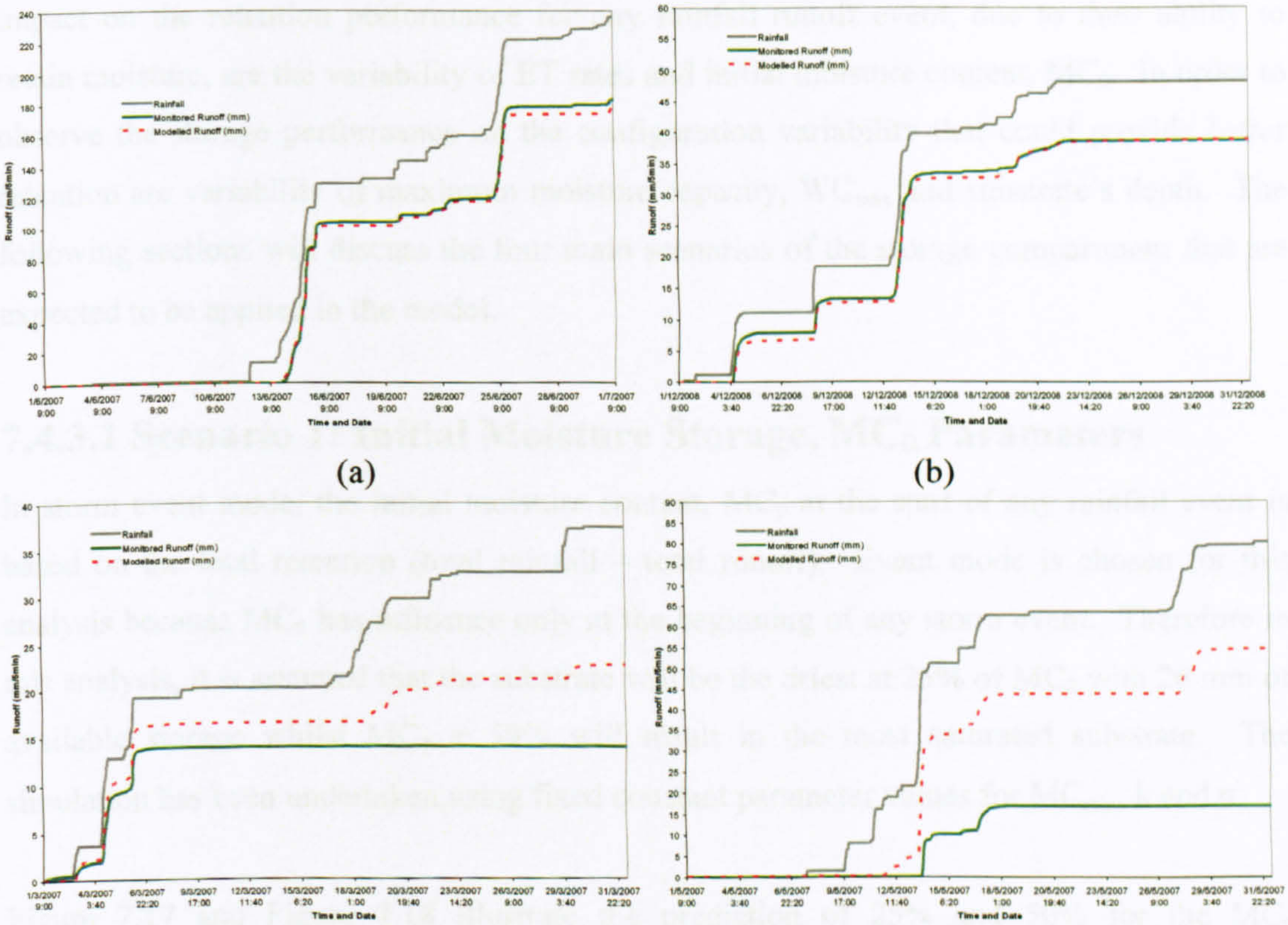


Figure 7.16: The example of cumulative profiles of rainfall, runoff and modelled runoff in (a) June 2007 (b) December 2007 (c) March 2007 (d) May 2007

In summation, the simple model performed relatively well in predicting the continuous simulation. In terms of their goodness of fit, $R_t^2 = 0.66$ might be the result of ET being used and were not particularly well represented. Some of the simulation can be well fitted to the events and some prediction required improvement. It is expected that if a better estimation of ET is used, the model will perform better. It can also be suggested that the Thornthwaite approach could be the best option for ET rates estimation; because it is directly related to the monthly local temperature. The analysis will be carried out in the next conference paper.

## 7.4.2 Model Application – Scenario Analysis

As the aim of this study is to develop a generic model, the model has been setup so that the system can be varied – in terms of parameter values. At this stage of the preliminary model development, there is no attempt to understand the system characteristic on the outflow vertically (i.e. k and n), yet, during this modelling only parameters that reflect the storage/retention capability have been adjusted. The critical parameters that expected to give

impact on the retention performance for any rainfall runoff event, due to their ability to retain moisture, are the variability of ET rates and initial moisture content, $MC_0$. In order to observe the storage performance on the configuration variability that could provide better retention are variability of maximum moisture capacity, $WC_{max}$ and substrate's depth. The following sections will discuss the four main scenarios of the storage compartment that are expected to be applied in the model.

### 7.4.3.1 Scenario 1: Initial Moisture Storage, $MC_0$ Parameters

In storm event mode, the initial moisture content, $MC_0$ at the start of any rainfall event is based on the total retention (total rainfall – total runoff). Event mode is chosen for this analysis because $MC_0$ has influence only at the beginning of any storm event. Therefore in this analysis, it is assumed that the substrate will be the driest at 25% of $MC_0$ with 20 mm of available storage whilst $MC_0$ = 50% will result in the most saturated substrate. The simulation has been undertaken using fixed constant parameter values for $MC_{min}$, k and n.

Figure 7.17 and Figure 7.18 illustrate the prediction of 25% and 50% for the $MC_0$ assumption with delayed and less runoff at the beginning of storm event for full available storage (Figure 7.17(a). Whilst for saturated substrate, an early and excessive runoff occurs at the beginning of the storm event as shown in Figure 7.18(a). Figure 7.17 (b) provides the cumulative profile of modelled runoff slightly lower than the monitored runoff. Figure 7.18(b) illustrates a similar modelled runoff as rainfall profile. This describes the early excessive runoff part and represents total retention of the event.

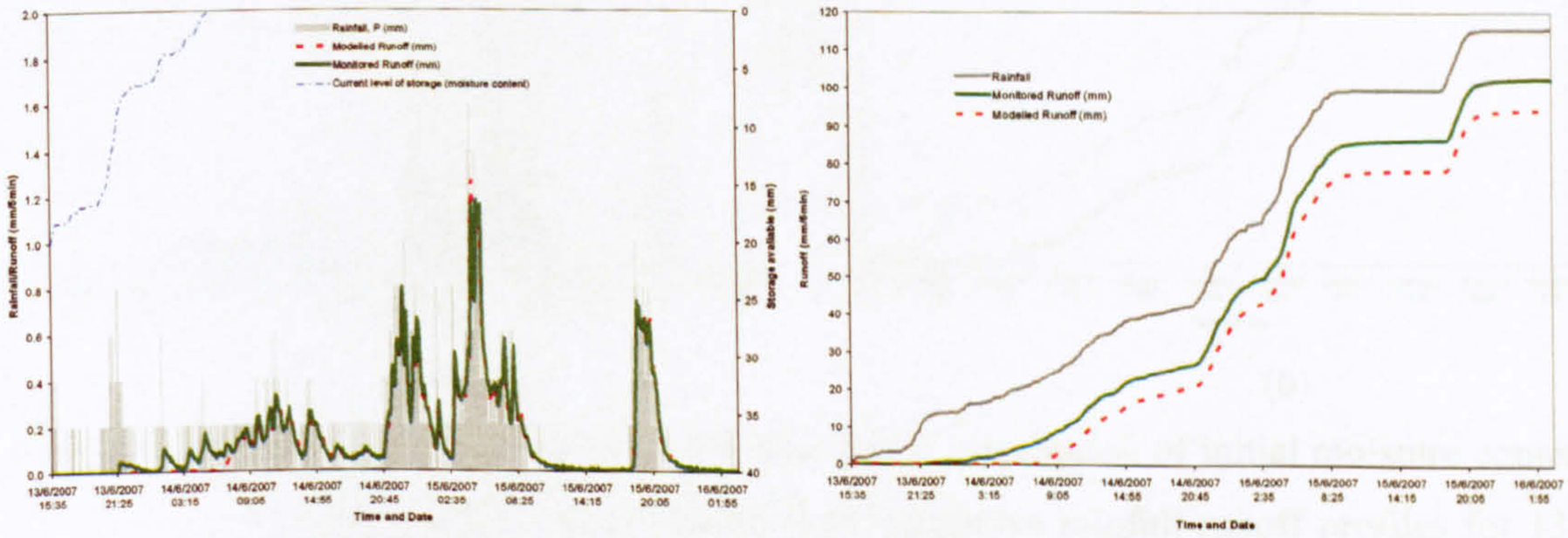


(a) (b)

Figure 7.17: (a) Model results for 13 – 16 June 2007; assumption of initial moisture content at 25%; (b) Cumulative rainfall runoff profiles for 13 - June 2007

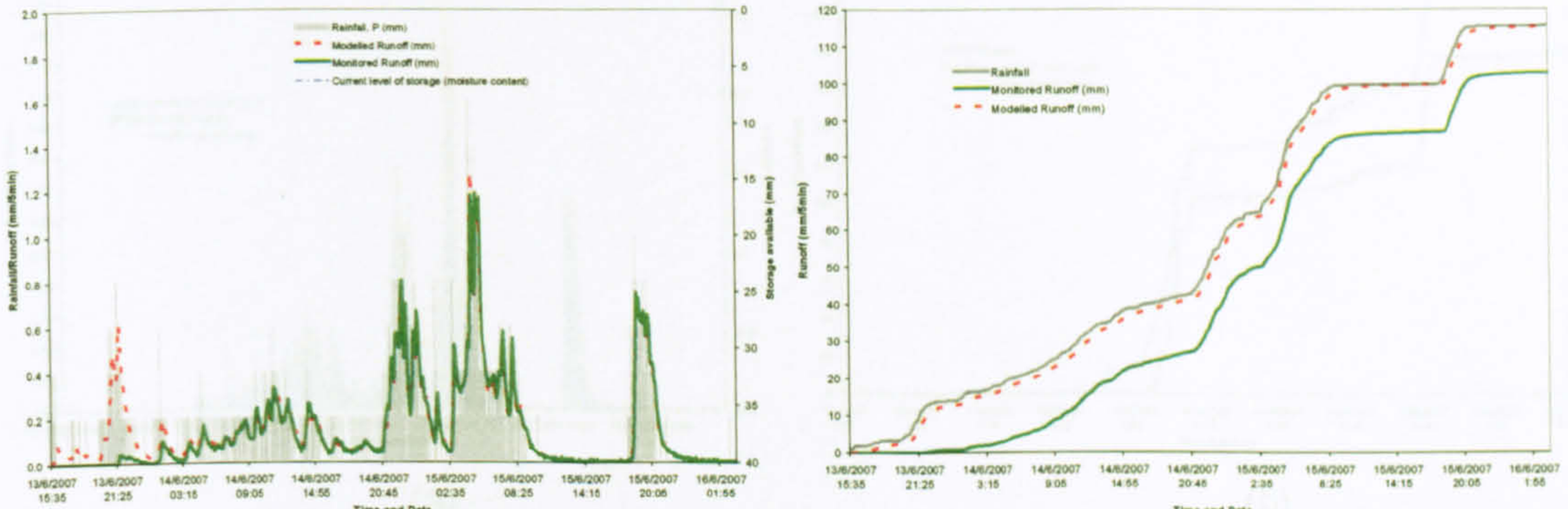


(a) (b)

Figure 7.18: (a) Model results for 13 – 16 June 2007; assumption of initial moisture content at 50% (b) Cumulative rainfall runoff profiles for 13 - June 2007

Using the best assumption for $MC_0$ (total rainfall – total runoff) for event mode, Figure 7.19 then illustrates the best simulation for both example events. The cumulative profiles clarify the same performance of both modelled and monitored runoff. Figure 7.20 shows the longer continuous (29 months duration) simulation with ET rate = 2.0 mm/day. This has similar simulation for the same event and the modelled runoff profile can still simulate the monitored runoff profile very well, until the end of month (Figure 7.20(b)) but with a slightly early runoff occurring.

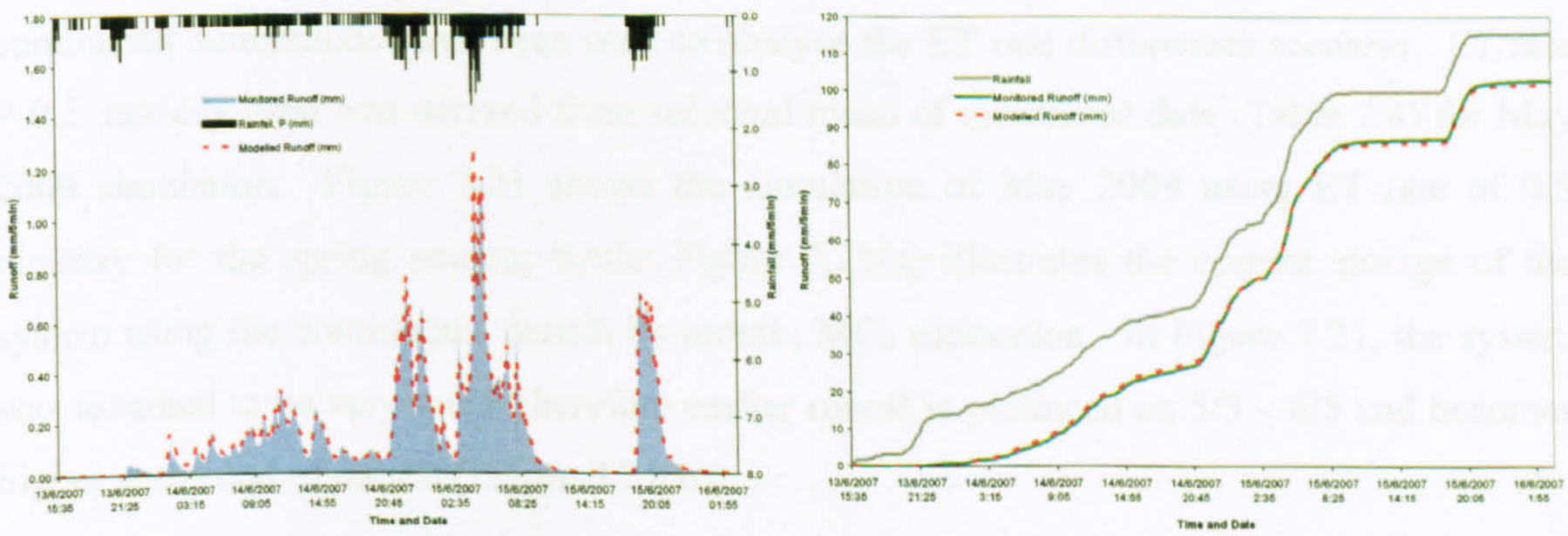


(a) (b)

Figure 7.19: (a) Model results for 13 – 16 June 2007; assumption of initial moisture content = total rainfall – total runoff; (b) Cumulative rainfall runoff profiles for 13 - June 2007

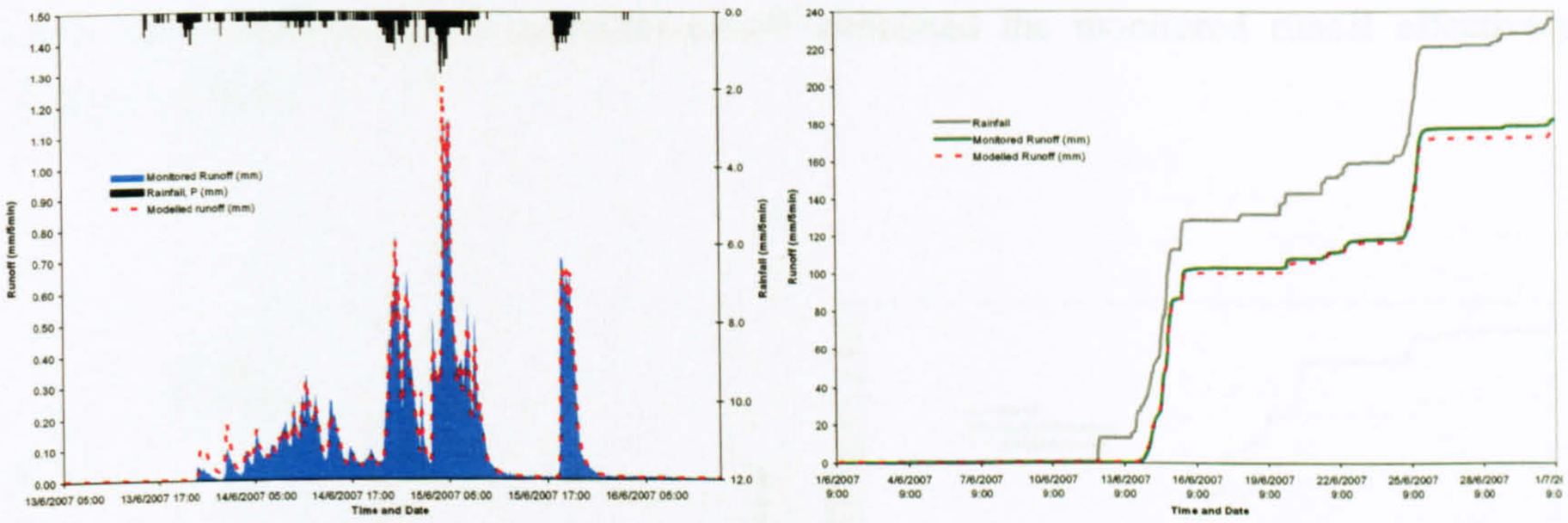


(a) (b)

Figure 7.20: (a) Close up modelled event for 13 – 16 June 2007 from June 2007 simulation; assumption of initial moisture content based on previous month (May 2007) last moisture condition (b) Cumulative rainfall runoff profiles for the whole month of June 2007

This analysis demonstrates that with the right amount of $MC_0$ for each storm following substrate condition, the model can predict storms very well. During continuous simulation, the roles of ET rates will be critical in order to describe the condition of the system for the whole simulation.

### 7.4.3.2 Scenario 2: Different ET Rates

In event simulation mode, no ET rate is considered for its initial losses, therefore both of the continuous simulations have been used to analyse the ET rate differences scenario. ET rate = 0.5 mm/day used was derived from seasonal mean of monitored data (Table 7.4) for May 2009 simulation. Figure 7.21 shows the simulation of May 2009 using ET rate of 0.5 mm/day for the spring season; whilst Figure 7.21(a) illustrates the current storage of the system using the continuous, month by month, $MC_0$ estimation. In Figure 7.21, the system was assumed to be very moist therefore earlier runoff is produced on 5/5 – 6/5 and becomes higher at the end of month (Figure 7.21(b)).

The ET rate has been recognised to play the main role in this matter. In Figure 7.22, still using the continuous simulation from Figure 7.21 for $MC_0$, best estimation of modelled runoff to the total monitored runoff is also used to estimate the best estimation ET = 2.2 mm/day. Therefore higher ET rate does increase the storage availability of saturated system within few dry days; runoff appears as monitored from the beginning until the end of the

event and cumulative total modelled runoff simulated the monitored runoff effectively (Figure 7.22(b)).

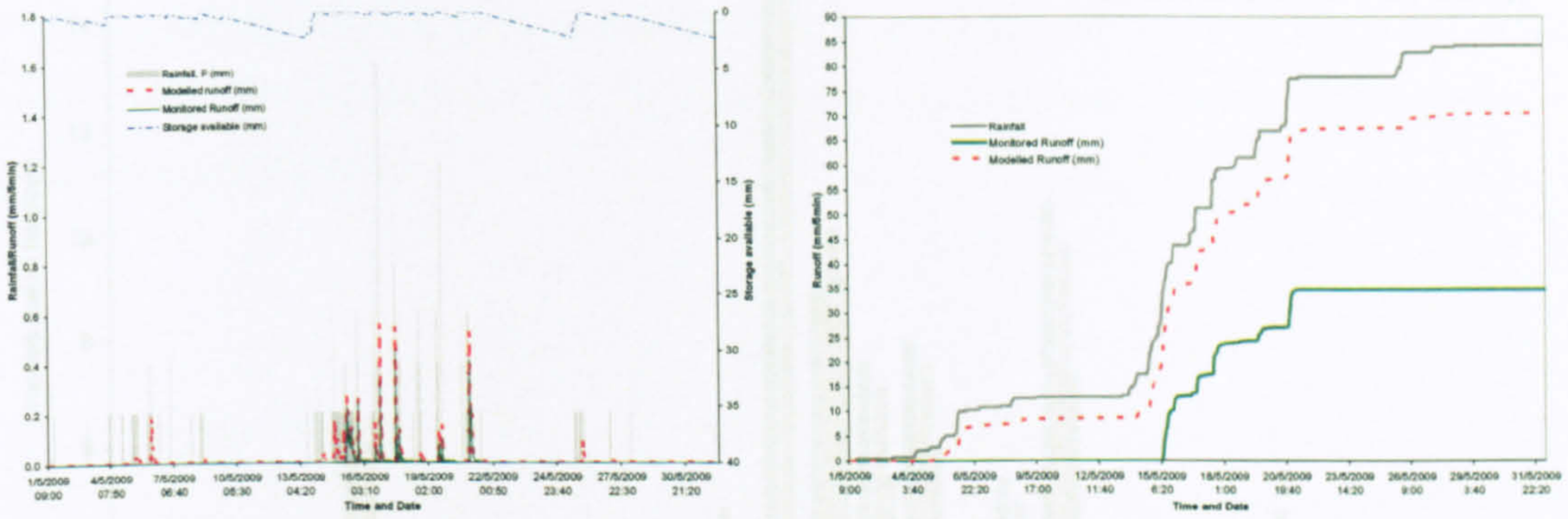


(a) (b)

Figure 7.21: (a) Model simulation for May 2009 using continuous $MC_0$ estimation with ET = 0.5 mm/day; (b) Cumulative rainfall runoff profiles for May 2009

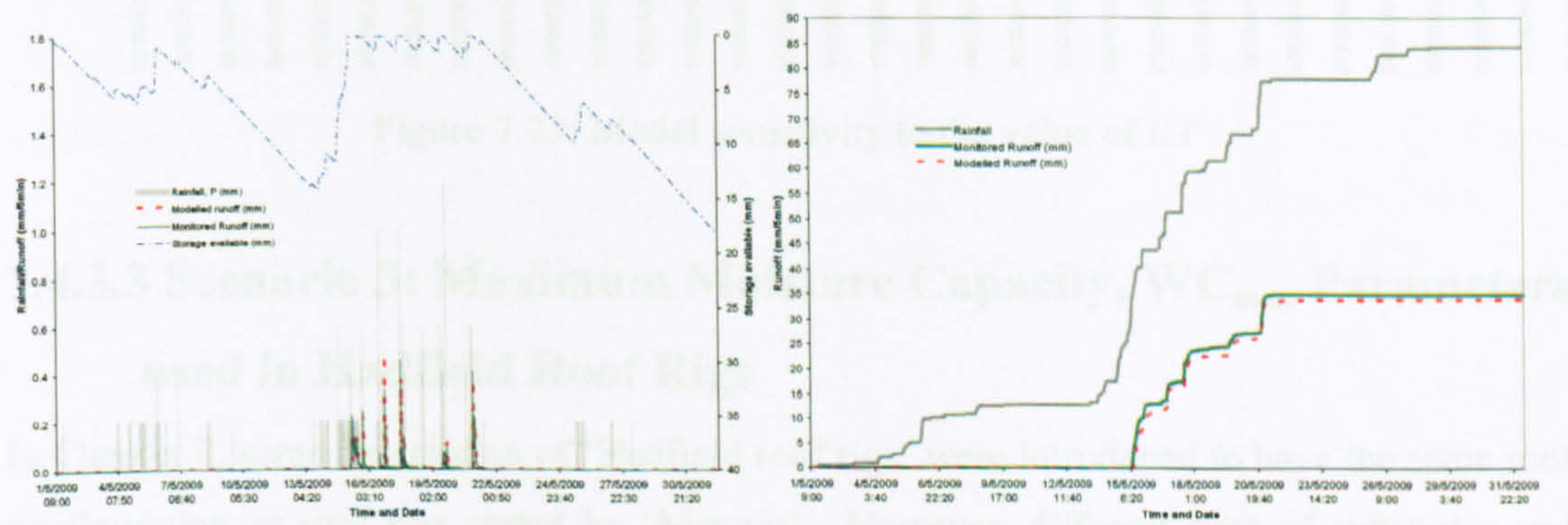


(a) (b)

Figure 7.22: (a) Model simulation for May 2009 using continuous $MC_0$ estimation with ET = 2.2 mm/day (b) Cumulative rainfall runoff profiles for May 2009

Figure 7.23 illustrates the sensitivity of monthly performance predictions for the correct identification of ET. It shows daily totals for rainfall, measured runoff, and modelled runoff; assuming ET rates from the seasonal mean of monitored data, 0.5 mm/day and the best estimation of 2.2 mm/day. Modelled runoff from ET rate of 0.5 mm/day significantly overestimates, by 50%, the total runoff over the period and also fails to retain the rainfall at all during 5 – 9 May and 26 – 28 May 2009. However, the 2.2 mm/day ET rate model was also slightly underestimated by 3% and simulated the current event storage very well.

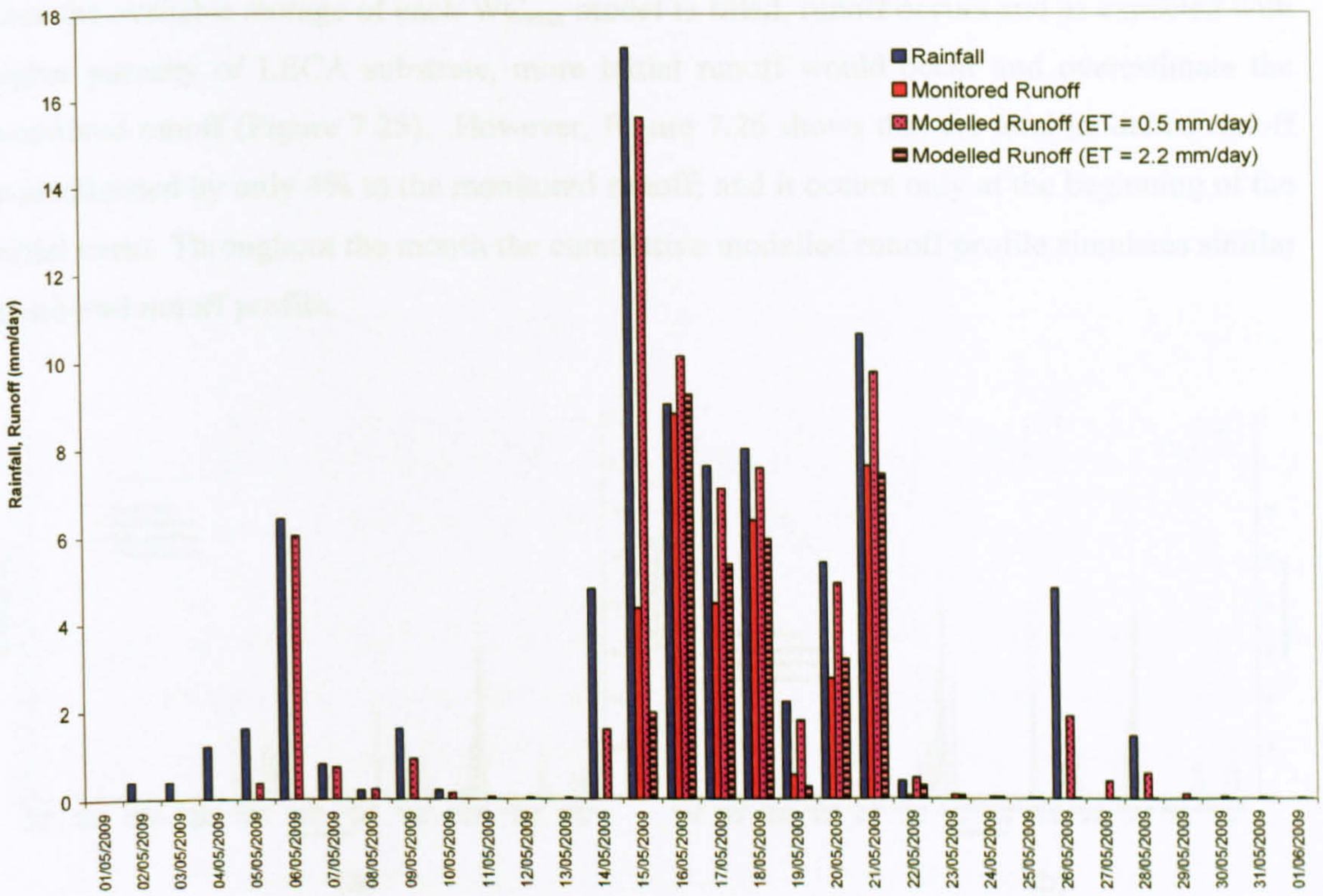


Figure 7.23: Model sensitivity to the value of ET

### 7.4.3.3 Scenario 3: Maximum Moisture Capacity, $WC_{max}$ Parameters used in Hadfield Roof Rigs

In Chapter 4, some description of 'Hadfield roof rigs' were introduced to have the same roof configuration as roof rigs stated by 'Mappin'. However, different type of substrates and vegetation were described. The model is expected to predict the same parameters of a green roof system but with different values due to their substrate characteristics, vegetation and climatic condition. The FLL tests on the Hadfield substrates showed that the LECA-based material exhibited an extremely low value of $WC_{max}$, at just 16%. It is assumed that this would result in significantly reduced retention when compared with the Mappin test rig substrate's $WC_{max}$ of 50%. This scenario will therefore consider the sensitivity of runoff profile to the value of $WC_{max}$. To model this scenario, all the parameters used were constant except for the $WC_{max}$.

Figure 7.24 compares the current storage available in the system between 16% and 30% of $WC_{max}$. Both systems by volume can only hold between 8% (6 mm) and 15% (12 mm)

maximum retention respectively compared with 20 mm in the monitored systems. Therefore once the available storage of each $WC_{max}$ model is filled, runoff occurs and as expected with higher porosity of LECA substrate, more initial runoff would occur and overestimate the monitored runoff (Figure 7.25). However, Figure 7.26 shows that the total modelled runoff overestimated by only 4% to the monitored runoff; and it occurs only at the beginning of the initial event. Throughout the month the cumulative modelled runoff profile simulates similar monitored runoff profile.

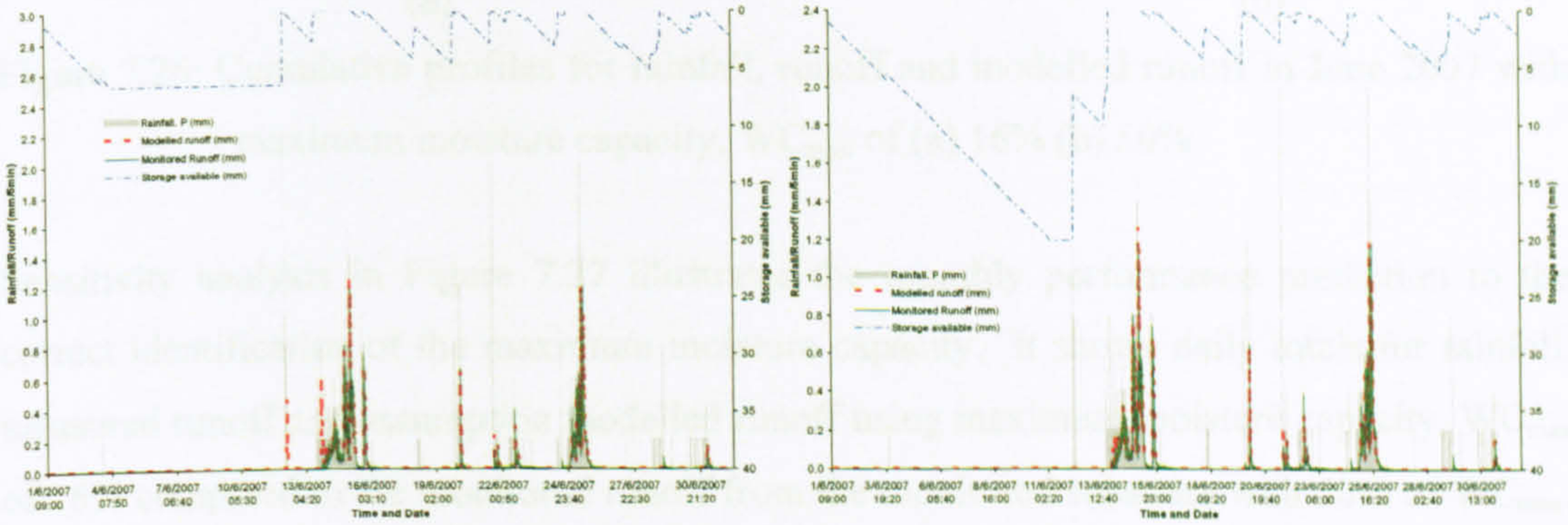


Figure 7.24: Model simulation for June 2007 with storage indicator using continuous simulation with maximum moisture capacity, $WC_{max}$ of; (a) 16% (b) 50%

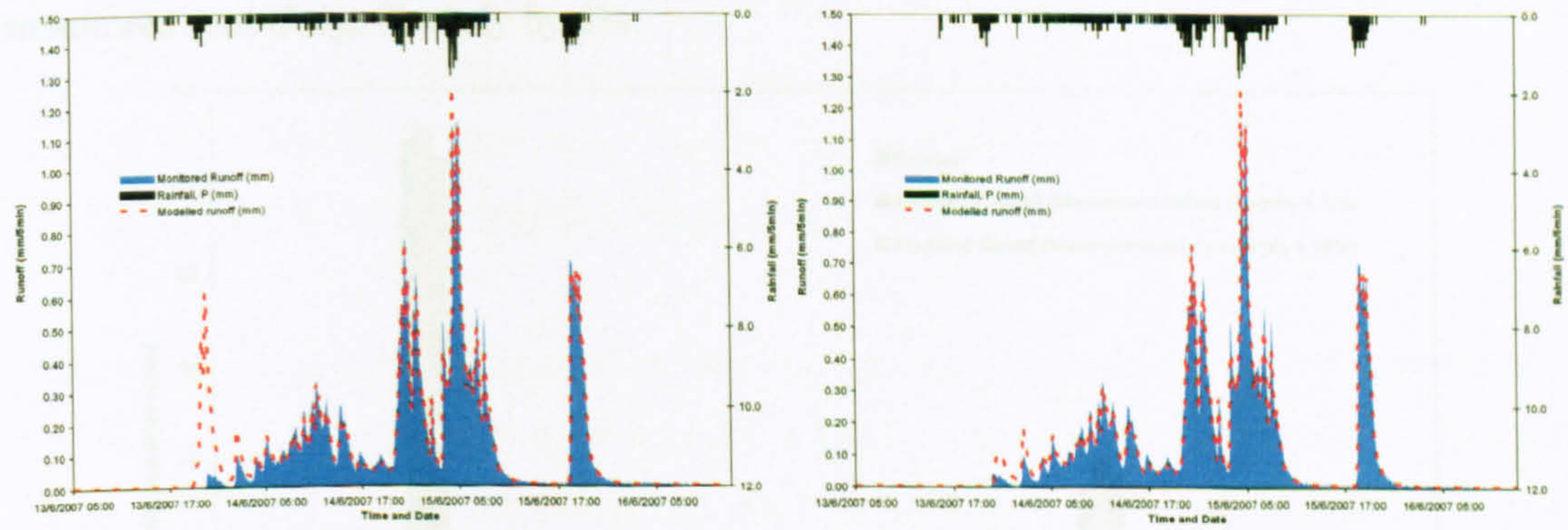


Figure 7.25: Model simulation for 13 – 16 June 2007 of June 2007 under longer continuous simulation with maximum moisture capacity, $WC_{max}$ of (a) 16% (b) 50%

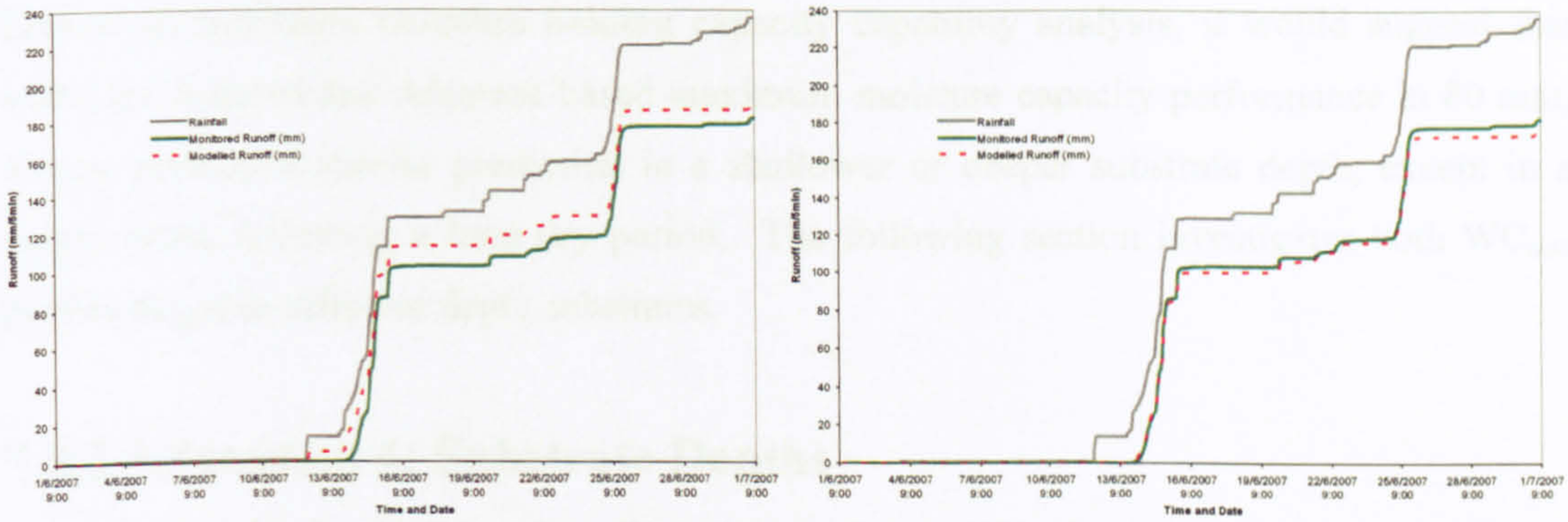


Figure 7.26: Cumulative profiles for rainfall, runoff and modelled runoff in June 2007 with maximum moisture capacity, $WC_{max}$ of (a) 16% (b) 50%

Sensitivity analysis in Figure 7.27 illustrates the monthly performance prediction to the correct identification of the maximum moisture capacity. It shows daily totals for rainfall, measured runoff and assumption modelled runoff using maximum moisture capacity, $WC_{max}$ of 16% compared to the monitored runoff from the monitored substrate with 50% of $WC_{max}$. The prediction suggests that although less $WC_{max}$ use is expected to have excessive runoff production; Figure 7.32 demonstrates that daily total rainfall still can be retained by both of the model systems with total modelled runoff from 16% $WC_{max}$ the model overestimated the monitored runoff significantly by 4%.

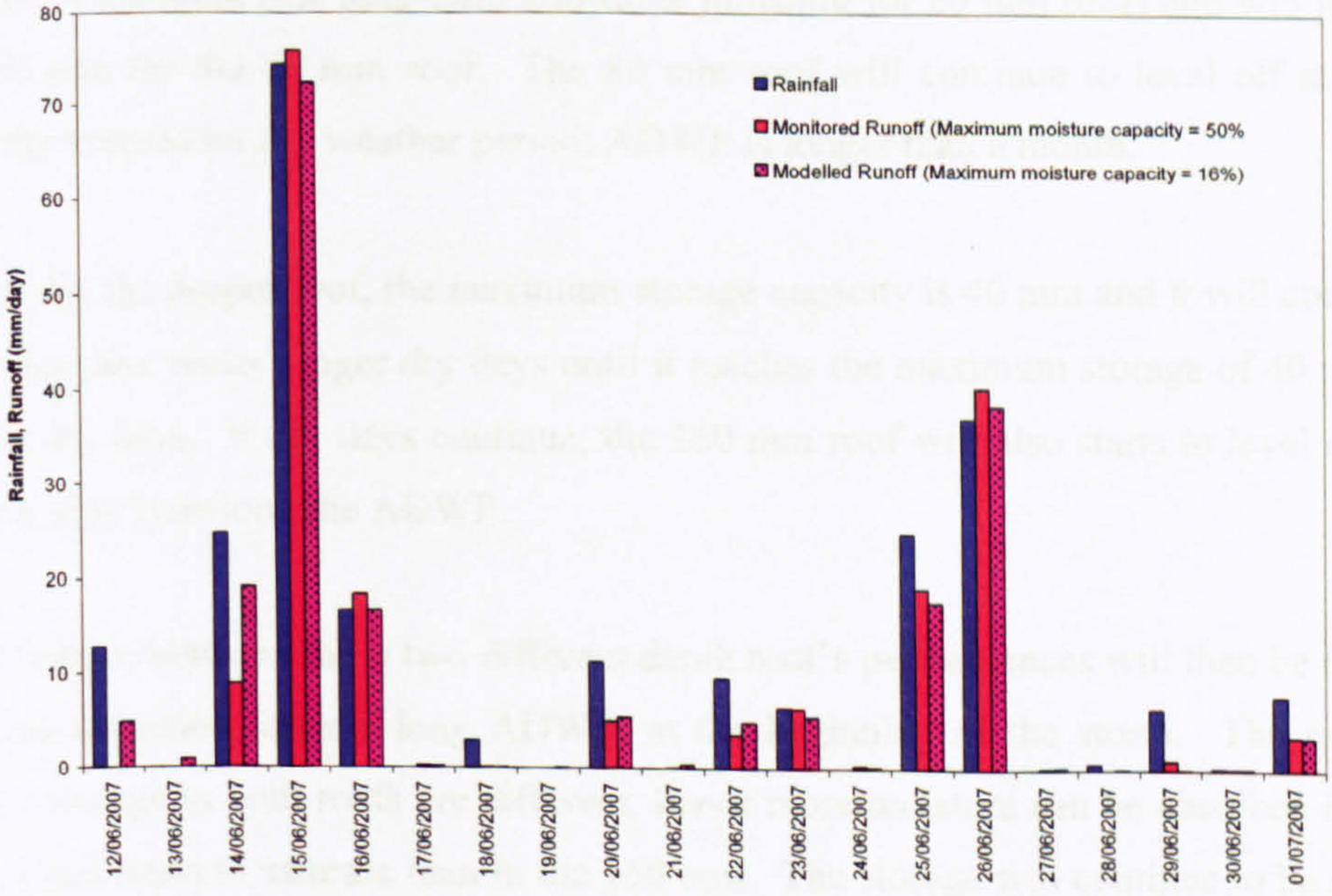


Figure 7.27: Model sensitivity to the value of $WC_{max}$

Following maximum moisture holding capacity capability analysis, it would suggest that with LECA-based and Alumasc-based maximum moisture capacity performance in 80 mm, it may perform a similar prediction in a shallower or deeper substrate depth, except in a single event, following a long dry period. The following section investigates both $WC_{max}$ performances in different depth substrates.

### 7.4.3.4 Scenario 4: Substrate Depths

It is expected that by doubling the substrate's depth to 160 mm it could retain more moisture from the monitored rig depth. This can be observed further in Figure 7.28 wherein the substrate with maximum moisture content, $WC_{max}$ = 50% under 80 mm (40 mm of moisture depth) is compared to a deeper depth at 160 mm. The assumption of minimum moisture content, $MC_{min}$ as being 25% has therefore become 20 mm of maximum storage available. Therefore, for a deeper roof with, $WC_{max}$ = 50% under 160 mm, become 80 mm of maximum available storage. The depth of $MC_{min}$ is also doubling as being 40 mm (of 40 mm maximum storage available).

Based on Figure 7.27, it is assumed that the system is saturated with a constant ET rate in both cases of 2 mm/day. Therefore it is expected that after 10 dry days, the moisture from the system will have lost at least 20 mm (10 days x 2 mm/day). It will therefore be reached at 20 mm of moisture (the long-term allowable moisture for 80 mm roof) and will just level off at 20 mm for the 80 mm roof. The 80 mm roof will continue to level off at 20 mm though the antecedent dry weather period; ADWP is longer than a month.

However for the deeper roof, the maximum storage capacity is 40 mm and it will continually lose its moisture under longer dry days until it reaches the maximum storage of 40 mm with about 20 dry days. If dry days continue, the 160 mm roof will also starts to level off at 40 mm, no matter how long the ADWP.

This difference between these two different depth roof's performances will then be observed under this condition (after a long ADWP) at the beginning of the storm. The maximum available storage in both roofs are different, hence more moisture can be absorbed in the 80 mm roof and starts to saturate than in the 160 mm. The storage will continue to be different in both cases until some extreme event occurs or during wetter months.

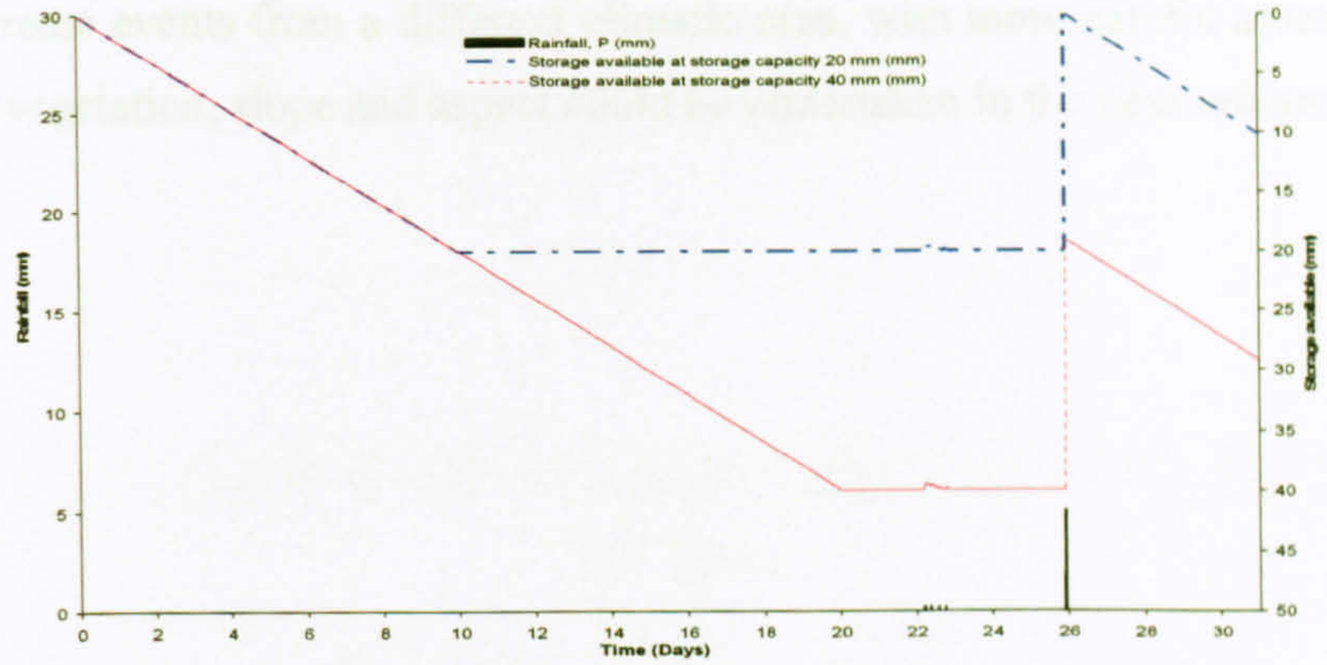


Figure 7.28: The assumption storage performance in the 80 mm and 160 mm substrate depths

## 7.5 Conclusion

Modelling activities discussed in this chapter have provided a better understanding of factors and relationships controlling the retention and detention performance. These activities also present the relationship between parameters used in the model such as moisture content parameters ($MC_{min}$, $MC_0$); substrate property ($WC_{max}$); substrate configuration (depth) and climatic variables (ADWP, ET rates) all of which represent the characteristics of the real green roof condition. Climatic variables such as type of design storm can be further investigated. It is felt that this preliminary model based on the Flood Studies Report (FSR, Volume II, Meteorology) (Wilson, 1990) June 2007 event and comparable to a 1 in 100 year return period rainfall event in the Sheffield area should be sufficient.

The conceptual model outlined has shown that the retention model can be determined from generic roof configuration characteristics (substrate depth and maximum moisture capacity, $WC_{max}$) and local climatic input data (rainfall, temperature for ET). However, the component of the detention model might requires further work to make it more generic; and the use of a small scale test plot for this analysis is expected to underestimate the potential of detention on a full-scale roof.

This model has attempted to provide more comprehensive information relating to the green roof design characteristics before it can be built either in small or full scale green roof construction. Further analysis, under different climatic conditions, using a variation of

arbitrary extreme events from a different climatic area, with more careful assessment of the influence of vegetation, slope and aspect could be undertaken in the next research project.

# CHAPTER 8

# CONCLUSIONS AND SUGGESTIONS FOR FURTHER WORK

## 8.1 Conclusions of the Thesis

This chapter summarises the main findings of this study regarding the hydrological performance of green roofs based on the long-term monitoring of the test rig on Mappin Building, University of Sheffield, between January 2007 and May 2009 under UK climatic conditions.

### 8.1.1 Green Roof Performance in Response to Monitored Storm Events

As summarized in Chapter 5, a new data set has been produced and we observed range of different events. During 29 months of monitoring, total of 200 storm events with 121 of them generated runoff and the remainder of 30% were fully retained. The maximum total rainfall depth observed was 115.8 mm with a maximum total runoff at 102.72 mm; with 11% of retention. A minimal of 1.4% retention was observed for a 46.8 mm rainfall event with 15 hours of dry days and 22.5 hours of rainfall duration. Regardless the season factors, the average retention was 69%, with average of peak reduction in runoff intensity was 65%. The minimal peak reduction was 8%. The longest runoff delayed at the start of rainfall was 33.3 hours with the average of 3.5 hours. Maximum lag time from peak rainfall to peak runoff was observed at 445 minutes (7.42 hours) with average at 58.4 minutes.

Monitoring of the single typical Alumasc test configuration revealed that during the study period, the maximum retention/initial loss observed from the test rig was 20 mm and this finding is similar to Villareal & Bengtsson (2005) where in shallow depth of 40 mm they observed 10 – 15 mm initial moisture content. However, in some cases the performance is less impressive than many commercial publicity materials suggest. For example, the roof

never retained more than 0.4 mm in saturated condition, and often – in damp conditions – retained less than 5 mm. The test rig still managed to retain moisture during the extreme events occurred in 2007. Although this was minimal during some storm events but retention during summer 2007 was 34% and the year in 2007 41%. The test rig also shows its capability to attenuate 65% of peak flow at most of the time with minimum of less than 10% attenuation during wet condition. This suggests that the seasonal and annual retention and detention does provide a quantitative benefit for storm water management.

The performance of retention and detention of the test rig however could not be easily explained by simple relationship or multiple regression between hydrological parameters (total runoff, volume retention, total retention, time to start runoff, peak runoff intensity, peak reduction and time lag) and the storm event characteristics (total rainfall, duration, intensity, ADWP, peak rainfall intensity and temperature/season). It seems reasonable to expect that the roof's responses to specific rainfall events might be influenced by various antecedent and storm event characteristics. However, on a storm-by-storm event basis, simple correlations between retention efficiency and a comprehensive range of hydrological parameters were not evident from regression on the data (Chapter 5). One example of the problems associated with the event-based regression approach is that the ADWP does not provide a robust indication as to exactly how much moisture is held in the substrate. After long periods in winter, moisture levels may remain quite high, because losses due to evapotranspiration will be low. On the other hand one might expect the substrate to be close to saturation following a short ADWP, but if the preceding event was only very small, following a long dry period in summer, it would not saturate the roof, and the substrate might actually still be in a very dry condition. These observations suggested that the physical moisture balance processes affecting the roof are too complex to be captured through simple statistical approaches, and that a continuous simulation approach should be adopted instead.

### 8.1.2 Experimental Studies

The conceptual model – initially outlined in Chapter 3 – comprises two compartments: i) a substrate moisture storage compartment; and ii) a transient storage compartment to be modelled using reservoir routing. Critical parameters required to describe the substrate moisture storage were highlighted as being the maximum moisture capacity ($WC_{max}$) and the rate of losses due to evapotranspiration (ET). It is expected that these parameters are

dependent on the substrate's physical characteristics and – to some extent – the influence of vegetation.

The German FLL *Guidelines for the Planning, Execution, and Upkeep of Green-Roof Sites* (FLL, 2002) procedure provides standard methods for the evaluation of green roof materials – substrate properties, including the estimation of maximum moisture capacity, $WC_{max}$. The substrate properties tests were undertaken for three different substrate compositions. It was noted that in some instances the substrates were not well-mixed, and that significant variations in the physical parameters were evident in repeat tests.

A new test was developed to establish evaporative loss rates from bare substrate. The test was intended to complement existing FLL standard test methods, and employed the same 150 mm test vessel as is used in those tests. The test procedure involved monitoring the sample's weight loss over an extended period (up to one month). The weight loss was assumed to equate to evaporated moisture, with the maximum possible moisture loss equating to $WC_{max}$ (saturated moisture content).

Maximum moisture capacity, $WC_{max}$ was estimated by fully drying the samples at the end of the test, and comparisons were made between this value and the FLL value (which is an indirect determination). Difference between the two were observed (quantify), and – once again – the lack of homogeneity/reproducibility in samples was suspected to contribute significantly to the observed $WC_{max}$ differences.

The laboratory evaporation tests suggested that moisture loss under constant temperature conditions will typically follow an exponential pattern, with high initial loss rates followed by reduced rates later on. In the analysis this was simplified to a two-stage linear model, with the transition position corresponding to the removal of the first third of the saturated moisture content.

It was hypothesised that the substrate moisture might never fall as low as zero, even during prolonged dry periods, and it was hoped that laboratory evaporation tests could be used to establish ambient minimum moisture content levels as a function of temperature and substrate characteristics. However, despite lengthy drying periods, samples exposed to the atmosphere under typical UK temperatures (10°C – 20°C) did not show evidence of reaching

a constant minimum. In some cases this reflects the facts that tests were terminated too soon, but several tests lasting one month or more failed to identify a constant low ambient moisture level.

The experiment evaporation, $E_e$ tests showed that for the substrates considered here, under UK climatic conditions, the maximum moisture retention was not fully restored even after one month of dry conditions. Typical substrate evaporation rates were in the order of 1 – 3 mm/day. These values imply that the moisture retention capacity of the roof may typically be only 2 – 6 mm after 48 hours, and 7 – 21 mm after a one week ADWP. Retention capacity is slow to be restored in a typical UK green roof installation.

The research set out to establish whether ET rates were affected by substrate physical characteristics. The laboratory evaporation rates did not show significant variations in evaporation losses from three different substrates. This may allow for some simplifications in modelling. However, ET – as opposed to evaporation alone – will also depend upon vegetation and interactions between vegetation and substrate. Further tests are required to assess whether substrate composition is more critical for ET rates than it is for evaporation alone. However, evaporation rates do show a strong dependence on temperature.

Although evaporation rates were not strongly influenced by substrate characteristics, the maximum water holding capacity was. It ranged from 16% to 50% for the substrates considered here; LECA-based mixture and Alumasc-based respectively. Modelling suggests that substitution of the lower $WC_{max}$ value into our model would result in 6% reduction in retention during the month of June 2007. This reduction was related to the current storage available in the system; reduced storage in the lower $WC_{max}$ of 16% than the 50%.

### 8.1.3 Model Development

Chapter 7 focused on calibration and validation of the conceptual model. The calibration and validation have been also demonstrated that the ET parameter for substrate moisture storage component is dependent on season for every storm to provide the accurate simulation. This has been illustrated in the full set of ET estimation from four different approaches where similar in seasonal and monthly trends in all of the data sets are evident (Figure 7.25). It was concluded that the ET Modified Thornthwaite formula provides a good initial estimate for modelling purposes. There appears to be potential to adapt the

Thornthwaite ET formula to provide monthly ET estimates from local temperature data. This finding might be contrary to the conclusion made by Mentens *et al.* (2003) who reported that without the slope angle, slope orientation, solar radiation, time of year and time of day parameter, the process of ET cannot be directly calculated for a construction of complete physical model using a generic Penmann-Monteith equation. The ET data determined through model fitting appears to be more consistent with other data sets when the temporal profile rather than total runoff is used as the basis for calibration.

The development of a standardized laboratory test for ET should enable differences resulting from substrate characteristics to be quantified, whereas long-term monitoring of test rigs will be used to assess the combined effects of vegetation and substrate.

Calibration suggested the appropriate values for parameters for the storage routing model as $k = 100$ and $n = 3.5$ and has been validated from independent storm events that using this values could provides a high level of confidence ($R_t^2 > 0.9$) in the basic model formulation to simulate the detention performance of green roof. Both low and high flow of runoff can be simulated very well.

Overall, the proposed hydrological model has been shown to reproduce monitored data, both during a storm event, and over a longer continuous simulation period. The storage within the substrate represents the roof's overall stormwater retention capacity (or initial losses). The analysis of long term continuous rainfall-runoff records from a test rig installed with a commercial extensive green roof system suggest that ET falls below 1 mm/day for much of the year under UK climatic conditions. The roof may require an antecedent dry weather period considerably greater than one week to recover its full retention capacity.

Conceptually the model is similar to others (e.g. Jarret, Villareal and Bengtsson), comprising moisture balance (retention) and reservoir routing (transient storage) compartments. However, in this case preliminary proposals have been made to move the model from being purely empirical (requiring site-specific calibration using monitored data) to being physically-based. The maximum moisture-holding capacity parameter ($WC_{max}$) may be determined by physical laboratory assessment of the substrate, whereas the ET parameter can be estimated using a modified form of Thornthwaite's equation.

Further work is required on the next study to identify independent physical determinants of the reservoir routing parameters, k and n, from the runoff rate relationship $Q = kH^n$; and to refine the ET predictions in response to the influence of vegetation. The routing parameter, k is expected to vary as a function of the roof's physical configuration; with greater delay (i.e. lower values of k) being expected for physically larger or deeper roofs; whereas the flow path will be longer. If n is 1.0, then Q will vary linearly as a function of depth, H. It is expected that if n is greater than 1.0, then an increase in depth (i.e. stored volume) will generate a larger increase in the outflow rate. A new field-based pilot-scale test facility has been established to capture performance data which will assist with the further development phases of the generic model.

In summation, this study has achieved the objectives where;

- A continuous longer time-series of data from a typical green roof configuration under UK climatic condition has been collected, analysed and interpreted;
- A generic conceptual rainfall-runoff model has been proposed, calibrated and validated using the experimental data from the monitored test rig;
- Laboratory experiments have been undertaken and relationships between measureable physical properties and model parameter values have been identified.

### 8.1.4 Engineering Impact of the Research

Overall the roof reduces the volume of stormwater discharged directly into sewers and watercourses by approximately 50%. This conclusion is based on a near-continuous 29-month data record, which included a storm event judged to have an (FSR) return period of 1 in 100 years. It may be argued, therefore, that widespread application of green roofs throughout a catchment might be expected to lead to improved quality in receiving waterbodies and/or cost savings through a reduction in the requirement for sewers.

The CIRIA SUDS Manual (C697, 2007) emphasises the importance for water quality of ensuring that SUDS: "capture and treat the runoff from frequent, small events"; and "capture and treat a proportion of the initial runoff (first flush) from larger and rarer events". The monitored data provides evidence that green roofs can make a significant contribution to achieving this objective. The roof fully-retained the runoff from many small events, and often retained 5-10 mm (i.e. the nominal first flush depth) from larger events.

However, the roof's volumetric retention capacity is finite, which means that the proportion of rainfall retained in large events tends to be far smaller. The maximum retention observed was 20 mm. This rainfall depth is approximately equivalent to what might be expected in Sheffield for a 1 yr return period 12 hr event, or a 10 yr return period 1 hr event (FEH CD-ROM). Clearly the green roof cannot provide complete protection from flooding from larger events, and needs to be used in conjunction with additional downstream measures as part of a SUDS treatment train.

The roof depends upon evapotranspiration (ET) to restore its retention capacity. The ET rate (which has been determined through several approaches) varies seasonally from around 0.5 mm/day up to 3.0 mm/day. This means that, even in summer, it may take a week or more to fully restore the roof's retention capacity after an event that fully saturates the substrate.
In terms of detention, the roof generally delays the onset of runoff, on average by 3.5 hours. On average the peak rainfall to peak runoff delay was 58 minutes and the peak attenuation was 65%. It should be noted, however, that these parameters are often difficult to determine from real storm data, and may be sensitive to the 5 minute time-step adopted for analysis. During large storm events, once the roof substrate had reached field capacity and runoff had started, the runoff peaks often followed the rainfall almost instantaneously. However, the green roof test plot is relatively small, and it is expected that this data underestimates the potential for detention on a full-scale roof.

A conceptual model for green roof rainfall-runoff prediction has been outlined, and it has been shown that the model's retention performance can be determined from generic roof configuration characteristics (substrate depth, substrate moisture-holding capacity) and local climatic input data (rainfall, temperature for ET). As shown in Chapter 7, in principle this component of the model could be implemented within drainage modelling tools (e.g. MicroDrainage, InfoWorks) to enable engineers to assess the performance of different roof configuration options. However the detention component of the model requires further work to move from empirically-calibrated routing parameters to something with more generic applicability. There is also considerable scope to enhance the retention component of the model, through more careful assessment of the influence of vegetation, slope, and aspect, amongst others.

In summary, the key engineering benefits from the research are:

1. An improved understanding of the role that green roofs may play in overall stormwater management strategies. They provide a source control for small events and 'first flush' rainfall depths, so have an important water quality enhancement function. However, Green roofs have finite capacity; in this instance not more than 20 mm. They should therefore be combined with other measures to provide protection from extreme events.
2. A preliminary generic modelling tool that enables drainage engineers to evaluate the performance green roofs as a function of selected configuration variables and in response to local climatic inputs.

## 8.2 Suggestion for Further Work

It was discovered that during this study, there are a number of works that can be suggested:

- In order to provide a confident and meaningful hydrological data collection, a mature test rig like ours (4 years old), the monitoring system need to be calibrated twice a year or at least at the beginning of spring time (the end of wet months that might affect the performance of the probe and water level);

- The maintenance of monitoring system is needed to be more systematic; as during this study period we lost a number of interesting extreme events when the solenoid valve leaked due to small debris becoming stuck in the valve opening. Filter is suggested to be installed at the end of gutter system, and more maintenance is required for the filter to make sure it always clean and could well filter the rainfall;

- Regarding the experimental work, it have been discussed that the homogeneity and reproducibility in samples was suspected to contribute the differences between $WC_{max}$ values during the test. Therefore, it needed to make sure that for the next test, the new, fresh and similar moisture condition batch of substrates to be used. This including for both physical properties experiment and the evaporation experiment. Repeat number of substrate physical characteristics test and evaporation tests for different season and month could provide confidence and better results;

- Following above suggestions, it is quite interesting to know how the performance physical properties of our mature substrate; as discovered by Getter *et al.* (2007), where the performance of $WC_{max}$ for their 5 years green roof is improving. Further tests also required to assess whether substrate composition is more critical for ET rates than it is for evaporation alone;

- Further experimental work regarding the establishment of evapotranspiration (with the influence of vegetation) rather than evaporation need to be conducted as demonstrated by Fassman *et al.*, (2008) and Rezaei and Jarret, (2006) in order to provide new data under UK climatic condition;

- As new field-based pilot scale test facility has been established on Hadfield Building, University of Sheffield, the hydrological performance of new 10 test rigs is expected to provide a range of hydrological information specifically on substrate and vegetation, therefore useful assessment can be made for further development phases of the generic model;

- Further calibration and sensitivity analysis for k and n on various types of rainfall events especially for the long-term performance, in order to tackle the problem occurred storms like in 31 July 2007 and 1 August 2007 that both appears to have high intensity rainfall (high rainfall with short duration); and also expected to be influenced by drainage layer, roof size and slope;

- During this study, the model has been undertaken using Microsoft Excel, it is suggested to have more robust software like MATLAB especially while conducting the long-term series performance.

# REFERENCES:


Alumasc (2007).
http://www.zinco.de/ausland/english/green_roof_systems/extensive/sedumcarpet.php
(Accessed on 19 July 2007)

Akagawa, Y., Matsumoto, Y. and Zaizen, M. (1997). The Inspection of Actual Runoff Control Facilities Five Years After Construction, Water Science Technology, 36(8–9), 373–377.

Argue, J. and Pezzati, D. (1998). Catchment "Greening" Using Stormwater In Adelaide, South Australia. Proc. 3rd Int. Conf. NOVATECH, Lyon.

Baraglioli, A., A. Guillon, Y. Kovacs, and C. Senechal, (2008) Studies on the Quantity Impacts of Green Roofs, 11th International Conference on Urban Drainage, Edinburgh, Scotland, UK.

Bass, B & Baskaran, B. (2001). Evaluating Rooftop and Vertical Gardens as an Adaptation Strategy for Urban Areas. CCAF IMPACTS AND ADAPTATION PROGRESS REPORT B1046) for 1)Adaptation & Impacts Research Group Environment Canada; 2) Institute for Research in Construction National Research Council Canada.

Bettes, R. (1996). Infiltration Drainage-Manual of Good Practice, CIRIA Report 156.

Beven, K.J. (1988) Rainfall – Runoff Modelling: The Primer, John Wiley & Sons Ltd. England

Brady, Nyle C.; Weil, Ray R. (1999). The nature and properties of soils: twelfth edition. Upper Saddle River, NJ: Prentice Hall. 881 p.

Burges, et al (1998) Hydrological Effects of Land-use Change in a Zero-order Catchment. Journal of Hydrologic Engineering, ASCE

Cabugos, L., Andrew J. Kaufman, Linda J. Cox, Tomoaki Miura And Dawn Easterday (2007) Feasibility Of Rooftop Landscaping With Native Hawaiian Plants In Urban Districts Of Hawai`I, Greening Rooftops for Sustainable Communities, Minnepolis.

CampbellSci, Campbell Science (2007) CR800 datalogger. http://www.campbellsci.com/cr800-datalogger (Accessed on 23 July 2007)

Carter, T.L. & Jackson, C.R. (2006). Vegetated roofs for stormwater management at multiple spatial scales. Journal of Landscape and Urban Planning. 80 (2007) 84–94.

Carter, T.L. & Rasmussen, T.C. (2005). Use of Green Roofs for Ultra-Urban Stream Restoration in the Georgia Piedmont (USA). Green Rooftops for Sustainable Communities Conferences, May 4 – 6, 2005. Washington, DC, USA.

Carter, T.L. & Rasmussen, T.C. (2006). Hydrologic Behavior of Vegetated Roofs. Journal of The American Water Resources Association. American Water Resources Association. Vol. 42 Pt. 5 pp. 1261-1294.

Chadwick A., Morfett J. and Borthwick M., (2004) Hydraulics in Civil and Environmental Engineering. Fourth Edition, Spon Press, London

Chow *et al.*(1988) Applied Hydrology. New York : McGraw-Hill, c1988.

CIRIA (2007) http://www.ciria.org/suds/ (Accessed on 28 April 2007)

Coffman, L. (2000). Low-Impact Development Design Strategies, An Intergrated Design Approach. EPA 841-B-00-003. Prince George's County, Maryland. Department of Environmental Resources, Programs and Planning Division.

Defra, Department of Environment (2005). 'Sustainable Drainage Systems: Summary of Issues, Consultation Responses and Proposed Next Steps'. Background paper accompanies the First Government Response. http://www.defra.gov.uk/environ/fcd/policy/strategy.htm (Accessed on 9 May 2007)

DeNardo, J.C, Jarret, A.R., Manbeck, H.B., Beattie, D.J., and Berghage, R.D. (2003). Green Roofs: A Stormwater BMP. Proceedings of the 2003 Pennsylvania Stormwater Management Symposium Held at Villanova University October 16-17, 2003. http://www3.villanova.edu/vusp/to/pasym03/index.html (Accessed on 30 Nov 2007)

Deutsch, B. et al (2005). Re-greening Washington, DC: A Green Roof Vision Based on Quantifying Storm Water and Air Quality Benefits. (http:// www.**greenroof**s.org/resources/**greenroofvisionfordc**.pdf (Accessed on 13 July 2007)

Dunnett, N. and N. Kingsbury (2004). Planting Green Roofs and Living Walls. Timber Press, Inc., Portland, OR.

EA, Environment Agency (2003) http://www.rochford.gov.uk/pdf/planning_quest_ans_sustainable_drainage_systems.pdf (Accessed on 9 May 2007)

EA, Environmental Agency (2007) Review of 2007 summer floods. (http://publications.environment-agency.gov.uk/pdf/GEHO1107BNMI-e-e.pdf) (Accessed on 23 May 2009)

ELT, Elevated Landscape Technologies (2006). http://www.elteasygreen.com (Accessed on 2nd July 2007)

Engineering Manuals (1994) Engineering and Design - Flood-Runoff Analysis. Publication Number: EM 1110-2-1417. http://www.usace.army.mil/publications/eng-manuals (Accessed on 13th July 2007)

Faraway, J.J (2005). Linear Models with R, Text in statistical science. Chapman & Hall/CRC Press Company, Boca Raton London New York Washington, D.C. http://lib.myilibrary.com.eresources.shef.ac.uk/browse/open.asp?id=23179&loc=

Fassman, E (2008) Effect of Roof Slope and Substrate Depth on Runoff, Greening Rooftops for Sustainable Communities, April 30 – May 2, Baltimore.

Fassman E. & R. Simcock (2008) Development and Implementation of Locally-Sourced Extensive Green Roof Substrate in New Zealand, World Green Roof Congress, London.

Fassman, E., R. Simcock, E. Voyde & J. Wells (2008) Quantifying Evapotranspiration Rates for New Zealand Green Roofs, EWRI International LID Conference, Seattle, Washington, 16 - 19 November.

Graham, P. & Kim, M. (2003). Evaluating the Stormwater Management Benefits of Green Roofs Through Water Balance Modeling. Greening Rooftops for Sustainable Communities, Chicago, Proceedings from the North American Green Roof Conference, 390-397.

Getter, K.L., Rowe, D.B. & J. A. Andresen (2007) Quantifying the Effect of Slope on Extensive Green Roof Stormwater Retention. Journal of Ecological Engineering 31: 225 – 231.

Grotehusmann, D., Khelil, F. & Sieker, M. (1993). Alternative Urban Drainage Concept and Design. Proc. 6th Int. Conf. Urban Storm Drainage, Vol. 2, pp. 1213–1218.

Hillel, D. (1998) Environmental Soil Physics. Academic Press USA.

Hilten, R.G., T.M. Lawrence and E. W. Tollner (2008) Modelling Stormwater Runoff from Green Roofs with HYDRUS-1D. Journal of Hydrology, 358: 288 – 293. Elsevier B.V.

Hutchinson, D. et al., (2003). Stormwater Monitoring Two Ecoroofs in Portland, Oregon, USA. Greening Rooftops for Sustainable Communities, Chicago, Proceedings from the North American Green Roof Conference, 372-389.

IGRA, International Green Roof Association (2007) http://www.igra-world.com/green-roof-benefits/public.html#storm (Accessed on 9 July 2007)

Jarret, A.R. & Berghage, R.D. (2008). Annual and Individual Green Roof Stormwater Response Models Greening Rooftops for Sustainable Communities, Baltimore, MD, April 30 – May 2.

Johnston, C., McCreary, K., Nelms, C. (2004). Vancouver Public Library Green Roof Monitoring Project. . Greening Rooftops for Sustainable Communities, Portland, Proceedings from the North American Green Roof Conference, 391-403

Kirkby, M.J., P.S. Naden, T.P. Burt and D. P. Butcher (1992). Computer Simulation in Physical Geography, 2nd Edition, John Wiley & Sons Ltd, England.

Kohler, M., M. Schmidt, F.W. Grimme, M. Laar & F. Gusmao, (2001) Urban Water Retention By Greened Roofs In Temperate And Tropical Climate, Sustainable Development, Vol.2, 38th EFLA World Congress (International Federation of Landscape Architects), Singapore.

Konrad, C.P. (2005) U.S Geological Survey, http://pubs.usgs.gov/fs/fs07603/ (Accessed on 4 May 2007)

LaBerge, K., Worthington, K., Mulvaney, P. & Bolliger, R. (2005). City of Chicago Green Roof Test Plot Study: Stormwater and Temperature Results. Greening Rooftops for Sustainable Communities, Washington, D.C., May 5-6, 2005, pp. 540-552.

Lando, P. (2004). Test Plots for a Light Weight, Low-Cost, Vegetative Roof in Commercial Applications. Greening Rooftops for Sustainable Communities, Portland, Proceedings from the North American Green Roof Conference, 404-410.

Linsley, R.K., Kohler, M.A. and Paulhaus.J.L.H. (1988) Hydrology for Engineers, McGraw Hill, London.

Liptan, T. & Strecker, E. (2003). EcoRoofs (Greenroofs) – A more sustainable infrastructure. EPA's PDF page. http://www.epa.gov/nps/natlstormwater03/20Liptan.pdf (Accessed on 9 July 2009)

Liu, K.K.Y. (2002). Energy efficiency and environmental benefits of rooftop gardens. Journal of Construction Canada, vol: 44 ,no. 2, p. 17, 20-23.

Liu, K. & Minor, J. (2005). Performance evaluation of an extensive green roof. Greening Rooftops for Sustainable Communities, Washington, D.C., May 5-6, 2005, pp. 1-11.

Livingroof.org (2007). http://livingroofs.org/ (Accessed on 4 May 2007)

Loder, M.A. And Peck, S. W., (2004) Green Roofs' Contribution To Smart Growth Implementation, Green Roofs For Healthy Cities

Lundberg, L. (2004). Swedish Research and its Links to Policy Development. Greening Rooftops for Sustainable Communities, Portland, Proceedings from the North American Green Roof Conference, 387-390.

Mansell, M.G. (2003) Rural and Urban Hydrology, Thomas Telford Limited, Great Britain.

Macdonald, K. & Jefferies, C. (2003). Performance and Design Details of SUDS. National Hydrology Seminar 2003. University of Aberdeen.

Macdonald, N. & Jones, P. (2006). The Retro-fitting of Sustainable Drainage Systems into established Urban Areas and its Interdiscipinary Demands: A Case Study of Glasgow. BHS 9th National Hydrology Symposium, Durham.

MacMillan, G. (2004). York University Rooftop Garden Stormwater Quantity and Quality Performance Monitoring Report. Greening Rooftops for Sustainable Communities, Portland, Proceedings from the North American Green Roof Conference, 461-474.

McCuen, R.H. (1941). Hydrologic Analysis and Design. Pearson: Prentice Hall, 3rd Edition.

MDE (Maryland Department of the Environment), 2002. Maryland's Stormwater Management Programme. Washington, Baltimore. http://www.mde.state.md.us/Programs/WaterPrograms/SedimentandStormwater/home/index.asp) (Accessed on 18 July 2007)

Mentens, J. , Dirk Raes & Martin Hermy (2006). Green roofs as a tool for solving the rainwater runoff problem in the urbanized 21st century?. Journal of Landscape and Urban Planning 77: 217–226.

Mentens, J. , Dirk Raes & Martin Hermy (2003) Effect of Orientation on the Water Balance of Greenroofs, Greening Rooftops for Sustainable Communities, Chicago.

Meteorology Office – Met Office (2010) http://www.metoffice.gov.uk/climate/uk/stationdata/sheffielddata.txt (Accessed on 1 January 2010)

Miller, C. (2004). Performance-Based Approach to Preparing Green Roof Specifications. Greening Rooftops for Sustainable Communities, Portland, Proceedings from the North American Green Roof Conference, 338-352.

Miller, C. (2003). Moisture Management in Green Roofs, Greening Rooftops for Sustainable Communities, Chicago.

Miller, C. & Pyke, G. (1999). Methodology for the Design of Vegetated Roof Covers. Proceeding of the 1999 International Water Resource Engineering Conference ASCE, Seattle, WA.

Montgomery D. C. & Runger G.C (1999) Applied Statistic and Probability for Engineers, 2nd Edition: page 464, John Wiley & Sons.Inc

Moran, A., Hunt, B. & Smith, J. (2005). Hydrologic and Water Quality Performance from Greenroofs in Goldsboro and Raleigh, North Carolina. Green Rooftops for Sustainable Communities Conferences, May 4 – 6, 2005. Washington, DC, USA.

Moran, A. (2004). A North Carolina Field Study to Evaluate Greenroof Runoff Quantity, Runoff Quality, and Plant Growth. M.S. Thesis, North Carolina State University, Raleigh, North Carolina.

Ngan, G (2004). Green Roof Policies: Tools for Encouraging Sustainable Design. Report from: Landscape Architecture Canada Foundation (http://www.gnla.ca/assets/Policy%20report.pdf (Accessed on 21 August 2007)

Palla, A, L.G. Lanza & P. La Barbera (2008) A Green Roof experimental Site in the Mediterranean Climate, 11th International Conference on Urban Drainage, Edinburgh, Scotland, UK.

Reeves, M.K. & Lewy, M. (2002). Modelling Sustainable Urban Drainage Structures. Environmental Expert.com Articles. http://www.environmental-center.com/articles/article1168/article1168.htm (Accessed on 12 February 2007)

Rezaei, F. et al., (2005). Evapotranspiration Rates from Extensive Green Roof Plant Species. ASAE Paper No 05-2150. Tampa, FL. July 17-20, 2005.

Rezaei, F. & A.R. Jarret (2006) Measurement and Predict Evapotranspiration Rate from Green Roof, Penn. State College of Engineering Research Symposium, University Park, Pennsylvania.

RSG, Retrofit SUDS Group (2003) http://retrofit-suds.group.shef.ac.uk/index.html (Accessed on 12 February 2007)

Rosenzweig, C., S. Gaffin, and L. Parshall (Eds.) (2006). Green Roofs in the New York Metropolitan Region: Research Report. Columbia University Center for Climate Systems Research and NASA Goddard Institute for Space Studies. New York. 59 pages. http://www.ccsr.columbia.edu/cig/greenroofs/index.html (Under Hydrology report) (Accessed on 20 February 2007)

Rowe, D.B., Rugh, C.L. & Durhman, A.K. (2006). Assessment of Substrate Depth and Composition on Green Roof Plant Performance. Green Rooftops for Sustainable Communities Conferences, May 11 – 12, 2006. Boston, USA.

Rowe, D B. Rugh, C L. VanWoert, N. Monterusso, M A. and D K Russell (2003) Green Roof Slope, Substrate Depth, and Vegetation Influence Runoff. Greening Rooftops for Sustainable Communities, Chicago, Proceedings from the First North American Green Roof Conference, 354-361

Seters, T.V., Lisa Rocha, MacMillan, (2007) Evaluation of the Runoff Quantity and Quality Performance of an Extensive Green Roof, in Toronto, Ontario. Greening Rooftops for Sustainable Communities, Minneapolis

Schraven, H., Durrant, J. & Kinney, T. (2004). Greenroof D esign Utilizing a Biostable Soil. Greening Rooftops for Sustainable Communities, Portland, Proceedings from the North American Green Roof Conference, 431-445.

Stahre, P. and Urbonas, B.R. (1990). Stormwater Detention for Drainage, Water Quality and CSO Management, Prentice Hall, New York.

Stovin, V.R. and Swan, A.D., (2003) Application of a retrofit SUDS decision-support framework to a UK catchment, Second National Conference on Sustainable Drainage, 23-24 June 2003, Coventry, UK.

Stovin V., Dunnett, N., and Hallam, A.(2007) "Green Roofs – getting sustainable drainage off the ground". Paper for NOVATECH 2007 - 6th Int. Conference on Sustainable Techniques and Strategies in Urban Water Management.

Stovin *et al.*, (2007) Green roofs – getting sustainable drainage off the ground. NOVATECH.

Straet, F., Beckers, E. & Degre, A. (2008). Hydraulic Behaviour of Greened Porous Pavements: A Physical Study. 11th International Conference on Urban Drainage, Edinburgh, Scotland, UK.

Swan, A., Stovin, V. & Reeves, M. (1999) Modelling Urban Drainage BMPs with HydroworksTM/ Infoworks TM. WaPUG Autumn Meeting 1999. UK.

Tan, P. Y. & Sia, A. (2005) A Pilot Green Roof Research Project In Singapore, Greening Rooftops For Sustainable Communities, Minnepolis

Takebayashi, H. & Moriyama, M. (2006). Surface heat budget on green roof and high reflection roof for mitigation of urban heat island. Journal of Building and Environment 42 (2007) 2971–2979

Takenaka Corporation (2001) Rooftop Greening Taking Advantage of Plant Characteristics and Not Requiring Care '*Load on Buildings Reduced Using Thin Layer Planting Base*'. http://www.takenaka.co.jp/takenaka_e/news_e/pr0103/m0103_02.htm (Accessed on 19 July 2007)

Taube, B. (2005) City Of Atlanta Greenroof Demonstration Project City Of Atlanta – Department Of Watershed Management, Greening Rooftops For Sustainable Communities, Minnepolis

Taylor, B.L. (2006). Planning a Green Roof Storm Runoff Monitoring System. Green Rooftops for Sustainable Communities Conferences, May 11 – 12, 2006. Boston, USA.

Taylor, B.L., Gangness & Ellison, (2005). Seattle Green Roof Evaluation Project: An Introduction. Green Rooftops for Sustainable Communities Conferences, May 4 – 6, 2005. Washington, DC, USA.

Taylor, B.L. & Gangnes, D.A. (2004). Method for Quantifying Runoff Reduction of Green Roofs. Green Roof for Healthy Cities Conferences, June 2 – 4, 2004. Portland, Oregon, USA.

Uhl, M. & L. Schiedt, (2008) Green Roof Storm Water Retention – Monitoring Results, 11th International Conference on Urban Drainage, Edinburgh, Scotland, UK.

USEPA (2007) 'International Stormwater BMP Database Project Background'. http://www.bmpdatabase.org/background.htm (Accessed on 11 May 2007)

VanWoert, N.D. *et al.* (2005). Green Roof Stormwater Retention: Effects of Roof Surface, Slope, and Media Depth. Journal of Environmental QUality. USA. Vol: 34, p. 1036-1044.

Viessman, W.,Jr. & Lewis, G.L. (2002). Introduction to Hydrology. Prentice Hall, Pearson Education, Inc. 5th Edition, USA.

Villarreal E.L. *et al.* (2004) Inner City Stormwater Control Using a Combination of Best Management Practices. Journal of Ecological Engineering 22 (2004) 279–298. (www.sciencedirect.com)

Villarreal, E.L. & Bengtsson, L. (2005) Response of a *Sedum* green-roof to individual rain events. Journal of Ecological Engineering 25 (2005) 1–7

Wacther, H.M., D. Lilly, B. Berkompas, W. Taylor, K.W. Marx (2007) City of Seattle Green Roof Policy Development through Extended Performance Monitoring as a basis for Hydrologic Modelling. Greening Rooftops for Sustainable Communities, Minneapolis

Whitelaw, E., Csla (2005) Vancouver's Public Library And The Urban Oasis – Robson Square, Cornelia Hahn Oberlander Landscape Architect, Greening Rooftops for Sustainable Communities, Minnepolis.

Wilson, E.M. (1969). Engineering Hydrology. 3rd Edition, Published: MacMillan Publishers Ltd. London.

Worden E. et al (2004) Green Roofs in Urban Landscapes. http://edis.ifas.ufl.edu/EP240 (Accessed on 18 July 2007).

Young, P., Jakeman, A. and McMurtie, R. (1980). An instrument variable method for model order identification, *Automatica,* 16, 281-294.

# Appendix 3.1

## Example of runoff conversion calculation using Microsoft Excel

| | A | B | C | D | E | F | G | H |
|---|---|---|---|---|---|---|---|---|
| 1 | **Transition** | **992.44** | **1195.99** | **mV** | | | | |
| 2 | **Zone** | Sensitive | Transition | Top | | | | |
| 3 | **Equation Type** | y=mx + c | $y= m*exp^{cx}$ | y=mx + c | | | | |
| 4 | **Parameter 1 (m)** | **0.0018** | **0.0066** | **0.0074** | | | | |
| 5 | **Parameter 2 (c)** | **1.0861** | **0.0047** | **7.0273** | | | | |
| 6<br>7<br>8 | TIMESTAMP | DiffVolt (mV) (x) | Rainfall Total (mm) | Rainfall Cumulative (mm) | Cum. Runoff Depth (mm) (y) | Remove lost runoff | 1 min added Runoff (mm) | Runoff Cumulative (mm) |
| 9 | 13/6/2007 20:38 | 717.2 | 0.2 | 0.2 | 0.20468 | 0.20468 | 0 | 0 |
| 10 | 13/6/2007 20:39 | 718.4 | 0.2 | 0.4 | 0.20302 | 0.20468 | 0 | 0 |
| 11 | 13/6/2007 20:40 | 720.4 | 0.0 | 0.4 | 0.21062 | 0.21062 | 0.00594 | 0.00594 |
| 12 | 13/6/2007 20:41 | 720.6 | 0.2 | 0.6 | 0.21098 | 0.21098 | 0.00036 | 0.0063 |

- Rows 1 – 5 : Calibration data for runoff conversion relationships;
- Rows 9 downwards : The conversion of runoff voltage response (mV) data into equivalent runoff depth (mm);
- Columns A – C : Raw data from the logger;
- Columns D : Cumulative rainfall (e.g : D10=C10+D9);
- Column E : The conversion of voltage runoff response (mV) into equivalent runoff depth (mm) using derived calibration equations, the transition points and 'IF' function. Each of these values was converted within their own water level zone;
  (e.g: = IF(B9<$B$1,$B$4*B9-$B$5,IF(B9<=$C$1,$C$4*EXP($C$5*B9),$D$4*B9-$D$5)))
- Column F : Data smoothing/discretising was carried out in this column to eliminate the negative values of runoff from the cumulative runoff depth using 'IF' function.
  (e.g : =IF(E10>F9,E10,F9))
- Column G : Equivalent runoff depth (mm) calculated. (e.g : G9 = F9-F10)
- Column H : Runoff cumulative will be needed again to refining the re-discreting processes.
  (e.g : H10=H9+G10)

# Appendix 4.1

**A program produced to allow the logger to read and scan the probe responses automatically:**

CR800 Program

```
'CR800 – Full Bridge
'Created by Short Cut (2.5) -

'Declare Variables and Units
Public Batt_Volt
Public Pressure1

Units Batt_Volt=Volts
Units Pressure1=mV

'Define Data Tables
DataTable(Hartini,True,-1)
        DataInterval(0,15,Sec,10)
        Average(1,Pressure1,FP2,False)
        Sample(1,Pressure1,FP2)
        Totalize(1,Pressure1,FP2,False)
EndTable

DataTable(Table2,True,-1)
        DataInterval(0,1440,Min,10)
        Minimum(1,Batt_Volt,FP2,False,False)
EndTable

'Main Program
BeginProg
        Scan(5,Sec,1,0)
                'Default Datalogger Battery Voltage measurement Batt_Volt:
                Battery(Batt_Volt)
                'Generic Full Bridge measurements Pressure1:
                BrFull(Pressure1,1,mV25,1,1,1,2500,True,True,0,_50Hz,1.0,0.0)
                'Call Data Tables and Store Data
                CallTable(Hartini)
                CallTable(Table2)
        NextScan
EndProg
```

# Appendix 4.2 (I)

## Experimental Procedure on Density, Water Capacity and Water

## A. Permeability Green Roof Media

**Reference**

Guideline for the Planning, Execution and Upkeep of Green-Roof Sites, 2002. Forschungsgesellschaft Landschaftsentwicklung Landschaftsbau (FLL), Bonn, Germany.

**Summary Of Method**

Cool/moist material with a loose volume of between 2100 and 2500 mL is compacted in a cylindrical container and the density calculated at moist (less than 20 % moisture), at maximum water capacity. The maximum water capacity is determined after total immersion of the sample in water for 24 hours and subsequent draining for 2 hours. The coefficient of absorption for the materials in compacted condition at maximum water capacity is determined by measuring the fall over a given period in the level of the water in which the materials are totally immersed.

**Equipment**

1. Cylindrical plastic or stainless steel containers with an inside diameter of 150 mm and a height of 165 mm and with a base perforated as follows:
   a. Radius interval 15°
   b. Perforation perimeter spacing 10 mm
   c. Perforation diameter 5 mm
   d. Number of perforations:

| | |
|---|---|
| centre | 1 x 1 = 1 |
| 90 ° intervals | 4 x 7 = 28 |
| 30 ° /60 ° intervals | 8 x 6 = 48 |
| 15 ° /45 ° /75 ° intervals | 12 x 4 = 48 |

2. Screening: 0.6 mm mesh wire, diameter 148 mm (2)
3. 7 mm steel plate, diameter 148 mm
4. Proctor hammer: 4.5 kg drop weight, 450 mm drop height
5. Plastic basins at least 200 mm height in which to place containers with media for immersion.
6. Drainage rack (for setting beakers on for drainage into sink after saturation)
7. 148 mm diameter non-woven fabric filters to cover the top of sample during saturation (cheese cloth)

8. 100 x 100 mm concrete or other weight to rest on top of sample during saturation
9. Plastic ruler (150 mm or smaller) with markings at 43 and 35 mm supported on a circular wire base.

**Procedure:**

Note: Testing is to be carried in in triplicate and the mean result for all analyses taken.
A separate determination of percent solids must be determined (see Method E1) for use in the calculations.

**A. Apparent density (volume weight)**

1. Place the wire mesh in the bottom of the container and weigh.
2. Fill the container to a depth of between 120 mm and 140 mm with a quantity of the material which must be cool/moist (generally less than 10-15 % moisture). If the material is too wet, allow it to dry before test measurement and placement in container. The container is filled to a level which will ultimately leave a depth of 100 mm or thereabouts after compaction.
3. Place the steel plate over the top of the material with which the container is filled and then strike 6 times with the Proctor hammer to compact it.
4. Find the depth of the sample (h) in its compacted state by making four cross-wise measurements from the upper rim of the cylinder to the surface of the sample and then subtracting the result from the internal height of the cylinder. The sample volume may be then calculated using the formula $\pi \times r^2 \times h$.
5. Find the weight of the container plus the sample, from which the weight of the container plus the fitted wire mesh is then subtracted to give the weight of the sample. Continue to Part B, below.

Apparent density at maximum water capacity is to be determined immediately after maximum water capacity has been found (see Part B, below). Check the height of the sample so as to take account of any swelling which may take place. Find the volume and weight of the sample as described above. Determine the apparent density on a dry weight basis from the percent solids determination (see Method E1.)

6. Calculations:

Density ($D_m$) under moist (as-received) conditions:

$$D_{moist} = \frac{mmoist}{V} \text{ (g/cm3)}$$

mmoist = mass (weight) in g in moist condition

V = volume in $cm^3$ in compacted condition

Density ($D_{max}$) under maximum water conditions (after performing Part B, below):

$$D_{max} = \frac{mmax}{V \text{ or } Vcor} \text{ (g/cm3)}$$

$m_{max}$ = mass (weight) in g at maximum water capacity

$V_{cor}$ = corrected volume in $cm^3$ if there is swelling after saturation.

Density ($D_{dry}$) on dry weight basis

$D_{dry} = D_{moist}$ x (% solids/100)

The results are expressed as the mean from the three replications.

## B. Maximum water capacity

1. After performing the density measurement (Part A, above), place the fabric filter and wire mesh on top of the materials inside the cylindrical vessel and weight these down with the concrete or other weights so as to prevent the contents from rising.

2. Place the vessels in the plastic basins and fill slowly with water until the level reaches approximately 10 mm below the top of the test sample. Dampen the surface of the test sample.

3. Add more water to the container until the level is 10 mm above the top of the test sample. Note, if the sample is highly organic, add water slowly so that water in the basin stays even with the level in the sample container and does not exceed it.

4. Check water level throughout the day and add more as necessary to maintain a level 10 mm above the top of the test sample.

5. After the sample have been totally immersed for 24 hours, carefully lift the vessel out of the basin until the water is just level with the sample surface. Quickly, transfer the sample to a tared pan. Weigh the sample and record as "weight saturated soil plus beaker before draining". This part of the procedure is not part of the FLL protocol, but will give a measurement of the total porosity (water-filled pores) which can be compared to the calculated total porosity based on the FLL guidelines.

6. After weighing, place the vessel on top of the draining board over a sink and leave it for two hours to drain. At the end of this period, dry the vessels thoroughly, remove the cover from the top of the sample, and find the combined weight of the vessel plus test sample.

7. Check the volume of the test sample at maximum water capacity by making four cross-wise measurements from the upper rim of the cylinder to the surface of the sample and then subtracting the result from the internal height of the cylinder. The sample volume may be then calculated using the formula $\pi$ x $r^2$ x h. Note, if the height after saturation is greater than the initial pre-satuaration height, the calculated volume would be Vcor in the equation below and that shown in section A7.

8. Calculate the maximum water capacity ($WC_{max}$) on a volume % basis as follows:

$$WCmax = \frac{(Mmax - Mdry) \times 100}{V \text{ or } Vcor} \text{ (Vol. \%)}$$

Mmax = mass (weight) in g at maximum water capacity

Mdry = mass (weight) in g in dry condition (=Mmoist * % solids/100)

The result is expressed as the mean from the three replications.

## C. Water permeability

The coefficient of absorption (mod. $K_f$) (water) for the materials in compacted condition inside the cylindrical vessels at maximum water capacity is found by measuring the fall over a given period in the level of the water in which the materials are totall immersed.

1. At the completion of the maximum water capacity measurement (Part B, above), cover the surface of the test sample with the wire mesh and place the ruler (supported on a circular stand) on top.
2. Fill the cylinder carefully from the top until the surface of the water is between 10 and 20 mm above the test sample.
3. Add water continuously as the water level drops to maintain the total immersion depth. Measurement commences as soon as water begins to flow evenly out of the perforated base.
4. Fill with water until the surface is above 45 mm on the ruler. Observe the water as the level drops and not the time taken for it to drop from 45 to 35 mm.
5. Perform the measurement 3 times on each of the 3 replicates and average the results
6. Calculate the water permeability (mod. $K_f$) as follows:

$$\text{mod. } K_f = \frac{1}{t} * \frac{1}{h + 4.0} \quad \text{(cm/s)}$$

h = depth in cm of the compacted test material (see A4)

t = the time in seconds for the water level to drop from 45 mm to 35 mm

The result is expressed as the mean of the three replications.

# Appendix 4.2 (II)

## Experimental Procedure on Total and Air-Filled Porosity Green Roof Media

**Calculated from assumed particle densities**

### Reference

VDLUFA Bulletin 6/1970, pages 126-128, with correction 6/1971, page 149. Simplified determination of pore volume using the FEIGE method.

### Summary of Method

Total porosity is calculated on the basis of a) the mineral and organic matter contents of the media, b) assumed particle densities for organic and mineral matter and 3) the measured bulk density of the media. A correction factor is applied for media with mineral matter greater than 70 %.

### Safety

There are no hazards associated with this procedure.

### Interferences

This procedure cannot be used for substrates which contain organic-synthetic foam type materials.

### *1.1 Parameters*

1. BD: Bulk density (volume dry weight); g/cm3
2. $M_{min}$ Percent mineral content of media, calculated as 100-percent organic matter
3. $M_{org}$ Percent organic content of media
4. $P_{s\text{-}min}$ Particle density for mineral substance: assume value of 2.65 g/cm3
5. $P_{s\text{-}org}$ Particle density for organic substance: assume value of 1.60 g/cm3

### *1.2 Calculations*

1. Total Pore Volume (Total Porosity): TPV
   a. For a pure mineral media,

$$TPV\ \% = 100 - (^{100}/_{P_{s\text{-}min} * BD})$$

   b. For mixed media (organic and inorganic):

$$TPV\ \% = 100 - (M_{min} / P_{s\text{-}min} + M_{org} / P_{s\text{-}org}) * BD$$

Since $M_{org} = 100 - M_{min}$, this equation can be reduced to:

$$TPV\ \% = 100 - (265 - M_{min} / 4.24 * BD)$$

c. For media containing greater than 70 % mineral matter (most green roof media), this equation is adjusted to

$$\mathbf{TPV\ \% = 100 - [(265 - M_{min} / 4.24 * BD) - 1.5]}$$

2. Air-filled porosity: AFP

The air-filled porosity is calculated as the difference between the TPV and the water held (%) at the maximum water holding capacity (WHC) as determined in Method E4.

$$\mathbf{AFP\ (\%) = TPV\ (\%) - WHC\ (\%)}$$

# Appendix 4.2 (III)

## Experimental Procedure on Particle Density and Porosity:

## Specific Gravity Method

**Reference**

Blake, G.R. 1986. Particle Density. *In* Methods of Soil Analysis, Part 1, Physical and Mineralogical Methods. Agronomy Monograph No. 9 (2nd edition). Soil Science Society of America, Madison, WI

Vomocil, James A. 1986. Porosity. *In* Methods of Soil Analysis, Part 1, Physical and Mineralogical Methods. Agronomy Monograph No. 9 (2nd edition). Soil Science Society of America, Madison, WI

**Summary of Method**

Particle density (total mass of solid particles to total volume) is calculated by determining the mass of the sample by weight and sample volume from mass of water displaced by the sample. Density of water is assumed to be 1 g/cm$^3$. The total porosity is calculated from the bulk density (see method E4) and particle density measurements.

**Safety**

Precautions should be taken when handling glassware on hot plate.

**Equipment**

1. 250 mL volumetric flask with wide neck (≥ 2mm ID).
2. Analytical balance sensitive to 0.001 g.
3. Hot plate
4. Hot mitts

**2 Reagents**

1. Distilled water

**Procedure**

1. Weigh clean dry volumetric flask.
2. Add 50-75 g of sample. Determine the percent solids of a duplicate sample (dry at 105 C)

3. Fill the flask with approximately 150 mL distilled water (about 2/3 the lower portion of the flask) taking care to rinse into solution sample particles that may have adhered to the neck.

4. To remove entrapped air, place the flask on a hot plate and boil gentle for several minutes. Agitate contents as necessary to avoid foaming and sample loss.

5. Remove the flask from the hot plate and cool to room temperature.

6. Fill the flask to the 250-mL calibration line with boiled, cooled distilled water at the same temperature as the flask contents.

7. Dry the flask thoroughly and weigh.

8. Remove the media from the flask and rinse contents thoroughly. Fill the flask with boiled, cooled distilled water and weigh. Alternatively, if calibration of flasks has been checked prior to use, record volume/weight of distilled water in flask as 250 mL (g).

**Calculations**

1. Calculated particle density as follows

$$D_p = \frac{d_w (W_s - W_a)}{(W_s - W_a) - (W_{sw} - W_w)}$$

$D_p$ = particle density
$d_w$ = density of water in grams per cubic centimeter at temperature observed (assume 1, for the normal temperature range in the laboratory)
$W_s$ = weight of volumetric flask plus sample (corrected to oven-dry weight)
$W_a$ = weight of volumetric flask
$W_{sw}$ = weight of volumetric flask plus sample and water
$W_w$ = weight of volumetric flask filled with water at temperature observed

2. Calculate total porosity as follows: (note see separate determination for bulk density, method E4)

$$TP\ (\%) = 100\ (1 - (D_b / D_p)$$

TP = total porosity
$D_b$ = bulk density
$D_p$ = particle density

3. Calculate air filled porosity as follows:

$$AFP\ (\%) = TP\ (\%) - WHC\ (\%)$$

AFP= air-filled porosity
TP = total porosity
WHC = water-holding capacity (% volume) (note: see separate determination, method E4)

# Appendix 4.3

## Example of calculation for Alumasc-HL physical properties

### 3.3.2.1 Percent Solids

$$\text{Percent of Solid} = 100\% \times \frac{\text{(Sample size (g) – weight of sample (after 24 hours) (g))}}{\text{Sample size (g)} \times 100}$$

$$= 100 \times \left( \frac{224.8 - 219.4}{228.4 \times 100} \right) \%$$

$$= 98\%$$

### 3.3.2.2 Density

1) Density ($D_{moist}$) under moist (as-received) conditions;

$$D_{moist} = \frac{m_{moist}(g)}{V(cm^3)} = \text{weight of compacted substrate (g) / volume of sample } (cm^3)$$

$$= 1469 \text{ g} / 1899.68 \text{ cm}^3 = 0.77 \text{ g/cm}^3$$

2) Density ($D_{max}$) under maximum water conditions (after performing maximum water capacity test)

$$D_{max} = \frac{m_{max}(g)}{V(cm^3)}$$

$$= \frac{\text{weight of sample minus container after 2 hours draining (g)}}{\text{volume of sample } (cm^3)}$$

$$= 2519.5 \text{ g} / 1982.74 \text{ cm}^3 = 1.27 \text{ g/cm}^3$$

3) Density ($D_{dry}$) on dry weight basis

$$D_{dry} = D_{moist} \times (\% \text{ solids} / 100)$$

$$= 0.77 \times (98/100) = 0.755 \text{ g/cm}^3$$

### 3.3.2.3 Maximum Water Capacity ($WC_{max}$)

$$WC_{max} = \frac{(M_{max} - M_{dry}) \times 100}{V}$$

$M_{max}$ = Weight of sample minus container after 2 hours draining (g)

Mdry = Weight of compacted substrate (g) × (% solids/100)

$$WC_{max} = \frac{(2519.5 - (1469 \times (98/100))) \times 100\%}{1982.74}$$

$$= 55\%$$

### 3.3.2.4 Water Permeability (mod. $K_f$)

$$\text{mod.}K_f = \frac{1}{t} \times \frac{1}{h+4.0} \; ;$$

t = time taken for water level to drop by 10 mm(s)

h = depth of sample in cm

$\text{mod.}K_f = (1/243.58) \times (1/((107.5/10)+4)) = 0.000278$ cm/s

### 3.3.2.5 Particle Density

$$D_p = \frac{d_w(W_s - W_a)}{(W_s - W_a) - (W_{sw} - W_w)} \; ; \; d_w = 1 \text{ g/cm}^3$$

$$= \frac{171.8 - 111.7}{(171.8 - 111.7) - (398.1 - 357.0)} = 3.163 \text{ g/cm}^3$$

### 3.3.2.6 Porosity

1) Total Porosity (TP) %

TP (%) = $100 \times (1 - (D_b/D_p))$ ; $D_b$ = bulk density = dry density

$= 100 \times (1 - (0.755/3.163) = 76.1\%$

2) Air-filled Porosity (AFP) %

AFP (%) = TP (%) – $WC_{max}$ (%)

$= 76.1 - 55 = 21.4\%$

**Green roof media analysis (Result on dry weight basis unless specific otherwise**

**(Source: Penn State University)**

| Analysis | Units | Penn State Result | FLL Guidelines for Intensive Sites |
|---|---|---|---|
| **Particle Size Distribution** | | | |
| □ 0.05 mm (FLL reference value based on < 0.06 mm) | mass % | 14.6 | ≤ 20 |
| Density Measurements | | | |
| Bulk Density (dry weight basis) | $g/cm^3$ | 0.8 | |
| Bulk Density (dry weight basis) | $lb/ft^3$ | 49.71 | |
| Bulk Density (at max. water-holding capacity) | $g/cm^3$ | 1.28 | |
| Bulk Density (at max. water-holding capacity) | $lb/ft^3$ | 80.15 | |
| Water/Air Measurements | | | |
| Moisture (as received basis) | mass % | 15 | |
| Total Pore Volume | vol.% | 69.3 | |
| Maximum water-holding Capacity | vol.% | 51.3 | ≥ 45 |
| Air-Filled Porosity (at max. water-holding capacity) | vol.% | 18 | ≥10 |
| Water Permeability (saturated hydraulic conductivity) | cm/s | 0.01 | ≥0.0005 |
| Water Permeability (saturated hydraulic conductivity) | in/min | 0.23 | |

# Appendix 5.1

## List of date for any activities and problems occurred during study period

| Date | Activities | Problems/description |
|---|---|---|
| 3rd May 2007 | start collecting data | Low level of water in the barrel due to dryness evaporation, pour in more water to get the water level back to normal (from the calibration) and ready to collect new data |
| 24th August 2007 | Downloaded data | Changed batteries and planning to change it every 2 months |
| 18th September 2007 | Downloaded data – re-calibration | Vegetation dried off. Dried days |
| 4th December 2007 to 13th December 2007 | Batteries changed at 14:00-15:00 | Lost data. Frost weather. Battery maintenance, it should be changed at least every 2 weeks-1month to avoid lost data. Less leaves, but showing some new fresh leaves growing. |
| 3rd January 2008 | Downloaded data | Everything was fine – snowy days |
| 15 January 2008 | Batteries changed | Greening vegetation, test rig saturated due to heavy rain. |
| 17 January 2008 | | The inconsistency of runoff data starting from this date |
| 19 Feb 2008<br><br>20-22 Feb 2008 | Batteries changed<br><br>20th 13:40 – due to frosty day, probe was taken out from barrel to avoid disruption<br>22th 10:40 – probe has been put in back | |
| 17 March – 4 April 2008 | The humidity gel for data logger should be swapped every two weeks.<br><br>Cleaned the rain gauge and weeding. | Lost data again. Got only 2 weeks of good data from 3rd March – 17th March.<br><br>Gutter flew away on 17th March and fitted back on 4th April. Checked on data in 29th March and it seems that the inconsistency in results happened since January 17th. The inconsistency in data may due to the frozen water collected in barrel, or because of the batteries. However, batteries were changed on 19th Feb and 3rd March 2008 and the inconsistency was back to normal after 3rd March, but not long until the gutter flown away on 17th March.<br><br>Humidity sign in logger box was in pink. |
| 22 april 2008 | Download data 4 Oct 07 – 22 Apr 08 for | Everything looks fine |

| | | |
|---|---|---|
| | analysis (of 4th – 22nd April).<br><br>Checked on the rig condition. The humidity label still in blue. | |
| 1st May 2008 | Battery changed; the time from logger was one hour late than exact time. Need to update daylight timer automatically | Wild flower and weeds on the rigs |
| 14th – 18th July 2008 | The thermocouple probes have been installed. | The program was adjusted |
| 29 Oct 2008 | Adding more water until the water level reached maximum level, and the valve opened and started new reading. | Logger failed to read data on 28-29 Oct 08, but it seems that the batteries have not connected to the cable was the cause to the failure. Data on 28-29 cannot be used. Fixed. |
| 12 Nov 2008 | Cleaned the rain gauge (14:00 – 15:00) | |
| 24 Nov 2008 | Batteries changed | |
| 17 Feb 2009 | Checked on the 2008 results | Most of February 2008 data produced no runoff, therefore the February storm events could be used.<br><br>Rainfall data also got some pattern during June, July, Aug, Sept 2008; where in each month, 2 or 3 data of one minute interval would be disappeared (i.e midnight at 00:00:00 will be lost) |
| 12 June 09 | Need to re-program the logger to automatically control (open) the valve when debris stuck within it | Lost data again on 10-12 June due to debris stuck in the valve opening during heavy rainfall in 10th June. |